International Journal of Computational and Engineering

DECEMBER 2016 VOLUME1 NUMBER4

Publisher: ACADEMIC PUBLISHING HOUSE
Address: Quastisky Building, Road Town, Tortola, British Virgin Islands
UK Postal Code: VG1110

E-mail: editorial@ij-ce.com
www.ij-ce.com

ACADEMIC PUBLISHING HOUSE

CONTENTS

Research on Application Level of Innovatory Information Technologies in Smart Grid

Xiaolong Li[1],Jing Zhou [2]*
[1.] State Grid Hebei Electric Power Corporation,Shijiazhuang, Hebei 050021,China
[2.] School of Control and Computer Engineering, North China Electric Power University, Beijing 102206, China

Abstract: With the rapid development, smart grid and information communication technologies have been integrated so tightly that it is imperative to evaluate the application level of innovatory information communication technologies for the informatization in smart grid. First of all, in this article, innovatory information communication technologies (internet of things, cloud computing, big data and so on) are summarized based on relative researches and applications in smart grid. Then, from three aspects (internet of things, cloud computing and big data), an evaluation index system with 21 indexes has been established to evaluate the application level of innovatory technologies in smart grid information system. Thirdly, an evaluation model has been built by combining order relation weight method and matter-element extenics. Finally, this evaluation model has been validated via a case of provincial power grid in China, which shows that the evaluation result on application level of innovatory technologies could help very well to make decisions, and be theoretically and practically significant for the informatization in smart grid nationwide.
Keywords: cloud computing; big data; smart grid; application level evaluation

1. INTRODUCTION

With the rapid development in China, the robust smart grid needs and depends more and more tightly on information communication technologies. [1]Especially, with the improvement of informatization in power grid, new technologies like distributed new energy, micro grid, electrical autos, smart home and so on are continuously introduced into smart grid so that the speed of data generation, the volume of data and types of data in power grid are increasing quickly. [2, 3]The sharp contradiction between the lag of information technologies and the rapid development of smart grid is getting more and more obvious.[4] Therefore, it has become an inevitable trend to research how to make new information communication technologies and smart grid integrated with each other.

New innovatory information communication technologies like big data, cloud computing and internet of things, cannot only change technology application, services and development ideas of electric enterprises, but also help to improve user experiences, to make enterprises and customers share values, to eliminate barriers among industries, to realize energy interconnection, to use energy efficiently, and to harmonically control energy and power.[5] Internet of things is an advanced technology to acquire and process information. It plays an important role while establishing smart grid by monitoring operational parameters and collecting related data on real time. Establishing internet of things based on smart grid application is an important way to promote information communication, and to make technologies and smart grid integrated with each other deeply. So far, internet of things technology has been widely researched and applied in the production process and customer services of smart grid. In production process, the internet of things technology has been used to monitor the transmission lines online, to manage field operation, to keep equipments safe, and to keep outdoor facilities from burglary. [6] In customer services, it has been used in smart appliances and smart home, wireless sensor security, to collect data of users' energy consumption, and so on. [7]Cloud computing technology with features of unique virtualization, massive data processing function, and high reliability can help electrical power software system (which is characterized with huge data, multi-type information, complicated computation, and independent resources) to analyze data efficiently and to save space on system disk. It has become an indispensible method that electrical enterprises analyze data in circumstance of new information technologies. Some scholars have introduced cloud computing technology into power grid restoration, user-side response, power flow analysis, distributed data management and dispatch system. [8,9]By making use of electric power big data, we can deeply analyze the extra values of massive data from electrical enterprises so to aid them make decisions on management and development in context of big data. At present, big data technology has been applied in processes of electricity generation, transmission, transformation, distribution, utilization and dispatch, and become the basis of information communication platform for enterprises[4].

To sum up, application depth and breadth of new innovatory technologies mentioned above will directly impact on the application architecture of power grid information system, and on further reform of informatization, interaction and automation in

smart grid[10] so to facilitate the transition of informatization structure and the upgrade in electric industry. In this article, by establishing an index system, the application levels of innovatory technologies used in the information system of power grid enterprises including big data, cloud computing and the internet of things have been analyzed and evaluated so to put forward decision references on application, construction and development of these technologies.

2. ESTABLISHING AN INDEX SYSTEM ON THE APPLICATION LEVELS OF INNOVATORY TECHNOLOGIES IN INFORMATION SYSTEM OF POWER GRID

With unprecedented depth and breadth, innovatory information communication technologies and power grid have been rapidly integrated with each other. Information communication system has become the centre in smart grid to support production, management and development for the new generation power grid [2]. In this article, an index system has been established based on three technologies (internet of things, cloud computing and big data) which deeply impact on the architecture of information system in power grid currently.

Internet of things is characterized with an advanced information acquiring and processing capability. It helps power grid system to improve the levels of intelligent perception measure and of network intelligent communication, and as well as enhance the capabilities to intelligently process signals and to aggregate information. Internet of things is applied to extract data which have specific meanings and values so to decrease the volume of data which will be transferred in network and to improve network performance, to enhance network automatic control capability, and finally to keep network safe.[7]The application level on internet of things could be mainly evaluated from 6 aspects as electric power intelligent perception measure level, intelligent signal processing capability, intelligent network communication level, information aggregating capability in internet of things, safety level in internet of things, and automatic control capability.

Cloud computing technology cannot only deal with complicated real-time calculation in electric power system, but also can improve memory power and virtualization technology level of power grid to promote resources integrating level. It is characterized with a strong expansibility. Besides, distributed computing can greatly enhance the parallel calculation capability of electric power grid so that information could be easily integrated and analyzed, and be kept safely and confidentially. Therefore, the application level of cloud computing technology will be mainly evaluated from 6 aspects as the physical architecture level of cloud computing, distributed cloud storage capability, virtualization technology level, deployment capability of intelligent cluster, distributed parallel computing capability, and the safety of electric power cloud computing.

The deep integration between big data technology and electric power is an inevitable course in the technological revolution for electric power. With regard to electric power big data, capabilities of storage& management, integration &analysis and data processing will become effective competition means for electric power enterprises. How to make use of big data generated in electric power system, and how to display and share them, will become core competition capabilities. The application of big data technology can comprehensively improve the levels on storage, integration, processing, analysis, display, safety and sharing of electric power data. Via further data mining & analyzing and knowledge discovery, implicit knowledge could be extracted from big data. Therefore, the application of big data technology will be evaluated from the following aspects as storage& management level of electric power big data, big data integration capability of electric power, processing capability of electric power big data, analysis capability of electric power big data, display capability, safety level of electric power big data, sharing service level of electric power big data, power grid topology simulation computing capability, implicit knowledge analysis and decision capability.

To sum up, a three-level index system on the application levels of new innovatory technologies as internet of things, cloud computing and big data as used in the information system of power grid has been established.(See Table 1)

Tab.1 Index system on the application levels of new innovatory technologies used in the information system of smart grid

First level	Second level	Third level
The application levels of new innovatory technologies used in the information system of smart gridA	The application level of internet of things technology(B1)	Electric power intelligent perception measure level(C11)
		Intelligent signal processing capability(C12)
		Intelligent network communication level(C13)
		Information integration capability for internet of things(C14)
		Safety level for internet of things(C15)
		Automatic control capability(C16)
	The application level of cloud computing	Physical architecture of cloud computing(C21)
		Distributed cloud storage capability(C22)
		Virtualization technology level(C23)

technology(B2)	Deployment capability of intelligent cluster(C24)
	Distributed parallel computing capability(C25)
	Cloud computing safety of electric power(C26)
The application level of big data technology(B3)	Storage & management level of electric big data(C31)
	Integration capability of electric big data(C32)
	Processing capability of electric big data(C33)
	Analysis capability of electric big data(C34)
	Display capability of electric big data(C35)
	Safety level of electric big data(C36)
	Sharing service level of electric big data(C37)
	Topology simulation computing capability of power grid(C38)
	Implicit knowledge analysis and decision capability(C39)

3. ESTABLISHING AN EVALUATION MODEL BASED ON ORDER RELATION WEIGHT METHOD AND MATTER-ELEMENT EXTENICS

3.1 matter-element theory

As one basic theory for extenics[11], matter-element is a method to describe things formally. The feature C and its valueV of the matter N are expressed as a triple in order as R=(N,C, V). N,C,V are three elements for the matter-elementR.[12-14]

When the matter N has multiple features, R could be expressed as an-dimension matter-element：

$$R=(N,c,v)=\begin{bmatrix} R_1 \\ R_2 \\ \vdots \\ R_n \end{bmatrix}=\begin{bmatrix} N\ c_1\ v_1 \\ c_2\ v_2 \\ \vdots\ \ \vdots \\ c_n\ v_n \end{bmatrix} \tag{1}$$

Here, $R_i=(N,c_i,v_i),i=1,2,\cdots,n$ is called sub-matter-element of R .

3.2 extension set

Extension setcan be used to describe the status that the matter is true or false, and the degree that the matter has some feature. A positive value means that the matter has the feature. The larger is the value, the higher is the degree, and vice versa. A negative value means that the matter does not have the feature. The value “0” means that the matter possibly has or does not have the feature.Correlation function is a common approach to describe extension set. In extenics, the distance between the point x on real axis and the intervalX0=(a,b) is defined as below[15]：

$$\rho(x,X_0)=\left|x-\frac{a+b}{2}\right|-\frac{b-a}{2} \tag{2}$$

3.3 establishing matter-element extenics evaluation model

(1)Determining classical threshold and sectional threshold

Given that there are totally t evaluation ranks. N_j stands for the j th evaluation rank, characteristic variable $c_i(i=1,2,\cdots,n)$ is defined within the range of v_{ji} (i.e. classical threshold). p stands for the overall rank, and at the same timecharacteristic variable $c_i(i=1,2,\cdots,n)$ is defined within the range of sectional threshold. p_0 stands for the evaluated matter-element, and meanwhile characteristic variable $c_i(i=1,2,\cdots,n)$ is defined as the data acquired via evaluation. Metter-element matrixes for classical threshold and sectional one are expressed as R_j and R_p, and the to-be evaluated matter-element is expressed as R_0 respectively as following,

$$R_j=(N_j,c_i,v_{ji})=\begin{bmatrix} N_j\ c_1\ v_{j1} \\ c_2\ v_{j2} \\ \vdots\ \ \vdots \\ c_n\ v_{jn} \end{bmatrix}=\begin{bmatrix} N_j\ c_1\ (\mathrm{a}_{j1},\mathrm{b}_{j1}) \\ c_2\ (\mathrm{a}_{j2},\mathrm{b}_{j2}) \\ \vdots\ \ \vdots \\ c_n\ (\mathrm{a}_{jn},\mathrm{b}_{jn}) \end{bmatrix} \tag{3}$$

$$R_p=(p,c_i,v_{pi})=\begin{bmatrix} p\ \ c_1\ v_{p1} \\ c_2\ v_{p2} \\ \vdots\ \ \vdots \\ c_n\ v_{pn} \end{bmatrix}=\begin{bmatrix} p\ \ c_1\ (\mathrm{a}_{p1},\mathrm{b}_{p1}) \\ c_2\ (\mathrm{a}_{p2},\mathrm{b}_{p2}) \\ \vdots\ \ \vdots \\ c_n\ (\mathrm{a}_{pn},\mathrm{b}_{pn}) \end{bmatrix} \tag{4}$$

$$R_0=\begin{bmatrix} p_0\ c_1\ v_1 \\ c_2\ v_2 \\ \vdots\ \ \vdots \\ c_n\ v_n \end{bmatrix} \tag{5}$$

(2)Determining weights based on order relation method

Weights could be determined based on order relation method without establishing judgment matrix,without conducting consistency test,and with characters of small computation volume and high utility. Besides, the numbers of indexes are not limited in this way. [16] Firstly, the hierarchical structure of the evaluation index system has been established. In this evaluation index system, 3-level architecture has been used. The target level is the application level of innovatory technologies in company information system framework. There are 3 first-level indexes and several second-level indexes. If evaluation index c_{mi} is more important than evaluation index c_{mj} on the same evaluation level $m(m=1,2,3)$, it is expressed as $c_{mi}>c_{mj}$. As for evaluation index

set $\{c_{m1}, c_{m2}, \cdots, c_{mk}\}$, k is the numbers of indexes on the evaluation level m. Then the order relation could be established according to the following steps:
1)Experts will choose the most important indexwhich they think it is, in index set $\{c_{m1}, c_{m2}, \cdots, c_{mk}\}$ and make it expressed as c^*_{m1}.
2)Experts will again choose the most important indexwhich they think it is, from the left $k-1$ index and make it expressed as c^*_{m2}.
3)Repeat the steps above.
In this way, a sole order relation could be defined as following,

$$c^*_{m1} > c^*_{m2} > \cdots c^*_{mk} \tag{6}$$

Given that experts' rational judgment on the importance between evaluation index c^*_{mi} and $c^*_{m(i+1)}$ is expressed as $w_{mi} / w_{m(i+1)}$ as following,

$$w_{mi} / w_{m(i+1)} = r_{i+1} (i = 1, 2, \cdots, k-1) \tag{7}$$

The value of r_{i+1} is given in Table2.

Tab.2 The given value of r_{i+1}

r_{i+1}	Description
1.0	Index c^*_{mi} is as important as index $c^*_{m(i+1)}$
1.2	Index c^*_{mi} is slightly more important than index $c^*_{m(i+1)}$
1.4	Index c^*_{mi} is more important than index $c^*_{m(i+1)}$
1.6	Index c^*_{mi} is critically more important than index
1.8	Index c^*_{mi} is extremely more important than index
1.1,1.3,1.5,1.7	intermediate values

Weights for the second level index is calculated as below,

$$w_{mk} = (1 + \sum_{j=2}^{k} \prod_{i=j}^{k} r_i)^{-1} \tag{8}$$

$$w_{mi} = r_{i+1} w_{m(i+1)} (i = 1, 2, \cdots, k-1) \tag{9}$$

In the same way, weight w_m for the first level index can be figured out. Finally, weights for each index could be calculated as below,

$$\omega_{mk} = w_m * w_{mk} \tag{10}$$

(3)Determining correlation degree and evaluation rank based on correlation function
The correlation function of each evaluation index to the j th evaluation rank is expressed as below,

$$K_j(v_i) = \begin{cases} \dfrac{-\rho(v_i, V_{ji})}{|V_{ji}|} & v_i \in V_{ji} \\ \dfrac{\rho(v_i, V_{ji})}{\rho(v_i, V_{pi}) - \rho(v_i, V_{ji})} & v_i \notin V_{ji} \end{cases} \tag{11}$$

Here, $\rho(v_i, V_{ji})$ stands for the distance from the to-be-evaluated matter element c_i to the classical threshold. $\rho(v_i, V_{pi})$ stands for the distance from the to-be-evaluated matter element c_i to the sectional threshold. $|V_{ji}|$ stands for the distance from index c_i to the classical threshold of the j th evaluation rank.
The correlation degree of the to-be-evaluated matter element to each evaluation rank is calculated as following,

$$K_j(p_0) = \sum_{i=1}^{n} \omega_i K_j(v_i) \tag{12}$$

Ranking formula is shown below,

$$\overline{K_j(p_0)} = \frac{K_j(p_0) - \min\{K_e(p_0)\}}{\max\{K_e(p_0)\} - \min\{K_e(p_0)\}} e = 1, 2, \cdots, t \tag{13}$$

4. CASE STUDY

4.1 determining the classical threshold

We will takethe practical application of innovatory technologies in information system of some electric power company in some coastal province in China to analyze and evaluate here below. The evaluation results are classified as 5 ranks as better(N_1), good(N_2), general(N_3), bad(N_4)and worse(N_5). According to experts' experience, classical thresholds of R_1, R_2, R_3, R_4 and R_5 are given individually. In table 3, classical threshold intervals for 3 second-level indexes are given. The values of classical threshold for third-level indexes are the same as the one for second-level indexes. Here, a, b are the lower limit and the upper limit respectively. The threshold R_1 has both lower and upper limits, and the left thresholds only have the lower limits.

Tab.3 The classical threshold settings for the application level of innovatory technologies in company information system framework

Index	R_1		R_2		R_3		R_4		R_5	
	a	*b*	*a*	*b*	*a*	*b*	*a*	*b*	*a*	*b*
B1	0.9	1	0.8	0.9	0.7	0.8	0.5	0.7	0	0.5
B2	0.9	1	0.8	0.9	0.6	0.8	0.5	0.6	0	0.5
B3	0.9	1	0.8	0.9	0.7	0.8	0.6	0.7	0	0.6

4.2 weights of index

Firstly, weighs of index system have been determined based on order relation method. Specifically, the importance among indexes is compared by provincial experts, and the resultsare shown in Table 4.

Tab.4Weights of each index for the application level of innovatory technologies in company information system framework

Importance order	importance degree	weight	Importance order	importance degree	weight	combination weight
impact of big data(B3)		0.43	Storage & management level of electric big data(C31)		0.18	0.077
			Processing capability of electric big data(C33)	1	0.18	0.077
			Analysis capability of electric big data(C34)	1.1	0.16	0.070
			Integration capability of electric big data(C32)	1.4	0.11	0.050
			Topology simulation computing capability of power grid(C38)	1.2	0.10	0.041
			Implicit knowledge analysis and decision capability(C39)	1	0.10	0.041
			Safety level of electric big data(C36)	1.4	0.07	0.030
			Display capability of electric big data(C35)	1.1	0.06	0.027
			Sharing service level of electric big data(C37)	1.3	0.05	0.021
impact of internet of things(B1)	1.4	0.31	Intelligent signal processing capability(C12)		0.22	0.067
			Automatic control capability(C16)	1	0.22	0.067
			Information integration capability for internet of things(C14)	1.1	0.20	0.061
			Electric power intelligent perception measure level(C11)	1.4	0.14	0.043
			Intelligent network communication level(C13)	1.2	0.12	0.036
			Safety level for internet of things(C15)	1	0.12	0.036
Impact of cloud computing(B2)	1.2	0.26	Physical architecture of cloud computing(C21)		0.21	0.055
			Deployment capability of intelligent cluster(C24)	1	0.21	0.055
			Distributed parallel computing capability(C25)	1.2	0.18	0.046
			Cloud computing safety of electric power(C26)	1.1	0.16	0.042
			Distributed cloud storage capability(C22)	1.3	0.12	0.032
			Virtualization technology level(C23)	1.1	0.11	0.029

4.3 COMPREHENSIVE EVALUATION ON THE APPLICATION LEVELS

To make the application of innovatory technologies deep into information system framework of this provincial electric power grid company, we firstly have evaluated the application levels of technologies as big data, internet of things, and cloud computing in its information system framework. Scores on each index given by experts are listed in the column 3, Table 5. According to formula(11)and formula $\omega_i K_j(v_i)$, weight for each index is calculated and listed in column 4 to 13, Table 5. Finally, according to formula(12)and formula(13), the correlation degree and the comprehensive evaluation rank could be figured out. See table 5:

Tab.5 Comprehensive evaluation result on the application level of innovatory technologies in company information system framework

Second-level index	Third-level index	Value of index	$K_1(v_i)$	$\omega_i K_1(v_i)$	$K_2(v_i)$	$\omega_i K_2(v_i)$	$K_3(v_i)$	$\omega_i K_3(v_i)$	$K_4(v_i)$	$\omega_i K_4(v_i)$	$K_5(v_i)$	$\omega_i K_5(v_i)$
B1	C11	0.59	-0.431	-0.019	-0.339	-0.015	-0.212	-0.009	0.450	0.019	-0.180	-0.008
	C12	0.81	-0.321	-0.021	0.100	0.007	-0.050	-0.003	-0.367	-0.024	-0.620	-0.041

	C13	0.87	-0.188	-0.007	0.300	0.011	-0.350	-0.013	-0.567	-0.020	-0.740	-0.027
	C14	0.72	-0.391	-0.024	-0.222	-0.013	0.200	0.012	-0.067	-0.004	-0.440	-0.027
	C15	0.64	-0.419	-0.015	-0.308	-0.011	-0.143	-0.005	0.300	0.011	-0.280	-0.010
	C16	0.72	-0.391	-0.026	-0.222	-0.015	0.200	0.013	-0.067	-0.004	-0.440	-0.029
B2	C21	0.78	-0.353	-0.019	-0.083	-0.005	0.100	0.005	-0.450	-0.025	-0.560	-0.031
	C22	0.88	-0.143	-0.005	0.200	0.006	-0.400	-0.013	-0.700	-0.022	-0.760	-0.024
	C23	0.69	-0.404	-0.012	-0.262	-0.008	0.450	0.013	-0.225	-0.007	-0.380	-0.011
	C24	0.89	-0.083	-0.005	0.100	0.005	-0.450	-0.025	-0.725	-0.040	-0.780	-0.043
	C25	0.79	-0.344	-0.016	-0.045	-0.002	0.050	0.002	-0.475	-0.022	-0.580	-0.026
	C26	0.87	-0.188	-0.008	0.300	0.012	-0.350	-0.015	-0.675	-0.028	-0.740	-0.031
B3	C31	0.92	0.200	0.015	-0.200	-0.015	-0.600	-0.046	-0.733	-0.056	-0.800	-0.061
	C32	0.93	0.300	0.015	-0.300	-0.015	-0.650	-0.032	-0.767	-0.038	-0.825	-0.041
	C33	0.83	-0.292	-0.022	0.300	0.023	-0.150	-0.011	-0.433	-0.033	-0.575	-0.044
	C34	0.82	-0.308	-0.021	0.200	0.014	-0.100	-0.007	-0.400	-0.028	-0.550	-0.038
	C35	0.89	-0.083	-0.002	0.100	0.003	-0.450	-0.012	-0.633	-0.017	-0.725	-0.020
	C36	0.95	0.500	0.015	-0.500	-0.015	-0.750	-0.022	-0.833	-0.025	-0.875	-0.026
	C37	0.87	-0.188	-0.004	0.300	0.006	-0.350	-0.007	-0.567	-0.012	-0.675	-0.014
	C38	0.94	0.400	0.017	-0.400	-0.017	-0.700	-0.029	-0.800	-0.033	-0.850	-0.035
	C39	0.74	-0.381	-0.016	-0.188	-0.008	0.400	0.017	-0.133	-0.006	-0.350	-0.015

$$K(p_0) = (-0.179,\ -0.050,\ -0.187,\ -0.414, -0.602)$$

$$\overline{K(p_0)} = (0.765,\ 1.000,\ 0.752,\ 0.341, 0.000)$$

In Table 5, the correlation degree of this provincial power grid company to the classical threshold of each rank is $(0.765,\ 1.000,\ 0.752,\ 0.341, 0.000)$, which shows that the evaluation result of this company ranks better, and reflects that the application level of innovatory technologies in this company is higher. By calculating, the correlation degrees of each rank to classical threshold are figured out for big data, internet of things and cloud computing respectively as following:

$$(0.778,\ 1.000,\ 0.333,\ 0.111, 0.000)$$
$$(0.125, 0.333,\ 1.000,\ 0.333, 0.000)$$
$$(0.415,\ 1.000, 0.792,\ 0.132, 0.000)$$

It is obvious that the application levels of big data technology and cloud computing technology rank good, and the one of internet of things technology ranks general. To comprehensively reflect the application level of innovatory technologies in information system framework of this provincial power grid company, we have analyzed and evaluated sub level indexes for 3 technologies and the results are listed in table 6.

Tab 6 Analysis on evaluation ranks for third-level index

Second index	Distribution of evaluation ranks for third-level index					Evaluation rank
	R_1	R_2	R_3	R_4	R_5	
B1		C12, C13, C16	C14, C15	C11,		R_3
B2		C22, C24, C26	C21, C23, C25			R_2
B3	C31, C32, C36, C38	C33, C34, C35, C37	C39			R_2

According to the evaluation results in Table 6, the comprehensive rank and the ranks for sub level indexes are both high for the application level of big data in this company, and mostly are good or better, which indicates that this company has deeply researched on the application of big data. the comprehensive rank for the application level of cloud computing is high, and the ranks for sub level indexes are general or good, which indicates that this company has been gradually applying cloud computing technology and bearing fruits currently. The application level of internet of things is lower than those of two formers, especially for some sub level indexes, the application level is bad, which indicates even this company has been gradually applying this technology, but the application level is still low. The evaluation process and results reflect the real situation on application level of innovatory technologies in company information system framework of this provincial power grid. The application of big data and cloud computing in this provincial power grid company is advanced and can

be referenced for follow-up similar evaluation. Besides, the comprehensive evaluation model has been proved as a feasible, scientific and rational evaluation method.

5. CONCLUSION

(1) Based on the depth and breadth of the innovatory technologies' application in company information system framework, an index system for the application level has been established. After describing and analyzing how to determine weight of index and how to choose the comprehensive evaluation model, order relation method and matter-element extenics method have been applied to this evaluation model. Via a case study on the application level of innovatory technologies in information system framework of a provincial power grid company, the evaluation model has been proved as a scientific, rational and feasible method.

(2)Evaluation on application level of innovatory technologies in company information system framework can not only measure the application level, but also help to improve the application level in this company. By comparing the evaluation results among provincial power grid companies, they can mutually supervise and learn from each other. Meanwhile, it can also provide practical management experience, and help to optimize the deployment and framework of information system.

6. ACKNOWLEDGMENT

This paper is supported by the Fundamental Research Funds for the Central Universities (Grant No.2015MS36) and the State Grid Corporation headquarters projects(Grant No.KJGW2015-020).

REFERENCES

[1] YU Yi-xin, LUAN Wen-peng.Smart Grid and Its Implementation[J]. Proceedings of the CSEE,2009,29(34):1-8 (in Chinese).

[2] LIU Jun, LV Jun-feng. Application of Data Mining Technologies in An Era of Big Data[N]. State Grid News,2012-05-15(10).

[3] FAN Mingtian, ZHANG Zuping, SU Aoxue, SU Jian. Enabling Technologies for Active Distribution Systems[J]. Proceedings of the CSEE, 2013,33(22)：12-18.

[4] ZHU Chaoyang, WANG Jiye, DENG Chunyu．Research and Design of Electric Power Big Data Platform[J]．Electric Power Information and Communication Technology,2015,13(6)：1-7.

[5] DUAN Junhong, ZHANG Naidan, ZHAO Bo, et al. Electric Power Information and Communication Technology, 2015,13(2)：92-95.

[6] Lu J,XieD,AiQ.Research on Smart Grid in China,Transmission& Distribution Conference & Exposition[C].Asia and Pacific,2009(10)

[7] LI Na, CHEN Xi, WU Fan, LI Xianzhen. Study of Information Aggregation Technology on the Internet of Things for Smart Grid[J]. Information and Telecommuni- cation Technology, 2010(2): 21-28.

[8] ZHANG Hao, HE Jinghan, YIN Hang, BO Zhiqian, Tony Yip. Power Grid Islands Service Restoration Based on Cloud Computing[J]. Proceedings of the CSEE, 2011,31(34)：77-84.

[9] CAO Zijian, LIN Jin, SONG Yonghua. Optimization Model for Resources Allocation of Cloud Computation in Active Distribution Networks[J]. Proceedings of the CSEE, 2014,(19):3043-3049.

[10] LI Xiangzhen, LIU Jianming. Telecommunications Network Technology, 2010,(8)：41-45.

[11] CAI Wen. Matter-element Model and Its Application [M]. Beijing: Scientific and Technical Documentation Press, 1994.

[12] KANG Zhi-qiang, ZHOU Hui, FENG Xia-ting, YANG Cheng-xiang. Evaluation of High Rock Slop Quality Based on Theory of Extenics[J].Journal of Northeastern Univeristy(Natural Science), 2007,28(12):1770-1774.

[13] Wang Yong-Hua, LuoGuo-Liang. Research on power quality evaluation based on matter-element extension model[J]. Applied Mechanics and Materials, 2013, 411-414: 2735-2741.

[14] Li Jinying, Li Panjuan. Risk assessment of wind power investment project based on matter-element extension model[J]. Open Fuels and Energy Science Journal, 2015,8(1): 52-57.

[15] YANG Yang. Research on Credit Evaluation of Commercial Bank Customer Based on the Theory of Risk Element Transmission[D].Beijing, North China Electric Power University, 2013.

[16] CHEN Wu, XU Xinyi, WANG Hongrui,etal.Fuzzy Synthetic Evaluation of Sustainable Utilization of Water Resources in Beijing City Based on Rank Correlation Method[J]. Journal of Economics of Water Resources, 2014,32(2)：19-24.

Effect of Miller Cycle and Compression Ratio on the Emission of High Power Natural Gas Engine

Hongyuan Wei, Xuejian Jiao, Wenqing Ge, Xiaoxiao Liang, Bo Li*
Shandong University of Technology, School of Transportation and Vehicle Engineering, ZiBo 255049, China

Abstract: In order to improve the economy and emission performance of high power natural gas engine , the application of miller cycle in high power natural gas engine is studied. Calculating and analyzing the influence of miller cycle mode, LIVC angle and engine geometry compression ratio on combustion performance and emission of high power natural gas engine. The results show that the application of miller cycle and improve the geometric compression ratio combination, with the increase of Miller cycle degree engine knock is suppressed, so the geometric compression ratio can be further increased, at the same time, the engine thermal efficiency increased and NOx emission is also improved. Miller cycle LIVC angle increases make the mixed gas flows down the quality of intake pipe increases, and the engine volumetric efficiency reduced, result the output torque of engine decline, detrimental to the engine power performance.When the geometric compression ratio is 13 and the LIVC angle is 24 degrees, The thermal efficiency is higher than that of other geometric compression ratio and LIVC angle, and the NOx emission can be reduced by 4.95%.The application of Miler cycle in the high power natural gas engine provides a theoretical basis for the improvement of thermal efficiency and emission performance of the high power natural gas engine.

Keywords: High power natural gas engine, Miller cycle, Effective compression ratio, Thermal efficiency, NOx emission

1. INTRODUCTION

With the wide application of petroleum resources, exploitation of oil reserves surged year resulted in serious decline, has become a major obstacle to the industrialization and modernization, seriously affecting people's lives and restricts the development of society, people want to make up for the development of new energy resources caused by energy crisis oil plummeted [1].Natural gas although it is also usedin the past, but the utilization rate is too less and resulting in a large number of waste, natural gas engines are mostly from other types of engine directly converted and thermal efficiency is not very high. In response to the energy crisis, natural gas is being used as a new type of clean energy has been widely used as the fuel of the engine, and it has been widely used in the fuel of the engine.

In order to improve the utilization of natural gas and the heat efficiency of natural gas engine, and reduce the emission of harmful gas, research scholars at home and abroad have already made a lot of research on high power natural gas engine.Tests [2-3] Studied for high power gas engine performance development method, combustion system parameters on the performance of natural gas engine. Test [4] used a prechamber spark plug and improve the lean limit and re matching of turbochargers and miller cycle mode and improves the power of the engine.High power engine fuel gas is mainly used to be developed, and the ignition technology, HCCI combustion technology, miler cycle technology, long stroke technology, EGR technology, and the integrated use of these technologies have made great progress.

Miller cycle technology to achieve the suppression of NOx emissions by changing the timing of the valve is easy to achieve, it is more suitable for high power natural gas engine to improve the emission of high power natural gas engine. Application of Miller cycle in high power gas engine, establish a AVL BOOST model of high power natural gas engine, the effects of Miller cycle angle and geometry compression ratio on engine combustion performance and emissions were simulated and studied, and matching geometry compression ratio and intake valve closing angle for engine.

2. SIMULATION MODEL OF HIGH POWER NATURAL GAS ENGINE

In an oilfield with high power natural gas engine as the prototype, combined with the related parameters of high power gas engine, the main parameters of the prototype are given in Tab. 1.

Table 1 Basic parameters of prototype engine

Element	Parameter
Engine type	V-Engine, 4 stroke
Air intake mode	Turbocharged Inter-cooled
Number of cylinders	8
Bore×Stroke/mm	190×210
Calibration torque/N.m	5300
Calibration speed/(r/min）	1000

Simulation software AVL BOOST was used to establish cycle simulation model of high power natural gas engine according to the relevant parameters of the prototype, as shown in Fig. 1.

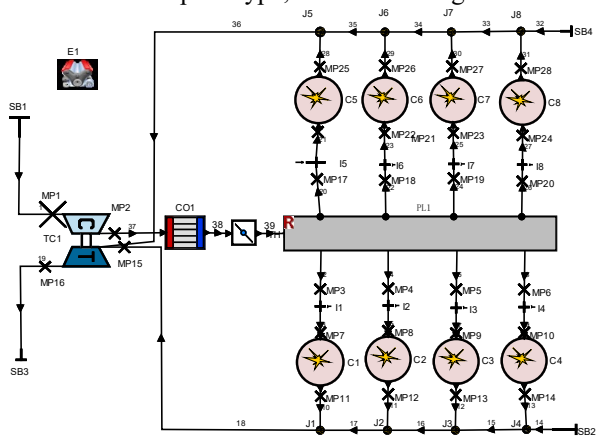

Figure 1 Cycle simulation model of high power natural gas engine

the Fractal quasi dimensional combustion model was used to calculate the combustion process in the simulation model. The combustion rate of the Fractal combustion model can be expressed by the formula:

$$\frac{dm_b}{dt} = \rho_u A_T S_L = \rho_u \left(\frac{A_T}{A_L} \right) A_L S_L \quad (1)$$

Where, m_b is the fuel mixture quality has burned; ρ_u is the concentration of the mixed gas is not burned; A_T is turbulent flame area; A_L is laminar flame area; S_L is laminar flame propagation velocity, which is affected by the temperature, pressure and the amount of waste gas in the cylinder.

3. MILLER CYCLE

The miller cycle was first proposed by the American engineer R.H.Miller in the last century in 40s[5]. The miller cycle by adjusting the engine intake valve closing time so that the pressure in the cylinder at the early stage of the compression stroke at a low value, thereby reducing the cycle temperature and pressure of the engine cylinder, the engine knock tendency decreases, NOx emission reduction[6-9], as shown in Fig. 2. The engine can continue to increase the compression ratio and improve the thermal efficiency of the engine. Miller cycle has been widely used as an important way to improve the performance of the engine.

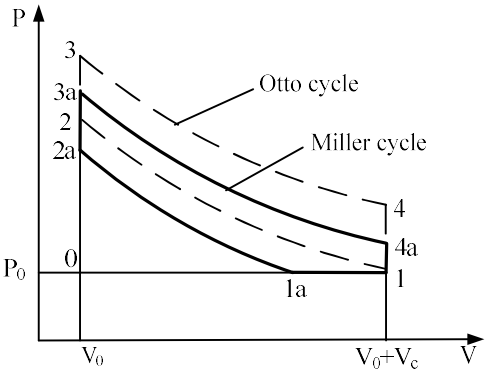

Figure 2 Miller cycle and Otto cycle Pressure-Volume diagram

3.1 Realization Form of Miller Cycle

The basic principle of miller cycle is to change the effective compression stroke and effective expansion stroke of the engine by changing the angle of the intake valve closing, so that the expansion stroke is greater than the compression stroke, thus reducing the effective compression ratio[10]. There are two main ways: Early Intake Valve Closing(EIVC)and Late Intake Valve Closing(LIVC)[11].EIVC to close the intake valve in advance and reduce the valve lift, the intake process stopped before the piston reaches BDC, reduces the engine air intake and advance a expansion cooling process. LIVC is generally used to maintain maximum valve lift unchanged and prolong the duration of valve opening, cylinder mixture poured into the air inlet and take away some of the heat, play a certain cooling effect. At present, the miller cycle is more than the way of using LIVC.

3.2 Effective Compression Ratio and Expansion Ratio

The miller cycle change the effective compression stroke of engine working process by adjusting the intake valve closing time, the effective compression ratio is less than the effective engine expansion ratio, thereby reducing the engine effective compression ratio and engine knock tendency[12-13]. Effective compression ratio is defined as the ratio of the volume at the time of the intake valve closing to the combustion chamber volume. And the effective expansion ratio is ratio of the cylinder volume at the time of the exhaust valve is opening to the combustion chamber volume. Effective compression ratio and expansion ratio are related to the volume of the cylinder at the time of closing the intake valve and opening the exhaust valve, which is related to the closing time of the intake valve and the opening time of the exhaust valve14-15].

The formula for calculating the effective compression ratio is:

$$\varepsilon_e = V_e / V_0 = V_e / (V / \varepsilon) = \varepsilon \cdot V_e / V \quad (2)$$

Where, ε_e is the effective compression ratio; ε is the geometry compression ratio; $V_e$is the cylinder volume at the time of the intake valve closing;$V_0$is the volume of the combustion chamber;V for the cylinder

volume when the piston at the BDC.

V_e can be changed according to the valve closing time, that is, the size of the V_e is corresponding to the intake valve closing time. The effective compression ratio shows a decreasing trend with the increase of the LIVC angle and reduce of the V_e.

The effective expansion ratio is calculated as:

$$\varepsilon_p = V_p / V_0 = V_p / (V / \varepsilon) = \varepsilon \cdot V_p / V \quad (3)$$

Where, ε_p is the effective expansion ratio;$V_p$is the cylinder volume at the time of the exhaust valve opening.

The engine uses miller cycle and not change the exhaust timing, so V_p is certain and the effective expansion ratio is proportional to the geometric compression ratio. Only by adjusting the valve closing time to change the size of the effective compression ratio, so that the value of the effective compression ratio is less than the effective expansion ratio.

4. SIMULATION RESULTS AND ANALYSIS

This paper uses improved geometric compression ratio combined with miller cycle to keep the effective compression ratio constant, by increasing the geometric compression ratio increases the engine effective expansion ratio, and improve engine thermal efficiency and NOx emissions. As shown in Fig. 3 is the calculated results in keeping the effective compression ratio unchanged based on the original model, LIVC angle with the change of the geometric compression ratio. As can be seen from the fig.3, with the increase of the geometric compression ratio(i.e. the increases of effective expansion ratio), the LIVC angle increases and the amplitude gradually becomes smaller, the valve opening time is prolonged and the degree of miller cycle is deepened.

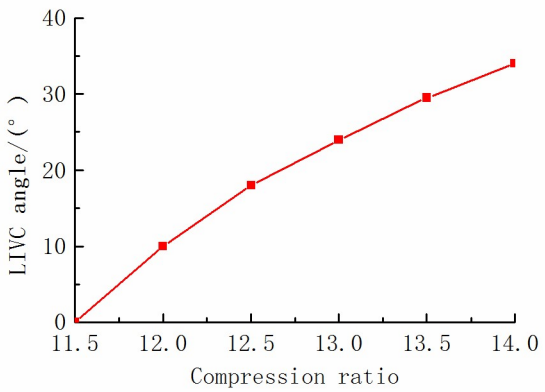

Figure 3 Change of LIVC angle with the geometric compression ratio

Under the premise of not changing the supercharger ratio of the engine, with the increase of LIVC angle the intake valve opening time increases, more mixed gas poured into the inlet, resulting in a decline in the engine volumetric efficiency and engine output torque dropped, is not conducive to engine power performance. In order to make up for the reduction of the intake air quantity, it is necessary to re match the supercharger ratio, so that the miller cycle engine can maintain the original intake amount and the engine power performance.

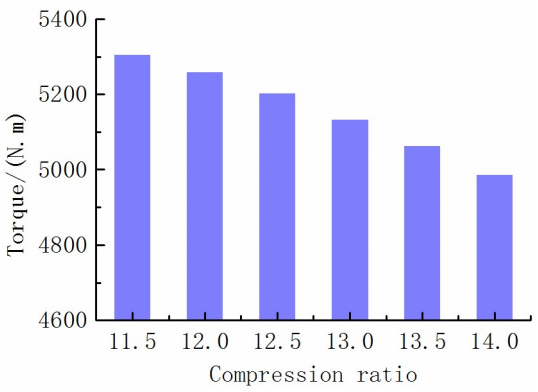

Figure 4 Variation of engine performance with geometry compression ratio

Studied in the changes of engine combustion and performance under six different geometry compression ratios with different LIVC angles, as shown in Fig. 5 below. With the increase of the geometric compression ratio, the combustion lag period decreases and the combustion heat release rate is accelerated, peak firing pressure rise, and the load of the engine body is increased. The geometric compression ratio is increased from 11.5 to 12~14, and the peak firing pressure is increased by 2.48%, 4.67%, 6.55%, 8.32% and 9.89% respectively.

At the same time, the LIVC angle increases with the increase of the geometric compression ratio, the cooling time increases at the beginning of the compression stroke, the temperature in the cylinder and the heat load of the engine decreases. The geometric compression ratio increases by 1, and the peak firing temperature can be reduced by 24K.

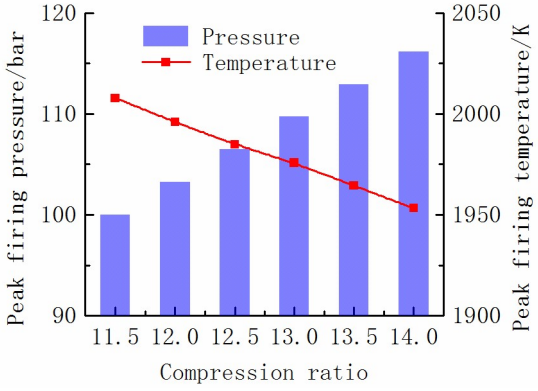

Figure 5 Change of combustion characteristics with geometric compression ratio

The increases of geometric compression ratio and LIVC angle, made the temperature of the engine combustion process is decreased, the NOx formation condition is limited and the production of NOx is reduced, the NOx through the exhaust valve and exhaust pipe emissions into the air reduction, environmental protection for the engine performance improvement plays a promoting role.

With the increase of LIVC angle, engine fuel consumption rate(BSFC) decreased first and then

increased, the thermal efficiency increases first and then decreases. When the economic performance in the geometric compression ratio of 13 and the LIVC angle is 24 degrees, get the maximum thermal efficiency.

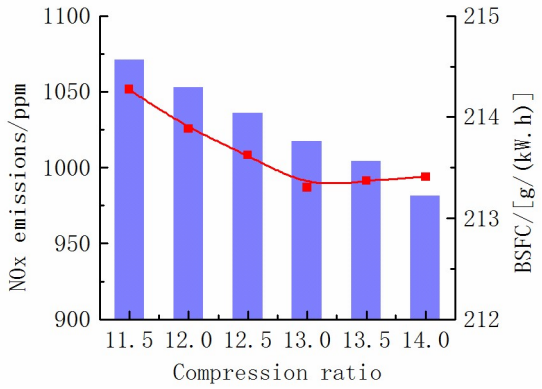

Figure 6 Change of NOx emission and gas consumption rate

5. CONCLUSION

(1)When the miller cycle and improve the geometric compression ratio method combining used with miller cycle deepened the engine peak firing pressure increases, the engine load increase, and the engine crude, but by the valve opening time is longer, the cylinder temperature drop in combustion process.

(2)Miller cycle LIVC angle increases make the mixed gas flows down the quality of intake pipe increases, and the engine volumetric efficiency reduced, result the output torque of engine decline, detrimental to the engine power performance.Miller cycle valve closure delay so that the cylinder temperature decreased, inhibiting the occurrence of knocking, to improve the geometric compression ratio provides a space.

(2)With the LIVC angle increase of the high power natural gas engine, engine fuel consumption rate(BSFC) decreased first and then increased, and the thermal efficiency increases first and then decreases. When the geometric compression ratio is 13 and the LIVC angle is 24 degrees of the high power natural gas engine, engine thermal efficiency is the best and the NOx emissions decreased by 4.95%.

6. ACKNOWLEDGMENT

This work is a project supported by Science and Technology DevelopmentProject of Shandong Province (Fund No.2014GGX103007), University Science and Technology Project of Shandong Province (Fund No.J11LD61), Natural Science Foundation of Shandong Province (Fund No.ZR2014EEQ031) and National Natural Science Foundation of China(Fund No.51505263).

REFERENCES

[1] Lu Jialiang, Zhao Suping. Optimization of energy consumption structure and natural gas industry development prospect in China[J]. 2013, 33(11):9-15.

[2] Li Shusheng. Study on Combustion System of the High Performance and barge Power Natural Gas Engine[D]. Shandong University, 2013.

[3] Li Quanwu. The Development of H12V190ZLT High Boost Pressure, Lean Burn Gas Engine[D]. Shandong University, 2008.

[4] Guo Zirui. The Simulation Optimization and Performance Improvement of Gas Engine[D]. Shanghai Jiao Tong University, 2012.

[5] R.H.Miller, Supercharging and internal cooling cycle for high output, Transactions of ASME 69(1947)453-457.

[6] R.H.Miller, H.U. Lieberherr, The Miller supercharging system for diesel and gas engines operating characteristics, CIMAC, 1957, in: Proceedings of the 4th International Congress on Combustion Engines, Zurich, June 15-22, 1957, pp. 787-803.

[7] Feng Kang. Fuel Saving Potential Study of Atkinson Cycle Applied on an Automotive Gasoline Engine[D]. Hunan University, 2012.

[8] Li Quanwu. The Development of H12V190ZLT High Boost Pressure, Lean Burn Gas Engine[D]. Shandong University, 2008.

[9] Federico Millo, Marco Gianoglio. Combining dual stage turbocharging with extreme Miller timings to achieve NOx emissions reductions in marine diesel engines[C].CIMAC Paper no. 210, 2010.

[10] Yang Cheng. Simulation and Optimization of Working Process for Miller Cycle Natural Gas Engine[D]. Jinlin University, 2013.

[11] Shi Xuehui. Simulation and Optimization of CNG Engine Based on Miller Cycle[D]. Jinlin University, 2014.

[12] Zhang Houshun, Chiu James, et al. Late Intake Valve Closing with Throttle Control at Light Loads for a Lean-Burn Natural Gas Engine[C]. SAE Paper, 1999-01-3458, 1999.

[13] Guo Zirui. The Simulation Optimization and Performance Improvement of Gas Engine[D]. Shanghai Jiao Tong University, 2012.

[14] Zhou Longbao. Internal combustion engine[M]. Beijing: China Machine Press, 2013.

[15] Zhou Song, Wang Yinyan, Ming Pingjian, et al. Working Process Simulation Technology of Internal Combustion engine[M]. Beijing: Beihang University Press, 2012.

Design of Friction and Wear Test Bench for Synchronizer

Kefeng WANG, Di LI, Wenqing GE, Peilin SHI, Bo LI*

Shandong University of Technology, School of Transportation and Vehicle Engineering, Zi Bo 255049, China

Abstract: The synchronization process of the lock ring synchronizer is mainly achieved by the friction effect, the friction generated when the inner cone of synchronizer ring is in contact with the outer cone of the gear ring which makes the meshing gear sleeve to synchronize rapidly with the synchronous ring. Synchronous friction increases the temperature of the friction cone, which has an impact on synchronous shift control process. In order to research the effect on the working performance of synchronizer when the friction cone temperature rise during synchronization process, the test bench has been designed which is used for the working process of the synchronizer.

Keywords: Synchronizer; Synchronization process; Test bench

1. INTRODUCTION

Generally, the key point of automobile transmission research is the working performance of synchronizer which is influenced by shift force, rotational speed difference, synchronous inertia and geometric structure of the synchronizer, in this situation, the effect of temperature between the friction cones on synchronizer working performance is ignored. Wang junwei[1] using ADAMS to analyze the effect of synchronizer locking feature parameters on synchronizer working performance; Xu wanli[2] analyzed the influence of lubricating oil and surface materials on transmission; J Kim[3] simulated the influence of shifting force on the manual transmission.

The synchronizer relies on the sliding friction between the friction cone to achieve the synchronization function, and the friction heat generated by the friction process has an effect on the coefficient of friction, which will further affect the working performance of the synchronizer. The friction heat is also affected by other conditions, such as the shift force and the rotational speed difference between the active side and passive side. A universal friction and wear test bench for synchronizer is designed, in order to obtain the relationship between these conditions and frictional heat.

2. RESEARCH STATUS OF FRICTION AND WEAR TESTING MACHINE

There are mainly three kinds of friction and wear testing machine in China, first one is the constant speed friction test machine based on DM-S and JF150D series models[4-5], which have simple structure and easy operation, but the working condition is fixed, and the actual working conditions can not be accurately simulated; The second one is JF160 type Chase friction test machine[6-8], which can provide many kinds of working conditions, but the price is expensive, structure is complex and the usage and maintenance personnel requirements is high; The third one is JF132 type bench wear testing machine[8-10], which equipment investment and test costs are high. In summary, these kinds of products can not complete the synchronization process experiment because of the higher price and the mismatched working conditions.

3. PRINCIPLE AND MAIN PARAMETERS OF THE FRICTION AND WEAR TESTING MACHINE

3.1 Principle of testing machine

The principle of the friction and wear testing machine of the synchronizer is shown in Fig.1. The rotational motion of the input shaft, inertia simulation device and the friction couple are driven by the driving motor, the axial move of the shifting fork-engagement sleeve and the friction couple are driven by the electromagnetic linear actuator, the friction surface temperature change of friction couple is recorded by infrared camera, and the rotating speed of the driving motor and the axial force of the electromagnetic linear actuator are applied to simulate the shift process of the synchronizer.

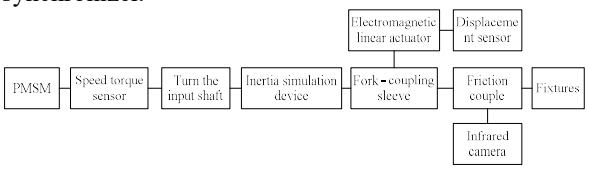

Figure 1 Principle diagram of friction and wear testing machine Determination of main parameters

The rotational speed difference, shifting force and the inertia of the synchronizer have influence on the shift time and the shift quality during the synchronizer shift process. Rotational speed, shift force and the input moment of inertia of the synchronizer are provided by the driving motor, the electromagnetic linear actuator and the inertia simulation device. Therefore, we need to determine the specific models and parameters of the driving motor, electromagnetic linear actuator, inertia simulation device and other equipment.

3.2.1 Rotational speed

The speed difference between the input and the output of the synchronizer has a great influence on the synchronization time. The temperature of the friction surface of the synchronizer is different because of the rotational speed difference and the synchronization time are different. Under the same synchronization time, the greater rotational speed difference, the higher temperature of the friction surface of the synchronizer, the worse the working performance. Shift one to shift two is the maximum rotational speed difference during the shift process. The rotational speed difference of both sides of the synchronizer are different, because of the different transmission gear ratio of shift one and two. Combined with the market models, the 0~1300r/min speed range of the friction and wear test bench for the synchronizer is determined, in order to meet the different models and different working conditions of the gear shift friction process.

3.2.2 Shift force

The size of shift force affects the temperature of the friction surface of the synchronizer, and indirectly affects the performance of the synchronizer. In a certain range, the temperature of the friction surface of the synchronizer will rise with the increase of the shifting force. The shift force can not be infinitely increased, we need to consider two principles[11]: first one is to meet the requirements of the service life of the synchronizer and the second is to meet the requirements of the working strength of the shift actuator. The shift force of the synchronizer friction and wear test bench is 0~1200N based on ABAQUS finite element analysis of the shift fork according to the test [11].

3.2.3 Inertia simulation device

The synchronizer input moment of inertia has a great impact on the synchronization time when the shift force and rotational speed difference is a certain. According to the equation (1), the greater the input moment of inertia of the synchronizer, the longer the synchronization time is. When the other boundary conditions are constant, the synchronization time increases and the temperature of the synchronizer friction surface also increases.

$$t_{s=}\frac{J_c \cdot \Delta\omega}{F \cdot \mu \cdot d} \cdot 2\sin\alpha \qquad (1)$$

Where t_s is the synchronization time; J_c is the input moment of inertia of the synchronizer; $\Delta\omega$ is the rotational speed difference; F is the shift force; μ is the friction coefficient between the friction cones; d is the average diameter of the friction cone; α is the half cone angle of friction cone.

3.2.4 Selection of the drive motor

The speed change function of the friction and wear testing machine of the synchronizer is realized by the driving motor. When we choose the drive motor, we not only have to consider its rated speed, but also have to consider its rated power and speed regulation. There are two kinds of speed regulation: first one is the AC motor frequency speed regulation, and the second is the DC motor rectifier speed regulation. According to the function of the test bench, the AC frequency speed regulation[12] is more advantageous, which has wide speed range, high precision, good smoothness, high efficiency and easy to realize the process automation.

The formula for calculating the power of the driving motor is equation (2)

$$P = \frac{T \cdot n}{9550} = \frac{2\mu \cdot F_n \cdot R \cdot n}{9550} \qquad (2)$$

Where P is the motor power; T is the torque of friction couple; n is the rotational speed of the friction couple; μ is the friction coefficient; F_n is the positive pressure of friction surface; R is the average radius of friction couple.

Put the limit parameters of the test bench into the equation (2), calculated the motor power.

3.2.5 Selection of infrared camera

The process of synchronous friction is short, and the temperature rise is changing fast. In order to better record the change of the friction surface temperature, the non-contact infrared camera is selected. The synchronization time is less than 0.5s, and the maximum temperature is less than 200℃ during the synchronization process. The German optris PI450 infrared camera is selected according to the above analysis, which model and technical parameters are shown in Tab.1.

Table 1 Model and main parameters of the infrared camera

Model	Sampling frame rate	Resolution	Temperature range	Standard temperature measurement	Minimum measuring distance
Optris PI450	80Hz	382*288	-20℃~900℃	±2℃	20mm

4. STRUCTURAL DESIGN OF FRICTION AND WEAR TESTING MACHINE FOR SYNCHRONIZER

4.1 Basic conception of the test bench

The basic idea of the synchronizer is to design a universal synchronous process test bench with variable speed, variable pressure and constant output function. It can not only test the influence of the friction heat of the synchronous process on the performance of the synchronizer, but also can meet the test requirement of multiple working conditions. The specific contents of the test bench are described as follows:

(1)Test piece

The test machine adopts the ring type friction couple

structure, and the size of the test piece is consistent with the size of the synchronizer.

(2)Working condition simulation

The real-time speed and shift force controllability shift process simulation can be achieved by the test machine, which can provide with different transmissions and gear ratios. In addition, the structure should be simple, and the cost should be low to meet the test function.

(3)Control section

The testing machine requires the speed, shift force, displacement, temperature and other parameters for real-time control. The same control software can be used with existing friction and wear testing machine, completing the predetermined condition test according to a certain test procedures.

(4) Data acquisition and processing

The computer data acquisition and processing system can monitor and measure the parameters such as speed, shift force, temperature, shift time and displacement in real time, and can calculate the friction coefficient.

4.2 Structure design of the test bench

The structure of the friction and wear test bench of the synchronizer is shown in Fig.2.

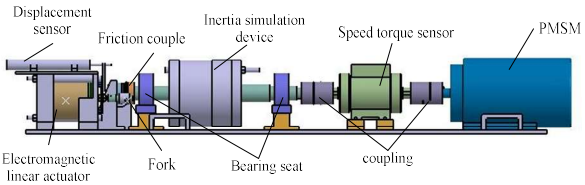

Figure 2 Friction and wear test bench

When the bench is working, the driving motor drives the main shaft to rotate through the torque sensor, the friction pair and the inertia disk are connected with the main shaft through the key groove, and rotate with the main shaft to the prescribed rotational speed. The electromagnetic linear actuators push the moving friction couple towards the static friction couple through the shifting fork-engagement sleeve, the displacement distance is controlled by the displacement sensor, and the output force is changed by the size of the current of the electromagnetic linear actuator. When the moving part of friction couple and static part of friction couple to achieve simultaneous shift, cut off the motor power supply, carry on the data acquisition and processing.

5. CONCLUSION

(1) According to the working principle of the synchronizer, a universal friction and wear test bench for synchronizer is designed. The influence of friction heat on the performance of the synchronization process is studied by collecting the experimental data and optimizing the process of synchronous friction, which is of great significance to improve the accuracy of the shift control.

(2) In order to reduce the cost and complexity for the friction and wear test bench, the friction process of the synchronous machine is simulated, and the influence of the transmission gear and the lubrication system on the friction process is ignored.

6. ACKNOWLEDGMENT

This work is a project supported by National Natural Science Foundation of China(Fund No. 51505263), Natural Science Foundation of Shandong Province (Fund No. ZR2014EEQ031), University Science and Technology Project of Shandong Province (Fund No. J11LD61), and Key Technology Research and Development Project of Shandong Province (Project No. 2015GGB01045).

REFERENCES

[1] Wang Junwei, Chu Chaomei, Miao Guo. Influence of Synchronizer Locking Feaure Parameter on the Performance of the Synchronizer[J]. Mechanical Transmission,2013,06:98-101.

[2] Xu wanli, zhao wei, su bin, xu ximeng, Investigation of manual transmission synchronizer failure mechanism induced by interface material/lubricant combinations, wear, 2015(328-329):475-479.

[3] J Kim,S Park,et al. Simulation of the shift force for a manual transmission[J]. Automobile Engineering, 2003,573-581.

[4] Zhao Xiaolou, Cheng Guangming, Wang Tieshan, Deng Shiqiao. The acyuality and development of friction and wear performance test of automobile friction material[J]. LUBRICATION ENGINEERING,2006,10:200-203.

[5] Shi Zhigang. Test Equipment and Developing Trend of Friction Materials for Automobile[J].Non-Metallic Mines,1998,05:57-58.

[6] Li Kang. Chase friction material testing machine and its testing range[J]. Friction and Wear,1987,4:44-49.

[7] S.K.Rhee. Comparison of CHASE Testing Machine and Inertia Test Stand for Motor Vehicle Friction Materials[J]. Friction and Wear,1986,3,48-53.

[8] A.HEISS. Comparison of Claus Friction Tester and Chase Testing Machine [J]. Friction and Wear,1991,4:45-47.

[9] Zhang Delin. Comparison of a CROSS Friction Testing Machine and Inertia Brake Testing Bench[J]. Automotive Technology,1994,05:32-35.

[10] Zhao Xi,Xu Lixiang, Dai Na, He Tao. Measurement and Control System of New Krauss Friction Tester Based on LabVIEW [J]. Journal of Hubei University of Technology,2011,05:55-57+77.

[11] Li Bo. Design and performance research of AMT shift system based on Direct-drive Technology[D]. Nanjing University of Science &Technology,2013.

[12] Qiu Dayin. The Development of Friction Material Tester with Adjustable Speed and Pressure[D].Jilin University,2009.

The Design of Online Travel Experience Systems based on the Virtual Reality

Zhao Jianguang,Fan Jingjing

Hebei Institute of Architecture and Civil Engineering, Department of Information Engineering

Abstract: Based on the analysis of the development of virtual tourism, this paper discusses the development principles and development steps of virtual reality modeling language. On this basis, VRML language is used to design the online experience system of snow and ice travel in ZhangBei County, which can improve the visibility and system stability.

Keywords: virtual reality; VRML; 3D

1. INTRODUCTION

With the development of economy and information technology, digital tourism to travel injected new vitality, using the existing Internet network platform combined with three-dimensional virtual technology, simulation technology, remote sensing technology, GPS technology, GIS platforms produce a variety of models digital Tourism application that allows people to stay at home, they can design itineraries to get detailed travel information, electronic map query, the virtual reality experience, sharing travel experiences, traveled the world to make the dream become a reality. Tourism tremendous economic potential and broad market prospects, the tertiary industry is emerging sunrise industry, is one of the fastest growing industries at the present stage country and the world's largest development.

Virtual reality tours and attractions and augmented reality is becoming a hot new, unprecedented realism to bring people to experience a sense of virtual reality technology based on digital tourism system. It has the following advantages in system construction, content organization, in the form of service aspects:

(1) gives the same sense of reality.

(2) the use of virtual reality technology, can provide a variety of services for visitors, including tours visual image products, virtual tours, self-guided, self-tours, customized tours, tourism, shopping, travel and other digital entertainment.

(3) provide for the management and decision support functions.

(4) to provide environmental information published tourist attractions, travel emergency assistance, travel route planning and publishing, tourist information and statistical analysis, decision support tourism development and other new digital tours.

(5) large-scale tourism development to environmental pollution, damage is very serious.

2. THE SYSTEM MODEL

The system uses VRML (Virtual Reality Modeling Language) referred to VRML, EAI interface technology and system design and development. EAI defines a VRML browser for Java classes, by EAI establish a link between VRML and the outside world, allowing users to immersive, realized through a browser online virtual tour.

System through VRML nodes and related fields to achieve, including: TouchSensor node, PlaneSensor node, SphereSensor node, CylinderSensor node, ProximitySensor node, Transform node implementations. Each node functions as follows:

Touchsensor node: receiving a mouse click action, starting the corresponding program.

Planesensor node: move the mouse to make the rotation, the formation of a rotating body.

Spheresensor Node: make the mouse to rotate into a rotating body.

Cylindersensor Node: make the mouse into the rotation around the Y axis.

Proximitysensor node: detecting a signal close to the observation point.

Transform Node: Control of linear transformation of the object.

3. THE SYSTEM DESIGN PROCESS TECHNOLOGY ROADMAP.

The main technology routes:

(1). field trips, scenic data acquisition, demand analysis.

(2). data processing, literature review, propose system solutions.

(3). spatial database data store large data platform.

(4). under the number micro-channel public platform, based on the development of micro-channel micro-snow travel sites.

(5). VRML three-dimensional modeling and Java programming.

(6). system testing and rectification.

4. CONCLUSION

The successful development of snow tourism VRML + Java virtual system, proved that the system has real-time, energy-efficient characteristics, stable operation.

5. ACKNOWLEDGEMENTS

This work was financially supported by the Education Department of Hebei Province youth fund project, project number: QN20131148. Hebei Institute of Architectural Engineering School Fund, NO: QN201414, Project Name: Based on the ski slopes of wireless sensor network security key

technology research. Hebei Institute of Architectural Engineering School Fund, NO: ZD201407, Project Name: Campus Card intelligent consumer terminal Key Technology Research. Hebei provincial science and technology plan special work projects, NO: 16236004D-8, Project Name: Tian Road ZhangBei grassland surrounding mountains outdoor tourism micro backpack sites and intelligent search field development. Zhangjiakou City Science and Technology Research and Development projects, NO: 1411052B, Project Name: XE-2000 permanent magnet synchronous wind turbine fault diagnosis and the development of early warning systems.Project of 2016 Science and Technology Program of Zhangjiakou City, NO: 1611059B, Project Name: Research and Development of ZhangBei Ice and Snow 3D Virtual Tour Online Experience System Based on Virtual Reality.

REFERENCES

[1] D.P.Roy,M.A.Wulder,T.R. Loveland,Woodcock C.E,R.G. Allen,M.C. Anderson,D. Helder,J.R. Irons,D.M. Johnson,R. Kennedy,T.A. Scambos,C.B. Schaaf,J.R. Schott,Y. Sheng,E.F.Vermote,A.S. Belward,R. Bindschadler,W.B. Cohen,F. Gao,J.D. Hipple,P. Hostert,J. Huntington,C.O. Justice,A. Kilic,V. Kovalskyy,Z.P. Lee,L. Lymburner,J.G. Masek,J.McCorkel,Y. Shuai,R. Trezza,J. Vogelmann,R.H. Wynne,Z. Zhu. Landsat-8: science and product vision for terrestrial global change research[J]. Remote Sensing of Environment. 2014

[2] Gyanesh Chander, Brian L. Markham,Dennis L. Helder. Summary of current radiometric calibration coefficients for Landsat MSS, TM, ETM+, and EO-1 ALI sensors[J]. Remote Sensing of Environment. 2009 (5)

[3] Blower J.D, Haines K,Santokhee A,Liu C.L. GODIVA2: interactive visualization of environmental data on the Web[J]. Philosophical Transactions of The Royal Society A. 2008 (1890)

[4] Thomas G.Van Niel,Tim R. McVicar,LingTao Li,John C. Gallant,QinKe Yang. The impact of misregistration on SRTM and DEM image differences[J]. Remote Sensing of Environment.2007 (5)

[5] K.G.Nikolakopoulos, E. K. Kamaratakis,N. Chrysoulakis. SRTM vs ASTER elevation products. Comparison for two regions in Crete, Greece[J]. International Journal of Remote Sensing.2006 (21)

[6] Cignoni, F.Ganovelli, E.Gobbetti, F.Marton, F.Ponchio, R . Scopigno. BDAM-Batched Dynamic Adaptive Meshes for High Performance Terrain Visualization[J]. Computer Graphics Forum.2003(3)

[7] Marian Werner.Shuttle Radar Topography Mission (SRTM) Mission Overview[J]. Frequenz. 2001 (3-4)

[8] Przemyslaw Prusinkiewicz.Modeling of spatial structure and development of plants: a review[J]. Scientia Horticulturae. 1998 (1) [9] James H. Clark. Hierarchical geometric models for visible surface algorithms[J]. Communications of the ACM. 1976 (10)

The Research and Design on Smart Home System based on Internet of Things

Fan Jingjing,Zhao Jianguang

Hebei Institute of Architecture and Civil Engineering, Department of Information Engineering

Abstract: In this paper, based on the analysis of the Internet of things and embedded systems, the design and implementation of the intelligent home networking system, focusing on the composition and principle of the system, the test system is stable.
Keywords: Smart Home; IOT; Embedded System

1. INTRODUCTION

Information Age lifestyle is changing the way people live, people put a higher demand for housing. Intelligent Community and the rapid rise in recent years to produce a new type of housing, from its people's lives needs, the integrated use of computer, information, communication, control, science and technology, home intelligent control systems, community information platform, security systems, property management systems and integrated information service system as the basis, using high-tech means to construct service platform to provide security for the residential tenants, environmentally friendly, efficient, comfortable and convenient living space. Visible intelligence community in one of the high-tech people a set of computer, communications, automation and control systems engineering and other settlements, reflecting the progress of human society, the inevitable demand for the development of productivity and knowledge economy era.

2. SMART HOME NETWORKING PART OF THE DESIGN AND IMPLEMENTATION OF PERCEPTION.

Perception part of the wireless sensor node implementations, different nodes according to the needs of different sensors, all the information collected by data transmission via wireless communication. Key design features RFID wireless sensor network nodes, control reader to read RFID tags on objects to achieve intelligent identification, positioning, tracking, monitoring and management (emphasis in design and implementation of district vehicle management system as an example).

Installed on the terminal stores the RFID tag object-related information, the reader for a variety of data and information in real time to take down the object. Being part of a network-aware objects to collect information to complete the analysis of information and decision-making process, and achieve or accomplish a specific task of intelligent applications and services, in order to achieve things and things, recognition and perception of persons and things, to play smart effect.

After specifically reader to read the data terminal, through the various gateways in the network layer transmission object information to the application layer, application layer information can retrieve or update information about an object, the same time, objects and tracking applications, according to the development in the host computer things information system, integrated management of objects in real time. For example, in each home-based home equipment such as: curtains, light bulbs, temperature and humidity, windows and doors controller, gas monitoring, intelligent home appliances etc. installation of smart wireless receiving device 51 as a single-chip controller, embedded intelligent home gateway uses ARM chip as the CPU, unified identification, management in this home all home devices and smart terminals.

3. INTELLIGENT HOME NETWORKING PART OF THE DESIGN AND REALIZATION OF THINGS.

Mainly through the existing products and smart home technology classification analysis, design of each intercommunication intelligent controller protocol and Internet protocol. To provide the necessary networking interface. Specifically, is the software and hardware connection, content and format of exchange of information, mutual control and linkage function between subsystems, each subsystem extension methods and so on. Thus enabling the respective separation equipment, functions and information is integrated into interrelated among the harmonization and coordination of the system, to achieve full sharing of resources and centralized, convenient management. Establish network-based Internet communications management algorithm for multi-task embedded control systems ARM technology, the system has good parallel processing performance, the use of multi-tasking functionality timeshare priority to the thread as a unit in real-time engineering work strong mandate for mission-critical and real-time is not strong non-critical time-sharing parallel processing.

4. CONCLUSION

Practice has proved that this system has real-time, energy-efficient features, can improve the overall level of intelligent management of intelligent home, its security, stability, degree of automation is manual management or close-recognition system can not be

achieved.

5. ACKNOWLEDGEMENTS

This work was financially supported by the Education Department of Hebei Province youth fund project, project number: QN20131148. Hebei Institute of Architectural Engineering School Fund, NO: QN201414, Project Name: Based on the ski slopes of wireless sensor network security key technology research. Hebei Institute of Architectural Engineering School Fund, NO: ZD201407, Project Name: Campus Card intelligent consumer terminal Key Technology Research. Hebei provincial science and technology plan special work projects, NO: 16236004D-8, Project Name: Tian Road ZhangBei grassland surrounding mountains outdoor tourism micro backpack sites and intelligent search field development. Zhangjiakou City Science and Technology Research and Development projects, NO: 1411052B, Project Name: XE-2000 permanent magnet synchronous wind turbine fault diagnosis and the development of early warning systems.Project of 2016 Science and Technology Program of Zhangjiakou City, NO: 1611059B, Project Name: Research and Development of ZhangBei Ice and Snow 3D Virtual Tour Online Experience System Based on Virtual Reality.

REFERENCES

[1] ZigBee Alliance.ZigBee Cluster library specification Wireless Personal Area Networks (WPANs). 2003

[2] ZigBee Alliance.ZigBee Specification. . 2012

[3] Roman Trchalik.ZigBee Gateways. 2006 EEICT 12th Conf .

[4] ZigBee Alliance.ZigBee Home Automation Public Application Profile. . 2012

[5] Shahin Farahani.ZigBee Wireless Networks and Transceivers. . 2008

[6] Texas Instruments. CC2530-ZNP Interface Specification . 2012

[7] CISCO. A Standardized and Flexible IPv6 Architecture for Field Area Networks: Smart-Grid Last-Mile Infrastructure. http://www.cisco.com/web/strategy/docs/energy/ip_arch_sg_wp. pdf . 2014

[8] RFC6282. http://tools.ietf.org/html/rfc6282 .

[9] Tatiana Bokareva, Nirupama Bulusu, Sanjay Jha.SASHA: Toward a Self-Healing Hybrid Sensor Network Architecture. Embedded Networked Sensors, 2005. EmNetS-II. The Second IEEE Workshop. 2005

Innovation and Practice of Cultivating Pattern for Scientific Research Ability of College Students

Chunli Wang[1,], Xiaodong Cai[2], Junli Zhang[1]*

[1] *Institute of Information Technology of Guilin University of Electronic Technology, Guilin, 541004, China*

[2]*School of Information and communication of Guilin University of Electronic Technology, Guilin, 541004,* China

Abstract：The cultivation of scientific research ability plays an important role in training college talents. In the age of big data, firstly the cultivation of scientific research ability starts from information retrieval what is very significant that how to retrieve the most valuable information. Secondly, the practice of scientific research can develop creative ability and innovative ability of college students. It is oriented to the project with tutor responsibility system, scientific research and classroom teaching combined to finish the scientific research training for college students in order to perfect the cultivation system of talents further.

Keywords：Information Retrieval; Research Ability; Talent Training; Tutor Responsibility System

1. INTRODUCTION

With the rapid increasing of knowledge and economy in modern age, international talents competition increasingly severe. The cultivation of high-level talents has become focus of national talent training. Colleges and universities is the cradle of training senior talents as the national reserve base of talent training. Cultivating capable, minded, technical and national development-adapted talents who are not only to possess strong professional knowledge, but also to have a certain scientific research ability. Insisting to the talent training mode of teaching, scientific research and industry-university cooperation to let college students participate in scientific research and practice in enterprises to improve students' scientific research innovation ability effectively. In our country:" The National Medium and long-Term Education Reform and Development Plan Outline (2010-2020) explicit pointed out the educational reform of strategic objectives, "by 2020, our country will achieve educational modernization basically, form learning society basically and become one of the human resources powerful nation." Thus it can be seen that the emphasis of talent training in our country. College students are precious human resources of the national development and national revival. In the era of rapid information development how to cultivate students' scientific research innovation ability is an important goal of talent cultivation in colleges and universities.

Firstly, the analysis of domestic and international research situation to improve college students' research scientific ability.

Organization and functioning of innovation team in colleges and universities mainly rely on key subject and scientific research base. Focus on certain innovative field or direction of major scientific projects in order to implement innovative team plan. Team members are basically constituted of the school or other colleges' related edge discipline with different titles of scientific researchers and graduate students, it shows the characteristics of the academic echelon. The overall goal is mainly to tackle key problems in science and technology. The concrete goal is mainly to obtain the expected results, getting original achievements of independent intellectual property rights, publishing research papers, developing academic communication, integrating the academic echelon and cultivating scientific research talents, etc. According to scientific research and school's developmental needs, innovation teams have various organized modes include: a team whose members are all the same subject or a team with interdisciplinary researchers; a team which consists of our school teachers or consists of the intercollegiate joint researchers; a team with relatively stable research direction and the researchers or a team is able to apply for project continuously. There is also a team with topic and task oriented liquidity.

Secondly, improving college students' scientific ability can enlighten innovative consciousness and stimulate creative thinking.

Innovative ability and innovative consciousness of college students can be greatly improved. Nowadays universities' students have creative consciousness but they are not good at making full use of it and create conditions actively. Their thought is prompt but it is lacked of creative thinking way. They have the creative enthusiasm but they are lacked a wide communication and comprehensive understanding of the society what cause their creative goal is not clear.

By participating in scientific researching projects, it can cultivate students' observation, stimulate students'

creative inspiration, and improve the sensitivity of information. In the process of scientific researching project, it can inspire students' innovation consciousness and stimulate students' creative thinking. It is only the consciousness can dominant the action, so cultivating students' innovation consciousness is the premise of college students to scientific research road.

Thirdly, the path of cultivating college students' scientific research innovation ability.

Improving the innovative ability of undergraduates is an important goal of college education. The participation of scientific research for undergraduate students which played an important role in improving their innovative quality. Forming an innovative team for scientific research is an important path that they participate in scientific research, cultivate innovation ability and practice ability. Rely on scientific research project of teachers and independent research of students, through hierarchical guidance, teaching to their aptitude, effective communication and multilateral incentives which can set up undergraduate scientific research innovative team mode under the guidance of tutor. It can effectively improve the comprehensive quality of students, promote the continuation and development of scientific research projects at the same time and achieve the effect of double harvest in training talents and research.

Improving the scientific research ability of college students must carry on the training of information retrieval.While college students are training in the scientific research that they always need to research materials. Considering on the experience of the predecessors which requires the students must master the effective information retrieval methods and understand their scientific research related database. So when college students are doing scientific research, they must carry on the training of information retrieval together. Teachers of library information retrieval need to be involved in training for students with a period of 24 hours.

2. MAIN CONTENT OF INFORMATION RETRIEVAL

2.1 The use and the retrieval method of periodical network

The main achievements of scientific research usually publish into the relevant article. When a student is looking for materials, you can find related content of your project through the journal net to search including which step you research in present and how to do a further research on the basis of foundation predecessors, etc. Now the nation's largest journal net and the most complete collection of journal net is CNKI. Besides CNKI research related papers, tracking periodical updates and paper submitted, there are translation assistant, reference books, scientific research assistants and standard terminology as many functions, Chinese knowledge network is an necessary resource for scientific research. Secondly, CNKI is still longyuan journal network, wanfang database and weipu news journal of network, these journal nets have their own characteristics. For scientific research, the journal net are complementary. The training for college students of journal net is good for cultivating students' thesis writing ability and base on the results of the integration for scientific research project.

2.2 Search and utilization of electronic books

Each university library can’t book collect all books, it will cause that the library don’t have the book which students need. But college students are required to get it immediately when they are doing the research project, at that time it will play the role in electronic books, the library's electronic resources are tend to buy super digital library, home of digital library e-book database and so on. These use of database requiret within the scope of the campus network, it will be limited to the network occasionally. The scope of the outer network can be used to "China national digital library" to solve urgent problem.

2.3 Retrieval and utilization of teaching video network

When university students are doing scientific research, they often encounter some strange knowledge, school don’t have some relevant courses, if a student only study by carrying textbooks independently which will be time-consuming and laborious. While using the network teaching video to learn the new contents and new knowledge will save time and effort which is the Internet age brings us convenience. There are many teaching video website as long as mastering only 3 or 5 websites that is unlimited. Nowadays moocs are very popular of teaching videos, many universities built moocs websites for students to do self-study. Comprehensive moocs lessons mean to “love lessons” which contains many moocs include video opening courses and resources shared classes freely. It provides a favorable platform for the students' self-study. In addition, the super star teacher pulpit, national library of China and reading show of knowledge base sites also have video teaching content. College students can learn it by themselves according to their own interests to compete the deficiency of class teaching and motivate students learning potential.

2.4 The method of detecting paper similarity

After writing the paper including journal papers and graduate thesis, most of them will have excessive repetitive rate to send it back. Therefore, it’s necessary for students to detect repetitive rate and make related some modification and then summit it. It is good for improving the passing rate. At present we provide three paper similarity detection sites for students, Super Star Found, ten Thousand Database and Weipu Database what all have the function of detecting the paper similarity. While CNKI paper detection is only test relevant department not to do

personal testing. Therefore, similarity detection of CNKI paper is not suitable for a personage to use.

3. FUNCTION AND SIGNIFICANCE OF INFORMATION RETRIEVAL

Information retrieval is the basic methods of college students to acquire knowledge. In modern information age, it is necessary to receive information fast, effectively and accurately, information retrieval technology will play an increasingly important role.

Avoid to duplicated research or delayed, scientific research has the inheritance and continuity, if it isn't do new information retrieval before doing research, and then it will repeat previous work or go a lot of detours. Cultivating students' scientific research ability, it must let them learn information retrieval. Each link of research needs to retrieve the latest information, otherwise the scientific research are empty talk.

Saving time of scientific researcher. Previous researchers always go to library for searching materials which spend a lot of time and the recall rate is low. Today, as long as you master methods of information retrieval which will greatly shorten the time of searching information. The recall rate also can get greatly improve to save a lot of time for the scientific research work and won more time and energy used in scientific research and innovation.

3.1 A short cut to acquire new knowledge

Basic knowledge and professional knowledge of college education is not enough to command the demand of the era of knowledge explosion, cultivating searching talents who must have self-learning ability and independent researching ability in the first place. Mastering the methods of the information retrieval which can help them to become self-taught to find a shortcut to absorb and use new knowledge, it is benefited forever.

3.2 Improve the scientific research ability for college students "tutor responsible system united guidance"mode

Due to the insufficient ability of students themselves and limited by the professional knowledge structure, students are tend to the not equal to their ambition when they engaged in scientific research work especially for independent college students. At the same time, some courses existed many subjects intersected. If it is only guided by one tutor, it will limit the creative thinking of students. Therefore, when guiding students' scientific research activities, in order to support scientific research subject and adhere to the "tutor responsible system, the united guidance" training mode is a kind of ideal model. The pattern is usually consisted of a strong sense of responsibility, high scientific research qualified teachers as project leader who are responsible for arranging scientific research tasks. Corpus mentor can be hold by those intermediate title. During the guidance of process, all tutors can have an opening, topic discussion, concluding and thesis writing to promote each other.

Mentor mainly guide the scientific research consciousness of college students, guiding students how to search the required data and carries on the analysis, sorting and utilization to help students straighten out the whole process of scientific research. Let them know what to do first and what to do after which to make its master the methods of scientific research, and smoothly complete research project research. After mastering the methods of scientific research, it is time to cultivate students' innovation consciousness, and choose those students with great, strong scientific research ability in training mode of deep study. Increasing the difficulty of the research and training surplus strong scientific research team which is a great effect to improve the innovative ability of college student. [2].

3.3 improvement of scientific research ability should be combined with undergraduate courses of college students

Students' professional knowledge basically learned in class of university stage, teachers' scientific research work and the students' scientific research should be trained into the teaching process to change the past simple teaching and question-and-answer method of teaching, teachers can set up relevant problems according to scientific research training in the classroom. Guiding students to think actively and apply their knowledge to scientific research. Let students can solve the problem in the process of dealing with new problem to put forward new problems, new ideas. Teachers should turn passive learning into active learning and encourage students to get out of the classroom and find methods to solve the problem in practice. It can make the students embrace to the forefront of scientific research and academic problems early, it will combine book knowledge and practice together. The innovation ability of students should be comprehensive motivated and maximize their potential. Thus it is useful to cultivate their independent thinking ways and ability of finding, analyzing and dealing with problem.

4. CONCLUSIONS

Transport students to the enterprise for exercising.

In the context of economic globalization, enterprises and universities college-business combined to train together which can achieve the purpose of mutual benefit. Enterprises can make use of the abundant academic resources of high universities to provide tailored talents for the enterprises. Colleges and universities can use high technology enterprise, management, and other resources of enterprises to provide practiced base for universities. It's good for improving students' overall quality and accept corporate culture early and cultivating team spirit of cooperation. In the process of combination between colleges and enterprises, enterprises arrange professional personnel to train for students operating

ability. They can turn the book knowledge into practical ability to lay a solid foundation of theory and practice for the scientific research [4].

The cultivation of the college students' innovation ability is the focus of education in colleges and universities, it is also a long and arduous process. The teacher must pay a certain effort in the process of scientific research to maximize potential of scientific researching students, cultivating their innovation spirit, broadening academic vision, encouraging bold thinking, guiding academic morality and scientific norms. Respecting the students' innovation passion and inspire the innovative motivation. Making a good guidance of students in the way of scientific research. But to cultivate the scientific research ability of college students only rely on teachers' effort is not enough, it needs to get relevant governments to provide encouragement and support in policy, it needs schools to provide strong scientific research platform in scientific research construction. Only when the government, school, teacher and student can work together, it will cultivate a high level of outstanding talents for the society and enhance the core competitiveness of countries[5].

5. ACKNOWLEDGMENT

This work was supported in part by a grant from Guangxi Guilin university of Institute of Information Technology of GUET in higher education of undergraduate course teaching reform project in 2015. "independent college" tutor + subject + students "innovation and practice of college students' scientific research ability training mode" (item number 2015 JGA417). And 2014, Guilin university of electronic science and technology graduate education teaching reform project "based on the collaborative innovation between colleges senior and personal training pattern in the center of the study" (project number YJG201402) which is one of the achievements.

REFERENCES

[1] Sunchao, Wu tianjiao, Chen yuzhe, Guochao, Yuan ming, Practical academic tutorial system cultivating innovative talents , Journal of animal ecology and practices , 2016:90-93.

[2] Zhang bingrong, Songxue, Exploration and practice of cultivating college students' scientific research innovation ability, Modern education management and practices , 2014:71-75.

[3] Li yangfan, Zhu xiaodong, Scientific research training plan and the college students' innovative ability training , Journal of China university teaching, 2011:24-25.

[4] Rao lingping, Hu pu, Hua xiaomei, Combining with the exploration and practice of the personnel training mode between colleges , China power education, 2009, 10:35 - 36.

[5] Yang sheng-xiang, Xi yusong, Training and cultivation of the college students' innovation ability in scientific research practice , Journal of higher education BBS, 2015, 09:57-59.

High Settling Positions Of Pb In Marine Bay Determined By Pb Sources

Dongfang Yang[1,2,3], Fengyou Wang[1,2], Sixi Zhu[1,2], Zhikang Wang[1,2] and Zhenqing Miao[4]

[1]Research Center for Karst Wetland Ecology, Guizhou Minzu University, Guiyang, 550025, China;

[2]College of Chemistry and Environmental Science, Guizhou Minzu University, Guiyang, 550025, China;

[3]North China Sea Environmental Monitoring Center, SOA, Qingdao, 266033, China;

[4]College of Fisheries, Zhejiang Ocean University, Zhoushan, 316022, China.

Abstract: Based on investigation data on Pb in bottom waters in Jiaozhou Bay in April July and October 1986, we analyzed the horizontal distribution of Pb in bottom waters, and reveal the high settling positions and the reasons. Results showed that Pb contents were 11.30-35.42 μg L^{-1}, and were meeting Grade IV in Chinese Sea Water Quality Standard, indicating that bottom waters in this bay had been heavy polluted by Pb. The pollution sources and source strengths of Pb were different in different seasons, leading to the different horizontal distributions and different high settling positions of Pb. Pb was mainly sourced from marine current in April and October, and the high settling position was in the open waters outside the bay mouth. Pb was mainly sourced from rivers in July, and the high settling position was in the inside of the bay mouth. In generally, by means of vertical water's effect, there were high settling processes in different seasons and positions, and the high settling positions were determined by the input of Pb.

Keywords: Pb, Distribution, High settling, Position, Source, Jiaozhou Bay.

1. INTRODUCTION

Pb contents in land, atmosphere, and ocean were increasing due to the rapid development of industry, agriculture and population. Many marine bays had been polluted by Pb finally since ocean was the sink of various pollutants [1-6]. By means of vertical water's effect [7], Pb contents were changing in waters in the bay. Therefore, understanding of the changing processes of Pb in marine bay is essential to environmental protection.

Jiaozhou Bay is a semi-closed bay located in Shandong Province, China. This bay had been polluted by various pollutants including Pb after China's reform and opening-up [1-6]. Based on investigation data in bottom waters in 1986 in this bay, the aim of this paper is to analyze the pollution level, distributions, and transfer processes, and to provide scientific basis for pollution control.

2. MATERIALS AND METHOD

Jiaozhou Bay is located in the south of Shandong Province, eastern China (35°55′-36°18′ N, 120°04′-120°23′ E), which is connected to the Yellow Sea in the south. This bay is a typical of semi-closed bay, and the total area, average water depth and bay mouth width are 446 km^2, 7 m and 3 km, respectively. There are a dozen of rivers, and the majors are Dagu River, Haibo Rriver, Licun Rriver, and Loushan Rriver etc., all of which are seasonal rivers [8-9].

The investigation on Cd in Jiaozhou Bay was carried on in April, July and Pctober 1986 in three investigation sites namely 2031, 2032 and 2033, respectively (Fig. 1). Pb in waters was sampled and monitored follow by National Specification for Marine Monitoring [10].

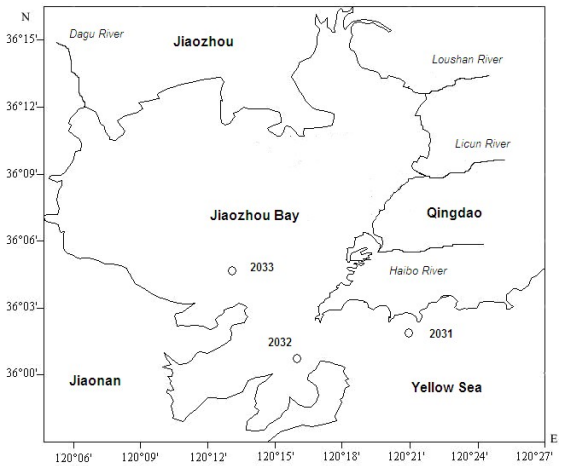

Fig 1 Geographic location and sampling sites in Jiaozhou Bay

3. RESULTS

Contents of Pb in bottom waters. Pb contents in bottom waters in April, July and October 1986 in Jiaozhou Bay were 11.30-18.17 μg L^{-1}, 22.20-34.33 μg L^{-1} and 22.48-35.42 μg L^{-1}, respectively (Table 1). In according to Chinese Sea Water Quality Standard, the pollution level of Pb was Grade IV, indicating that this bay had been heavy polluted by Pb in 1986.

Table 1 Pb contents in bottom waters in Jiaozhou Bay in April, July and October

Month	April	July	October
Content/μg L^{-1}	11.30-18.17	22.20-34.33	22.48-35.42
Grade	IV	IV	IV

Horizontal distributions of Cd in bottom waters. The three sampling Sites of 2031, 2032 and 2033 were located in the open sea, the bay mouth and the inside of the bay mouth, respectively (Fig. 1). In April 1986, high value region was occurring in Site 2031 in the outside of the bay mouth, and the contour lines were parallel and decreasing from the high value center (18.17 μg L^{-1}) to Site 2033 inside of bay (11.30 μg L^{-1}) (Fig. 2). In July 1986, high value region was occurring in Site 2033 inside the bay, and the contour lines were parallel and decreasing from the high value center (34.33μg L^{-1}) to waters inside the bay mouth (22.86 μg L^{-1}) (Fig. 3). In October 1986, high value region was occurring in Site 2031 in the outside of the bay mouth, and the contour lines were parallel and decreasing from the high value center (35.42 μg L^{-1}) to Site 2033 inside of bay (22.48 μg L^{-1}) (Fig. 4).

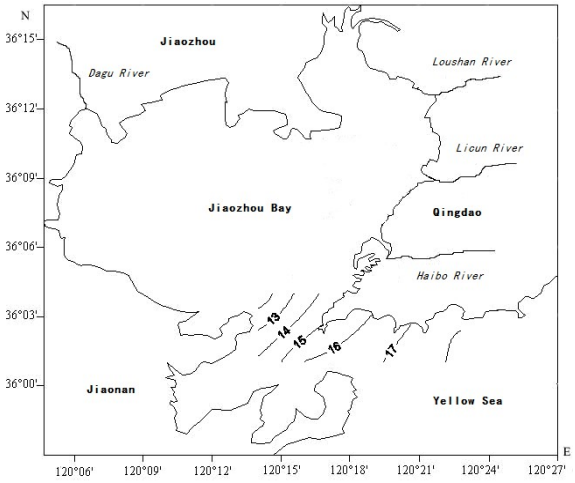

Fig 2 Horizontal distribution of Pb in bottom waters in April 1986/μg L^{-1}

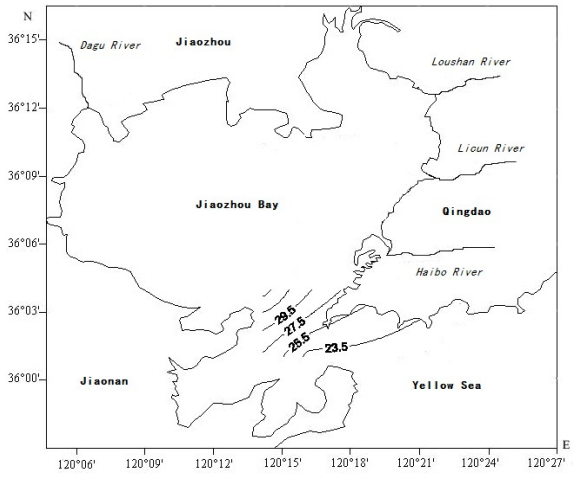

Fig 3 Horizontal distribution of Pb in bottom waters in July 1986/μg L^{-1}

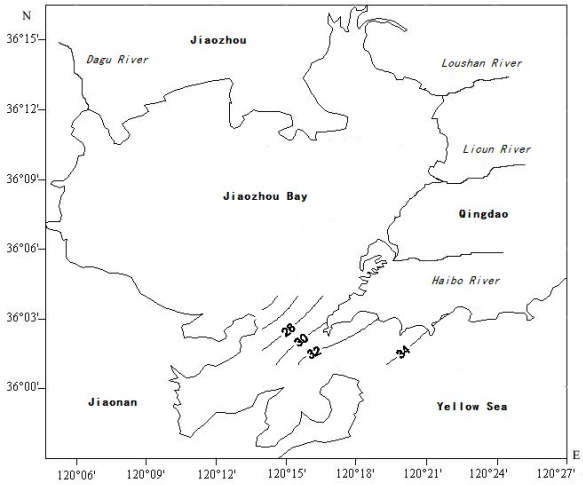

Fig 4 Horizontal distribution of Pb in bottom waters in October1986/μg L^{-1}

4. DISCUSSION

Pollution level of Pb. The major Pb sources in Jiaozhou Bay were stream flow and marine current. Pb was originally transported to surface waters, and then was settled to bottom waters. Hence, by means of vertical water's effect [7], Pb contents in bottom waters were 11.30-35.42 μg L^{-1}, and were meeting Grade IV in Chinese Sea Water Quality Standard. In generally, Jiaozhou Bay had been polluted by Pb since 1986.

Migration process of Pb. By means of the water exchange between the open waters and the bay waters, the contents of the substances in Jiaozhou Bay were decreasing continuously [11]. In April 1986, Pb contents in bottom waters were 11.30-18.17μg L^{-1}, and were decreasing from the open waters to the bay mouth, indicating that there were low settling process inside the bay, yet high settling process outside the bay. In July 1986, Pb contents in bottom waters were 22.20-34.33 μg L^{-1}, and were increasing from the open waters to the bay mouth, indicating that there were low settling process outside the bay, yet high settling process inside the bay. In October 1986, Pb contents in bottom waters were 22.48-35.42 μg L^{-1}, and were decreasing from the open waters to the bay mouth, indicating that there were low settling process inside the bay, yet high settling process outside the bay.

In April and October, Pb was mainly sourced from marine current whose source strength was 25.60-27.40 μg L^{-1}, and Pb contents in bottom waters outside the bay mouth was 11.30-35.42 μg L^{-1}, and the high settling position was in the open waters outside the bay mouth in April and October. In July, Pb was mainly sourced from rivers whose source strength was 25.82-44.12 μg L^{-}, and Pb contents in bottom waters inside the bay mouth was 22.20-34.33 μg L^{-}, and the high settling position was inside the

bay mouth in July. Finally, we revealed the migration process of Pb that in any times, Pb was originally arrived at surface waters, and than was crossing water body and settling to sea bottom by means vertical water's effect. Hence, the high settling position was in the inside of the bay mouth in July. In generally, by means of vertical water's effect, there were high settling processes in different seasons and positions, and the high settling positions were determined by the input of Pb.

5. CONCLUSIONS

Pb contents in bottom waters in April, July and October 1986 in Jiaozhou Bay were 11.30-18.17 μg L^{-1}, 22.20-34.33 μg L^{-1} and 22.48-35.42 μg L^{-1}, respectively, and this bay had been heavy polluted by Pb in 1986. Pb was mainly sourced from marine current in April and October, and the high settling position was outside the bay mouth. Pb was mainly sourced from rivers in July, and the high settling position was inside of the bay mouth.

The migration process of Pb was that in any times Pb was originally arrived at surface waters, and than was crossing water body and settling to sea bottom by means vertical water's effect. In generally, by means of vertical water's effect, there were high settling processes in different seasons and positions, and the high settling positions were determined by the input of Pb.

6. ACKNOWLEDGEMENT

This research was sponsored by Doctoral Degree Construction Library of Guizhou Nationalities University, Education Ministry's New Century Excellent Talents Supporting Plan (NCET-12-0659), the China National Natural Science Foundation (31560107), Major Project of Science and Technology of Guizhou Provincial ([2004]6007-01), Guizhou R&D Program for Social Development ([2014] 3036) and Research Projects of Guizhou Nationalities University ([2014]02), Research Projects of Guizhou Province Ministry of Education (KY [2014] 266), Research Projects of Guizhou Province Ministry of Science and Technology (LH [2014] 7376).

REFERENCES

[1] Yang D F, Su C, Gao Z H, et al.: Chin. J. Oceanol. Limnol., Vol. 26(2008): 296-299.

[2] Yang DF, Guo JH, Zhang YJ, et al.: Journal of Water Resource and Protection, Vol. 3(2011): 41-49.

[3] Yang DF, Zhu SX, Wang FY, et al.: Applied Mechanics and Materials, Vol. 651-653(2014), p. 1419-1422.

[4] Yang DF, Geng X, Chen ST, et al.:Applied Mechanics and Materials, Vol. 651-653 (2014), p. 1216-1219.

[5] Yang DF, Ge HG, Song FM, et al.: Applied Mechanics and Materials, Vol. 651-653 (2014), p. 1492-1495.

[6] Yang DF, Zhu SX, Wang FY, et al.:Applied Mechanics and Materials, Vol.651-653 (2014), p. 1292-1294.

[7] Yang DF, Chen Y, Gao ZH, Zhang J, et al.:Chinese Journal of Oceanology and Limnology, Vol. 23(2005): 72-90.

[8] Yang DF, Wang F, Gao ZH, et al.: Marine Science, Vol. 28 (2004), p.71-74.

[9] State Ocean Administration. The specification for marine monitoring: Beijing, Ocean Precess, (1991).

[10] Yang DF, Wang FY, He HZ, et al.: Proceedings of the 2015 international symposium on computers and informatics, Vol. (2015), p. 2655-2660.

[11] Yang DF, Wang FY, Zhao XL, et al.:Sustainable Energy and Enviroment Protection, Vol. (2015), p. 191-195.

The Impact of Delayed Retirement on China's Employment Market

Hui Huang

Business school, Huanggang Normal University,Hubei,438000,China.

Abstract: As one of the hot topic in today's society, delay retirement problem has been widespread concern. Today, all walks of life to delay the retirement of different views. Supporters stand in the aging population, pension gap etc. analysis showed that the delay retirement can bring many positive effects in these aspects, opponents will mainly focus on the delay argument retirement may give jobs "crowding out effect", especially the negative impact on the employment of young people. Based on the Chinese retirement system and the employment present situation analysis, from two angles and the negative impact of delay retirement on the job market positive effect, a comprehensive analysis of the effect of delay retirement employment effects, and puts forward some suggestions for the related policies China delay retirement system.

Keywords: Delayed retirement, employment, Effect

1. INTRODUCTION

In today's world, population aging is a common problem facing the world, the aging society brings heavy economic burden to support young people, and because of the shortage of young labor, will affect the economic and social development. Since China has been pursuing fewer eugenics of family planning policy, making China's growth the rate has been at a low level, low birth rate and average life expectancy continues to increase, so that our country has earlier entered the aging society. Since 2003, China's GDP growth of nearly 4 times the average annual growth rate of 10.7%, the rapid economic growth and promote the medical and health protection in China development, resulting in China's social population structure has undergone great changes, China has inevitably entered the aging trend of.2010, the sixth national census data show: China's population aged sixty and over accounted for 13.26% of the population aged sixty-five and over accounted for up to 8.87%. Some domestic scholars pointed out: by 2050, our country will face every 100 working age population need to burden 48.5 old people. Zheng Bingwen (social insurance experts, China Latin American Academy of Social Sciences Institute) has pointed out: because of the deepening degree of population aging, China currently has nearly half of the province's pension deficits, personal pension accounts "empty account" more than 1700 billion yuan [1-3]. In order to cope with the aging population economic and financial consequences, looking abroad, many countries have implemented a flexible retirement system to deal with this problem. In our country, whether it should take a flexible retirement system should consider China's basic national conditions.

2. OVERVIEW OF DELAYED RETIREMENT AND EMPLOYMENT

(1) Introduction of China's current retirement system

The current retirement system in China originated from the notice of the financial and Economic Committee of the financial and Economic Committee of the government of the people's Government of China on 1950, This is the first new China with retirement related regulations, then by several times of adjustment, it gradually forming China's retirement system, formed a continuation of the retirement system, provisions of China's current pension system can be divided into age, working conditions, physical conditions, working conditions and working conditions of the residual [4-7]. The title of six categories, each category according to the relevant provisions of the concept can be retired or early retirement or retirement age delay conditions. Specific provisions are as follows:

(2) Current retirement policy in foreign countries

At present, the world has entered the aging society in 68 countries and regions. In order to cope with the aging of the population to reduce the supply of labor, pension deficits, dependency ratio of population increase and other issues, many foreign countries have taken some measures, of which the most important is to adjust the retirement policy. Here in several typical countries as examples to illustrate [7].

U.S.A: Since 1983, the United States began to develop. The United States adopted a retirement policy setting method of elastic retirement age to minimize delay retirement to various economic and social impact. In 2003, 65 years of age for employees, the government decided to extend their retirement age of two months; in 2004 four month extension and so on; until, extended to 67 years, so that people have enough time to adjust.

France: The current statutory retirement age for male and female workers, for 60 years.2010 years, in the economic crisis, the aging of the population, the unemployment rate rising under the pressure of reform, the French government began to implement progressive retirement policy. The specific measures

are: the completion of the retirement age from 60 years to 62 years of delay in 2018, according to the every 4 month extension rate of gradual reform, in order to alleviate the pressure and reduce government pension payments to extend the retirement effect. At the same time, the French have to pay full social contribution to the French government in forty-one years and three months to retire in gold and receive a full pension after retirement.

Table 1 Chinese retirement conditions

Age condition	Male cadres and male workers no difference, 60 years of age to retire, Female cadres and female workers differences, female cadres over 55 years of age, female workers over 50 years of age to retire.
Length of service	Cadres and workers, whether it is a normal retirement or early retirement, must work for 10 years before they meet the conditions, but the number of cadres is to participate in the work of life, workers are calculated by the continuous length of service.
health condition	Working life of 10 years, the hospital proved to be completely lost the ability to work, men and women over 50 years of age, the full age of female cadres can be retired in advance; Continuous service for 10 years, in addition to the hospital certificate, must be confirmed by the labor appraisal committee completely lost the ability to work, male workers over 50 years of age, female workers over 55 years of age can pressure for early retirement.
work - related injuries	After the hospital confirmed that cadres, workers proved by the hospital and the labor appraisal committee, completely lost the ability to work, no age, work experience and continuous service restrictions apply for early retirement pressure.
working condition	In the body the loss of heavy labor workers, men over 55 years of age, women over 45 years of age, and over 10 years of continuous service, can the pressure for early retirement.
Title Condition	A few senior experts need to work in the consent of the person, according to the cadre management authority by the appointment and removal authority approval, may be appropriate to extend the retirement age. Associate Professor, Associate Research Institute and senior professional titles at the same level, not more than 65 years old; Professor, senior researcher and expert level with the title of the longest pressure does not exceed 70 years.

Japan: Japanese pension age is 60 years old, so Japan's retirement age is 60 years old. But as Japan entered the aging society, in order to guarantee the balance of pension, in 2004 the Japanese government requirements before the year 2013 completion of the extension of the retirement age, to extend the requirements will receive the pension age to 65, but the adjustment period of male and women are different. Therefore, the present stage of Japan's statutory retirement age is 65 years old.

Britain: The current retirement policy is: 65 year old male, female 60 years old.2006 years the British government released a report on the reform of the endowment insurance system of the project, according to the content of the program me, in 2024 the British government will put Britain the retirement age is extended to 66 years, the retirement age for men and women; and finally in 2044 to extend at the age of 68.

Other countries have begun to gradually implement the extension of retirement age programs, such as Germany, Brazil.2011, Germany's legal retirement age has reached 67 years old.2003 years, Brazil will be the retirement age from 55 years old to 60 years of age.

(3) Comparison of domestic and foreign retirement policies

Compared with the foreign policy of retirement, the current retirement policy in China has the following problems:

a. the retirement age is low

With the rapid development of economy and society, the life expectancy of the population is increasing, the length of education is prolonged, which is not matched with the current retirement age of our country, and it appears that the current retirement age is low.

There is no doubt that the new China to now, China's average life expectancy of the population in the rapid growth. According to the Chinese statistical yearbook data shows: 2000-2010 years, China's average life expectancy of male population growth from 69.63 years to 72.38 years of age, women's average life expectancy from 73.33 years old to 77.37 years old ten years of growth. The average life expectancy in the continue to improve, and improve the speed of the male female, improve the life expectancy of the population slowly. Compared to other developed countries is also growing, and most countries have been or are ready to adjust the retirement policy, along with our country still 1993 retirement policy, there is no reform.

With the education of young people in our country to continue to extend, if not adjust the retirement policy will make the human capital investment is long and short payback period, resulting in a waste of human resources, and to dispel people's enthusiasm for investment in human capital.

b. large differences in retirement population

Gender differences and identity differences are the main differences in retirement age.

For developed countries, the retirement age for men and women is the biggest difference of 5 years old, and their minimum retirement age is 60. In our

country, and the retirement age of workers was 10 years old. The retirement age for men and women the gap is too large, the retirement age for women is low makes women work less, not conducive to full play female workers, especially the role of female workers with higher education, makes people more reluctant to female human capital investment. Therefore, in order to adapt to the changing development of the laws of nature and society, should adjust the retirement policy. In addition to gender differences, the differences of status is China's current retirement policy problems. There are differences the retirement age between workers and cadres is not reasonable. So, our retirement age should be how to adjust? Of course cannot be directly modeled by some developed countries' efforts, we should be based on China's current retirement age to adjust the retirement age, the development of the retirement policy is not only to meet the requirements of China's current stage and can be suitable for future development.

3. ANALYSIS ON THE IMPACT OF DELAYED RETIREMENT ON EMPLOYMENT

(1) The positive impact

a. Increase labor supply, ease the shortage of labor

The sixth national census data show that China's population aged 60 and above accounted for 65, 13.26% years of age and more than 8 of the population accounted for 87%. Early in the second national census data show that China is the world's only elderly population over countries. Today, China's population aging intensifies, "silver wave" has been sweeping the country. China's implementation of family planning has been for several years, has been in the control of population growth, which makes the new population to reduce the number of labor can not be replenished. After the aging of the population, followed by a serious shortage of labor. Zheng Bingwen, director of the world social security research center of Chinese Academy of Social Sciences, also said that the aging population means increasing burden on the elderly, but also means that the reduction of labor input. The total working age population in China will be reduced from 970 million in 2010 to 870 million in 2050. Quantitative and technical economics China Academy of Social Sciences analysis room director Li Jun said, is expected to 2050, China's 15 year old to 59 year old working age population will decline to 710 million, less than in 2010 about 230 million people.2030 years later, China's labor supply will be seriously inadequate.

In the long term, China's aging population, China's first time facing the demographic dividend disappeared, the process will experience a serious shortage of manpower. The delay retirement age from the increase in the elderly workers working life and reduce the number of workers to leave the two to solve the overall labor shortage, and increase the supply of labor, alleviate the labor force lack of status. In the world, countries facing labor shortage problem of aging caused by impact, is usually taken to extend retirement age to solve. Experience shows that this is an effective way to solve the problem of insufficient labor.

b. To promote the accumulation of human capital and make full use

Human capital (Human Capital) refers to the workers by education, training, experience, migration, health care and other aspects of the investment and accumulation of knowledge and skills acquired knowledge and skills. This can bring benefits to its wages, thus forming a specific capital. Delayed retirement age has a significant impact on human capital accumulation delay retirement age can increase the working life of the future, it will affect the workers on human capital investment decision. Human capital theory, knowledge and skills of workers in the structure of human capital is the most important part of the knowledge and skills are gained through education and training, personal education investment decision is a return the education cost analysis based on the growth of [[16]. years of working experience, education investment income will be extended, which will extend the workers human capital to stimulate investment, promote workers to increase Education, improve their level of education, increase the professional, practical experience of training, these are conducive to the accumulation of human capital of workers.

Delay retirement age to make full use of human capital has a positive impact to extend our average life expectancy, social average years of education and improve the average level of education to improve the quality of workers, education level has improved significantly. To enhance the utilization of human capital to explain life after moves. If you do not consider the actual situation of China's labor force. In accordance with the statutory retirement age limit for workers, will cause a lot of waste of human resources. At the same time, older workers in the same industry, the same post has accumulated rich experience, if they will continue to work in companies will bring great benefits, but also can save the training for the new employees. The cost of delay retirement the age of older workers can make full use of waste heat of the body, promote the effective utilization of human capital.

(2) The negative impact

a. Delay the retirement age will squeeze unemployed employment, the employment problem has become more and more serious

The employment problem has always been in China in recent years in efforts to solve the important problems of.2010 years of the government work report, Premier Wen Jiabao called the employment priority is to protect and improve people's livelihood, points out the severe employment situation, the work can not have the slightest slack, we will continue to

implement a proactive employment policy, the central government will invest 43 billion 300 million yuan for the promotion of employment. Report of the eighteenth National Congress of the Communist Party of China pointed out that employment is the basis of people's livelihood. To implement the strategy of giving priority to employment and a more active employment policy to do youth employment and the transfer of rural labor force to focus on college graduates, the urban poor, veterans' employment of labor force in China. In recent years the oversupply of university enrollment in recent years, the delay retirement age for unemployed workers to enter the labor market will bring more difficult to have a greater negative impact. Based on this situation, any action that may have a negative impact on employment will be infinitely magnified. Many researchers believe that the delay retirement age in the labor market will have a crowding out effect, crowding out labor jobs, the employment problems of unemployed workers are more serious.

b. Squeeze the unemployed jobs, especially young labor

Delay retirement age makes the original statutory retirement age of workers to continue in the job, it will have a crowding out effect, crowding the unemployed workers jobs. Some researchers believe that the delay retirement age will not occupy youth jobs, because the elderly retired and vacated positions for young workers are not necessarily appropriate. However, the delay retirement age although treatment industry did not have direct effect but still indirect squeeze, squeeze out the unemployed jobs. Because while young and old labor labor does not necessarily exist direct substitutes, but indirect substitution relationship exists. Reach the legal age of older workers back body quit work, although there may be no suitable substitute to young workers, but his job can have a certain work experience to share; and have some work experience one vacant post, can by the young labor force to share. In real work, the majority of enterprises can not be selected to meet the requirements of the staff, most of the selection mechanism is based on the concept and principles to carry out a person job match.

c. To make old workers at a disadvantage.

At present, China's workforce is approaching retirement transition and transition generation. With the continuous reform, the development of modern industry, the emergence of high-end industry, professional phenomenon, elderly labor has been unable to meet the enterprise more and more high requirements. Due to historical reasons, the old labor endowments, human capital investment, innovation ability, new skills have compared to the overall young workers are at a disadvantage, which makes them at a competitive disadvantage in the labor market. In our country, the aging labor education level is generally low, compared with the young labor force. So far, the old workers compete with young workers in the workplace is in a weak position. Once to extend the retirement age, it will aggravate the disadvantage of old workers, so that they fall into a more competitive disadvantage. Furthermore, China's labor force is brought in a large proportion of city process of rural labor force, and they are mostly engaged in heavy physical labor. This part of the labor force into old age, physical condition as before, it is difficult to engage before work. Delayed retirement age on the part of labor force is completely will make them into one disaster after another. The more a disadvantage.

d. Invisible employment dominance

Our current retirement age is the last century follows the basic provisions of 50s. With the rapid development of economy and society, now the retirement age reveals many problems. The retirement age is low, the retirement age differences and early retirement problem is most prominent. A series of problems inevitably in the retired population in many of the "retired" phenomenon. This kind of person is nominally retired, but continues to hold jobs, not for the unemployed for jobs. In addition, the legal retirement age of workers in terms of employment has a special advantage, that employers continue to employ do not need to pay a large number of social insurance costs, you can save a lot of labor costs for enterprises. The "incentive mechanism", is bound to exacerbate the "retired" phenomenon. Many early retirement staff actually did not really drop out of the workforce, delay retirement age is only the dominance of hidden employment. So, "returned without" retirement, only a nominal retirement, they are still in on the job, to make explicit the hidden employment effects of delay retirement age.

4. CONCLUSION

a. Proposed progressive retirement system

Although the long delayed retirement on employment is not affected, but the short-term impact is still not to be ignored, so it is necessary to avoid, as far as possible in the process of implementation, reduce its positive impact on employment, the best way is to implement a progressive retirement system. That year the retirement 6 months, every two years to extend the retirement program for 1 years, through reasoning and analysis, the employment impact of new employment population is very large. Therefore, in order to avoid the impact of reduced employment, a year extension of time as short as possible, but not too short, too short to solve the problem of employment, pension payment the population aging problem, but can not be eliminated. Therefore, in the process of progressive retirement, the gradual progress of the interval to be too large, it is recommended to 2-3 months each year for the best, the longest do not exceed 6 months.

b. Proposed flexible retirement system

Our current retirement system is too rigid, without

considering the average number of years of education extension, increase the cost of human capital reality. Make full use of rigid rules to reach the statutory retirement age of retirement must not conducive to human resources. But the provisions of the statutory retirement age is too high, in some ways it is not conducive to the early work of the laborers, the nature of the work on one hand they decided their larger body loss, on the other hand due to manual workers general education is short, see the earlier work, will delay the retirement age, extra loss of their bodies. Therefore, the delay in the retirement age can not engage in one size fits all, and should establish a flexible two sets of retirement provisions.

c. Supporting a reasonable population policy

Reasonable population policy is a prerequisite for the healthy development of a country's economy. The impact of family planning policy on Chinese population at the same time, the economic Chinese no trivial matter, also played a certain role. However, the current economic development in Chinese compared to twentieth Century has been a qualitative leap, today's situation is different from the time, so at that time the population policy in some areas is not suitable to now. The family planning policy in line with national conditions Chinese in early development, but now the population is no longer China pressure factors of economic development, so the family planning policy should be given some reform, because if you continue to implement strict birth control policies, will reduce the birth rate will weaken the delay retirement policy effect. After the adjustment of the policy should be in line with the current situation of China, improve the China population structure, the current China Economy plays a role in promoting.

REFERENCES

[1] AnderwA Samwick. New evidence on pensions, social security, and the timing of retirement. Journal of Public Economics . 1998

[2] Axel Brsch-Supan. Incentive effects of social study on labor force participation: evidence in Germany and across Europe. Journal of Public Economics . 2000

[3] OECD."Increasing Employment: The Role of Later Retirement". OECD Economic Outlook . 2002

[4] Queisser, M, E. Whitehouse." Neutral or Fair Actuarial Concepts and Pension-System Design.". Social, Employment and Migration Working Paper, No.40 . 2006

[5] Romain, Duval."Retirement Behaviors in OECD Countries: Impact of Old-age Pension Schemes and Other Social Transfer Programs.". OECD Economic Studies . 2003

[6] Matthew Flynn. Who would delay retirement? Typologies of older workers. Personnel Review. 2010 (3)

[7] Terry A. Beehr, Sharon Glazer, Norma L. Nielson, Suzanne J. Farmer. Work and Non-work Predictors of Employees' Retirement Ages. Journal of Vocational Behavior . 2000 (2)

Research on the Present Situation and Improvement of the Public Participation in Air Pollution Control - Taking Anshan as an Example

Wu Tingting[1], Zhao Liling[2],Zhu Yingming[3]

[1] School of economics and law, University of Science and Technology Liaoning, Anshan, Liaoning, China

[2] Civil three Court, Anshan MTR Eastern District People's court, Anshan, Liaoning, China

[3] Zhongshan Environmental Protection Bureau Dalian branch, Dalian, Liaoning, China

Abstract: In response to the fog and haze, improve air quality, the government of Liaoning Province, the implementation of the blue sky project in Liaoning province. As a key demonstration city, Anshan has achieved initial success, but in the process of development, there are still some problems to be solved, one of which is public participation. Under this background, this paper takes Anshan city of Liaoning Province as the study area, through the analysis of the present situation of air pollution in Anshan City, investigation and summary of air pollution control in the degree of public participation, analyzes the reasons, and puts forward specific measures to improve public participation in air pollution control.

Keyword: Air pollution; Public participation; Way

1. INTRODUCTION

The new "environmental protection law", "air ten" in 2014 and “air pollution prevention law has amended and promulgated”in 2016, in highly stressed the importance of air pollution prevention and control law, requiring local should be based on their characteristics and the system of prevention and control of atmospheric pollution on the basis of the status quo, to revise and improve the relevant system area. This paper tries to sum up the Anshan City air pollution control in the degree of public participation on the basis of the actual research and analysis, summarized the reasons, finally put forward specific measures and suggestions to improve public participation in air pollution control, this will not only promote the innovation of public participation mechanism in the field of air pollution control, give full play to the initiative of the public, at the same time in order to provide a new way for the government to control air pollution, to achieve the prevention and control of atmospheric pollution in "good governance" to provide targeted countermeasures.II.

2. The explanation of the basic theory of public participation

2.1Meaning of public participation

Public participation refers to the social behavior of the people, organizations, units or individuals as the main body, in accordance with the rights and obligations that they enjoy. Including the participation of the subject, the scope of participation and participation in the way. The environmental law system of public participation in the public and its representatives according to the national environmental legal rights of participation in environmental protection system, the government or the environmental protection administrative departments rely on the public's wisdom and strength, environmental policy, laws and regulations, determine the development of construction project system, but also should include damage to the citizen or organization environment public environmental rights or interests, and participation in environmental protection by law to request relief and compensation behavior.

2.2 The scope of public participation

The scope of public participation can be studied from two aspects of horizontal and vertical. From the horizontal perspective, it should include the public's right to know, the right to express the public's desire, the public's right to supervise the public, the public's right to question, the public's right to litigation, etc.. From the longitudinal perspective, the scope of public participation should include four processes: the plan stage participation, the process participation, the end participation and the behavior participation.

2.3 The mode of Public participation

The way of public participation, including two ways: direct participation and indirect participation. Direct participation is the direct participation of the public in the form of individual social affairs management, directly express their wishes, interests and aspirations. Indirect participation is the indirect expression of their own interests and opinions by means of Representatives and organizations. The specific methods include: questionnaire survey, visit, held a

forum, hearing, argumentation, public opinion, hire supervisors, etc.

3. Typical examples of foreign public participation in air pollution control

Since the beginning of the industrial revolution, developed countries have experienced the first pollution, after the treatment of environmental protection on the road, although the economy has made tremendous gains, but the environment has paid a painful price. Old industrial countries in the UK, due to sulfur dioxide, soot and other excessive emissions, London was once a "death"; the United States has also experienced the bitter experience of atmospheric pollution. As one of the developed countries of Japan, in the process of the blind pursuit of rapid economic development has not spared, "yokkaichiasthma incident" became Japan's century of war.

However, after the air pollution control Shushiji years, London had taken off the fog hat, the United States and Japan's air quality has also improved significantly, the basic control of air pollution. In this paper, according to Britain and the United States and Japan environmental protection development and achievements, summarize the management experience, and provide reference for air pollution control in China, so that we avoid the old road of the developed country, and the vision of exploration for air pollution control in China road.

3.1 BRITAIN

On the one hand, the London smog incident broke out, the British Parliament started the legislative process, which lasted three years, in 1956 enacted the world's first air pollution prevention and control law, "Clean Air Act", the law must shut down coal-fired power plants in London City; designated non-smoking area, prohibit the use of smoke in the non-smoking area in fuel; in order to reduce coal consumption, large-scale transformation of city residents traditional stoves, and actively promote the use of natural gas. Then has promulgated the "air pollution control act", the cap on the industrial fuel sulfur is clearly defined; "environmental law" for the first time asked the government to formulate the national air quality strategy. Revised "air quality strategy", added to the PM2.5 (can be inhaled particulate matter) monitoring requirements. On the other hand, the active participation of all the people in the United kingdom. British universities, environmental organizations and the media to actively participate in the governance of air pollution, the force can not be ignored. All is the air pollution control practitioner. Private enterprises are also actively involved in the improvement of air environment action. In Britain today, environmental protection has become a way of life, King's College London launched a "London air" mobile phone software, on the basis of in the Greater London area 100 observation station monitoring data, free of charge to the user push London air quality, urged the public to live greener life.

3.2 U.S.A

Since the event of photochemical smog in Losangeles, the United States introduced and implemented a series of laws and regulations to encourage public participation, so that the air quality has been significantly improved. First of all, through the development of laws, strict standards. In 1955, the United States introduced the "air pollution control law" to provide technical support for local control of air pollution. 1963 "clean air law" for the first time said: "air pollution is a national issue across the region", "air quality control law" division of air quality control area. In 1970 the United States Congress passed the landmark clean air law, set up the environmental protection department, greatly strengthened the government's rights and responsibilities. Second, the use of market mechanisms to control pollution. As the air pollution control measures become more and more economical for industrial enterprises, the environmental protection department cited the market regulation mechanism, which will be divided into a number of units according to the area of the plant, each year on the various units

An annual reduction of emissions, emissions below the prescribed amount of the plant can be no "use" of the discharge amount of the market transactions, the supply of those who did not complete the plant emission reduction targets. The more factory emissions, the more profitable in the trading market. The government only needs to monitor the total emissions of the region, the mechanism not only effectively supervise the plant emissions reduction work, but also encourage factories to improve production technology and equipment to reduce emissions. Finally, pay great attention to the public participation. Losangeles smog incident, the air pollution has aroused public concern, to promote the vigorous development of environmental protection movement, more and more people to participate in environmental protection activities. Even the attention of the air pollution and the action taken to become an important standard to measure the outstanding people of Losangeles. In addition, the United States Environmental Protection Agency in order to let the public know the air quality at any time, a special website, as long as the public access to the site to enter the address of the zip code, you can find the day of air quality.

3.3JAPAN

The government through the review mechanism, the hearing system to encourage people to express their views before the environmental laws and regulations, policies, planning process and major environmental action, at each stage of large-scale construction project bidding procedures, actively arrange seminars, public hearings, airing the way to listen to the views of residents, in order to minimize the risk of decision.

In addition, citizen participation in environmental protection is more reflected in the behavior of participation, according to a survey, most people travel to consciously take public transportation, even the public polished stone in the decoration of houses, will also be a person with the vacuum bag in the grinding machine, to prevent dust into the air.

To sum up the experience of the management of air pollution in the developed countries, the state attaches great importance to environmental legislation, and gradually improve the environmental legal system, according to the law is the basis of the legitimate and reasonable management of air pollution. From the history of national atmospheric pollution, that we can not ignore the power of the public. Each of us is a manufacturer of air pollution, and actively participate in and enjoy the environmental right is also so as to solve the problems of air pollution also requires each of us so we say that the public is the basic power of the prevention and control of atmospheric pollution. The improvement of the quality of the atmosphere environment, both need to be determined by the government to develop and implement relevant policies, strict management, and actively promote innovation in the field of science and technology, but also need to establish and improve the public participation system. In raising public awareness of environmental protection and legal awareness, while giving the public environmental protection participation right, the right to know the environmental information, environmental public interest litigation, etc., and effectively make the public to participate in environmental protection.

4. Nvestigation and existing problems of public participation in air pollution control in Anshan City

4.1 Investigation on the current situation of the public participation in air pollution control in Anshan

From the Anshan Municipal Environmental Protection Bureau survey, the current atmospheric pollutants in Anshan is mainly sulfur dioxide, soot, dust.

Mainly from industrial pollution sources, mobile pollution sources, urban dust, pollution sources and other pollution sources, etc.. Anshan, as one of the 113 key cities nationwide environmental monitoring, Liaoning blue sky project focused on the city, the Anshan municipal government has taken a series of measures to promote public participation in the construction of atmospheric governance.

The air pollution index (API) is a method of reflection and evaluation of air quality, the air pollutant concentration of several routine monitoring is simplified as a single concept refers to the numerical form, and fractionation of air pollution and air quality. The classification of air pollution index is detailed in table.

TABLE 1 Air pollution index range and the corresponding air quality level

Air pollution index（API）	Air quality level	Air quality status
0-50	I	excellent
51-100	II	good
101-150	III1	Slight pollution
151-200	III2	Slight pollution
201-250	IV1	Moderate pollution
251-300	IV2	Moderate heavy pollution
301-350	V	Heavy pollution

TABLE2 Statistical table of air quality level during the period of "12th Five-Year" in Anshan City

Grade	I	II	III	IV	V	Better than II days	API	Air quality level	Primary pollutant
2011	13	224	99	18	6	237	82	II	PM10
2012	11	218	103	21	7	229	80	II	PM10
2013	10	195	123	24	8	205	91	II	PM10
2014	12	198	132	12	6	210	90	II	PM10
2015	14	219	100	22	5	233	87	II	PM10

1) Institutional settings

Anshan City Environmental Protection Bureau in order to protect the public's right to know the environmental information, since 2013 to increase the publicity of information, mainly reflected in the following aspects:

First of all, in order to make the people of Anshan city in a timely manner to understand the quality of air environment in Anshan information, Anshan monitoring station and Anshan city gas.Like the Bureau in Anshan television, radio, Internet and other media published on the same day, the next day forecast.And the next 72 hours Anshan city environmental air quality forecast, the establishment of environmental quality forecasting and early warning system.

Secondly, the implementation of the construction project environmental impact assessment document

approval information publicity system. Anshan Municipal Environmental Protection Bureau. January 1, 2014 onwards, to further standardize the acceptance of the EIA approval publicity, publicity, including the name of the project. Construction site, the date of acceptance, real-time service status, etc., while for the convenience of public access to the annex. The full text of the EIA document publicity. The implementation of this system has not only improved the information disclosure system of eia,. At the same time effectively protect the public interest, to further improve the environmental information disclosure.

Finally, improve the environmental supervision system. Anshan Municipal Environmental Protection Bureau in a timely release of the official website of the project sewage charges, corporate sewage.Status, and other environmental information, environmental information, regularly publish air quality rankings, and the implementation of the mandatory disclosure of environmental information for key enterprises system, in order to protect the people's right to know.

2) Environmental publicity

Anshan City Environmental Protection Bureau has a publicity Center, is responsible for environmental protection publicity and education work. Make full use of all kinds of media, and actively promote the work of environmental protection, construction, guidance, valuable advice, information, information. At the same time, Anshan city center actively cooperate with the community to actively carry out the green community building activities. In the community to set up environmental protection propaganda window, to promote environmental protection knowledge, to save energy, water, and other environmental protection act vigorously promote, promote resource recycling. Regular environmental science and technology seminars, to explain the daily life of the small common sense of environmental protection.

3) Public participation channels

Anshan Municipal Environmental Protection Bureau has 12369 environmental hotline, convenient for the public to report all kinds of environmental pollution or ecological damage events at the same time, the Anshan Municipal Environmental Protection Bureau website has a public interactive column, for public reaction to events timely reply.

The survey shows that as the environmental authorities in Anshan, the Anshan Municipal Environmental Protection Bureau attaches great importance to the public power in environmental protection, actively engaged in environmental publicity work, also in public efforts to gradually increase the environmental information, through the creation of environmental protection hotline, the website opened public opinion feedback column actively listen to the voice of the public, but in the the survey also learned that in the Anshan area is almost the end of the relief of public participation, participation in the plan is only present in environmental impact assessment, and public participation in environmental impact assessment in the "Questionnaire" in the form of ordinary citizens to participate in the "hearing", "demonstration" will be less and less.

4.2 Existing problems

Through the analysis and summary of the information collected by the field survey, the problems of the public in the air pollution control in Anshan include:

1) Environmental awareness is weak, the low participation of public welfare activities.

Public awareness of environmental protection is relatively weak, and put into action the environmental behavior is less and less. The survey found that the residents of the degree of education and environmental awareness is proportional, and the environmental satisfaction is inversely proportional to. Among them, the higher the degree of public education, the greater awareness of the seriousness of the problem of air pollution, environmental awareness, and the worse the satisfaction of environmental conditions.

2) Much of the public participation in the end relief is involved, has not yet penetrated into the prevention of participation and participation in the process".

Most respondents said that only in the enterprise excessive emissions behavior in conflict with their own interests, will report or complain. And eighty percent of respondents said that the construction of major construction projects in Anshan area, and did not seek their own views, but not heard of and participated in the environmental impact assessment and environmental protection hearings. It is not difficult to see that this end relief to participate fully exposed the weak awareness of the public in Anshan, it is bound to greatly reduce the public participation in the influence of air pollution control.

3) Civil environmental protection organizations are weak

China's environmental protection NGO from its inception to now, the change is happening. The garbage from planting, bird watching, to "the development planning in offerwords"; from "turn tail man" to "in the interests of the group asked the game for the right to know, the right of discourse". This allows us to see the role of them in the field of environmental protection. However, in the harvest gratifying results at the same time, we also find that the real influence of environmental protection: NGO is very few, there are many disadvantages of the current development of environmental protection NGO. Its main manifestations are: limited quantity, serious shortage of funds, and the public's trust in environmental organizations.

4) Enterprises lack the sense of social responsibility and participation

Enterprises are the major contributors to air pollution,

this should take the responsibility of the main force of air pollution control. Status of air pollution in Chifeng area: the investigation is still a "government single center" governance model, this should take the main responsibility of enterprise pollution and no positive move, at least not "active" move. This thing in the governance of air pollution, the government and enterprises has been in a "guerrilla warfare" state for a long time, the government policy tightening, enterprises will put out pollution response style; government policy has slowed down, enterprises for pollution control. The study found: many enterprises to reduce production costs, many environmental protection equipment in the production process only acts as a "decoration", in an idle state, only to deal with the higher check the time to open.

5) The absence of existing public participation system

Read the laws and regulations of environmental protection in China, although there are relevant provisions on the principle of public participation. However, there are many defects, the concept of "public" is not clear. General concept refers to the relative official people, and those who are more involved in environmental protection conditions and the ability of the group of the "public" excluded from participation in eligibility. The most prominent problem is:

First, the lack of operational principles of public participation. At present in our country, it is too much emphasis on the participation principle. Public participation mechanism is not perfect, the way of participation, methods, channels and other procedures are not clear, not specific. So when citizens in the face of specific environmental issues, citizens do not know what way to participate in, and even some citizens in order to cause the government to pay attention to the problem of illegal means to solve the problem.

Secondly, the public access to environmental information of a single channel. Information disclosure is the prerequisite and basis for effective public participation, it is also the basic guarantee of the public's right to know, "measures for the disclosure of environmental information (Trial)" although there are on the "public information", but for the species, the extent of the information disclosure without specific requirements. Therefore, in practice, a lot of projects carried out, are in the surrounding public has not been informed of the situation, it has been approved and started.

Again, the public expression system is low. In the current legal system of our country, the implementation of the people's Congress system and the political consultation system. Representatives of the public election, during the meeting, through the NPC deputies or CPPCC members to reflect the aspirations and wishes of the public. In addition, the expression of public opinion expression mechanism is not perfect, bottom-up and low communication system.

Finally, the lack of judicial protection system. The judicial protection of public participation is the final remedy umbrella, however due to the lack of judicial protection system of public participation in environmental protection activities, the public participation in the destruction and hinder, hamper for public participation in environmental protection, personal sanctions are not clear.

5. Countermeasures and suggestions on improving public participation in air pollution control

5. 1 Raising awareness of environmental protection of citizens' atmosphere

To sum up the practical experience of the management of air pollution in the developed countries, and to the public participation. The basis of public participation is the improvement of environmental awareness. The survey shows that: the overall level of public awareness of environmental protection in Anshan area is low. People call for improvement in the atmospheric environment, behavior and performance is too cold. Complaining about the phenomenon of more and less knowledge and less knowledge is widespread. Therefore, to enhance public awareness of the environment has no time to delay. Raising awareness of environmental protection is a long-term and arduous task, and it must be realized in many ways.

On the one hand, it shall determine the public's environmental rights and the status of the specific content through legislative means, let citizens know that they have more rights, will arouse their attention to environmental problems, and actively join in environmental protection consciousness.

On the other hand, should actively promote environmental publicity and education activities environmental publicity and education is an important way to improve citizen awareness of environmental protection, but also determine the extent and depth of citizen participation.

5.2 Increase environmental organizations to participate in the intensity of air pollution control

The government should increase efforts to foster environmental protection organizations. Environmental protection organization is engaged in social welfare undertakings, is to share the responsibility for the government, so the government should support the development of environmental protection organizations, increase support efforts.

On the one hand, it should be appropriate to relax the conditions for the establishment of environmental protection organizations. Modify the "dual management system" of the current "single management system", in order to avoid administrative departments when swaying, passing each other. In the amount of funds, the number of members, etc., to relax the requirements of the establishment.

On the other hand, the government has given financial support. The government should provide direct financial support, the establishment of government funding mechanism for environmental organizations, such as the annual budgeting, governments at all levels according to their actual situation, the environmental protection organization funding included in the government fiscal expenditure year.

5.3 Establish and perfect the laws and regulations of the public to participate in the management of air pollution

Anshan Municipal Environmental Protection Bureau has 12369 environmental hotline, convenient for the public to report all kinds of environmental pollution or ecological damage events at the same time, the Anshan Municipal Environmental Protection Bureau website has a public interactive column, for public reaction to events timely reply.

The survey shows that as the environmental authorities in Anshan, the Anshan Municipal Environmental Protection Bureau attaches great importance to the public power in environmental protection, actively engaged in environmental publicity work, also in public efforts to gradually increase the environmental information, through the creation of envi. In addition, people's awareness of the damage caused by pollution also requires a long process, so the extension of the statute of limitations is extremely important.

1) Establish procedure law to determine the mechanism of public participation in the whole process

The existing public participation system in our country pays more attention to the following: after the pollution incident, it is allowed to carry out the inspection.The "end" of a complaint or an accusation ". And environmental problems such as air pollution can be passed through the public.Public participation in decision-making in advance to prevent the. If a citizen is only involved in the pollution control after the pollution incident.In theory, it is bound to increase the cost of governance. From an economic point of view, such a system is not scientific, should be given.Improve, establish "plan participation", "participation in the process" and "end to participate in" as one of the whole process of participation.System and realize the good governance of environmental management".

2) Establish a smooth flow of information feedback channels

On the one hand, through the news media to understand the new environmental policy, new initiatives to share the success of environmental governance case,

To provide new ways and methods of environmental governance, but also to strengthen the typical set of negative environment, the destruction of the environment

Individuals, units, organizations should be exposed; the government regularly publish environmental bulletin, bulletin, guide the public attention to environmental issues, the establishment of a public crisis on the environment, and urge the public to take action, and actively participate in environmental protection. Can also be through the hotline, the public mailbox, to facilitate the public to reflect the problem at the fastest speed to investigate, to solve.

On the other hand, improve the interactive mechanism to enhance the interactive effect

The promotion of the interactive effect of the government and the people is not only reflected in the increase in the number of public participation, but also reflected in the feedback efficiency and quality of government departments. Establish and improve the interaction mechanism, the implementation of the responsibility of the government departments responsible for communicating with the public. The implementation of the accountability system, urging its active participation in the government and the public interaction, to avoid the emergence of a question and answer, and without reason, and so on.

3) Establishment of environmental public interest litigation system

Environmental public interest litigation is a lawsuit brought by a legal person, a natural person or a social organization to a people's court for the maintenance of the public interest. Although the current law of our country has already made clear regulations on environmental public interest litigation, there are some relevant judicial interpretations, but there are still a lot of problems in practice. Lead to the public can not effectively protect their own environmental rights and interests. Specifically, it should also relax the plaintiff's prosecution qualifications. Appropriate extension of the prescription of action. At present, China's environmental litigation prescription for 3 years, the longest period of not more than 20 years. The environmental damage with the potential of some pollutants, long, and will not produce immediate damage effect, it needs to pass through the migration, transformation and enrichment of a series of links, can lead to the fact that the damage occurred. In addition, people's awareness of the damage caused by pollution also requires a long process, so the extension of the statute of limitations is extremely important.

4) Improve the incentive mechanism

Should be implemented to encourage the public to actively participate in the incentive measures for air pollution control, the government should give incentives to the public in the air pollution control, thereby encouraging them to actively participate in the governance of atmospheric pollution. Evaluation of clear public rewarded conditions and standards, by which the level of incentives and rewards, to establish a complete evaluation system, incentives to develop application, review, evaluation, and other

relevant details published issued by the program, thus reducing the award review process subjective.

6. CONCLUSIONS

This paper is on the basis of public participation of a large number of relevant theoretical research, summarizes the successful experience of developed countries for air pollution control, combined with the present situation of air pollution in Anshan City, air pollution control model is still the "government leading" management mode. Non governmental organizations, citizens in the air pollution control in the presence of a strong dependence on psychology, participation is not high. In this paper, we put forward a model of air pollution control in the "government market society", and analyze the feasibility of the model. Study on the public participation in air pollution control in Anshan. Finally, improve the public air pollution prevention and control countermeasures and suggestions, namely: participation to improve citizen awareness of environmental protection; emphasize the importance of environmental NGO in the environmental protection; to develop the whole process of the participation of the public participation mechanism, perfecting the laws and regulations of public participation in environmental protection.

7. ACKNOWLEDGEMENTS

[1]Anshan social science research key topic in 2016, the project name: "blue sky project" in the background of the Anshan air pollution prevention and control of the legal research, the subject number: as20162048.

[2] University of Science and Technology Liaoning Youth Fund Project in 2016, the project name: Public participation in air pollution prevention and control in Anshan city.

REFERENCES

[1] Li Qing ping. The new development of environmental law and the interaction between control and democracy [M], People's court press, 2006:39.

[2] Wang Qun, Tan Jiangtao. Another "invisible hand" Ostrom Eleanor and the "multi center" theory, Journal of Opening times, 2010.06.

[3] Liu Jianzhen, Crack public participation problems to promote air pollution control, Environmental protection, 2013.11.

[4] Wang Qun, Tan Jiangtao. Another invisible hand, Eleanor Ostrom and the "multi center" theory, 2010, (06):140 ~ 150.

[5] Yu cheng. Some problems on constructing environmental public interest litigation system, modern law. 2004, (03):157 ~ 161.

A Novel Coarse-grained Parallel Evolutionary Algorithm for Intrusion Detection

Xuan Li[1], GuanYu Hu[2]*
[1]Science and Technology on Information Systems Engineering Laboratory, National University of Defense Technology, Changsha; 410073, China;
[2]School of Information Science and Technology, HaiNan Normal University, Haikou, 571158, China

Abstract: An coarse-grained embarrassingly parallel evolutionary algorithm—Solution Genetic Evolution Algorithm (SGEA) has been designed and its effectiveness has been tested. In traditional evolutionary algorithms, such as Genetic Algorithm, solutions of a problem are treated as chromosomes; and the genes of the chromosome are the components of the solutions. while in SEGA, we go one level deeper—that solutions are treated as genes inside chromosomes, while nucleotides inside genes are the components of the solutions. The solution genes are classified in accordance with the subspace of the solution space, each sub-space is a class of proteins, and a solution gene belongs to a particular type of protein. The concept of multi-level populations on the basis of the different classes of proteins in the sub-space is also created. SGEA is very suitable for parallel computing, because of its individual independent of each other, and the calculation process is coarse-grained. SGEA also solves problems of genes expression and internal information flow, it separates the functional significance and position of the genes. We have chosen some parallel test cases to evaluate SGEA in a cluster instead of BBOB. The results show that, SGEA is super-linear performance, and it has a good global search capability and fast computation capability in reasonable times. In a test using Intrusion Detection with KDD'99 dataset, the experimental results show that SGEA has increased total detection rate, and proves its practicality.
Keywords: Solution Genetic Evolution Algorithm, internal information flow, bad gene, good gene, Learning-operator, similar genetic cluster

1. INTRODUCTION

Evolutionary algorithms are random search methodologies, which inspired by Darwin's theory of evolution. They solve optimization problems by simulating the process of biological evolution. Evolutionary Algorithms are algorithm clusters; including genetic algorithms, evolutionary program design, evolutionary programming, and evolutionary strategies. Genetic Algorithm (GA), proposed by Holland in 1975 [1], has been one of widely used evolutionary algorithms. GA turns the solution into individual (chromosome) by encoding, and uses selection, crossover and mutation operations to find out the optimal solution. The characteristics of the genetic algorithm do not dependent on the inherent nature of the problem solving, do not require differentiable of optimization functions. (GA has implicit parallelism, but its local search capability is not good, evolutionary will be premature [2].)

Currently, the researches of the Evolutionary Algorithms focus on two areas: applications and theories. In applications, it is used to solve combinatorial optimization problems [3-6] initially, and it has applied to a number of areas now: automatic control, multi-objective function optimization, engineering design, Bio-engineering and economic fields, etc.

In theory researches, scholars have been focused on enhancing local search ability and improving its evolution premature phenomenon. Cloned environment evolution operator and adaptive exploration operator were introduced [7] to improve GA's global search ability. And an improved crossover operation was proposed [8] to improve the efficiency of GA crossover operation and improve GA's convergence. Some scholars have designed a genetic algorithm use multiple of population [9-14], and they also considered other intelligent algorithms which can applied to the genetic algorithm [15-16]. Kargupta and Goldberg proposed a gene expression genetic algorithm (GEGA) [17] in 1998.The algorithm mentioned: in natural evolution, the flow of information mainly through two channels, external information flow (transmission of genetic information in the iterative process of evolution) and internal information flow (internal expression of genetic information). At present, most of evolutionary algorithms only use external information flow, such as genetic algorithm selection, crossover and mutation operations, while the internal flow of information is rarely utilized. GEGA emphasizes the role of gene expression; this helps to retain the body's inherent genetic characteristics. There are some algorithms that focus on the evolution of the internal flow of information, for example, Gene Handling Genetic Arithmetic (GHGA) [18]. We believe that the recently proposed optimization algorithms based on membrane computing also contain the evolution of the internal flow of information, (see ref. [19] and [20]), which genetic operation is assumed to be carried out within the cell membrane. With the development of computing power and cluster

technology, the parallel evolutionary algorithms get more and more attention and has greatly development, parallel evolutionary algorithm can improve the diversity of population and greatly reduce the computation time. There are three main types of parallel evolutionary algorithms [21]: master-slave model, fine-grained model, and coarse-grained model. Above all, we propose and design a new parallel evolutionary algorithm: Solution Gene Evolution Algorithm (SGEA), to better utilize the gene expression and the internal flow of information. It is well known that genes consist of specific nucleotide sequences that contain the genetic information in DNA or RNA molecules. And genes express their own genetic information by the synthesis of proteins, thus genetic information is passed to the next generation in macroscopic characters, and in this process chromosomes are the carriers of the genetic information. In traditional GA, chromosomes correspond to potential solutions of a problem to be solved; its genes are the components of the solution after encoding. Then it uses the selection, crossover and mutation operations to search the optimal solution. However, in the crossover-operation, swapping genes is to swap solution components essentially, this causes each new individual after cross appear anywhere randomly in the solution space, so the each new individual does not inherit any of the characteristics of their parents. The same problem also appeared in the mutation operation, mutated individuals have no apparent connection with parents. The individual's genes do not express the characteristics of solving the problem in traditional genetic algorithm, thus the full advantages of evolution is not utilized.

In this paper, we are attempting to create an coarse-grained embarrassingly parallel evolutionary algorithm, its individual's genes can express the genetic characteristics, establish the connection of parents and new individual. In this algorithm, the genes are classified in accordance with the sub-space (we call the proteins), and use the number of the good genes and the bad genes to reflect the individual's overall fitness; the essence of Solution Genetic Evolution Algorithm. Inspired by the quotient space [22], we establish the concept of multi-level populations in SGEA. The solution genes that belong to same class of proteins are called the similar genetic clusters; we use the Learning-operator in the similar genetic clusters, to enhance the ability of local search. Both the individuals and the multi-level populations of SGEA are distributed in the node of cluster. Several well-known test cases are chosen to test SGEA and to compare it with some traditional algorithm. The results of the test show that the algorithm has improved performance compared to the tested traditional algorithms; and exhibits some advantages in practical applications.

The paper is organized as follows. In Section 2, we will introduce Solution Genetic Evolution Algorithm (following abbreviated as SGEA). In Section 3, we will describe the specific operation of SGEA. Learning-operator and the Multi-level populations will be demonstrated in this Section, too. In Section 4, we will exam and compare the difference between SGEA and Multi-group Genetic Algorithm. Finally, in Section 5 and Section 6, we design the process and the parallel computing of the algorithm. In Section 7, we analyzed the simulation results of the experiments.

2. THE BASIC PRINCIPLES OF SGEA

In SGEA, genes, not chromosomes, are treated as solutions, which can be represented by their fitness values; the space coordinates of solutions are the nucleotides that constitute a gene, and a chromosome is an individual that composed by a number of solution genes, its three-dimensional shape as shown in Fig.1. Fig.1 illustrates a three-dimensional fitness landscape, its two-dimensional solution space is divided into a number of blocks, each block represents a class of proteins, potential solutions in a block is called solution gene, the coordinates that constitute a solution gene called nucleotides, the fitness value of solution gene is called a protein.Obviously, the similar proteins formed by different genes in the same block can have different fitness values to determine their quality, good or bad. This is like a gene which synthesize a part of the organism are also better or worse.The chromosome consists of a number of solution genes, so that parents characteristics can be inherited to the new individual, as shown in Fig.2.

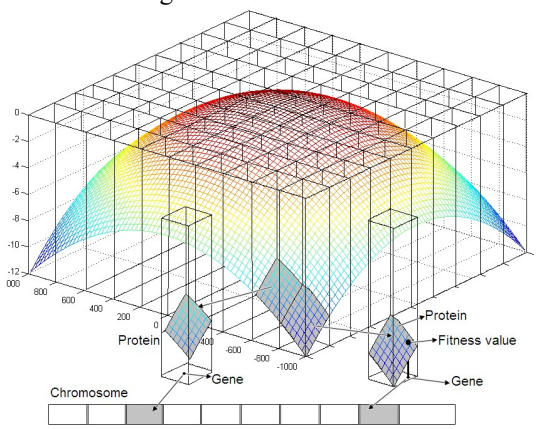

Figure 1 The three-dimensional shape of SGEA

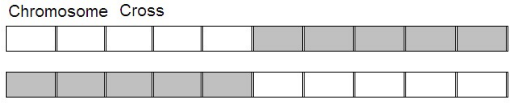

Figure 2 The chromosome cross

Fig.2 describes the crossover-operation between two chromosomes, where each of the gene blocks is a solution. The child generation will inherit parent's protein information. In this way, the chromosome constituted by solution genes can be seen as an individual constituted by a number of proteins, the genetic operators operating on the potential solution

set of the problem, rather than merely changing the location of the individual. Individual's advantages or disadvantages no longer depend on the fitness value, rather on the average merits of multiple proteins which constitute its own.

3. THE OPERATORS OF SGEA

3.1 Selection-operator

The chromosomes that carry a lot of solution genes cannot be able to describe by a fitness value, we use smooth fitness value instead:

$$\overline{f}_i = \sum_{i=1}^{n} f_i / n \tag{1}$$

(1) is the average fitness value of i-th chromosome, n is the number of proteins.

$$\overline{\overline{f}}_i = \overline{f}_i \times \alpha + f_{i,\min} \times (1-\alpha) \tag{2}$$

(2) is the smooth fitness value of i-th chromosome, where α is a coefficient. The smooth fitness values represent the individual's ability to adapt, taking into account the average evolution and partial evolution, reflect the evolutionary direction of the individual (solving the minimum, for example). For similar proteins (same subspace of the solution space), a gene is marked as a bad gene, if it is the worst among all the similar genes, or a good gene, if it is the best. Sometimes, a genetic defect in a biological body will lead to lower its survival chance or, in some cases pre-mature death, so in SGEA if the numbers of unqualified genes are excessive, the chance of being eliminated in the selection-operation will increase, even if its smooth fitness value is excellent, this cannot be done in a simple genetic algorithm. In referencing RED (Internet router congestion algorithm), we set the selection probability P_i as follows:

$$\overline{\overline{f}}_i^{'} = 1 / \overline{\overline{f}}_i \tag{3}$$

$$PS_{i,temp} = \overline{\overline{f}}_i^{'} / \sum_{j=1}^{m} \overline{\overline{f}}_j^{'} \tag{4}$$

(4) is the temporarily selected probability of i-th chromosome, m is the number of individuals.

$$PS_i = PS_{i,temp} / (1 + count_i \times PS_{i,temp} - count`_i \times PS_{i,temp}) \tag{5}$$

Count $_i$ is the number of bad genes of i-th chromosome, count`$_i$ is the number of good genes of i-th chromosome.

3.2 Crossover-operator

Crossover-operation exchanges part of specific genes between two chromosomes based on a probability. We use the single-point crossover to random pairing of individuals, and randomly set the location of the crossing points in this paper. The crossover operation in SGEA is the same as traditional genetic algorithm, except that the concept of gene. In addition, similar to the selection operation, we consider a chromosome's adaptability as the crossover probability, each chromosome will be given a crossover probability, to simulate excellent individual of the nature can get more mating, so for those chromosomes who have experienced the Selection-operator have to compete for mating rights. Selection probability indicates the individual's adaptability: we use it to indicate a cross-probability:

$$PC_i = PS_i \tag{6}$$

Individuals who have larger crossover probability will first choose the better individual to cross, until all individual cross finished or only one individual remains un-crossed. In the traditional genetic algorithm, there is only one crossover probability, it controls the number of the times of crossing, chromosomes are randomly selected to perform cross. Crossover probability of enhanced algorithm in this paper represents the ability of individual mating, the cross will become more directly and more purposeful, which is also in agreement with the idea of directed evolution in GGA. Its essence is filtered random evolution in nature, directly to the target of evolution. Fig. 3 describes the vertical comparison of genes, and takes the number of bad genes and good genes in the similar protein to the factor of Selection-operator and Crossover-operator.

3.3 Mutation-operator

The Selection-operator and Crossover-operator mentioned above do not change the solution's position in space, genes in SGEA need to have mutation as an individual in traditional genetic algorithm. The Mutation-operator in SGEA is identical with the traditional Genetic Algorithm, both of them are change the component of gene based on a probability, but mutation operation in SGEA only be confined to the sub-space.

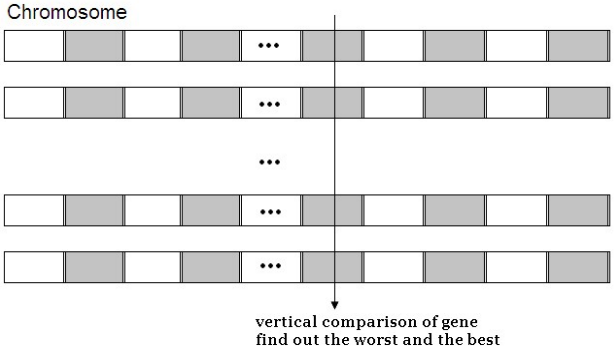

Figure 3 vertical comparison of genes

3.4 Learning-operator

Learning-operator means to learn from the good genes among the similar genetic clusters. When each time SGEA selects a good gene of a class of protein, the others will move closer to the good genes. Because the component of gene in traditional algorithm does not contain the genetic characteristics, therefore Learning-operator is not suitable for traditional algorithm. SGEA provides us with a new understanding of the population genetic algorithm, the range of the population can be multi-angles, multi-levels, as shown in Figure 4, 5,and 6.

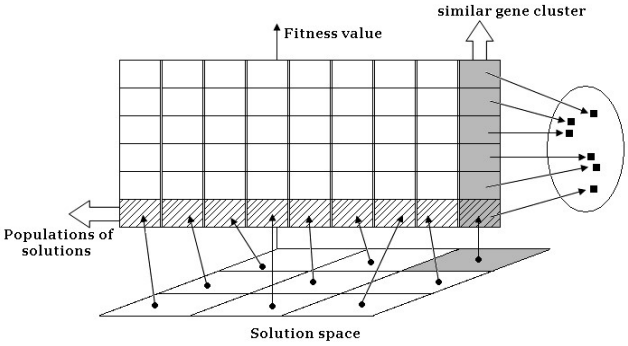

Figure 4 multi-level populations and the similar genetic cluster

Fig. 4 describes multi-level populations in SGEA. In the specific realization, the population that constituted by individuals in SGEA is as a cell array, the internal element is a solution of the solution space. Each line constituted a population of solutions whose solution was distributed in the different class of proteins (sub-space). Each column constituted the similar genetic clusters whose solutions are distributed in the same class of proteins (sub-spaces).

Fig. 5 describes the crossover operation in the populations of solutions, each grid represents a sub-space of the solution space. The genetic operation in the population of solutions is coarse-grained, this operation which exchange a lot of solution gene randomly is similar to the individual migration between populations of GA.

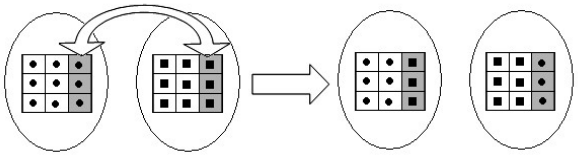

Figure 5 The Crossover-operator in the population of solutions

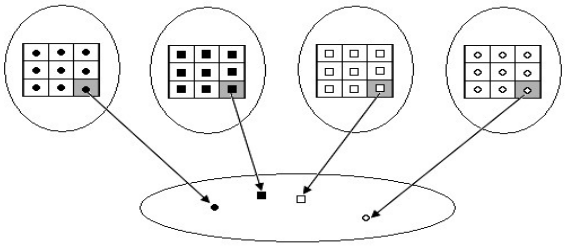

Figure 6 The learning operation in the similar gene cluster

Fig. 6 describes the process that different solutions in same subspace constituted the similar genetic cluster. The internal of the similar gene cluster can perform fine-grained operation.

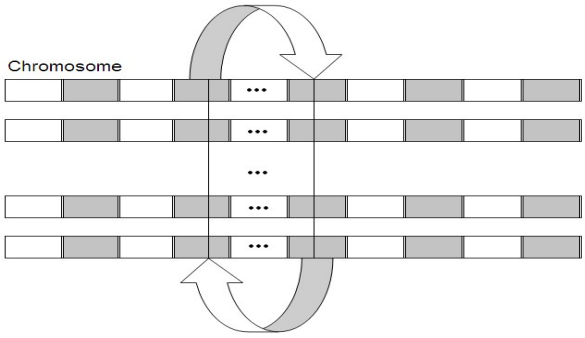

Figure 7 Swap-gene-operator

In short, Learning-operator is carried out inside the similar genetic clusters, its purpose is fine tuning of the optimal solution, enhances its local search capabilities of the algorithm. The solutions of the similar genetic clusters come from the same sub-space, but belong to different individuals; it is not only involved in the operations of the genetic algorithm, but also participates in Learning-operator of similar genetic clusters. We can complete the learning process by some populations algorithm, such as CMA-ES etc., but each iteration only executed once. Because the other operations are not changed to the individuals of the similar gene cluster except mutation-operator, so algorithm is having continuity in the similar genetic clusters.

3.5 Swap-gene-operator

Swap-gene-operator refers to the overall sequence swap of genes between two similar gene clusters, such as shown in Fig. 7.Fig..7 illustrates the gene swap process of Swap gene-operator, exchange probability is referred to Pe. Although the position of a gene in chromosomes is not important, Swap-gene-operator will give crossover-operator of next generation to different states. Swap-gene-operator must change the whole column location of a gene in given chromosomes as shown in Figure 7, otherwise, if a similar genetic cluster is out of order, it will be difficult to find the number of good or bad genes. The functional significance and the position of the gene is independent of each other [23], for example, the genes that controlled skin growth do not have any effect on the heart, traditional genetic algorithms do not have such distinction. The structure of the encoded string has important influence on the individual's fitness value.

4. SGEA and Multi-population Genetic Algorithm

SGEA seems to be similar to the Multi-population Genetic Algorithm, but the former as the solution to the gene, some solutions constitute individuals; the latter as the solution to the individuals, some individuals constitute the population, both have the essential difference. In recent years, along with the development of parallel distributed processing technologies, many Multi-population Genetic Algorithm (MPGA) models are developed [9, 10, 11]. In MPGA individuals are divided into several sub-populations, genetic operation is carried out

independently in each sub-population, and allow individuals to migrate between sub-populations. The creative migration path was designed between sub-populations, including how to determine the migration path between populations, migration frequency, selection mechanism, alternative strategies and so on. [12, 13, 14] Recently, Membrane Optimization Algorithm that based on Membrane Computing [24] is also reported, which resembles MPGA, In Membrane Optimization Algorithm, the population is divided into several membranes which use different internal optimization algorithm and independent evolution. There will be communication strategy between the membrane [25, 26].The chromosomes in SGEA are the same as sub-populations of MPGA, but different from MPGA and its variants. The potential solution is seen as a complete individual's gene in SGEA, the major differences between SGEA and Multi-population Genetic Algorithm are as follows:

(1) The solution is as genes in SGEA, genetic operation is completed on population level;

(2) Probability of selection is determined by the smooth fitness value and the number of the bad gene in SGEA;

(3) Exchange solution in crossover-operation of SGEA, crossover probability is determined by the number of good genes;

(4) The genes that constitute individual of SGEA are limited in the sub-space. Each sub-space is seen as a protein;

(5) SGEA possesses Multi-level populations, the similar genetic clusters and unique Learning-operator.

5. Flow SGEA

In general, we simplify the operating environment of SGEA; we assume that the solution space is two-dimensional, which is easy to divide into subspaces. In the complex multi-dimensional environments, such as the Intrusion Detection, we use the space partitioning method or only split one dimension. The design process of the SGEA is as follows:

(1) Initialization protein: split the solution space;

(2) Generate individuals: generate a solution randomly in each sub-space, these solutions constitute an individual;

(3) Generate individuals until the requirements are met;

(4) All individuals constitute a cellular array;

(5) Calculate the fitness value of each gene, and generate a fitness value matrix;

(6) Calculate the number of bad genes and the number of good genes of each individual;

(7) Calculate the average fitness value and the smooth fitness value of each chromosome;

(8) Start the genetic operations: Selection-operator; Crossover-operator; Mutation-operator; Learning-operator; Swap-gene-operator.

(9) Achieve the required solution to stop evolution.

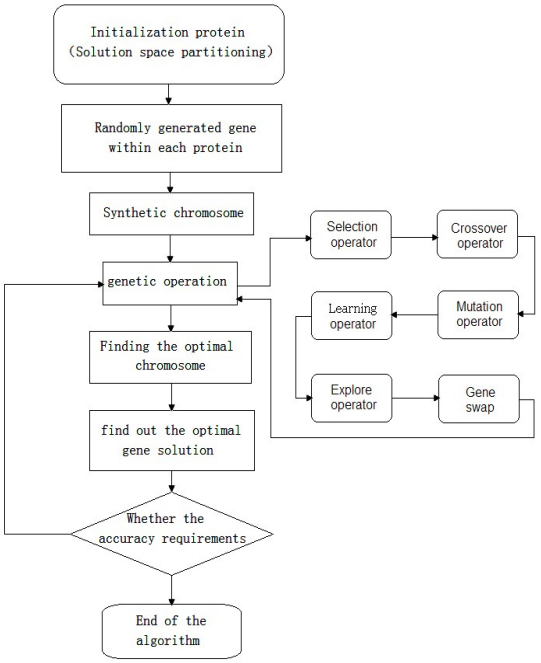

Figure 8 The process flow of SGEA

Fig. 8 illustrates the process of SGEA. The genetic operation loop of SGEA with the Learning-operator, runs within each sub-space in each iteration.

6. THE PARALLEL COMPUTING OF SGEA

6.1 Parallel environment

SGEA needs more solutions during the evolutionary process, it will increase the quantity and the time of computation. So in SGEA, the individuals and the operators are distributed in the node of cluster, in order to make up for the shortcomings of the running time. SGEA uses the MATLAB parallel toolkit as the operating environment, and we built a LAN cluster which include 45 nodes, each worker node uses the PC which CPU is AMD Sempron Processor 3000+ 1.16GHz, 1GB memory. Master node uses the Server which CPU is Intel Core i7-3632QM 2.2GHz, 8GB memory, as shown in Fig.9.The master node plays two roles: job manager and client. Client run the main program. Job manager assigns specific tasks to the worker, and collects the result of each worker. The task of job manager is as follows:(1) Initialization parameters; (2) Generate initial individuals; (3) Passing the parameters and initial individuals to the worker; (4) Receiving the new individuals and its fitness value; (5) Select the best individual. The worker task is as follows: (1) Receiving the parameters and initial individuals from master; (2) perform specific operations; (3) Generate new individuals; (4) Calculate the fitness value; (5) Passing new individuals and its fitness value to the master. In the process above, communication between worker and master occurs only once in a generation, most of the calculations concentrated in workers. So SGEA is a coarse-grained embarrassingly parallel evolutionary algorithm.

6.2 Parallel testing

There are many standard to test the parallel

evolutionary algorithm [27]: run time, cost of optimizing, operating rate of evaluation function, and speed-up. Traditional speedup is defined as [21]:

$$S_n = \frac{T_1}{T_n} \quad (7)$$

T_1 is the longest run time of the best serial optimization algorithm, T_n is the longest run time of the parallel optimization algorithm in n processors. We use the formal weak speedup [28] instead: compared with the serial and parallel time of the same algorithm, its percentage is:

$$\eta_n = \frac{S_n}{n} \times 100\% \quad (8)$$

We test the formal weak speedup of SGEA with many functions in different dimensions. 10 dimensions as an example, the formal weak speedup is 124.2516%, more than 100%, the result is [29] super-linear performance.

7. CASE STUDY

To further test the algorithm effect in high dimension practical applications, we chose the Intrusion Detection with KDD'99 dataset to test the SGEA, and compared detection rate, false negative and false positive with other algorithms. Using BP neural network as the classifier, which have 56 parameters, the test equivalent to 56 dimensions optimization, the results are shown in Table 1.

8. SUMMARY

Potential solutions are treated like genes of an individual in SGEA, and each gene is classified as protein (sub-space); genetic operations are completed in solutions of the population. Select-operator screens solutions of the population, Crossover-operator exchanges solutions of the population. In comparing to Multi-population Genetic Algorithm, SGEA puts forward multi-level populations, and the similar genetic clusters, as well as the Learning-operator and many other operators. SGEA solves the problem of gene expression and internal information flow. Evaluation results of selected cases show that SGEA has a good global search capability; and it can quickly find the global optimum with Learning-operator. SGEA has improved performance on most test cases. In addition, in complex optimization problems, such as IDS, SGEA shows good performance. However, the search accuracy of SGEA is not as good as we expected in the significantly perturbed functions (e.g., Ackley function).SGEA is more suitable for parallel computing environments because of space segmentation and multi-level populations; we will further study in the realization of SGEA in the parallel environment. Further improvement and theoretical support of SGEA will be the focus of future work

.

Hostname	Reachable	Cores	Status	Up Since	Name	Count
CHINA-7B2FF53B5 (192.168.8.254)	yes	1	running	2013-10-12 08:39	JM	0
Dell	yes	4	running	2013-10-12 12:36		4
worker1 (192.168.8.27)	yes	1	running	2006-01-02 11:44		1
worker10 (192.168.8.156)	yes	1	running	2006-01-01 22:46		1
worker100 (192.168.8.100)	yes	1	running	2006-01-01 21:47		1
worker101 (192.168.8.101)	yes	1	running	2013-10-12 14:04		1
worker11 (192.168.8.157)	yes	1	running	2006-01-02 03:58		1
worker12 (192.168.8.158)	yes	1	running	2006-01-01 13:12		1
worker13 (192.168.8.159)	yes	1	running	2006-01-01 22:17		1

Name	Hostname	Status	Up Since	Workers
JM	CHINA-7B2FF53B5	running	2013-10-12 08:38	45

Worker				MJS		
Name	Hostname	Status	Up Since	Connection	Name	Hostname
worker11_worker01	worker11	idle	2006-01-02 03:57	connected	JM	CHINA-7B2FF53B5
worker12_worker01	worker12	idle	2006-01-01 13:15	connected	JM	CHINA-7B2FF53B5
worker13_worker01	worker13	idle	2006-01-01 22:15	connected	JM	CHINA-7B2FF53B5
worker15_worker01	worker15	idle	2006-01-01 20:48	connected	JM	CHINA-7B2FF53B5
worker16_worker01	worker16	idle	2006-01-02 02:39	connected	JM	CHINA-7B2FF53B5
worker17_worker01	worker17	idle	2006-01-02 03:30	connected	JM	CHINA-7B2FF53B5
worker18_worker01	worker18	idle	2006-01-02 04:29	connected	JM	CHINA-7B2FF53B5
worker19_worker01	worker19	idle	2006-01-02 09:33	connected	JM	CHINA-7B2FF53B5
worker1_worker01	worker1	idle	2006-01-02 11:42	connected	JM	CHINA-7B2FF53B5
worker20_worker01	worker20	idle	2006-01-02 04:41	connected	JM	CHINA-7B2FF53B5
worker21_worker01	worker21	idle	2006-01-02 04:30	connected	JM	CHINA-7B2FF53B5

Figure 9 The process flow

Table 1 The rate of False Negative and the False Positive of IDS with various algorithms

Attack / Algorithm	%	Total	Normal	Dos	Probe	R2L	U2R

BP	DR	90	97.45	98.93	83.50	49.89	33.33
	FN	7.82	0	1.07	16.50	50.11	66.67
	FP	2.18	2.55	0	0	0	0
GA-BP	DR	89.91	97.30	98.27	77.34	50.53	35.42
	FN	8.84	0	1.73	22.66	49.47	64.58
	FP	1.25	2.70	0	0	0	0
PSO-GP	DR	87.85	84.20	94.58	87.19	88.79	41.67
	FN	4.82	0	5.42	12.81	11.21	58.33
	FP	7.33	15.8	0	0	0	0
Improved PSO-GP	DR	87.18	97.55	98.27	85.96	14.26	64.58
	FN	11.69	0	1.73	14.04	85.84	35.42
	FP	1.14	2.45	0	0	0	0
SGEA-BP	DR	91.25	97.50	98.34	86.25	47.52	35.33
	FN	7.64	0	1.66	13.75	52.48	64.67
	FP	1.11	2.50	0	0	0	0

FN: False Negative; FP: False Positive; DR: Detection rate.

9. ACKNOWLEDGEMENTS

This work is partially supported by the Natural Science Foundation of China under Grant No.71671186.

REFERENCES

HOLLAND J H, Adaptation in natural and artificial systems, Cambridge: MIT Press, 1975.

Ming-Zhou, ShuDong-Sun, The Principle and Application of Genetic Algorithm, National Defense Industry Press, 2001.

J.Berndt D, Watkins A, Investigating the performance of genetic algorithm based software test case generation, Proc of the 8th IEEE International Symposium on High Assurance Systems Engineering. 2004, (4): 261-262.

NingGuang-Xu, ZhiYong-Xiao, JinShou-Yu, Adaptive genetic algorithm to solve container loading problem, Control and Decision. 2007,(22):1280-1283.

Karabulut K, Inceoglu M. M, A hybrid genetic algorithm for packing in 3D with deepest bottom left with fill method, Proc. of the 3rd International Conference on Advances in Information Systems. 2004,(3261): 441-450.

Singh A, Baghel A S, A new grouping genetic algorithm for the quadratic multiple knapsack problem, Proc. of the 7th European Conference on Evolutionary Computation in Combinatorial Optimization, Berlin: Springer, vol 4446, 2007, 210-218.

Hu Xia, Jian Zhuang, Li Zhong-wang, Environment Based Synergic Immune Genetic Algorithm. Journal of Xi-An Jiao-Tong University, 2009,(43): 80-84.

LiangWei-Cai, Xia-Li, Improvement on crossover operation of genetic algorithms, System Engineering and Electronics, 2006, (28): 925-928.

Grefenstette J.J, Parallel Adaptive Algorithms for Function Optimization, Technical Report CS-81-19, Vanderbilt University, Computer Science Department, Nashville, 1981.

E.Cantú-Paz, A Survey of Parallel Genetic Algorithms, Calculateurs Paralleles.Resaux et Systems Repartis, 1998,(10):141-171.

D.Whitley, A Review of Models for Simple Genetic Algorithms and Cellular Genetic Algorithms. In V.Rayward-Smith, editor, Applications of Modern Heuristics Methods, 1995, 55-67.

E.Cantú-Paz, Migration Policies, Selection Pressure, and Parallel Evolutionary Algorithms, Technical Report IlliGAL Report No.99015, University of Illinois at Urbana-Champaign, 1999.

E.Cantú-Paz, Parallel Genetic Algorithms with Distribut Panmictic Populations,Technical Report IlliGAL Report No.99006,University of Illinois at Urbana-Champaign, 1999.

E.Cantú-Paz, Topologies, Migration Rates, and Multi-Population Parallel Genetic Algorithms, Proceedings of the Genetic and Evolutionary Computation Conference, 1999, 91-98.

Yogeswaran M, Ponnambalam S G, Tiwari M K, An efficient hybrid evolutionary heuristic using genetic algorithm and simulated annealing algorithm to solve machine loading problem in FMS, International Journal of Production Research, 2009,(47):5421-5448.

Oh S K, Pedrycz W, Park H S, Genetically optimized fuzzy polynomial neural networks, IEEE Trans on Fuzzy Systems, 2006,(14):125-144.

Kargupta H, Revisiting GEMGA: Scalable evolutionary optimization through linkage learning, Proc. of IEEE International Conference on Evolutionary Computation, IEEE Press, 1998.

Long Fu-Luo, The Theory and Application of GeneHandling Genetic Arithmetic, Hunan University, 2001.

JinHui-Zhao, Research on Bio-inspired Optimization Algorithms based on Membrane Computing and Applications. ZheJiang University. 2010.

FengTao-Han, A Study of Endoplasmic Reticulum Inspires Membrane Computing Optimization

Algorithms, ZheJiang University. 2011.
Erick Cantú-Paz. Efficient and Accurate Parallel Genetic Algorithms. Kluwer Academic Publishers,1998.
Zhang L, Zhang B, The theory and application of Problem solving-The theory and application of quotient space granular computing, beijing. Tsinghua University Press, 2007.
Min-Zhou, ShuDong-Sun, Genetic Algorithms: Theory and Applications, BeiJing: National Defense Industry Press.1999, 65-68.
Păun G, Computing with Membranes, Journal of Computer and System Sciences, vol.61, 2000, 108-143.
Nishida T Y, An approximate algorithm for NP-complete optimization problems exploiting P systems, Proceedings of Brain-storming Workshop on Uncertainty in Membrane Computing, 2004, 185-192.
Huang Liang, Membrane computing Optimization Method. Hang Zhou, Zhejiang Univers, 2007.
Xu Youzhun, Zeng Wenhua. The Development of Parallel Evolutionary Algorithms. Pattern Recognition and Artificial Intelligence, vol 18, No 2, 2005, 183-192.
Enrique Alba, Marco Tomassini. Improving flexibility and efficiency by adding parallelism to genetic algorithms. Statistics and Computing, 2002, 12(2):91-114.
Enrique Alba, Antonio J. Nebro, and José M. Troya. Heterogeneous Computing and Parallel Genetic Algorithms. Journal of Parallel and Distributed Computing, 2002,62(9):1362-1385.

Research on the Use of Auxiliary Tennis Wall to Improve the Tennis Technology in College Physical Education

*Yongshan Peng**
School of Physical Education, Jiangxi University of Finance and Economics, Nanchang 330013, China

Abstract: Through the literature documentary, the expert interview and induction, the paper makes a systematic analysis on the tennis ball sense training and six methods for tennis technical training with tennis wall, pointing out the key points in each technique, each stage, and the notes as well. The paper finally concludes the concrete suggestions to the practical application.
Key words: Colleges and universities, Auxiliary tennis wall, tennis training methods

1. INTRODUCTION

In the recent ten years, it is well known that tennis has become more and more popular in China. The unique charm and style of tennis has also been sought after by college students, and tennis has become one of the most popular sports in the school. From the east to the west, from key universities to ordinary institutions, tennis has become the most popular selective course with numerous students. So, in recent years, many colleges and universities have expanded or built new courts, and the number of tennis courts has increased a lot comparing to that in ten years ago. Due to the increasing number of students, the number of tennis courts in most colleges and universities are far from meeting the needs of teaching and training, let alone the needs of students in their spare time. And tennis is a sport activity with higher technical requirements which is difficult to learn, so it is difficult for the students to master five basic tennis technologies. In this case, taking advantage of auxiliary tennis wall is a better way to explore the tennis training, so that the majority of college students can still take tennis practice in spite of less training partners, less coaches, less tennis courts and training funds. It has important practical significance to increase the frequency of practice and effectively improve the tennis technology. In this article, the author proposes the method of using auxiliary wall to practice tennis, which can provide useful help for the majority of tennis learners, especially for the beginners in a short time.

2. BASIC CONCEPT OF TENNIS WALL

Tennis wall is also known as tennis practice wall, or auxiliary practice wall. It is a flat wall perpendicular to the ground, which is an assistant for the tennis training in the course of tennis practice. The standard tennis wall should have special height, width, hardness, and smooth surface. Special line type should be marked and the shape of tennis balls should be drawn on the wall for tennis practice. But in fact, specifications in most of the tennis walls are not as strict as the tennis courts with international standards, because there is no uniform standard for tennis wall. Due to the training needs of tennis wall, there are still certain standards for tennis wall. For example, the height of the wall is not below 5 meters, to avoid stroking the ball behind the wall; the standard width of doubles tennis court is 10.97 meters, so the width of tennis wall should be 1-2 meters wider than that; the distance from the tennis net to the baseline in the court should be 11.885 meters. Thus, the length of incidental ground should reach more than 15 meters as a sufficient buffer. In fact, due to various restrictions, most tennis wall can not meet the above requirements. A flat wall of ordinary building, even the interior wall can also be used as a tennis wall. Sometimes, some tennis fans play tennis on the wall, and those walls all can be called the tennis wall.

3. THE APPLICATION OF TENNIS WALL IN TENNIS TEACHING AND TRAINING

3.1 To improve ball sense with the tennis wall

For tennis learners, regardless of the beginner or intermediate, senior players, the ball sense is the basis of the smooth completion of the tennis technology. The feeling is the handle of tennis, which is the stability of the movement and the control ability of stroking, mainly including the muscle feeling and the observation, thinking and judgment of the ball, player, court and time in the practice. For the beginners, the most important thing is the practice for of the ball exercises, the beginners can practice by using the following methods: 1. face to the wall, throw to the wall, after the ball hitting the wall and landing, catch the ball with both hands; when mastering the skill. then catch it with one hand; 2. face to the wall, throw to the wall, after the ball hitting the wall without landing, catch the ball with both hands, then catch it with one hand; 3. stand at a distance of 3-5 meters long from tennis wall, the forehand, grip with medium strength, stroking, when the ball rebounding, catching the ball with the hand without

racket; 4. after the progress, the practice can be a bit more difficult, do not catch ball with hands, but continuous stroking to the wall, fully understanding the feelings of racket and ball controlling; 5 after a period of practice, the control of the ball can be increased to a certain level, standing 4-5 meters away from the wall, appropriately increasing the hitting strength, stroking, rebounding, before landing, stroking again, which is mainly enable learners to appreciate how racket absorb the ability to rebound the ball. It can improve the ability to control the ball, enhance coordination, softness in the practice, and improve ball controlling on different speeds and strength of the.

3.2 The practice of forehand and backhand drive with tennis wall

3.2.1 The forehand and backhand drive is the most basic and important technology with the highest using frequency in tennis. In tennis training and teaching, the learners should do special technology practice in order to further improve the tennis technology.

3.2.1.1 The forehand and backhand drive practice of beginners can be divided into four stages. In the first stage, a group of three or four students can stand at a distance of 5-6 meters from tennis wall (including a player, two or three assistants), one assistant can stay in the place sending tennis balls to the player in the free-fall way for the forehand and backhand drive (one or two assistants stand behind the player to catch the rebound ball which the former assistant fails to catch), that is from sending to driving. At first, the player can hold the racket, when the assistant sending the ball bouncing to a suitable height, the player should hit the ball to the wall high up to more than 1 meter with 50% of the total strength. After a period of practice, the drive turn to stable, the trainer can release the ball in the auxiliary to shoot and after the ball, and the player can hold the racket after the sending, which causing two actions to combine into a complete continuous movement. This practice can form a correct stroking movement.

3.2.1.2 When the learners' technology of forehand and backhand drive keeps stable, they may come to the second stage of the practice (the assistant starts to throw the ball to the learner in a distance, and the learner practice stroking to the wall. One or two assistants catch the bouncing balls behind the learner, and send the balls to the former assistant feeding the ball. After hitting 10 balls, the learner and other assistants change their positions with each other, which mean the former learner becomes an assistant feeding balls for the next learner.). In the process, the placement of dropping balls are required to be stable, and the bounce height are basically the same, the speed of the bouncing ball should be slow. So in the practice, the balls should be much softer and lighter with poor elasticity.

3.2.1.3 When the learners can easily and stably complete the second phase of the practice, they can enter the third stage without assistants (the learner continuously does the practice of forehand and backhand drive by himself or herself). In the process, the placement of the practice should be from far to near, the power from small to big, and gradually improve the difficulty, and then the placement from near to far, the power from big to small, which can improve the stability of ball sense and the control of the ball; finally, from the near to the long distant, the power form the small to big. Through the repeated practices, the technology of baseline can be improved into a higher level. In the process, the judge of learners should be accurate and ready for hitting the ball, try to maintain the correct movement, hitting the ball 1-2 meters high on the wall.

3.2.1.4 Practice in the fourth stage

For those learners who have above basic tennis technology, they can improve the technology of forehand and backhand drive by controlling the ball placement and changing the running route of the balls. First, the learner should stand in the distance of 10-12 meters away from the tennis wall, and continuously forehand and backhand stroke in different positions, and the balls are required to hit to the appointed region on the tennis wall; the learners are required to take correct judge in time, so they can move and backswing swiftly, before hitting, they can have a clear judge on the line shot and cross shot. Thus, the correct judge on the line shot and cross shot and the control on the hitting route could improve the consistency of ball placement.

3.2.2

For the balls with lower hitting point, far away from the wall, with slower bouncing speed, back spin or the falling balls, the racket face should be open to touch the ball to avoid the ball back to the wall below one meter, which is called "below the net"; for the balls with high hitting point, top spin with high speed or the bouncing ball in the rising, the racket face should be a bit closed in the moment of touching the ball, to avoid returning the high ball; for the balls in other states, in the moment of touching the ball, the racket face should be perpendicular to the ground or in a slightly backward state.

3.2.3 Notes for the forehand and backhand practice with the auxiliary tennis wall

(1)First of all, the power for the stroking should not be too big, so as not to increase the difficulty of the next return;

(2)It must proceed in an orderly way and step by step. In the beginning, people should try to reduce the difficulty of the exercise, then gradually increase the difficulty; soft balls can be used in the first stage of the practice, then the slightly hard ball,

and people gradually increase the difficulty of the exercise.

(3)Third, in the practice of forehand and backhand, learners should practice top spin as far as possible, which can improve the continuity and consistency of the return and control the ball placement and route.

3.3 Practice of forehand and backhand volley with tennis wall

3.3.1 Volley is an effective way to get score in tennis competition, especially doubles tennis. Due to the high speed, short time of volley, learners are required to have rapid response ability and correct movement.

3.3.1.1 Before the practice of volleying, learners can do the swing practice with back against the wall, mainly taking backswing, and then they can check whether the hand or racket can reach the wall. If touching the wall, it means the action is the oversize movement, which should be avoided in the volley.

3.3.1.2 In the beginning of the volley practice, two people can be in a group, the learner standing in the distance of 3-5 meters from tennis wall, while the assistant feeding toss balls to the learner with the back against the wall. The learner softly hits the ball back to the assistant by volley, and the assistant catch the ball by hand, and they continuously practice toss-volley. After 10 balls, they change their position with each other. In the practice, they are required to do the alternating exercises with forehand and backhand, and the assistant should point out the problems and shortcomings of the learner in the process.

3.3.1.3 The learner practice forehand and backhand volley with the wall by himself or herself. The learner can be close to the wall and hit it to the wall, when the ball bouncing back but not grounding, the learner should do the continuous stroking as many as possible. When stroking, the learner should pay attention to the body balance, taking body forward, and the ball must be hit in front of the body. Keeping practice without the power, the learner should focus on the correct volley movement, the ball sense with the fixed wrist, the control of racket and the hitting time.

3.3.1.4 The following practice is to improve the control of the placement of volley with the tennis wall. The learner stands in the distance of 3-5 meters from tennis wall with position shift, and practices the forehand and backhand cross shot. It allows learners to have the sense of moving, so as to strengthen the movement ability, and the binding capacity of forehand and backhand.

3.3.1.5 In the practice of midfield volley, the learner stands in a distance of 6 - 8 meters from tennis wall. Firstly, the learner hits the ball to the wall, then fast forward 2 - 3 meters according to the stroke strength and bounce, stroking to the wall again by using volley. In the practice, the learners are required to move forward quickly, leading to the accurate cohesion of fast moving and volley. Through these phases of practice, forehand and backhand volley can be effectively improved.

3.3.2 Notes on the practice of forehand and backhand volley: the change of the racket face angle

(1) When the height of hitting point is lower than the net, the racket face angle should be in the open state, and people can hit the ball with the racket forward and upward and the hitting power should not be too large, preventing the back ball "out of bounds".

(2) When the height of hitting point is close to the net, the racket face angle should be in the open and slightly backward state, and people can hit the ball with the racket forward and the hitting power should not be too large, preventing the back ball "out of bounds".

(3) When practicing volley in high hitting point, the racket face angle should be in the open and backward state, and people can hit the ball with swinging the racket downward and the hitting power should be large for the volley.

3.4 Practice of serving and receiving with the tennis wall

3.4.1 In the practice of toss with the tennis wall, taking the wall as a reference, learners can practice toss. Firstly, people should draw a line on the wall in a suitable height, the learner leans to the wall with one side and the hand in the side does hold the racket, and then start to toss. The learners are required to toss to the line every time and self-observe the height and position of the ball, so as to enhance the stability of service ball route and the placement. When the ball trajectory is straight and the toss height is accurate, the learners can enter the next stage of practice.

3.4.2 In the practice of serving in a suitable height, learners can stand in the distance of 12 meters from the wall, and serve to the left and right half region of the wall in various types of serve. The ball should be hit to the marked region up from the ground 1 - 1.5 meters, and the serve should be in a smooth state. Then, the following practice is to control the service placement. The learner stands in a distance of 12 meters from the wall, and tries to serve to the expected region.

3.4.3 In the practice of receiving with tennis wall, after serving, the learner should swiftly move and hit the bouncing balls by using stroke, volley, smash, and lob, which is the receive practice. Because the high speed and impact force of the bouncing ball are close to the actual service speed, this service practice can be basically equal to the training in pair.

3.5 Practice of overhead smash with the tennis wall

Firstly, the learner can make a mark in the ground

in a distance of 2m far from the wall, then back to the distance of 8m away from the wall, and the learner starts to serve to the mark. When the ball landing and then bouncing forward to the wall, and immediately bouncing to up high, which seems like a tennis lob from the opponent, at this time the learner should be rapidly in the place to do overhead smash again to the marked spot, and then bounce to the wall, and repeat the practice to improve the overhead smash.

4. CONCLUSIONS

It is an effective method of using tennis wall in colleges' tennis teaching, which can solve the problems like being lack of tennis courts and tennis courses, large number of learners in colleges and universities, and also can enhance the comprehensive skills of learners, improve the teaching efficiency. But in practice, learners should pay attention to the following points.

(1) In the practice with tennis wall, the power and strength should not be too large, and the learners should focus on completing the whole technical movements and correct the shortcomings, in order to improve the ball sense and consistency.

(2) The tennis wall is a kind of auxiliary means, which can not completely replace the actual court. So the practice with tennis wall should be combined with the practice in tennis court, which can cultivate the ball sense in the court.

(3) The practice with tennis wall is relatively boring, and the learners in the practice should have patience and perseverance, so as to accumulate a ball sense and experience and improve their skills.

REFERENCES

[1] Shim J, Carlton L G, Chow J W, et al. The use of anticipatory visual cue by highly skilled tennis players. J Motor, 2005, 37(2): 164-175.

[2] Jones C M, Miles T R. Use of advance cues in pre-dicting the flight of a lawn tennis ball, Journal of Hu-man Movement Studies, 2009, 4(1): 231-235.

[3] Huys R, Canal-Bruland R, Hagemann N. Global information pickup underpins anticipation of tennis shot direction. J Motor Behav, 2009, 41(2): 158-170.

[4] Pherson M C, Sue L. Expert-novice differences in planning strategies during collegiate singles tennis com-petition. J Sport Psycho, 2000, 22(1): 39-62.

Hydrogen Desorption Property and Mechanism of Mg95Ni5+NbF5 Prepared by Hydriding Combustion Synthesis and Mechanical Milling

Lingjun Wei
Jiangsu Key Laboratory of Advanced Food Manufacturing Equipment and Technology, Jiangnan University, Wuxi, P. R. China

Abstract: The hydrogen desorption peoperty and mechanism of Mg95Ni5+NbF5 composite prepared by hydriding combustion synteesisi and mechanical milling(HCS+MM) was investigated. The hydrogen desorption kinetics of Mg95Ni5 composite with 0.1,0.2,0.5,1mli%NbF5 after 3,5,7,10h mechanical milling(MM) at 473,493,523K were measured respectively. At 523K,Mg95Ni5 composite with 0.5mol%NbF5 milled for 5h can be desorb 5.1wt.% of H2 in 60min. The apparent activation energy of the Mg95Ni5+0.5 mol% NbF5 system calculated by Arrhenius equation is only 127.74 kJ/mol,which is lower than the pristine system. XRD ecamination suggested that the formation of MgF2 and Nb-series products with carious high calence states may cantribute to kenetic improvement.
Keywords: Materials Science; Hydrogen desorption property; NbF5;Catalytic effect

1. INTRODUCTION

Magnesium hydride has been considered as a strong candidate for the storage medium for vehicular application because of the high theoretical hydrogen capacity (7.6 wt.%), high abundance and low cost [1]. However, the high operating temperature (>573K) and slow kinetics limit its wide application commercially. Recently, several approaches have been used to settle these questions, including element substitution, the addition of catalysts and new preparation methods [2-4]. It was found that the addition of transition metals and/or their oxides, and even some non-metal materials by mechanical milling could accelerate the hydrogen adsorption/desorption [5-7].

The reaction between F- ions in aqueous solution and Mg has been shown to create a highly reactive and protective fluorinated surface, which has a high affinity to hydrogen [8]. In addition, the products by a displacement reaction between MgH2 and transition metal fluoride catalyst during mechanical milling or the process of hydrogen absorption and desorption could activate the hydrogen desorption of MgH2 effectively [9-11]. Considering the transition metal ions with high valence state and function of F- anion, NbF5 is therefore of great interest for enhancing the performance of hydrogen desorption of Mg-based hydrogen storage alloys as a source of these both species.

HCS was first developed by Akiyama et al. [12], which is basically a powder metallurgy method for direct production of hydrides of magnesium-based alloys from powder mixture of metals under pressurized hydrogen and elevated temperatures. This method has several advantages over conventional ingot metallurgy method for the preparation of Mg-based hydrogen storage alloys, including low energy consumption [13], short processing time and high activity of the product that need no activation. In the previous study, we found that the mechanism of high activity of Mg2NiH4 prepared by HCS can be attributed to pure composition, loose and porous morphology, a large number of micro fissures and crystal defects, and an outmost layer of Mg(OH)2 instead of MgO on the surface [14, 15]. Furthermore, considering mechanical milling which can synthesis various metastable hydrogen storage alloys such as amorphous, nanocrystalline and extended solid solutions phases, we combined HCS and MM (HCS+MM) to expect to improve the hydrogen storage properties. Based on this novel method [16], the hydrogen sorption performance of Mg-based hydrogen storage alloys can be improved dramatically [17-19]. The HCS+MM product of Mg95Ni5 reached maximum capacity of 5.56 wt.% at 373 Kwithin only 100 s, whereas its dehydrogenation property was still not ideal [19]. It is the main research subject of our group recently to ameliorate the hydrogen desorption property.

In the present paper, the result for Mg95Ni5 composites containing NbF5 prepared by hydriding combustion synthesis and mechanical milling is reported. This investigation aims to enhance, especially, the dehydrogenation kinetics at the lower temperature. As expected, Mg95Ni5 composite with 0.5 mol% NbF5 milled for 5 h can desorb 5.1 wt.% hydrogen in 60 min at 523K.

2. EXPERIMENTAL

The starting powders of magnesium (99.9% in purity,

<74 μm in size) and nickel (99.99% in purity, 2~3 μm in size) with atomic ratios 95: 5 (Mg95Ni5) were used directly for hydriding combustion synthesis without any compressive treatment. Some details of the operation of the HCS process have been described in Ref. [18]. In the process of synthesis, the synthesis reactor was heated to 853K under a hydrogen atmosphere of 2.0 MPa at a heating rate of 10K/min, and keep this temperature for 60 min to ensure completion of the combustion synthesis between metallic powders, then the reactor was kept at 613K for 120 min so as to guarantee a high yield of hydride during the cooling period.

The as-prepared Mg95Ni5 composite was mechanically milled with 0.1, 0.2, 0.5 and 1 mol% NbF5 (99% in purity, Alfa Asear) for 3, 5, 7 and 10 h under argon atmosphere by using a planetary milling apparatus with stainless steels vial (50 ml) and balls at 200 rpm. The ball-to-power weight ratio was about 30:1. The as-milled sample was taken out in the glove box filled with Ar atmosphere to avoid sample self-igniting because of high activity.

Hydrogen desorption performance of Mg95Ni5-NbF5 composites were examined in vacuum by an automatic Sieverts' apparatus (AMC Inc, USA) at 473, 493 and 523K. The structures of the samples after mechanical milling and dehydrogenation were characterized using X-ray diffraction (XRD) with Cu Kα radiation.

3. RESULTS AND DISCUSSION

A. Optimization of the addition amount of NbF5

Fig. 1 shows the desorption profiles at 473K of the HCS+MM products of Mg95Ni5 + x mol% NbF5 (x=0, 0.1, 0.2, 0.5, 1) mechanically milled for 10 h. It is observed that in all cases, the addition of NbF5 markedly improves the dehydriding kinetics. However, a saturation limit is reached for 0.5 mol.% of NbF5. This is different to the 2 mol.% optimum amount NbF5 reported by Luo [20] and Recham [21] et al. The reasons for such difference mainly attribute to the different compositions and the preparations of the samples.

The rate limiting steps of the reactions for different catalyst contents are different. For the Nb2O5 additive system, the reaction is three dimensional growth controlled with catalyst contents lower than 0.2 mol% at 523K [22]. However, the recombination rate is high enough and the kinetics rate-limiting step is changed to interfaced-controlled with catalyst contents above 0.2 mol%. As the Nb2O5 content increases, the catalytic effect reaches a limit, because the recombination rate of hydrogen atoms is not the determining step anymore [23]. In our Mg95Ni5-NbF5 system, the addition amount of NbF5 has the same effect to the rate limiting of dehydrogenation. When the content of NbF5 reaches 0.5 mol%, the dehydrogenation kinetics shows the fastest.

Further increasing the NbF5 content, the kinetics becomes slower. The addition of 0.5 mol % NbF5 may be a point to change the kinetic rate-limiting step. The more details about rate-limiting step need further investigation.

To figure axis labels, use words rather than symbols. Do not label axes only with units. Do not label axes with a ratio of quantities and units. Figure labels should be legible, about 9-point type.

Color figures will be appearing only in online publication. All figures will be black and white graphs in print publication.

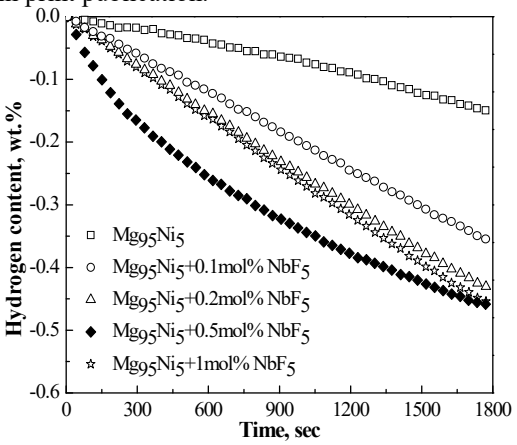

Figure 1 Hydrogen desorption profiles of the HCS+MM products of Mg95Ni5 + x mol% NbF5 (x=0, 0.1, 0.2, 0.5, 1) mechanically milled for 10 h measured at 473K in vacuum.

B. Influence of milling time

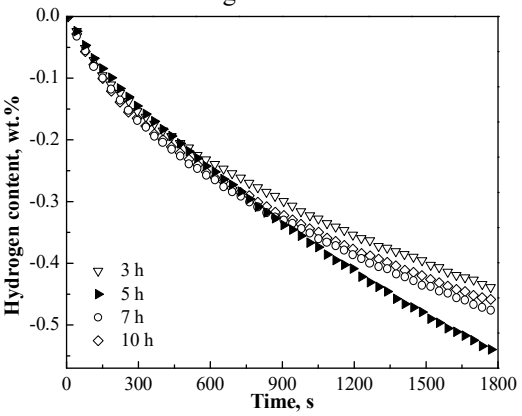

Figure 2 Hydrogen desorption profiles of the HCS+MM products of $Mg_{95}Ni_5$ + 0.5 mol% NbF_5 mechanically milled for 3, 5, 7, 10 h measured at 473K in vacuum.

Fig.2 shows the hydrogen desorption profiles at 473K of the samples of Mg95Ni5 + 0.5 mol% NbF5 mechanical milled for different time from 3 h to 10 h. Apparently, a longer milling time leads to a more kinetic enhancement. Nevertheless, it is also found that increasing milling time to exceed 5 h causes a decrease in the hydrogen desorption capacity since excess milling time may be mainly ascribed to the particles agglomeration and the partially oxidized Mg during the milling.

C. Hydrogen desorption performances at different temperatures

Desorption properties of Mg95Ni5 + 0.5 mol% NbF5 milled for 5 h were investigated from 473K to 523K (see Fig. 3). The composites desorbed about 2.3 wt.% and 5.1 wt.% H2 in 60 min at 493K and 523K, respectively. A small hydrogen amount, namely 0.7 wt.% in 60 min is also desorbed at 473K. This phenomena highlight that the HCS+MM products of Mg-based hydrogen storage materials could desorb hydrogen at much lower temperatures than the thermodynamics limit.

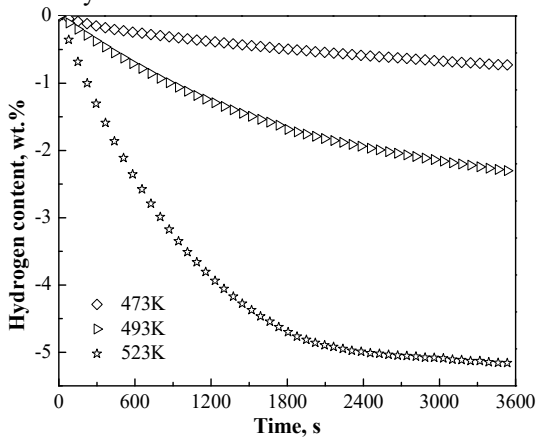

Figure 3 Evolution of the hydrogen desorption profiles of the HCS+MM product of $Mg_{95}Ni_5$ + 0.5 mol% NbF_5 milled for 5 h with decreasing desorption temperature measured in vacuum.

The comparison of the hydrogen desorption profiles at different temperatures shows faster kinetics and higher capacity for Mg95Ni5 + 0.5 mol% NbF5 than that for Mg95Ni5 in Fig. 4. At 473, 493 and 523K in 60 min, Mg95Ni5 desorbs nearly 0.3, 1.5 and 4.4 wt.%, however, Mg95Ni5 + 0.5 mol% NbF5 desorbs 0.7, 2.3 and 5.1 wt.%, respectively. The Johnson-Mehl-Avrami (JMA) model is the most popular model for analysis of Mg-based hydrogen storage materials [24, 25], which is expressed by the following general formulation:

$$\alpha = 1 - \exp\left(-kt^{n}\right) \quad (1)$$

Where α is the fraction desorbed for the hydride at time t. Both the rate k and the Avrami exponent n are constant with respect to time, which generally reflects the nucleation and growth morphology and dimensionality, as well as the rate-limiting process. Fig.5 presents the JMA plots of ln[-ln(1-α)] vs ln(t) for the dehydrogenation of the HCS+MM products at different temperatures. The plots show good linearity (R2>0.99) in the range of α<0.7. For the HCS+MM product of Mg95Ni5, the value of n is decreased from 1.08079 at 523 K to 0.71479 at 473 K, which suggests that at lower temperatures, the hydrogen diffusion along the MgH2/Mg interfaces cannot be neglected because a value of n=0.5 in the JMA model indicates a diffusion-controlled process. However, For the HCS+MM product of Mg95Ni5+ 0.5 mol% NbF5, the Avrami exponent n is determined to have values of 1.10763 (R2=0.99913) at 523 K, 1.14558 (R2=0.99864) at 493 K and 1.11378 (R2=0.99633) at 473 K, indicating the nearest integer as n=1. It is more likely that growth of the Mg nuclei is limited by hydrogen reassociation on the surface as proposed by Mitlin et al [24]. Therefore it is reasonable to assume that NbF5 may help the hydrogen diffusion along the MgH2/Mg interfaces at the lower temperatures.

To further study the dehydrogenation kinetics of these composites, the activation energy for desorption was calculated according to the Arrhenius formulation as

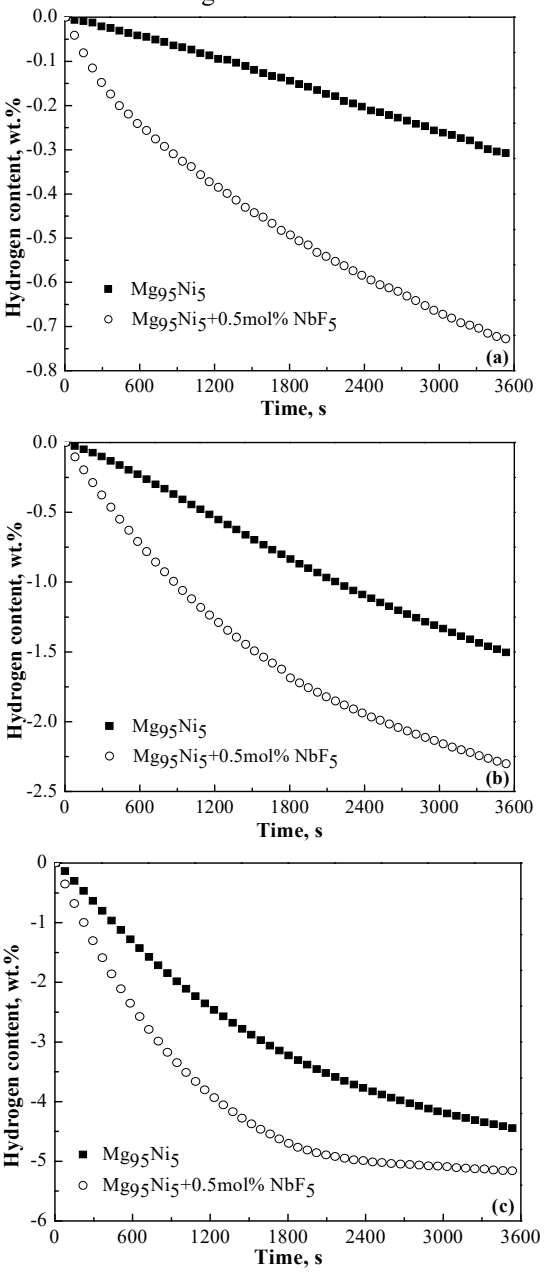

Figure 4 Hydrogen desorption profiles of the HCS+MM products of $Mg_{95}Ni_5$ and $Mg_{95}Ni_5$ + 0.5 mol% NbF_5 milled for 5 h measured in vacuum under different temperatures: (a) 473 K; (b) 493 K; (c) 523K.

$$E_A = -RT \ln\left(\frac{k}{k_0}\right) \quad (3)$$

where EA is the activation energy, k is a temperature-dependent reaction rate constant determined by JMA equation, R is the gas constant and T is the absolute temperature. Fig.6 shows the Arrhenius plot for the HCS+MM products. The apparent activation energy, E_A was calculated as 147.71 kJ/mol for the Mg95Ni5 system, which was close to the value for as-received

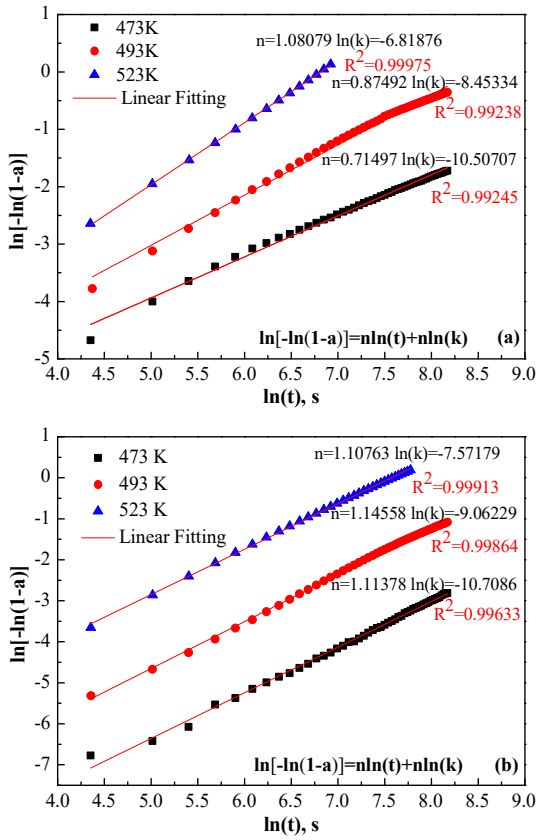

Figure 5 JMA plots of ln[-ln(1-α)] vs ln(t) for the dehydrogenation of the H.CS+MM products at different temperatures: (a) $Mg_{95}Ni_5$; (b) $Mg_{95}Ni_5$ + 0.5 mol% NbF_5. The reacted fraction of α<0.7 was used.

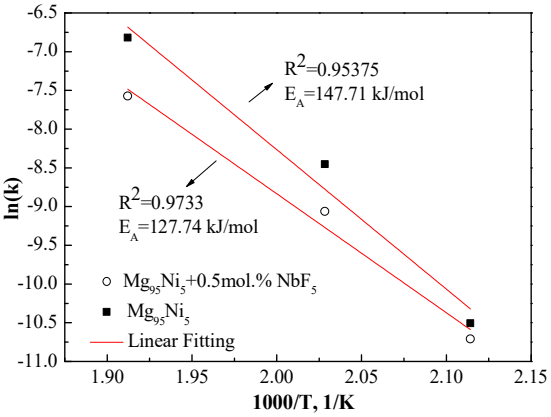

Figure 6. Arrhenius plot for the H2 desorption of the HCS+MM products of Mg95Ni5 and Mg95Ni5 + 0.5 mol% NbF5.

commercial MgH2 (153 kJ/mol) obtained by Choi et al [26]. With the addition of NbF5, the apparent activation energy decreased to 127.74 kJ/mol. This result suggests that NbF5 has an obvious catalytic effect on the dehydriding reaction of MgH2.

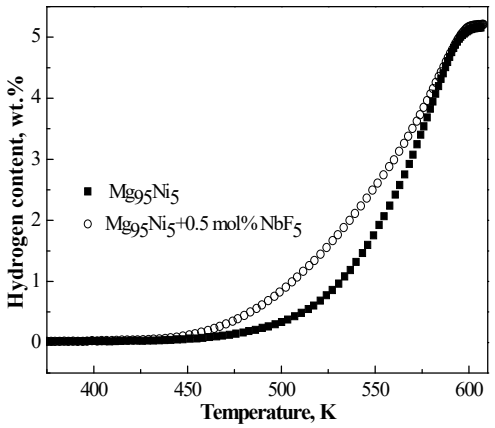

Figure 7 The amount of hydrogen desorbed as a function of the temperature of the HCS+MM products of Mg95Ni5 and $Mg_{95}Ni_5$ + 0.5 mol% NbF_5. The average heating rate was 20 K/min.

The HCS+MM products of Mg95Ni5 and Mg95Ni5 + 0.5 mol% NbF5 were heated in the evacuated sample chamber while the rise in pressure was recorded so as to examine the desorption property. Fig.7 shows the amounts of hydrogen desorbed as a function of temperature of Mg95Ni5 together with Mg95Ni5 + 0.5 mol.% NbF5. It can be seen that the dehydriding onset (the temperatures at which hydrogen begins to release from the materials in Fig. 7) of Mg95Ni5 + 0.5 mol% NbF5 was lowered comparing with that of Mg95Ni5. The dehydriding onset of the HCS+MM products was decreased by approximately 30 K, from 465 K without catalyst to 435 K with 0.5 mol.% NbF5.

D. Structural characterization and discussion

Fig. 8 presents the XRD patterns of the as-milled Mg95Ni5 with and without 0.5 mol% NbF5 as well as those after dehydrogenation at 523K in vacuum. It is observed that the diffraction patterns of the as-milled samples with and without NbF5 addition are quite similar. The peaks corresponding to MgH2, Mg2NiH4, Mg2NiH0.3 and Mg are detected in both of the as-milled products. For the HCS+MM product of Mg95Ni5 + 0.5 mol.% NbF5, the trace of MgF2 is hardly detectable, neither are Nb-series products due to its small volume fraction (Fig.8, b). However, the formation of MgF2 is visible after dehydrogenation at 523K (Fig.8, d) due to the reaction between Mg and NbF5. As a matter of fact, such phenomenon was reported by Recham [21] and the formation of MgF2 was further supported by XPS measurements [20]. The product of MgF2 could improve the hydrogen desorption kinetics of Mg-based hydrogen storage alloys effectively [27]. The reason of this improvement may be attributed to the high electronegativity of fluorine anions which lead to a

further weakening of the surface Mg2Ni-H and Mg-H bonds.

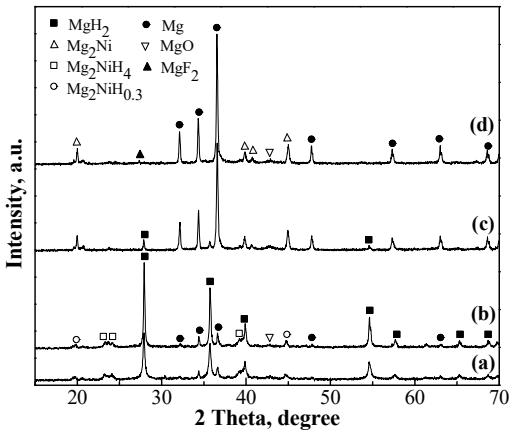

Figure 8 XRD patterns for $Mg_{95}Ni_5$ (a) milled, (c) dehydrogenationed and $Mg_{95}Ni_5$ + 0.5 mol% NbF_5 (b) milled, (d) dehydrogenationed.

According to previous observations, it is not a complete reduction of NbF5 into Nb but a partial transformation to Nbx+-containing compounds in period of the formation of MgF2 phase [20]. During dehydrogenation, the Mg-H bond of MgH2 is activated by catalyst. During the process, the electrons of the bonding orbitals of the MgH2 are donated to the unoccupied orbitals of catalyst. In succession, the electrons of the occupied orbitals of catalyst are back donated to the antibonding orbitals of the MgH2 [28]. Comparing with the valence electron configurations of Nb, Nbx+ is 4d4-x5s1 with various d electron orbitals, which increase the electron exchange action with MgH2 to result in the easier dissociation of Mg-H bonds.

Comparing patterns of c and d in Fig. 8, we found that MgH2 was not detectable in Mg95Ni5 with 0.5 mol% NbF5 whereas little trace of that was visible in Mg95Ni5 after dehydrogenation at 523K in 60 min, which also approved the catalytic effect of NbF5.

4. CONCLUSION

The hydrogen desorption property of Mg95Ni5 prepared by hydriding combustion synthesis is improved by adding NbF5 . The addition of NbF5 accelerates the dehydriding kinetics, in particular at the lower temperature 473K. The apparent activation energy of the Mg95Ni5 + 0.5 mol% NbF5 system calculated by Arrhenius equation is only 127.74 kJ/mol, which is lower than the pristine system. XRD examination suggested that the formation of MgF2 and Nb-series products with various high valence states may contribute to kinetic improvement. In order to clarify the catalytic effect of NbF5, further investigations such as X-ray photoelectron spectroscopy (XPS) are required.

5. ACKNOWLEDGEMENTS

This work was supported by the National Natural Science Foundation of China (NSFC) (Grant Nos. 51471087, 51401086, 51571112), Natural Science Foundation of the Jiangsu Higher Education Institutions of China (No. 13KJA430003), the Fundamental Research Funds for the Central Universities (No.1072050205152030), and the Priority Academic Program Development of Jiangsu Higher Education Institutions (PAPD).

REFERENCES

[1] K-F Aguey-Zinsou, J-R Ares-Fernández, “Hydrogen in magnesium: new perspectives toward functional stores”, *Energy Environ Sci*., vol. 3, pp. 526-543, 2010,.

[2] V. M. Skripnyuk, E. Rabkin, “Mg3Cd: A model alloy for studying the destabilization of magnesium hydride”, *Int J Hydrogen Energy*, vol. 37, pp. 10724-10732, 2012.

[3] G. Liu, Y. J. Wang, F. Y. Qiu, L. Li, L. F. Jiao, H. T. Yuan. “Synthesis of porous Ni@rGO nanocomposite and its synergetic effect on hydrogen sorption properties of MgH_2”, *J Mater Chem,* vol. 22, pp. 22542-22549, *2*012.

[4] K. J. Jeon, H. R. Moon, A. M. Ruminski, B. Jiang, C. Kisielowski, R. Bardhan, J. J. Urban, “Air-stable magnesium nanocomposites provide rapid and high-capacity hydrogen storage without using heavy-metal catalysts”, *Nature Mater*., vol. 10, pp. 286-290, 2011.

[5] H. Gasan, O. N. Celik, N. Aydinbeyli, Y. M. Yaman, “Effect of V, Nb, Ti and graphite additions on the hydrogen desorption temperature of magnesium hydride”, *Int J Hydrogen Energy*, vol. 37, pp.1912-1918, 2012.

[6] A. Anastasopol, T. V. Pfeiffer, A. Schmidt-Ott, F. M. Mulder, S. W. H. Eijt, “Fractal disperse hydrogen sorption kinetics in spark discharge generated Mg/NbOx and Mg/Pd nanocomposites”, *Appl. Phys. Lett.*, vol. 99, pp. 194103-194105, 2011.

[7] M. Konarova, A. Tanksale, J. N. Beltramini, G. Q. Lu, “Porous MgH2/C composite with fast hydrogen storage kinetics”, *Int. J. Hydrogen Energy*, vol. 37, pp. 8370-8378, 2012.

[8] F. J. Liu, S. Suda, “Properties and characteristics of fluorinated hydriding alloys”, *J Alloys Compd*, vol. 231, pp. 742-750, 1995.

[9] L. Xie, Y. Liu, Y. T. Wang, J. Zheng, X. G. Li, “Superior hydrogen storage kinetics of MgH2 nanoparticles doped with TiF3”, *Acta. Mater*, vol. 55, pp. 4585-4591, 2007.

[10] I. E. Malka, M. Pisarek, T. Czujko, J. Bystrzycki, “A study of the ZrF4, NbF5, TaF5, and TiCl3 influences on the MgH2 sorption properties”, *Int. J. Hydrogen Energy*, vol. 36, pp. 12909-12917, 2011.

[11] F. M. Mulder, S. Singh, S. Bolhuis, S. W. H. Eijt, “Extended solubility limits and nanograin refinement in Ti/Zr fluoride-catalyzed MgH2”, *J Phys Chem C*, vol. 116, pp. 2001-2012, 2012.

[12] T. Akiyama, H. Isogai, J. Yagi. “Hydriding combustion synthesis for the production of hydrogen storage alloy”, *J Alloy Compd*, vol. 252, pp. L1-L4, 1997.

[13] I. Saita, T. Akiyama, "Exergy analysis of hydriding combustion synthesis". *J Chem Eng Jpn*, vol. 39, pp. 525-530, 2006.
[14] D. M. Liu, Y. F. Zhu, L. Q. Li, "Mechanism of the high activity of Mg2NiH4 produced by hydriding combustion synthesis based on the analysis of phase composition, particle characteristic and grain size", *Int. J. Hydrogen Energy*, vol. 32, pp. 2455-2460, 2007.
[15] D. M. Liu, Y. F. Zhu, L. Q. Li, "Crystal defect analysis and surface characteristics of Mg2NiH4 produced by hydriding combustion synthesis", *Int. J. Hydrogen Energy*, vol. 32, pp. 2417-2421, 2007.
[16] L. Q. Li, X. F. Liu, "Technology of preparing high purity and activity magnesium-based hydrogen-storage alloy". China and CN1598018, 2004.
[17] X. F. Liu, Y. F. Zhu, L. Q. Li, "Hydriding characteristics of Mg2Ni prepared by mechanical milling of the product of hydriding combustion synthesis", *Int. J. Hydrogen Energy*, vol. 32, pp. 2450-2454, 2007.
[18] X. F. Liu, Y. F. Zhu, L. Q. Li, "Hydrogen storage properties of Mg100-xNix (x=5, 11.3, 20, 25) composites prepared by hydriding combustion synthesis followed by mechanical milling (HCS + MM)", *Intermetallics*, vol. 15, pp. 1582-1588, 2007.
[19] H. Gu, Y. F. Zhu, L. Q. Li, "Structures and hydrogen storage properties of Mg95Ni5 composite prepared by hydriding combustion synthesis and mechanical milling", *Mater. Chem. Phys*., vol. 112, pp. 218-222, 2008.
[20] Y. Luo, P. Wang, L. P. Ma, H. M. Cheng, "Hydrogen sorption kinetics of MgH2 catalyzed with NbF5", *J. Alloy Compd*, vol. 453, vol. 138-142, 2008.
[21] N. Recham, V. V. Bhat, M. Kandavel, L. Aymard, J. M. Tarascon, A. Rougier, "Reduction of hydrogen desorption temperature of ball-milled MgH2 by NbF5 addition", *J Alloys Compd*, vol. 464, pp. 377-382, 2008.
[22] G. Barkhordarian, T. Klassen, R. Bormann, "Effect of Nb2O5 content on hydrogen reaction kinetics of Mg", *J. Alloys Compd*, vol. 364, pp. 242-246, 2004.
[23] G. Barkhordarian, T. Klassen, R. Bormann, "Kinetic investigation of the effect of milling time on the hydrogen sorption reaction of magnesium catalyzed with different Nb2O5 contents", *J. Alloys Compd.*, vol. 407, pp. 249-255, 2006.
[24] W. P. Kalisvaart, A. Kubis, M. Danaie, B. S. Amirkhiz, D. Mitlin, "Microstructural evolution during hydrogen sorption cycling of Mg-FeTi nanolayered composites", *Acta Mater*, vol. 59, pp. 2083-2095, 2011.
[25] C. Y. Zhu, T. Akiyama, "Zebra-Striped Fibers in Relation to the H2 Sorption Properties for MgH2 Nanofibers Produced by a Vapor-Solid Process", *Crystal Growth Design*, vol. 12, pp. 4043-4052, 2012.
[26] Y. J. Choi, J. Lu, H. Y. Sohn, Z. Z. Fang, "Hydrogen storage properties of the Mg-Ti-H system prepared by high-energy-high-pressure reactive milling", *J. Power Sources*, vol. 180, pp. 491-497, 2008.
[27] E. Ivanov, I. Konstanchuk, B. Bokhonov, V. Boldyrev, "Hydrogen interaction with mechanically alloyed magnesium-salt composite materials", *J. Alloy Compd.*, vol. 359, pp. 320-325, 2003.
[28] T. Muneyuki, A. D. Wilson, K. Hideaki, H. Nakanishi, H. Aikawa, "Mg-H dissociation of magnesium hydride MgH2 catalyzed by 3d transition metals", *Thin Solid Films*, vol. 509, pp. 157-159, 2006.

Path Identification of Camera-based Smart Cars

Wenyu Wang,Wenfeng Song,Yaohua Xu,Yi Han
Chang'an University, School of Automobile, Xi'an, Shannxi, 710064, China

Abstract: In this article, the mechanism of collecting information of road image of the smart car based on camera OV7620 and the microcontroller MK60DN512ZVLQ10 is introduced. Meanwhile, an algorithm aiming at image processing that only needs to traverse the pixels once to complete filtering and binarization of the images is also presented. This algorithm can reduce the computational burden of the microcontroller and improve its processing ability. In addition, it also introduces three kinds of edge detection algorithms, which are used to identify both sides of the road border, and hence provide a basis for subsequent control algorithm.
Keywords: camera OV7620, image filtering, binarization process, edge detection.

1. INTRODUCTION

Driverless operation technology [1] has become a hot topic in the auto industry. In order to promote the progress of this technology, The NXP Cup National University Intelligent Car Race yearly invites students to make an automatic guiding car on particular track [2], using the model car as a platform. In earlier years, most competitors would use XS128 [3], a 16-bit chip made by Freescale Company, as the control chip for smart cars. However, because of its slow processing speed, the car's speed has been seriously influenced. Now the 32-bit processing chip is widely used. Except for using camera [4] as the main image sensor, we can also use the inductor to detect electrified wires laid in the driveway [5], or use the photoelectric sensor [6] and so on as sensors to perceive the external environment. But the camera has a clear advantage. It can collect a greater amount of information and is good for later analysis. At the same time, it has a good foresight which can reach more than 1m. This provides guarantee for the high speed of the smart cars. Literature [7] introduced a kind of method to make smart cars based on the camera. Literature [8-10] presented related control algorithm of camera-based smart cars. Through some relevant research on the path recognition of the track from the perspective of image processing algorithm [11], we propose a new algorithm of fast filtering and binarization.

2. THE MICROCONTROLLER AND CAMERA

The microcontroller is the "brain" of a smart car, so it must have enough hardware resource and powerful computing capacity.MK60DN512ZVLQ10[12]is a kind of 32-bit microcontroller based on ARMCortex-M4, which is launched by Freescale Company. It has 144 pins, uses LQFP encapsulation, and has abundant interfaces that can be connected with external devices. The main modules used in the smart cars are as follows: the DMA (Direct Memory Access) module to receive signal data collected by the camera; PWM (Pulse Width Modulation) module to output signal to the control steering gear and drive the motor; PIT (Periodic Interrupt Timer) module to set time to trigger the interrupt program; UART(Universal Asynchronous Receiver and Transmitter) module to implement data communication between the microprocessor and the upper machine, which is convenient to debug the program.

The camera is just like "eyes" of a smart car. It provides road information on current path for the microcontroller, and then transmits real-time collected information to the microcontroller to be handled. OV7620[13]is a digital CMOS camera, needing low supply voltage which is 5v. It also has lower power consumption. VSYNC pin, the field interruption signal, is the main pin of OV7620. It is used to determine whether an image has begun; HREF pin, the horizontal interrupt signal, is used to judge whether a line of image has begun; Y0-Y7 are data output pins, which are used to output the image pixel data collected by the camera; PLCK is a pin to synchrony the pixel signal. A cycle represents that the pixel value of a point is passed from Y0 to Y7; the 5v pin and GND pin are used to supply power for the camera.

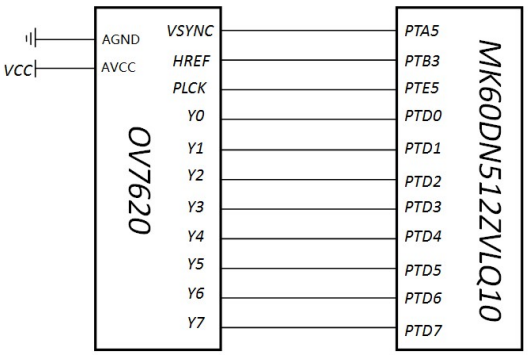

Figure 1 The interface circuit diagram between OV7620 and K60

Pin connections betweenOV7620 and K60 are shown in Fig.1.Horizontal signal, field signal and pixel

interrupt signal are respectively on pin PTB3, PTA5 and PTE5, which are external interrupt trigger pins on K60; Y0 - Y7 is correspondingly linked to PTD0 - PTD7 which are common IO ports of K60.

3. ROAD IMAGE ACQUISITION

In order to reduce the influence of external environment and improve the identification efficiency of smart cars, we use the road path with blue background and black-edged white path as shown in Fig.2.

Figure 2 The road path for the smart cars

The image information collected by the camera is represented by a two-dimensional array. Each element of the two-dimensional array represents the gray value of one pixel. For OV7620 camera, we can collect image information according to waveforms of the field interrupt signal VSYN, horizontal interrupt signal HREF and pixel interrupt signal PCLK. Using oscilloscope to check the waveforms of the above three interrupt signals, we can see their timing relationships as shown in Fig.3.

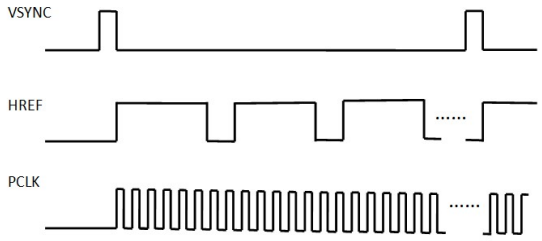

Figure 3 Timing relationships of OV7620

It can be measured that the above three signals' cycle are respectively 16.48ms, 63.58μs (only high level represents the output of gray levels of pixels, roughly 47.4μs), and 73ns. Since 1s/16.48ms = 60.6, 16.48ms / 63.58μs = 259 and 47.4μs / 73 ns = 649, the resolution of OV7620 camera can reach nominal 640 * 240. At the same time, its frame rate is 60 frame /s.

In view of the image acquisition of smart cars, the frame rate which is 60frame/s is enough. But 640 * 240 resolution contains too much data, which will increase the calculation amount of the microprocessor. So on the premise of guaranteeing the image resolution, we use 320 * 200 resolution and that will be enough. For the number of rows, we adopt the method of interlacing collection, through which we can just save 320 lines of data among the original 640 lines to the microprocessor. For the number of columns, we abandon the top 20 and rear 20 data of each line according to the pixel interrupt signals PCLK. Then we only need to store the middle 200 data. So we can collect the right road gray image with suitable size as shown in Fig.4.

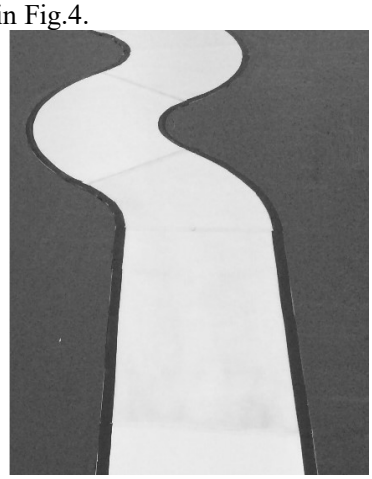

Figure 4 Gray image of the road path

4. IMAGE FILTERING AND BINARIZATION PROCESSING

Salt and pepper noise are common in image acquisition of smart cars, which can cause black and white noise points of the image. Too much black and white noise points will cover the valid data about road information. This will increase the extraction difficulty of the follow-up edge. So it is necessary to filter out noises in order to improve the quality of the image.

Camera OV7620 can output 8-bit data, and the gray values range from 0 to 255. Binarization processing is to set a threshold value to convert gray levels of the pixels into two values, such as 0 and 1. If the grey value is equal to or larger than the threshold value, then we can determine the corresponding pixel to be white and its value becomes1; otherwise, we determine the corresponding pixel to be black and its value becomes 0.

The traditional operation method of image preprocessing[14] is image filtering and the following binarization processing. However, this requires traversing the pixels two times, which relatively needs large amount of calculation. Therefore, a new algorithm which can complete filtering and binarization processing at the same time through smaller amount of calculation is put

forward in this paper. Specific algorithm steps are as follows:

(1)Judge whether the gray value of all pixels of the first 3 * 3 pixel area are all less than the threshold that is preset.

(2) If so, the nine points will be condensed into a black dot and its grey value is 0; otherwise, they will be condensed into a white dot and its grey value is 1.

The schematic diagram of filtering method is shown in Fig.5. If the gray value is the biggest, namely 255, it is pure white. If the gray value is the smallest, namely 0, it is pure black. If a pixel in the diagram is white, its grey value is considered to be greater than the threshold. If the pixel is gray, its gray value is considered to be less than the threshold value.

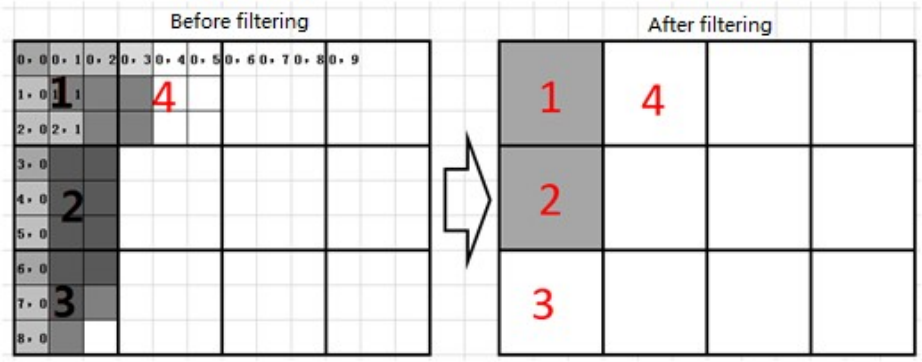

Figure 5 Schematic diagram of filtering method

There are nine pixels in the first area before filtering, namely (0, 0), (0, 1), (0, 2), (1, 0), (1, 1), (1, 2), (2, 0), (2, 1) and (2, 2). Gray values of the nine pixels are all less than the threshold. After filtering, these nine pixels turn to be a pixel point. Since the gray values of the nine pixels are all less than the threshold before filtering, this pixel is seen as a black dot. Similarly, there are nine pixels in the second area before filtering and their gray values are all less than the threshold. But these nine pixels in the second area turn to be a black pixel after filtering.

There are nine pixels in the third area before filtering, but there is a pixel whose gray value is greater than the threshold. Then after filtering, the nine pixels in the second area turn to be a white pixel. Similarly, there are six pixels among the nine points whose gray values are greater than the threshold in the fourth area, so these nine pixels turn to be a white pixel after filtering.

In the schematic scheme, there are totally 108 pixels before filtering. While after filtering, they become 12 pixels. Namely, the size of the original image is reduced by 9 times through the filtering program.

The advantage of this method is its stricter judgment conditions based on specific environment. It will only need to traverse all the pixels once. Besides, it reduces 1/9 of the original image size. So not only its computational complexity is small, but the path identification in the next step is also been simplified. However, the downside of this approach is that if a continuous black area is too small, you may mistake it to be white. For example, if the black edge is too narrow, it might be mistaken for white. The probability of misjudgment is bigger especially at the way edge in the distant place. But in this article, the black area and the white area are continuous, and the actual edge width can reach 2.5cm. With the right installation height and angle of the camera and suitable threshold, misjudgment won't occur as far as the camera can see. The algorithm turned to be feasible after repeated test. The image after filtering and binarization is shown in Fig.6.

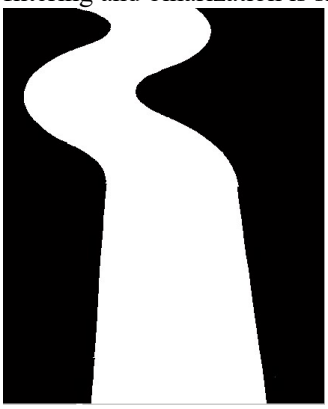

Figure 6 The image after filtering and binarization

5. PATH IDENTIFICATION

Path identification is analyzing road information according to the image signal which is sent back from the camera, and then calculating the movement track of smart cars.

The commonly used edge detection algorithms are mainly direct edge detection algorithm and edge tracing algorithm.

5.1 Direct edge detection algorithm

Since the pixel value of the white path is obviously greater than that of the blue background and the black edge, we can set a suitable threshold to

convert the original road image to the binary one as shown in Fig.6 according to the real environment. We can see from Fig.6 that only the driveway is white while the background is black. Based on the binary image, we adopt the method of comparing each pixel one by one, and then subtract the neighboring pixel from the left-most line to the right in turn. If the difference between data i and data i+1 is 255(difference between black and white pixels), then mark the position of point i to be a. If the difference is 0, then move on to the right. Continue to subtract after finding the position a. If the difference between data point a+ j and data pointa+j-1is -255, and then mark the location to be b. If the difference is 0, move on to the right again. Then the position of the black line of the left edge is considered to be a, and the position of the black line of the right edge is considered to be b. So the center coordinate of the driveway is (a+b)/2. The disadvantage of the direct edge detection algorithm is that it needs to calculate each pixel of each row. The load is heavy for the microcontrollerK60, and it takes up too much system resources. It is bad for the performance of the system. Diagram scheme of the algorithm is shown in Fig.7.

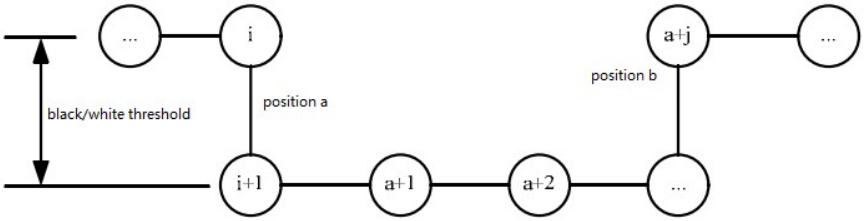

Figure 7 Diagram scheme of the direct edge detection algorithm

5.2 Edge tracing algorithm

This algorithm is simplified by direct edge detection algorithm. Take the left edge for example, if the left edge of some line has been found, since the edge points of the adjacent two rows on both sides are close, when we look for the left edge of the next line, we can search it near the left edge of the previous line. The edge tracing algorithm greatly simplifies the direct edge detection algorithm and needn't to compare with each pixel. The algorithm is simple and practical. Besides, it doesn't need to deal with the whole image, occupies less system resources and is good for the performance of the smart car.

5.3 Cross-edge detection algorithm

But both the above two methods need to test the whole image. In this paper, a simpler algorithm is adopted. That is retrieving each point to find the position of the target point in the image according to the algorithm. It is called the cross-edge detection algorithm as shown in Fig.8.

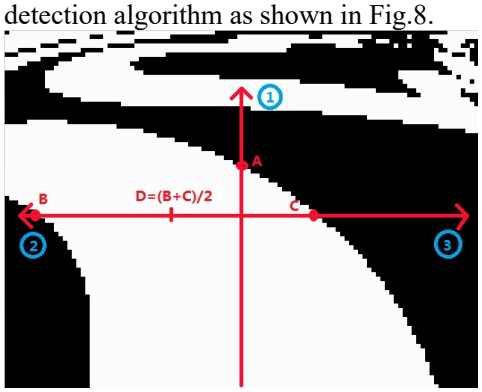

Figure 8 The cross-edge detection algorithm

Steps of cross-edge detection algorithm are as follows:

(1) Retrieve from mid-point of line zero of the image to the first line, then second line until to the midpoint of the last line. Then find A, the first black spot and record the line with point A to be line a.

(2) Retrieve from the midpoint of line (a-n) (n is determined by the debugging experiment), and then find B, the first black spot, which is seen as the left edge.

(3) Retrieve from the midpoint of line(a - n), and then find C, the first black spot, which is seen as the right edge.

(4) Find each midpoint of B and C in line (a-n) and record it as D. D=(B+C)/2.

(5) See point D as the current position of the smart car. The difference between point D and the midpoint of the line (a – n) is the amount of yaw.

As is shown in Fig.9, if the place where point A lies is far away enough, such as after the 60th line, then it is considered to be small curve called "S" or straight. The steering angle is small at this place.

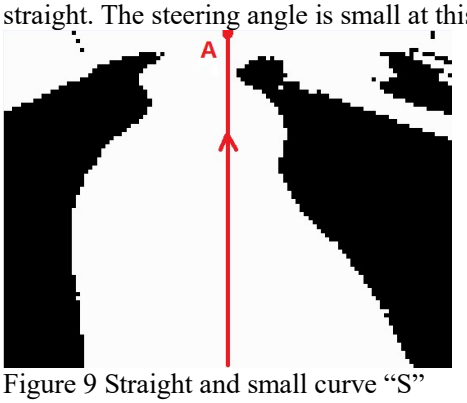

Figure 9 Straight and small curve "S"

When the smart car is running out of the path, we can use the detection algorithm to test the road image. As is shown in Fig.10, if point A is detected

to be very close to the edge, such as less than 20 lines, then the steering angle becomes larger.

Figure 10 The image of the smart car running out of the path

When the smart car is going to drive near the crossroads, two cases will occur. The first is that point A is far away from the edge, which is shown in Fig.11, and it will be considered to be straight or small curve "S". Another case is that point A doesn't appear to be far away enough. But at this time, point B and point C is certainly to be on both ends around the image, and the steering gear return to the middle control position, and then the smart car goes straight forward. The probability of the second case is very small. It only occurs when the direction is not adjusted before running into the crossroads.

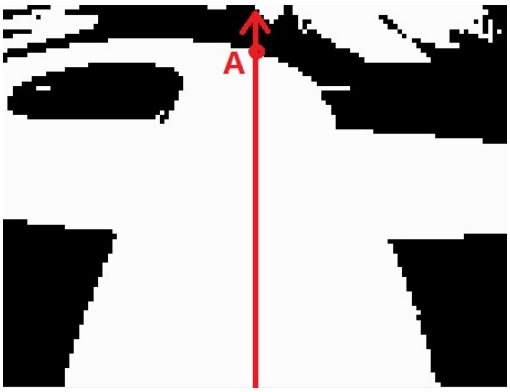

Figure 11 Path of the crossroads

5. RESULT

As to the image preprocessing algorithm, the oscilloscope can be used to measure how much time the new algorithm consumed compared to how much time the traditional algorithm did. The result is shown in Tab.1.

Table 1 Time consumption of the new algorithm and the traditional algorithm

Algorithm	new algorithm	Traditional algorithm(filtering only)	Traditional algorithm(binarization only)	traditional algorithm(filtering and binarization)
time-consumption (μs)	691	536	314	857

We can indirectly represent the difference of the above three algorithms through car speed. Tab.2 shows the average speed of the same smart car on the same track. The difference of their procedural programming is just about the path recognition part. Other parts, including image preprocessing, speed control and direction control, are all the same.

Table2 Average speed of three edge detection algorithm

Algorithm	direct edge detection algorithm	edge tracing algorithm	cross-edge detection algorithm
average speed (m/s)	2.21	2.36	2.59

6. DISCUSSION

As can be seen from the above results, the processing speed of the new algorithm is slow compared with the traditional algorithm(binarization only). However, for the camera-based smart car, using the traditional algorithm means using filtering to remove noise and binarization algorithm to deal with road image. Therefore, from the result of the experiment data, we can know that the processing speed by the new algorithm (691μs) is increased by 19.37% compared with the traditional algorithm (857μs). As a result, the processing time of the microcontroller is saved and the processing speed is also improved, which lay the foundation for the increase of the smart car speed.

Different tracks, such as straightway and curve, the edge condition is different, so even the same path identification method will cost different time to deal with the images collected by the camera. Thus we can't simply decide which algorithm has more superiority just by comparing the time-consumption of the above three algorithms. We can use the idea of controlling the variables, which only changes the code that is used to path identification in the program and evaluates the three algorithms according to the average speed of the smart cars. We can know from the experimental results that when using cross-edge detection algorithm, the smart car can reach the highest speed. This shows that the algorithm has faster processing speed, and at the same time, the processing cycle of the micro controller is short as well as the control cycle of smart cars. So we can control the direction and speed of the smart car in time.

7. CONCLUSION

This article provides a new algorithm by studying path identification of camera-based smart car. The new algorithm combines the traditional filtering

with the binarization. It only needs to traverse each pixel of the image to complete the image filtering and binarization. At the same time, three kinds of path identification methods are also introduced, including the cross-edge detection algorithm which has high efficiency. Using this identification algorithm, we can greatly save the resources of the microprocessor, which shortens the control cycle and improves the real-time control system of the smart car. On this basis of the above work, we have made a smart car based on the camera as shown in Fig.12.Based on the quickness of the above algorithm, the top speed of our smart car can reach 3.1 m/s and the average speed can reach 2.59 m/s.

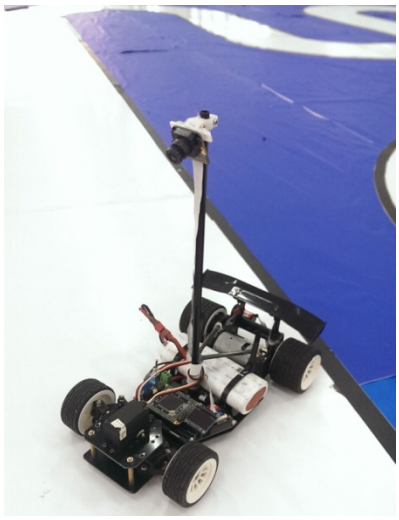

Figure 12 The smart car based on the camera

REFERENCES

[1] Row, S. 2013. The future of transportation: connected vehicles to driverless vehicles. What does it mean to me? . Ite Journal, 83(10), 24-25.

[2] Wuwei C, Mills K, Wenwu S. 2004.A new navigation method for an automatic guided vehicle. J Robot Syst 21(3):129–139.

[3] Wang J. 2011.The Design of the Smart Car Track Recognition Devices Based on XS128 MCU[J]. Value Engineering.

[4] Lukac R, Plataniotis KN. 2006. Single-sensor camera image compression[J]. IEEE Transactions on Consumer Electronics, 52(2):299-307.

[5] Xiang, W. U., & Wang, G. 2015. Control research and realization of the intelligent vehicle based on the electromagnetic navigation. Journal of Sichuan University of Science & Engineering.

[6] Intelligent Vehicle Navigation System Based on Photoelectric Sensor DispersedArrangment[J]. Electronic Engineering & Product World, 2007.

[7] Ran L I, Hai-Jun L I, Yang C. 2014.Disgn of Smart Car Tracing Method Based on Camera Image[J]. Computer Knowledge & Technology.

[8] Qu S C, Tian Y, Chen C. 2011.Fuzzy PID Control for Intelligent Smartcar System with CCD Camera[J]. Key Engineering Materials, 467-469:433-436.

[9] Ke Q, Que D, Lu W. 2015.The Design of a Smart Car Based on a Kind of Dynamic Threshold Algorithm and Speed Control Algorithm[J]. Lecture Notes in Electrical Engineering, 334:871-878.

[10] Corona D, De Schutter B.2008. Adaptive cruise control for a SMART car: A comparison benchmark for MPC-PWA control methods[J]. IEEE Transactions on Control Systems Technology, 16(2):365-372.

[11] A Rosenfeld, A C Kak. 1983. Digital Picture Processing. Beijing Science Press,57-190.

[12] Chen B, Huang X. 2016.Design and implementation of laser scanning rangefinder based on the Freescale MK60[J]. Microcomputer & Its Applications.

[13] Jiang Z, Wang M, Gong W. 2010.The video capture and processing research on Smart car road information based on OV7620 camera[C]// International Asia Conference on Informatics in Control, Automation and Robotics. IEEE Press,108-111.

[14] RafaelC.Gonzalez,Richard E. Woods.2007. Digital Image Processing[M]. Prentice Hall.

The Research on Combined Optimization Scheme of Chemical Elements in Deformed Steel Bar

Yue WU[1], ZiJiao WU[1], Yang PENG[1], Yan LI[2]*
[1]College of Mechanical Engineering, North China University of Science and Technology, Tangshan 063000, Heibei, China
[2]College of Science, North China University of Science and Technology, Tangshan 063000, Hebei, China

Abstract: In this paper, based on the 2016 Problem APMCM B third questions, using modern statistics, on the impact of chemical elements on the performance of the rebar to study, to design the composition of the optimization program. First, a random sampling of 10% of the data. The relative efficiency of the data was screened out by using DEA model, and the relative efficiency of the sample data was 1, and 155 relatively effective data were selected for further optimization. Then, according to the meaning of the problem, the use of national standards in the performance requirements of the conditions to limit the maximum content of Cr elements, other elements of the minimum target, the list of linear programming equation, see equation (4) to solve the Cr content which can increase up to 0. 039, other elements can be reduced to a maximum of 0. 339.
Keyword: deformed steel bar, Composition optimization design, DEA, LP

1. INTRODUCTION

The chemical composition of steel is the ultimate effect of hot-rolled steel structure and basic elements. Most of the deformation of steel using micro-alloying method to adjust the proportion of ingredients to improve the structural properties [1-5]. In this paper, the influence of chemical elements on the properties of rebar is studied. By using modern statistics, the optimal combination scheme is designed to achieve the purpose of ensuring product performance and controlling production cost.

2. DEA SCREENING VALID DATA

Data envelopment analysis（DEA）based on the concept of relative efficiency, According to the multi index input (input) and multi output (output), the decision making units of the same type are evaluated with relative effectiveness or benefit. In this case, 12 kinds of alloying elements, equal to the input required for the production of threaded steel samples, And the three indexes that reflect the mechanical properties of the threaded steel are equivalent to the output. We want to use the minimum input to achieve maximum output, the relative efficiency is the largest, DEA model can be used to screen out the relative efficiency of the largest data, and further optimization.

2. 1 DEA MODEL THEORY

There are n decision-making units DMU_i (1≤i≤n). Each unit has a m entry $x_{1i}, x_{2i}, \ldots, x_{mi}$ and S item output $y_{1i}, y_{2i}, \ldots, y_{si}$（which $x_{ji}, y_{ji} > 0$）. The following input - output matrix[6-9].

	DMU_1	⋯	DMU_i	⋯	DMU_n
Input 1	x_{11}	⋯	x_{1i}	⋯	x_{1n}
Input 2	x_{21}	⋯	x_{2i}	⋯	x_{2n}
…	⋯	⋯	⋯	⋯	⋯
Output m	x_{m1}	⋯	x_{mi}	⋯	x_{mn}
	y_{11}	⋯	y_{1i}	⋯	y_{1n}
Input 1					
Input 2	y_{21}	⋯	y_{2i}	⋯	y_{2n}
…	⋯	⋯	⋯	⋯	⋯
Output s	y_{s1}	⋯	y_{si}	⋯	y_{sn}

The input and output of the DMU_i is recorded as a vector form:

$$x_i = (x_{1i}, x_{2i}, \cdots, x_{mi})^T,$$
$$y_i = (y_{1i}, y_{2i}, \cdots, y_{si})^T$$

record as:

$$X = \begin{bmatrix} x_1 & x_2 & \cdots & x_n \end{bmatrix},$$
$$Y = \begin{bmatrix} y_1 & y_2 & \cdots & y_n \end{bmatrix}$$

X is a multi-index input matrix and the Y is a multi output matrix.
Suppose:

$$v = (v_1, v_2, \cdots, v_m)^T \text{ and}$$
$$u = (u_1, u_2, \cdots, u_s)^T$$

Is the input and output of the weight vector, The total input I_i and the total output O_i of the DMU_i are respectively:

$$I_i = v_1 v_{1i} + v_2 v_{2i} + \cdots + v_m v_{mi} = x_i^T v$$
$$O_i = u_1 y_{1i} + u_2 y_{2i} + \cdots + u_s y_{si} = y_i^T u$$

Obviously, the smaller the total input I_i, the greater the total output O_i, the higher the efficiency of the DMU_i. So, DEA with the total output of the ratio of the total input to measure the size of the effectiveness of DMU_i. Let:

$$E_{ii} = \frac{O_i}{I_i} = \frac{y_i^T u}{x_i^T v}$$

E_{ii} is called the efficiency evaluation index. In the above formula, the weight vectors u and v are to be determined, Each of these components is nonnegative(record as $u \geq 0, v \geq 0$). For each one DMU_i, Find the weight vector that maximizes E_{ii}. Therefore, the C2R model of DEA is obtained. ($\overline{P}$):For each one DMU_i, Solve the following maximization problem:

$$\begin{cases} \max \dfrac{y_i^T u}{x_i^T v} = E_{ii} \\ s.t. \dfrac{y_i^T u}{x_i^T v} \leq 1 (1 \leq j \leq n), u \geq 0, v \geq 0 (\overline{P}) \end{cases}$$

T

his is a fractional programming problem, Let

$$t = \frac{1}{x_i^T v}, \ \omega = tv, \ \mu = tu$$

Then ($\overline{P}$)can be changed into equivalent linear regression problem:

$$\begin{cases} \max y_i^T \mu = E_{ii} \\ s.t. y_j^T \leq x_j^T \omega, x_i^T = 1, \omega \geq 0, \mu \geq 0 (P) \end{cases}$$

The solution of linear programming (P), ω_i^* and μ_i^* is called the optimal weight vector, is to make the DMU_i efficiency value E_{ii} to reach the maximum value of the weight vector. (As a solution to the linear programming, ω_i^* and μ_i^* are not unique.)

Define

(1)If the solution of linear programming (P) ω_i^*, μ_i^* satisfy: $E_{ii} = y_i^T \mu_i^* = 1$, DMU_i is known as weak DEA effective(C^2R);

(2)If the solution of the linear programming (P) solution exists $\omega_i^* > 0, \mu_i^* > 0$ and $E_{ii} = y_i^T \mu_i^* = 1$, DMU_i is known as DEA effective (C^2R).

In order to facilitate testing the effectiveness of DEA, General considerations (P) for the dual model of the equation form(With slack variables and non-Archimedes infinity ε):

$$\begin{cases} \min (\theta - \varepsilon (e_1^T s^- + e_2^T s^+)) \\ s.t. \sum_{j=1}^{n} \lambda_j x_j + s^- = \theta x_i \sum_{j=1}^{n} \lambda_j y_j - s^+ = y_i \\ \lambda \geq 0, s^- \geq 0, s^+ \geq 0 \end{cases}$$

Inside, $s^- = (s_1^-, s_2^-, \cdots, s_m^-)$ is a slack variable in the m entry, $s^+ = (s_1^+, s_2^+, \cdots, s_s^+)$ is a slack variable in the output of the s item; $\lambda = (\lambda_1, \lambda_2, \cdots, \lambda_n)$ is a combination of DMU n coefficient; $e_1^T = (1,1, \cdots,1)_{1 \times m}$, $e_2^T = (1,1, \cdots,1)_{1 \times s}$; ε is a very small number. (General take ε=10^{-6})

Suppose the optimal solution for the linear programming(D_ε) are λ^*, s^{*-}, s^{*+}, θ^*, then

(1)i $\theta^* = 1$ f, DMU_i is known as weak DEA effective(C^2R);

(2)if $\theta^* = 1 \ s*^- = 0, s*^+ = 0$, DMU_i is known as DEA effective (C^2R).

2. 2 DEA MODEL SOLUTION

As the subject is given a large sample data in the appendix, So with the help of SPSS software randomly selected about 10% of the samples for analysis. Import the sample data, By the procedures in Appendix I of this paper, the relative efficiency value of each sample can be obtained.

$$E = \begin{bmatrix} 0.990 & 0 & \cdots & 0 \\ 0 & 0.999 & \cdots & 0 \\ \cdot & \cdot & \cdots & \cdot \\ \cdot & \cdot & \cdots & \cdot \\ \cdot & \cdot & \cdots & \cdot \\ 0 & 0 & 0 & 0.931 \end{bmatrix}$$

Inside, $E_{508} = 0.85884$ is the smallest relative efficiency value of the extracted samples. 51. 08% of the data relative efficiency value of 1. By the definition of knowledg, the relative efficiency value is equal to 1 of the sample, at least weakly effective, and the relative efficiency value is not equal to 1 of the sample, which is not weakly efficient. In order to confirm the validity of the relative efficiency value equal to 1 and to analyze the relative efficiency value is not equal to 1 of the sample, Need to use model D_ε.

By program II, the solution of this problem:

$$\lambda^* = \begin{bmatrix} 0 & 0 & \cdots & 0 \\ 0 & 0 & \cdots & 0 \\ \cdot & \cdot & \cdot \ \cdot \ \cdot & \cdot \\ \cdot & \cdot & \cdot \ 1 \ \cdot & \cdot \\ \cdot & \cdot & \cdot \ \cdot \ \cdot & \cdot \\ 0 & 0 & \cdot \ \cdot \ \cdot & 0 \end{bmatrix}$$

$$s^{*-} = \begin{bmatrix} 0.011 & 0.019 & \cdots & 0.0014 \\ 0.0083 & 0 & \cdots & 0 \\ \cdot & \cdot & \cdots & \cdot \\ \cdot & \cdot & \cdots & \cdot \\ \cdot & \cdot & \cdots & \cdot \\ 0.0027 & 0 & \cdots & 0 \end{bmatrix}$$

$$s^{*+} = \begin{bmatrix} 5.57 & 0 & \cdots & 0 \\ 0 & 1.43 & \cdots & 0 \\ 0 & 0 & \cdots & 0 \end{bmatrix}$$

$$\theta^* = \begin{bmatrix} 0.990 & 0.999 & \cdots & 0.904 & 0.932 \end{bmatrix}$$

As can be seen from the above solutions, the relative efficiency value is equal to 1 of the sample, if $\theta^* = 1$ and Relaxation variable $s^{*-} = 0$, $s^{*+} = 0$, From the theorem, it is relatively effective. The relative effective data accounted for 22. 3% of the sample data, so the screening of the 155 relatively effective data to further optimize the solution.

3.SOLUTION OF COMBINATORIAL OPTIMIZATION

3. 1 CORRELATION ANALYSIS

Q is content of 11 elements other than Cr. Using SPSS software, put the Cr content and Q correlation analysis of the results in Tab. 1.

Table 1 The correlation

		Cr	Q
Cr	Pearson The correlation	1	-0. 080**
	Significant(both sides)		0. 000
	N	7123	7123
Q	Pearson The correlation	-0. 080**	1
	Significant(both sides)	0. 000	
	N	7123	7123

Cr and Q were significantly correlated at the level of 0. 01, and both of them showed a negative correlation. Indicating that Cr content increased, while the other elements content decreased, which meets the meaning of the problem.

3. 2LINEAR PROGRAMMING SOLVING

With the help of the SPSS software, the regression analysis of tensile strength, yield strength and elongation at break as the independent variables were carried out [10]. The results were as follows:

$$\sigma_b = 22.5Q - 253\omega_{cr} + 632 \quad (1)$$

$$\sigma_s = -207Q - 16\omega_{cr} + 455 \quad (2)$$

$$\delta = 0.15Q + 2.4\omega_{cr} + 24.6 \quad (3)$$

Represents the sum of the contents of 11 elements, representing the content of Cr elements. According to the national standard GB 1499. 2-2007 draws the critical index of each kind of performance and comes to the constraint of linear programming:

$$\begin{aligned} &\max\ \omega_{cr} \\ &\min\ Q \\ &s.t.\begin{cases} 22.5Q - 253\omega_{cr} + 632 \geq 630 \\ -207Q - 16\omega_{cr} + 455 \geq 500 \\ 0.15Q + 2.4\omega_{cr} + 24.6 \geq 20.25 \end{cases} \end{aligned} \quad (4)$$

Solution: $Cr \leq 0.039, Q \geq 0.339$

So the Cr content can be increased up to 0. 039, other elements can be reduced to a maximum of 0. 339.

4. CONCLUSIONS

(1)Using the DEA model to screen out the relative efficiency of the largest data, screening out 155 relatively effective data to do further optimization.

(2) Using the national standard requirements for conditions, to maximize the Cr content, other elements in the minimum target, list the linear programming equations, and then solved by the content of Cr can be up to 0. 039, other elements can be reduced by up to 0. 339.

REFERENCES

[1] Huilin Gao. Analysis and review on the yield ratio of pipeline steel [J]. pipe welding, 2010, 06:10-14.

[2] Minghao Huang, Feng Xu, Guojian Huang. Discussion on Factors Affecting Yield Ratio of Pipeline Steel [J]. pipe welding, 2008, 03:20-23+85.

[3] Xinya Li, Ling Jin, Li Liu. Chongqing municipal general undergraduate colleges and universities performance evaluation——An empirical study based on Data Envelopment Analysis [J]. Journal of Southwestern Normal University(Natural Science Edition), 2015, 12:145-151.

[4] Yousen Wang, Hao Xu, Efficiency evaluation method of parallel production system based on Data Envelopment Analysis [J]. Operations Research Transactions, 2015, 04:25-36.

[5] Guoliang Yang, Wenbin Liu, Haijun Zheng. Data envelopment analysis method(DEA) summarize [J]. Journal of systems engineering, 2013, 06:840-860.

[6] Desheng Wu. Research on some theories and methods of data envelopment analysis [D]. University of Science and Technology of China, 2006.

[7] Lijun Han, Zhigang Gao, Xufang Fang, Yue Kou. Analysis of influencing factors on properties of screw steel [J]. Technology and enterprise, 2013, 10:359.

[8] Yuwei Peng, Shouxian Wu, Xiaozhan Xu. Application of MATLAB in data envelopment analysis[J]. Journal of Southwest Nationalities College (Natural Science Edition), 2002, 02:139-143.

[9] Lingyun Lang, Ke Xie, Yankun Guo. Effect of vanadium on Microstructure and mechanical properties of 20MnSi steel for construction[J]. Foundry Technology, 2016, 09:1818-1820.

[10] Yang Li, Longfei Zuo, Jianchun Zhang, Han Ma. Effect of alloy elements on the properties of HRB600 reinforced high cuby[J]. Journal of materials heat treatment, 2016, S1:61-67.

Study on the Chemical Element and Deformed Steel Bar Based on Neural Network Model Correlation analysis

Huan Wang[1], Jingshuo Yang[2], Tong Zhang[3], Jie Li[4]*
[1]School of Economics, North China University of Science and Technology, Tang'shan 063000, China
[2]School of Mechanical Engineering, North China University of Science and Technology, Tang'shan 063000, China
[3]College of Science, North China University of Science and Technology, Tang'shan 063000, China
[4]College of Metallurgy and Energy, North China University of Science and Technology, Tangshan 063000,Heibei,China

Abstract: Hot-rolled bars are mainly used in the framework of reinforced concrete components, the chemical composition of different elements in steel will affect the structural properties of steel, adding trace elements to steel will not only significantly improve the performance of steel, but also can effectively control the cost of production. A Case Study of Mathematical Modeling Contest for College Students in the Asia - Pacific Region in. In this paper, based on the data of chemical elements and steel performance, the BP neural network model is established by using the multiple linear regression equation. The primary and secondary factors affecting the performance of deformed bars are analyzed and their correlations are analyzed.
Keywords: BP neural network model , Multiple Linear Regression Model , Error gradient descent method , Dimensionless processing.

1. INTRODUCTION

Hot-rolled ribs are mainly used in the framework of reinforced concrete components, performance is reflected in the tensile strength, yield strength and elongation after fracture. The chemical composition of the steel is the ultimate structural properties of hot-rolled steel is the basic elements. The micro-alloying method was used to add expensive trace elements to the steel. The BP neural network model was used to establish the three-layer nonlinear network structure of chemical elements and properties. The corresponding weights and thresholds were calculated by the BP neural network toolbox, Then integrated into the intuitive equation, which adjust the composition ratio, can improve the structural performance, while effectively guaranteeing performance and control of production costs[1].

2. AN OVERVIEW OF BP NEURAL NETWORK

BP neural network is a feedforward network, the minimum variance of learning, because of its connection weights adjustment is used in the reverse propagation of the learning algorithm, also known as error back propagation network (BackPropagation).

BP algorithm from both positive and negative aspects of the same time: forward propagation of the input information and back-propagation error information. The forward propagation of the input information is the propagation of the sample data from the input to the output. The back propagation of the error is the correction of the weights and thresholds from the output to the input. The flow chart is shown in Figure 1 below[2].

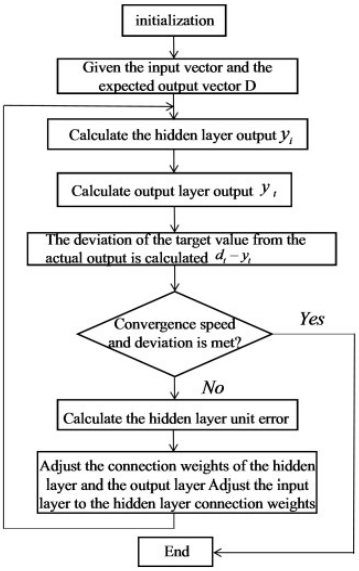

Figure 1. BP neural network algorithm flow chart

The corresponding BP algorithm is divided into two stages:

2.1 signal back propagation

When the input layer input information,  the hidden layer i node to receive information net_i

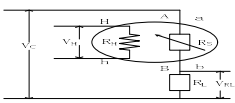 (1)

Hidden layer of the i node output net_i :

$$net_k = \sum_{i=1}^{q} w_{ki} y_i + a_k \quad (2)$$

Output layer of the k node output y_k:

$$y_k = \psi(net_k) \tag{3}$$

2.2 forward propagation of oerrors

Error propagation, that is, the error you want to spread from the output layer by item to calculate the output error, and then according to the error gradient to calculate the threshold and the weight value, and then the revised threshold and weight input corresponding position.

For each sample p there is a quadratic error criterion function of

$$E_p : E_p = \frac{1}{2}\sum_{j=1}^{p}\sum_{k=1}^{l}(T_k^p - o_k^p) \tag{4}$$

According to the error gradient descending method in order to correct: the output layer weight value of the correction Δw_{kl} ,Output layer threshold of the amount of correction Δa_k ,Hidden layer weight of the amount of correction Δw_{ij} ,Hidden layer threshold of the amount of correction $\Delta\theta_i$.

$$\Delta a_k = -\eta\frac{\partial E}{\partial a_k}$$

$$\Delta w_{ij} = -\eta\frac{\partial E}{\partial w_{ij}}$$

$$\Delta\theta_i = -\eta\frac{\partial E}{\partial\theta_i} \tag{5}$$

Output layer weight adjustment formula:

$$\Delta w_{kl} = -\eta\frac{\partial E}{\partial w_{kl}} = -\eta\frac{\partial E}{\partial y_k}\frac{\partial y_k}{\partial net_k}\frac{\partial net_k}{\partial w_{kl}} \tag{6}$$

Output layer threshold adjustment formula:

$$\Delta a_k = -\eta\frac{\partial E}{\partial y_k}\frac{\partial y_k}{\partial net_k}\frac{\partial net_k}{\partial a_k} \tag{7}$$

Implied layer weight adjustment formula:

$$\Delta w_{ij} = -\eta\frac{\partial E}{\partial y_i}\frac{\partial y_i}{\partial net_i}\frac{\partial net_i}{\partial w_{ij}} \tag{8}$$

Hidden layer threshold adjustment formula:

$$\Delta\theta_{ij} = -\eta\frac{\partial E}{\partial\theta_i} = -\eta\frac{\partial E}{\partial y_i}\frac{\partial y_i}{\partial net_i}\frac{\partial net_i}{\partial w_{ij}} \tag{9}$$

3. MODEL ESTABLISHMENT AND SOLUTION

3.1the variable is determind

The input variable $x_i(i = 1,2\cdots 12)$ is determined from the twelve chemical element data contained in the deformed bars given in Annex 1, and the yield variable $y_k(k = 1,2,3)$ is defined as the yield strength, the tensile strength and the elongation after fracture.

3.2 immeasurable steel treatment

Standardization formula for dimensionless processing: $Z_i = \dfrac{x_i - \bar{x}}{s_i}$

3.3 determination of the number of nodes in hidden layer

There is a great correlation between the number of hidden nodes in BP neural network and the progress of BP neural network: the number of nodes is too small and the training capacity of God will become weaker and cannot finish the calculation accurately. , The training time of the neural network becomes longer, and the neural network may appear over-fitting. So the selection of the appropriate number of nodes in order to maximize the performance of neural network play.

Determine the number of implicit layer nodes m formula: $m = \sqrt{i + k}$

Among them, i is the number of output variables, k is the number of input variables. From this we can determine the number of hidden layer nodes 4.

3.4 bp network structure determination

According to the error gradient descent method, the weights of the input layer to the hidden layer are obtained(Table 1,Table 2,Table 3).[3]

Table 1 Tensile strength factor of the element input layer to the hidden layer weight

C	MN	S	P	Si	Ceq
1.8407	0.3380	-0.5029	0.1317	-0.3717	-1.7601
0.9954	-0.5856	-1.9539	0.1643	4.0375	-0.7584
0.4204	2.6431	0.9990	-0.4203	1.2259	-3.9967
-1.0626	0.0586	0.6906	-0.3464	-0.2157	1.1990
V	Cr	Ni	CU	MO	ALT
0.2869	7.5920	-2.4282	-1.5886	1.5112	0.0215
1.0415	-6.6642	5.6774	-7.4456	1.4337	-1.4515
1.6115	2.6103	-0.9263	2.5830	2.4779	1.4048
0.0179	-5.6374	1.2676	2.6541	-1.8530	15.4616

Table 2. Yield strength factor of the element input layer to the hidden layer weight

C	MN	S	P	Si	Ceq
0.9108	0.6473	-0.0631	0.4231	0.1491	0.7811
0.4587	0.1016	-0.2473	-0.3033	1.2214	-1.0161
-0.5924	0.1823	0.6367	0.2090	0.5290	0.5821
0.4634	0.0025	0.6854	0.2910	0.0793	0.8633
V	Cr	Ni	CU	MO	ALT
0.7719	0.7449	-0.3107	0.2847	-0.0397	0.0999
-0.0155	-2.1653	-1.1158	-0.8584	0.4909	0.8964
0.6444	-0.0667	-0.0679	0.8971	0.5968	0.2119
0.1747	-0.9193	1.0578	0.6722	-0.0854	-0.2665

Table 3. Percentage elongation after fracture factor of the element input layer to the hidden layer weight

C	MN	S	P	Si	Ceq
-0.3164	0.4261	-0.3372	-0.0122	0.2110	0.1895
-0.0636	-0.4941	0.0321	0.0230	-0.6676	0.3354
0.4435	0.9280	0.8910	-0.3562	1.0194	-1.1479
-0.6332	-1.2235	-1.4022	0.5855	-1.0208	1.6345
V	Cr	Ni	CU	MO	ALT
0.2388	-1.8934	1.5215	4.4306	-2.8926	3.4491
-0.2585	1.4184	-0.9533	-2.1240	2.1727	-8.5244
0.6446	-1.6460	1.3001	-0.8854	-1.7832	2.6836
-0.8899	1.9997	-1.7766	2.0120	1.9729	-1.4207

Tensile strength：

Threshold for input layer to hidden layer:

$$\theta_i = (2.2692,-5.4969,4.5685,13.4152)^T \quad (10)$$

The weight of the hidden layer to the output layer:

$$w_{kl} = (0.2352,0.0634,-0.1047,0.2304)^T \quad (11)$$

Threshold of the hidden layer to the output layer:

$$a_k = -0.0914 \quad (12)$$

Yield strength:

Threshold for input layer to hidden layer:

$$\theta_i = (-1.8294,-2.0878,-0.3244,2.3605)^T \quad (13)$$

The weight of the hidden layer to the output layer:

$$w_{kl} = (0.0475,0.1092,-0.6606,0.3266)^T \quad (14)$$

Threshold of the hidden layer to the output layer:

$$a_k = -0.0404 \quad (15)$$

Percentage elongation after fracture:

Threshold for input layer to hidden layer:

$$\theta_i = (5.2368,-8.7679,1.5814,0.2564)^T \quad (16)$$

The weight of the hidden layer to the output layer:

$$w_{kl} = (-0.7787,-1.5269,-1.8444,-1.1984)^T \quad (17)$$

Threshold of the hidden layer to the output layer:

$$a_k = -2.1444 \quad (18)$$

4.THE RESULTS ARE OBTAINED AND CONCLUSION

From the above calculation, we can get the regression equation of the three properties of the deformed steel bars.

$$y_1 = 583.97x_1 + 319.287x_2 + 579.369x_3 - 8.004x_4$$
$$+71.514x_5 - 44.309x_6 + 0.002x_7 - 47.873x_8$$
$$+67.987x_9 + 813.452x_{10} + 22.923x_{11} + 39.690x_{12}$$
$$y_2 = 391.736x_1 + 226.512x_2 + 584.402x_3 - 21.227x_4$$
$$+58.066x_5 - 34.048x_6 + 0.001x_7 - 101.046x_8$$
$$+66.190x_9 + 529.329x_{10} - 205.150x_{11} + 33.978x_{12}$$
$$y_3 = 25.551x_1 + 12.668x_2 + 11.501x_3 + 13.760x_4$$
$$+2.485x_5 - 5.299x_6 + 29.609x_7 + 9.505x_8$$
$$+11.131x_9 + 30.316x_{10} - 241.217x_{11} + 7.332x_{12}$$

The main secondary factors affecting yield strength are Mn and Ni, respectively; the main secondary factors affecting the elongation after fracture are Cu and Ni, respectively; the main secondary factors affecting the tensile strength of the deformed bars are Ni and Mn, Cu and Ni.

REFERENCES

[1] ZHANG Wei-wei, ZHAO Cheng-lin, LI Guang-bang, WANG Li-juan. Application of BP Neural Network in Iron and Steel Industry [J]. 2010,04:16-20.

[2] LUO Yu-chun, DOU Hong-ji, CUI Fang-fang. Analysis of the relationship between BP neural network structure and function approximation ability based on Matlab[J]. 2007,24:88-90.

[3] Li Yang, Zuo Longfei, Zhang Jianchun, Ma Han. Effects of alloying elements on the properties of HRB600 steel bars[J]. Journal of Materials Heat Treatment,2016, S1:61-67.

Multivariate Linear Based on the Theory of the Lasso and its Related Analysis and its Application

*Yuhan Li,HaoMen,Shichao Yu,Aimin Yang**

North China University of Science and Technology,Tangshan 063000,China

Abstract: Based on Lasso multivariate linear regression method, a model of the influence of chemical elements on properties of deformed steel bar. First of all, the variables selection in the multiple linear regression equation was optimized by using Lasso and its correlative theory. Then the tensile strength, yield strength, yield ratio and elongation at break are analyzed, and the improved multiple linear regression model was established. Finally, the function relationship between elements and properties are obtained.

Key words: elongation at break; Lasso; multivariate linear regression; yield ratio

1. INTRODUCTION

Linear model is one of the important branches of modern statistical theory. For the linear regression model, the accuracy of the model depends on the choice of variables and the value of the regression parameters [1,2]. In this paper, the lasso algorithm is applied to the multivariate linear regression to improve the performance of the deformed steel bar [3,4].

2. THE ESTABLISHMENT OF THE IMPROVED LINEAR MULTIPLE REGRESSION MODEL

(1)The concept of Linear Multiple Regression model

General multivariate linear model in form is to generalize a unitary dependent variable X to the more dependent variable $X_1,...,X_p$. The concept of test point is the same as the unitary station. It can be written as follow [5]:

$$Y=\begin{pmatrix} y_{11} & \cdots & y_{1q} \\ \cdots & \cdots & \cdots \\ y_{n1} & \cdots & y_{nq} \end{pmatrix} \tag{1}$$

It is also known as the design matrix. Observations are p dimensional vector. It is $n\times p$ order matrix.

$$X=\begin{pmatrix} x_{11} & \cdots & x_{1p} \\ \cdots & \cdots & \cdots \\ x_{n1} & \cdots & x_{np} \end{pmatrix} \tag{2}$$

The corresponding matrix of the error is:

$$\omega=\begin{pmatrix} \omega_{11} & \cdots & \omega_{1p} \\ \cdots & \cdots & \cdots \\ \omega_{n1} & \cdots & \omega_{np} \end{pmatrix} \tag{3}$$

Among them, the matrix of the unknown parameters is:

$$B=\begin{pmatrix} \beta_{11} & \cdots & \beta_{1p} \\ \cdots & \cdots & \cdots \\ \beta_{1p} & \cdots & \beta_{np} \end{pmatrix} \tag{4}$$

This is a $q\times p$ order matrix. The j column β_j affect the results of the j. The gotten general multivariate linear model is [6]: $X=YB+\omega$

In the estimates of unknown parameter matrix B, we can use a dollar of least square method. At the state of unitary situation, making $\hat{\beta}$ be the estimation of β, and discussing the sum of the squares of the residuals $\hat{\omega}\cdot\hat{\omega}$, minimizing it, the gotten is the least squares estimate. Now we are to clear in what sense the sum of the squares of the smallest was conducted. Generally speaking, there are four conditions minimize the sum of squares:

1)To minimize the maximum characteristic root of $\hat{\omega}\cdot\hat{\omega}$, that is, find out $\hat{\beta}$ and let

$$\max eig\{(X-Y\hat{B})^T(X-Y\hat{B})\}\le\max eig\{(X-YB)^T(X-YB)\}$$

is established for all the matrix B.

2)After the residuals in column ω, find out $\hat{\beta}$ to make the minimum number $\hat{\omega}\cdot\hat{\omega}$. It means

$$trac(X-Y\hat{B})^T(X-Y\hat{B})\le trac(X-YB)^T(X-YB)$$

is established for all the matrix B.

3) Being the minimum the sense of nonnegative matrix. It is to say that finding out $\hat{\beta}$, make

$$(X-Y\hat{B})^T(X-Y\hat{B})\le(X-YB)^T(X-YB)$$

is established for all the matrix B.

4) being the minimum in the sense of the determinant. It means finding out $\hat{\beta}$, making

$$\left|(X - Y\hat{B})^T(X - Y\hat{B})\right| \le \left|(X - Y\hat{B})^T(X - YB)\right|$$

is established for all the matrix B.

The desires $\hat{\beta}$ is very similar to the unitary least-square method:

$$\hat{B} = (Y^T Y)^{-1} Y^T X ,$$

It is also a least squares estimate of multivariate linear model.

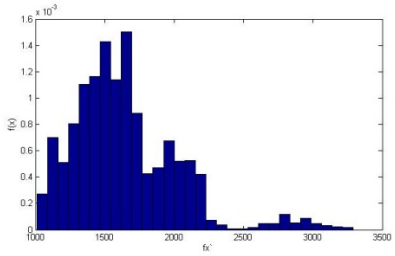

Fig 1 Multiple linear fitting

(2)Regression of Lasso and related method to multiple linear

In the above four kind of sense of minimum has been proved. It should be considered from the perspective of practical application and use the relatively simple method. Based on the Lasso estimate definition [7,8].

a) The biggest characteristic value compression estimation

Trace is several characteristic value of matrixand matrix. The biggest characteristic value of it plays an important role. A kind of the biggest characteristic is:

$$\hat{B}(eig) = \arg\min trac\{(X-YB)^T(X-YB)\}, s.t. \max eig\{B^T B\} \le t。$$

This method, directly using the matrix eigenvalues, shows the number of embodies the matrix characteristics

b) Estimate matrix trace compression

In order to simplify the complicated calculation, from four smallest meaningful discussions before we know, the use of a matrix trace compression estimated is

$$\hat{B}(trac) = \arg\min trac\{(X-YB)^T(X-YB)\}, s.t. trac\{\hat{B}B\} \le t$$

It has the advantage that the determinant compression estimation method. And ithas the multiple linear regression model parameters for the characteristics of the vector matrix. It can have reduced the computation complexity [9].

In the above several estimates it can be known that in the form of Linear Multiple Regression model for variable selection is the key algorithm. The regression algorithm at smallest Angle and Lasso algorithm is difficult to be applicate here, so we choose using stochastic simulation algorithm to solve the problem.

It need to compute the constraint. The first step is to change the calculating maximum constraints $T = \sum_j \left|\hat{\beta}_j^0\right|$,penalty function listed to the estimation algorithm before. If it is in the norm compression estimation m_1 , the corresponding maximum constraints changes to $T = \sum_i \sum_j \left|\hat{\beta}_{ij}^0\right|$. If it is in the determinant compression estimates, the corresponding maximum constraints changes to $T = \det(\hat{B}^{0T}\hat{B}^0)$, , in which $\hat{B}^0$ is the least square matrix of the original Linear Multiple Regression.

In step 4 of stochastic simulation algorithm, to calculate residual SSE, unary Linear Multiple Regression, and get a numeric value is convenient. In a Linear Multiple Regression model, what we get is a matrix, using the method of this article set forth in section 2.1.1 matrix is the second residual error [10].

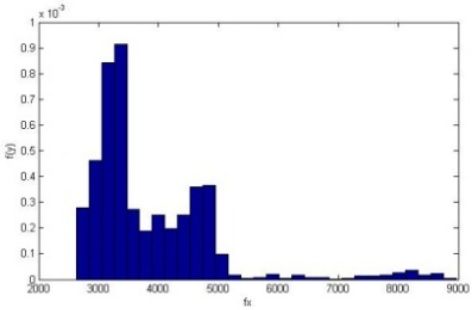

Fig 2 Multiple linear fitting

3. SOLUTION OF THE MODEL

Through using Linear Multiple Regression model analysis C, MN, V, CR, NI and deformed steel tensile strength, yield strength and deformation of the reinforcement of the relationship between the elongation at break, it can be deformed steel tensile strength, yield strength and deformation of the reinforced elongation at break and C, V, CR, MN, NI element, the multiple linear relationship between its expression, as shown below:

$$T = 645.6344C + 146.3963Mn + 5.1766V + 224.1721Cr - 274.1676Ni + 145.4744$$

$$Y = 647.64388C + 76.3496Mn + 1.8900V + 424.7270Cr - 291.9525Ni + 133.2878$$

$$P = 647.64388C + 76.3496Mn + 1.8900V + 424.7270Cr - 291.9525Ni + 133.2878$$

T means Tensile strength, Y means Yield strength, P means percentage elongation after fracture.

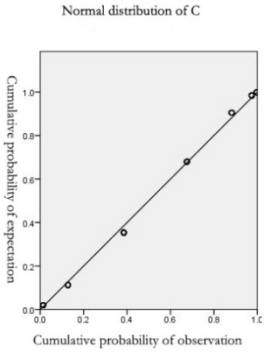

Fig 3 Normal distribution of C

The ratio of yield strength and tensile strength is called the yield ratio. It is a reaction of steel utilization and use of safe and reliable. The yield ratio

and C, MN, V, CR, NI the relationship between as follows:

$$Y/T = 0.0839C + 0.0061Mn + 0.7498V + 0.2620Cr - 0.0781Ni \quad (5)$$

Y/T means Tensile strength/Yield strength.

REFERENCES

[1] R. Dennis Cook, Xin Zhang. Simultaneous Envelopes for Linear Multiple Regression[J]. Technometrics, 2014, 57(1): págs. 11-25.

[2] Marrero P D, et al. Linear Multiple Regression with Variable Selection by a Successive Projections Algorithm Applied to The Analysis of Anodic Stripping Voltammetry Data[J]. ElectrochimicaActa, 2014, 127(5):68-78.

[3] Valente G, Castellanos A L, Vanacore G, et al. Linear Multiple Regression of High-Dimensional FMRI Data with Multiple Target Variables[J]. Human Brain Mapping, 2014, 35(5):2163–2177.

[4] Farkas A, Vajna B, Sóti P L, et al. Comparison of Multivariate Linear Multiple Regression in Micro-Raman Spectrometric Quantitative Characterization[J]. Journal of Raman Spectroscopy, 2015, 46(6):566–576.

[5] Li Jun. Prediction method Using the Multivariate Linear Multiple Regression Based on the Factor Analysis and its Applications on the Share Price Forecast[D].Nanjing University,2014.

[6] Li Ying. Based On Time Sequence And Multiple Linear Multiple Regression Of Rural Cigarette Sales Forecasting[D].Yunnan University, 2015.

[7] ZhouChen,etc.Research on Water Requirement in Northeast Area Based on Multiple Linear Multiple Regression [J]. Mathematics in Practice and Theory,2014,01:118-123.

[8] Zhang B, Lai L. Multiple Change-Points Estimation in Linear Multiple Regression via Sparse Group Lasso[J]. IEEE Transactions on Signal Processing, 2015, 63(9):2209-2224.

[9] Li Y, Nan B, Zhu J. Multivariate sparse group lasso for the Multivariate Multiple Linear Regression With an Arbitrary Group Structure[J]. Biometrics, 2015, 71(2):354–363.

[10] Lockhart R, Taylor J, Tibshirani R J, et al. A significance test for the lasso[J]. Annals of Statistics, 2014, 42(2):413-468.

[11] Wasserman L. Discussion: "A significance test for the lasso"[J]. Annals of Statistics, 2014, 42(2):501-508.

[12] Reid S, Tibshirani R, Friedman J. A Study of Error Variance Estimation in Lasso Regression[J]. Statistica Sinica, 2014.

[13] Hansen N R, Reynaudbouret P, Rivoirard V. Lasso and probabilistic inequalities for multivariate point processes[J]. Bernoulli, 2015, 21(1).

The Research on Prediction Model of Temperature and C Content in Metal Smelting

Fanbei Kong[1],Xiangyu Xu[1],Bo Zhao1,Aimin Yang[2,*]

[1]Yi Sheng College,North China University of Science and Technology,Tangshan Hebei,063000,China

[2]College of Science,North China University of Science and Technology,Tangshan Hebei,063000,China

Abstract: In the process of metal smelting, there is great economic and environmental benefits in the online prediction of temperature T and C content. In this paper, an online prediction model is established based on the improved BP neural network algorithm combined with the rule of metal smelting and the conjugate gradient method .The cross test results results show that the model can be used to solve the prediction problem of metal smelting.

Keywords: BP neural network; factor analysis; metal smelting law; conjugategradient method; online prediction.

1. INTRODUCTION

In the metal smelting process, there has a huge economic and environmental benefits for the online prediction of temperature T and C content. However, because people are not fully grasp the real reaction mechanism, accurate and timely online prediction effect is very difficult to achieve.

The temperature prediction model of T and C content of optical information based on data is an important branch of the prediction model [1]. In order to reduce the number of input data, try to find one or more characteristic values of light intensity data, which will be used as input to reduce the complexity of the model calculation, and enhance the applicability of the model.

A convenient and efficient BP neural network model [2] with high accuracy is established in this paper,which combined with optical information characteristics and time t, gas accumulation consumption and other variables. Achieving the temperature T, C content online accurate prediction and improving the smelting efficiency and output value.

2. EXPERIMENTAL

2.1 study area

In order to realize the prediction of the temperature T and the key elements of the content of C, combining the conjugate gradient method and BP neural network algorithm, prediction model of T and C in temperature making up the standard BP neural network itself may fall into the local minimum point, learning step length fixed caused by the lack of long training time and shortcomings [3], get more ideal training accuracy and shorter training time.

Model training process is as follows:

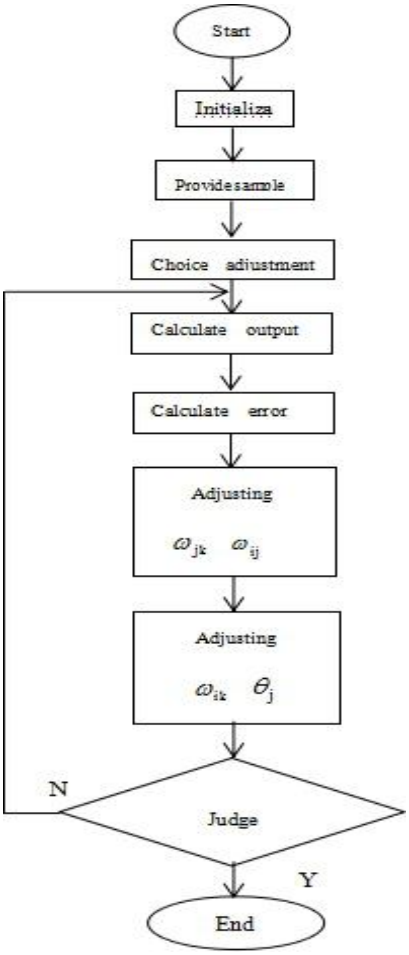

Figure 1 model training process

(1)The output layer node outputs:

$$Z_j = f(\sum_j w_{jk} y_j - \theta_k) = f(net_k) \quad (1)$$

Among them, f is the output layer activation function, and θ_k is the threshold value of the output layer.

(2)Similarly, the output of hidden layer node is:

$$y_j = g(\sum_j w_{jk} y_j - \theta_j) = g(net_j) \quad (2)$$

Among them, g is the hidden activation function and also the hidden layer threshold .

(3)The error function of the neural network [4] is defined:

$$E = \frac{1}{2}\sum_{k}(t_k - z_k)^2 \quad (3)$$

Among them, the expected value of the output node is t_k, and the output value of the network computing is z_k.

(4)The Connection weight coefficient and threshold value of the output layer network.

$$\Delta w_{jk} = \eta \cdot (t_k - z_k) \cdot f^{'}(net_k) \cdot y_j \quad (4)$$

(5)The closed value of the output layer θ_k

$$\Delta\theta_k = -\eta \frac{\partial E}{\partial \theta_k} \quad (5)$$

$$\theta_k(n+1) = \theta_k(n) - \eta\delta_k \quad (6)$$

(6)The connection weight coefficient and threshold value of the hidden layer network.

$$\Delta w_{ij} = \eta^{'} \cdot \delta_j \cdot x_i \quad (7)$$

(7)The adjustment of the threshold of the hidden layer nodes.

$$\Delta\theta_j = -\eta^{'} \frac{\partial E}{\partial \theta_j} = -\eta^{'}\delta_j \quad (8)$$

$$\theta_j(k+1) = \theta_j(k) - \eta^{'}\delta_j \quad (9)$$

2.2 THE TRAINING RESULTS OF THE MODEL

Considering the actually requirements, system of pre training accuracy is set as 0.0001, and the batch mode error convergence condition is relatively simple to achieve shorter training time [5]. In this way, making use of the algorithm mentioned above and the construction of the network model, you can put the sample data into the model after normalization for training, training a one note for a Epoch, figure 2 shows the training process of the network model, when running to 127 Epochs, the training accuracy can meet the requirement of training results, as shown in Figure 2.

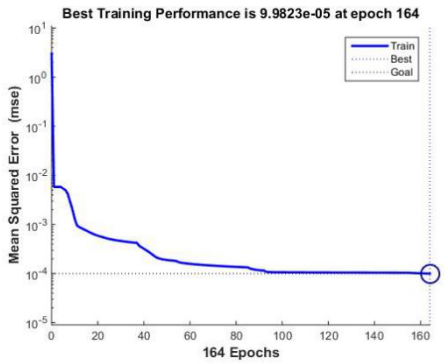

Figure 4 network training process

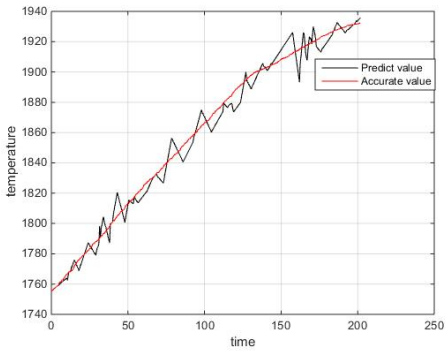

Figure 5 the training value and the actual value distribution (temperature T)

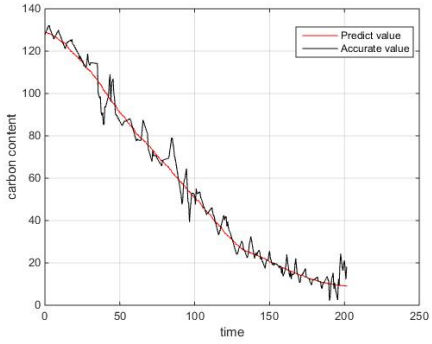

Figure 6 the training value and the actual value distribution map (C content)

3. SUMMARY

What can be seen from the above results, this paper established the neural network prediction model for the algorithm has obvious effect, and fitting with satisfactory results of their training sample data, because the accuracy of the training error and the prediction error within 5S was above 76%, and the system response time is less than 2S, One end to meet the requirement of converter prediction. Although these results basically meet the requirements of the forecast, to further improve the prediction accuracy, the following problems also need to be solved.

(1)The selected training samples in the model are compressed. Artificial [6]to the abnormal data of the furnace discarded, so as to ensure the rationality of the model samples, and the furnace was abandoned more than the larger furnace interference by the scene, so the above model was established for the furnace condition only good furnace Times, for the interference of the furnace is not a better solution. But this interference is produced by the whole process and the environment caused by the need for smelting departments to coordinate and solve.

(2)The input data used in the model are collected after the off-line processing, we analyze the law of data is built on the data obtained in the information. In the process of real-time acquisition, it is difficult to obtain certain input values, for example, the time of the highest point of the image at the end of the converter steel-making in the input, because the image feature value is affected by the blowing

process Interference fluctuates greatly, so it is difficult to judge the highest point accurately.

REFERENCES

[1]Aula M, Leppanen A, Roininen J. Characterization of Process Conditions in Industrial Stainless Steelmaking Electric Arc Furnace Using Optical Emission Spectrum Measurements[J]. Metallurgical and Materials Transactions B, 2014, 45(3):839-849.

[2]ShiZhandong.Comparativeanalysis and Improvement Research of converter end point control model[D]. Chongqing University , 2008.

[3]WenHongyuan.Research on Modeling and prediction of BOF end point mouth radiation information[D]. Nanjing University of Science and Technology, 2009.

[4]WangKun.Based on spectrum analysis and support vector machine algorithm for the end point carbon classification of converter steelmaking [D]. Nanjing University of Science and Technology, 2015.

[5]ShuaiLi.Prediction model of converter end point based on Grey RBF neural network [D]. Northeastern University, 2014.

[6]YuanwangPan,YanminShao,ChangShen.Flame multispectral analysis technology to predict end point carbon based on [J]. Metallurgy in Anhui , 2015 (1): 1-3.

The Influence of Chemical Element on Blast Furnace Slag

*Yujing Li, Peng Zhang, Xiang Li, Aimin Yang**

Electrical Engineering, North China University of Science and Technology, Tangshan 063000,China

Abstract: Blast furnace slag is the skeleton of reinforced concrete member, in which the chemical composition is the basic element that affects the structural properties of deformed bars. In this paper, the effects of chemical elements on the properties of deformed bars are studied. carried out the following discussion: First of all, 12 factors were used as 12 variables, and two main factors were analyzed by SPSS, and two principal factors were obtained. Secondly, 12 types of impact factors were classified according to the relevance to get the main factors affecting the performance of deformed bars were C, Mn and Ceq, and the minor factors were Cr, Ni and Cu. Finally, the correlations among the influencing factors were analyzed. The results showed that the correlations of Cr and Mn were significant at 0.01 level. On the basis of the analysis, the influence of chemical elements on the main structural properties of rebar was analyzed.

Keywords: Blast furnace slag; Factor analysis; Chemical element

1. INTRODUCTION

Hot-rolled ribbed bar is commonly known as deformed blast furnace slag, it's mainly used for skeleton of reinforced concrete component and it requires certain mechanical strength, bending and deformation properties, fabrication weld ability in use. The chemical composition in steel is the basic element that influences the final structure property of hot rolled steel. There is no clear dependency between the blast furnace slag like tensile strength, yield strength and percentage elongation after fracture, elements like C, Mn, S, P, Si, Cr, Mo, Cu, Ni, Alt, V and other influence factors, Most blast furnace slag adopts micro alloying method, that is to add expensive microelement (such as Mn alloy material, V alloy material, etc.) into steel, adjust the composition proportion and to improve structure property. In order to guarantee the properties and control the production cost effectively at the same time. Modeling to study the influence of blast furnace slag properties on chemical element and optimize the composition. In this paper, the factor analysis method is used to analyze the structure and properties of rebar and its main chemical elements, and the main influencing factors and secondary factors are studied.

2 PRIMARY AND SECONDARY FACTORS AFFECTING THE BLAST FURNACE SLAG

This section uses factor analysis to determine the primary and secondary factors affecting the blast furnace slag, and the correlation between the factors were studied.

2.1 DETERMINE PRIMARY AND SECONDARY FACTORS BASED ON FACTOR ANALYSIS

Factor analysis can be regarded as the extension and extension of principal component analysis. The idea is to find out the most information that can reflect the original variables synthetically through the study of the relations among variables, Then the original variables are grouped according to the size of the correlation, so that the correlation among the variables within the group is high, while the correlation between the variables of different groups is low. In this section, we use 12 factors as the 12 variables. We use factor analysis to reduce the dimension. We use a few factors to represent the original variables.

According to the 12 known variables given in the annex, the specifications 1 and 2 deformed bars are analyzed separately. The following takes the specification 1 as an example to establish the mathematical model of factor analysis:

$$X_i = a_{i1}F_1 + \cdots + a_{im}F_m + \varepsilon_i \ (m \le 12) \quad (1)$$

$$\begin{bmatrix} X_1 \\ X_2 \\ \vdots \\ X_{12} \end{bmatrix} = \begin{bmatrix} \alpha_{11} & \alpha_{12} & \cdots & \alpha_{1m} \\ \alpha_{21} & \alpha_{22} & \cdots & \alpha_{2m} \\ \vdots & \vdots & & \vdots \\ \alpha_{121} & \alpha_{122} & \cdots & \alpha_{12m} \end{bmatrix} \begin{bmatrix} F_1 \\ F_2 \\ \vdots \\ F_m \end{bmatrix} + \begin{bmatrix} \varepsilon_1 \\ \varepsilon_2 \\ \vdots \\ \varepsilon_{12} \end{bmatrix}$$

Where $F_1, F_2, \cdots, F_m$ is the common factor, is the unobservable variable, and their coefficient $a_{i1}, a_{i2}, \cdots, a_{im}$ is the factor load. ε_i is a special factor that can not be included by the first *m* common factors. And the following conditions are satisfied:

$$\operatorname{cov}(F, \varepsilon) = 0 \quad (2)$$

That is,F, ε is not relevant;

$$D(F) = \begin{bmatrix} 1 & & & \\ & 1 & & \\ & & \ddots & \\ & & & 1 \end{bmatrix} \quad (3)$$

That is, $F_1, F_2, \cdots, F_m$ is not related to each other, the variance is 1;

$$D(\varepsilon)=\begin{bmatrix}\sigma_1^2 & & & \\ & \sigma_2^2 & & \\ & & \ddots & \\ & & & \sigma_8^2\end{bmatrix} \quad (4)$$

That $\varepsilon_1,\varepsilon_2,\cdots,\varepsilon_i$ is not related to each other, the variance is not necessarily equal, subject to normal distribution $\varepsilon_i \sim N\left(0,\sigma_i^2\right)$

2.2 MODEL ESTABLISHMENT

Import the original data In the SPSS to normalize original data and then consider if and there is a certain linear relationship between the original variables.

SPSS was used to calculate the correlation matrix among the variables, the correlation coefficients were observed, and the KMO test and Bartlett sphericity test were used to judge the correlation coefficient. The results of the software analysis are shown in Tables 1.

Tab 1 KMO Test and Bartlett Sphericity Test

The Kaiser-Meyer-Olkin metric for sampling adequacy		0.428
Bartlett's Sphericity Test	Approximate chi-square	34475.199
	df	66
	Sig.	0

As can be seen from Table 1, most of the correlation coefficients in the correlation matrix are greater than 0.3, the KMO statistic is 0.428, the Bartlett's sphericity test is approximately 34475.199, the degree of freedom is 66, and the bilateral test value is 0.000. Indicating that there is a strong correlation between the concentration of elements, indicating that factor analysis can be carried out. Using SPSS to do the factor analysis of gravel map, shown in Figure 1:

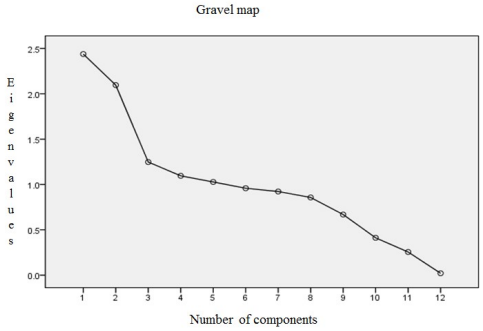

Fig 1 Factor analysis of gravel plot

It can be seen from the above factor analysis of gravel map of the first two factors significantly larger eigenvalues, solid selection of two principal components as a factor is more appropriate. Using SPSS to calculate the load of each variable on the principal component, the results are shown in Table 2:

Tab 2 The main component load

	Ingre	dient
	1	2
C	0.752	0.185
MN	0.767	-0.12
S	-0.04	0.01
P	0.195	0.273
SI	0.423	-0.59
Ceq	0.94	0.188
V	0.402	-0.12
Cr	0.052	0.88
Ni	0.086	0.545
Cu	-0.1	0.692
MO	0.042	-0.14
ALT	-0.03	-0.05

From the analysis of Table 3, the first principal factor showed strong positive correlation with C, Mn and Ceq. The second principal factor showed a strong positive correlation with Cr, Ni and Cu.

In the same way, the influencing factors in specification 2 are analyzed. The obtained factor analysis gravel map and each principal component load are shown in the appendix. It can be seen from the analysis that the specification 2 is consistent with the principal component factor of the blast furnace slag which is extracted from the specification 1. Therefore, the study of blast furnace slag impact factors can be divided into two categories. The main factors are: C, Mn, Ceq; secondary factors: Cr, Ni, Cu.

Combined with the blast furnace slag and the characteristics of these six influencing factors,

(1) C is the most important element except iron, the strength of steel increased, plasticity, toughness, especially low-temperature impact toughness decreased with the increasing of carbon content, and corrosion resistance, fatigue strength and cold bending performance was significantly decreased at the same time. The addition of Mn in the steel can play a role of solid solution strengthening. Ceq represents the carbon equivalent, Ceq values can generally assess the weldability of steel.in a certain range.

(2) secondary factors mainly refer to Cr, Ni, Cu and other residual elements, content is not much, but have the impact on the performance of steel. Among them, Cr and C, Fe to form carbide, to improve the hardness and wear resistance of steel, and Ni content in steel exceeding the standard, will result in increased kainite microstructure of steel, the yield point of steel is unknown, steel performance strange, the main function of adding the Cu element is that the Cu element can be deposited on the surface of the stainless steel. as additional microelectrodes, to promote a very small anode current to passivation state.

The main influence of the blast furnace slagis analyzed by SPSS.

3. CONCLUSIONS

In addition to the weak correlation between Cr and MN, the rest were significant in the 0.01 level. In accordance with the different interaction between the carbon, alloying elements commonly used are divided into non-carbide-forming elements and carbide-forming elements of two categories. Carbide forming elements include V, Mo, Cr, Mn, etc., which can be combined with carbon in the steel to form carbides, such as VC, MnC, etc., these carbides generally have high hardness, high melting point and stability, if They are small particles and evenly distributed in the steel, it will significantly improve the strength of steel, hardness and wear resistance.

REFERENCES

[1] Wang Mingjun, Liu Xinbin, Li Zhongmin. Study on the mechanical propertiesand chemical composition of 20MnSi steel [J]. Metallurgical Standardization &Quality,2000,04:1-2.

[2] Sun Deshan, The relationship between principal component analysis and factoranalysis and software implementation [J]. Statistics and DecisionMaking,2008,13:153-155.

[3] Wang Shuang. Effect of Micro - alloying and Rapid Cooling on theMicrostructure and Properties of Hot Rolled Ribbed Bar [D]. NortheasternUniversity,2006.

[4] Li Yang, Zuo Longfei, Zhang Jianchun, Ma Han. Effect of alloying elements onthe strength-flex ratio of HRB600 blast furnace slag s [J]. Transactions of Materials andHeat Treatment,2016, S1:61-67.

[5] Tirumalai S. Srivatsan,Kannan Manigandan, Andrew M. Freborg, Thomas Quick.Investigating and Understanding the Cyclic Fatigue, Deformation, and FractureBehavior of a Novel High Strength Alloy Steel: Influence of Orientation[J]. steelresearch int.,2012,843.

The Influence of Chemical Element on Properties of Deformed Steel Bar

Deyi Liu[1],Doudou Ge[1],Shanbiao Wang[2], Shujuan Yuan[3,]*
[1] College of Information Engineering, North China University of Science and Technology, Tangshan, 063000, China
[2]College of Electrical Engineering, North China University of Science and Technology, Tangshan, 063000, China
[3] College of Science, North China University of Science and Technology, Tangshan, 063000, China

Abstract: Based on the data given in Annex I, delete the error is relatively large data, The principal component analysis is performed by randomly extracting 500 sets of data using the principle of flip-flop. The main factors affecting the yield point, tensile strength, hardness, and other properties of the steel are Mn, C, Ceq, Cu, Al and Si, the secondary factors are V, P, S, Cr, Ni, Mo. However, P and S are harmful elements in steel, reducing the yield point of steel and tensile strength. In the end, the correlation of elements was analyzed using SPSS. $|r| > 0.8$, indicating that the elements are highly correlated, included Ceq and C, Cu and Cr. $0.8 > |r| > 0.5$, indicating that the correlation between the elements is low, included Si and Cu, Si and Mn, Ni and Cr, Ni and Cu. Other elements are essentially irrelevant.
Keywords: Principal component analysis, Multiple regression analysis, Correlation analysis

1. INTRODUCTION

Deformed steel contains a variety of chemical elements, such as C, Mn, S, P, Si, Cr, Mo, Cu, Ni, Alt, V, these elements have an impact on the yield strength of the steel, the tensile strength after fracture and the elongation at break. For example, manganese is a good deoxidizer and desulfurization agent, it would be improved the hot workability of steel and improved the yield point of steel. Mn content is high, can weaken the corrosion resistance of steel, reducing the welding performance. Increased carbon content in steel, yield point and tensile strength increased, but the plastic and impact resistance. Based on the chemical elements in the deformation of the steel principal component analysis, the effects of chemical elements on the properties of steel were investigated, what's more, discuss the correlation between the elements.

2. PRINCIPAL COMPONENT ANALYSIS

Principal Component Analysis (PCA) is one of the most multivariate statistical methods used in social and economic problems. The principle is to reduce the original dimension by using the dimensionality reduction method to minimize the loss of the original data. , Which is a linear combination of the original indicators, which not only maintains the primary information of the original indicators, but also is not related to each other, simplifies the complex problems and seizes the main contradictions to analyze.

Suppose there are n samples, there are p observation index $(p < n)$, the original data matrix , and the correlation coefficient matrix. The eigenvalues of the correlation coefficient matrix are calculated. The eigenvalues are and the eigenvectors, then the i principal component is

Usually by the size of the cumulative contribution to take the first k , in most cases the first few principal components have been representative of the original indicators of most of the information.

a. The original observation of p indicators were standardized.n is the number of samples, p is the number of original indexes, and s is the sample standard deviation. The correlation coefficient matrix R is obtained from the normalized data matrix.

b.The characteristic λ and the characteristic vector l of the correlation coefficient matrix R and the contribution rate c_i are obtained

Cumulative contribution rate

c. The Determine the principal components .

d.Calculate the comprehensive evaluation value

3. THE PRINCIPAL COMPONENT ANALYSIS OF ELEMENT

Annex 1 gives the raw data for two sets of deformed steels, which are subject to pretreatment due to the large amount of data.Using the data sheet given in Annex 1, calculate the average of the 12 chemical elements of the two deformed rebar, and then filter the data. Exclude the data with mean values of -0.05 and 0.05, under the standard data selected randomly selected 500 groups of data. Then the principal component analysis method was used to determine the main and secondary factors affecting the deformation of steel bars. And then to these major and secondary factors for correlation analysis to find the relationship between elements.

The results of principal component analysis of chemical elements by SPSS are as follows:

According to the total variance statistic table of the solution, the cumulative contribution rate of the variance of the element is obtained. The chemical composition of the principal component is more than 85%. That score matrix, you can explain the principal component of the load on each variable, which can be derived from the main component of the expression:
So as to get the comprehensive score formula
,The extracted data into expression validation, calculate, the results of the calculation shown in the following table:
Table 1 Chart one Element Weight Form

η_C	η_{Mn}	η_S	η_P	η_{Si}	η_{Ceq}
0.082	0.510	0.010	0.013	0.181	0.171
η_V	η_{Cr}	η_{Ni}	η_{Cu}	η_{Mo}	η_{Al}
0.011	0.010	0.004	0.006	0.001	0.001

According to the above table, according to the size of the η value, the main factors affecting the yield strength, tensile strength and elongation at break of the deformed bar are Mn, C, Si, all of these elements are large, Deformed steel content is relatively high, so these are the main factors affecting the deformation of steel. Ceq and other chemical elements of the small η, as a secondary factor. In the steelmaking process, manganese is a good deoxidizer and desulfurization agent, manganese content increased, will yield point, tensile strength and hardness increased a lot, weaken the corrosion resistance of steel, reducing welding performance. Silicon steel in the process of adding silicon as a reducing agent and deoxidizer, silicon can significantly improve the elastic limit of steel, yield point and tensile strength. Nickel can increase the strength of steel, while maintaining good plasticity and toughness. 0.5% of vanadium in steel can be refined grain structure, improve strength and toughness. The main and secondary factors play an important role in the process of steel making, and some secondary factors can replace the main factors to achieve the purpose of saving costs.

4. CORRELATION ANALYSIS

Use SPSS software to make the correlation matrix among the factors
According to the chart can draw such a conclusion, $|r| > 0.8$, indicating that the elements are highly correlated, included Ceq and C, Cu and Cr. $0.8 > |r| > 0.5$, indicating that the correlation between the elements is low, included Si and Cu, Si and Mn, Ni and Cr, Ni and Cu. Other elements are essentially irrelevant.
The chemical elements in the deformed steel are not only related to the content, but also have some relevance in the realization of the function. For example, C,Si,Ni and Cu can increase the yield point and tensile strength, so that the steel to maintain good plasticity and toughness. Si, Mo and Cr has the effect of improving corrosion resistance and oxidation resistance, and can produce heat-resistant steel. V has the characteristics of oxidation resistance and corrosion resistance, and have the characteristics of endure high temperature. S, P are to increase the brittleness of steel, so that the weld ability of steel deterioration, reducing the plasticity of steel, ductility and toughness, are all harmful elements in steel. Steel due to the interaction of various elements, closely linked, but also have their own characteristics, making the use of more extensive steel.

5. CONCLUSION

Deformed steel in our daily life has been widely used. In this paper, chemical elements of deformed steels are classified by principal component analysis of chemical elements, including major and minor elements. Mn, Si and C are the main components, and Cr, Ni and V are the minor components. And then the chemical elements contained in the deformation of the steel were analyzed, the interaction of each element analysis and discussion. $|r| > 0.8$, indicating that the elements are highly correlated, included Ceq and C, Cu and Cr. $0.8 > |r| > 0.5$, indicating that the correlation between the elements is low, included Si and Cu, Si and Mn, Ni and Cr, Ni and Cu. Other elements are essentially irrelevant.
All in all, C, Cr, Ni and other chemical elements play an important role. In order to obtain the greatest benefit we need to understand, to master.

REFERENCES

[1] Jinxing Xie, Optimization Modeling and LINGO Software, Beijing: Tsinghua University Press, 2005.
[2] Caifu Yang, high-strength steel construction of the latest technological progress, Steel Research Institute, 2009-05-18.
[3] ZhenglinKe, Lasso and its related methods in the application of multiple linear regression model [D]. Beijing Jiaotong University, 2011.
[4] Tao Pan, Low Cost V-N Microalloyed High Strength Research and Production, China Conference, 2009-07-18.
[5] Yushan Zhang, multiple linear regression analysis of the case study [J]. Science and Technology Information, 2009,09: 54-56.
[6] Qiyuan Jiang, mathematical model (second edition), Beijing: Higher Education Press, 1993.

Simulation Study On Melting Process Of Iron Tailings In Blast Furnace Slag

Fang GAO[1], Shulei YANG[1], MinHua BIAN[2], Weixing LIU[3,]*
[1] College of Metallurgy and Energy, North China University of Science and Technology, Tangshan 063000, Heibei, China
[2] College of Information Engineering, North China University of Science and Technology, Tangshan 063000, Heibei, China
[3] North china university of science and technology, The ministry of education key laboratory with modern metallurgical technology, Tangshan 063000, China

Abstract: In the conditioning process of blast furnace slag, the temperature field distribution of iron tailings melting is an important basis for judging whether or not soaking. This paper uses the method of thermodynamic calculation, the solid phase, liquid phase and fuzzy region are regarded as continuous medium, under the premise of considering the chemical reaction, the diffusion and temperature distribution equations in three-dimensional coordinate system are established, the simulation of the change rule of the temperature field of iron tailings during the melting process is carried out by coupling simulation. Micro describes the inner link between the iron tailings physical parameters with melting slag, and the time required for heat homogenization was obtained.
Keywords: iron tailings, continuous medium, coupling simulation, temperature field

1. INTRODUCTION

In the process of preparing high value-added thermal insulation material by using direct-fiber-forming process of quenched and tempered blast furnace slag[1], melting modifying agent of iron ore tailings is the key technology of fiber directly into blast furnace slag, and directly determining the quality and yield of the fiber. Because the iron tailings in the slag melting behavior is carried out under high temperature, and it is not easy to observe and calibrate. There are few studies on the melting of iron tailings in blast furnace slag at home and abroad, mainly concentrated in the study of SiO_2, CaO, MgO style single substances dissolved in molten slag, erosion behavior, the influence of various factors on its dissolution and the homogenization behavior of the alloy in molten steel[2].

The melting of iron tailings is a solid-liquid phase change problem[3], the melting process of iron tailings in slag is divided into two stages, the first stage, iron tailings in the hot slag environment under the surface chemical reaction. The second stage, liquid molten slag-solid solution mixed state-solid iron tailings surface reaction products melt penetration between the melting and diffusion, liquid slag-solid solution mixed state-the temperature of the transfer of solid iron tailings[4], and then achieve the overall soaking process. Based on the above two stages, in this paper, the material diffusion model and the energy conservation equation of iron tailings in the melting process of blast furnace slag are constructed, simulation of the changes of temperature field during the melting process of iron tailings, then get the time that the iron tailings are be heated, and providing the theoretical and technical support for the direct fiber-forming process of blast furnace slag.

2. THE CHEMICAL REACTION ANALYSIS OF IRON TAILINGS MELTED IN BLAST FURNACE

In the quenching and tempering process, when the solid iron tailings particles are added into the slag system, using the phase diagram module in the thermo scientific software FactSage 7.0. Selecting FToxid database, the slagging reaction during the quenching and tempering process was simulated and computed. According to the data in the table, in order to facilitate compare the change of the slag produced by the change of the composition change, set the Al_2O_3 content is 16%, the SiO_2-CaO-MgO- Al_2O_3 four phase diagram is obtained as shown in Fig.1.

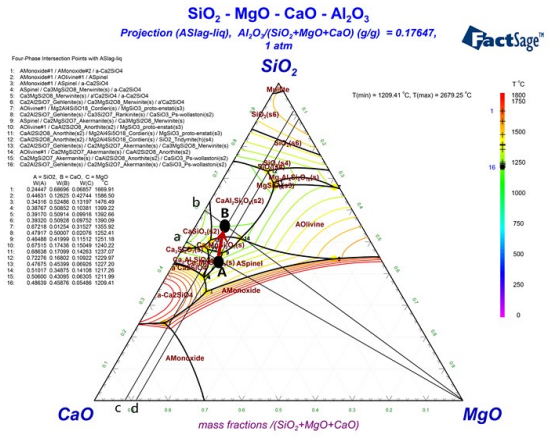

Figure 1 Quaternary phase system of SiO_2-CaO-Al_2O_3-MgO when weight of Al_2O_3 equals to 16%

As can be seen from the phase diagram analysis, the main chemical reaction in the changing process of slag and iron tailings occurs as follows:

TABLE 1 CHEMICAL REACTION BETWEEN IRON TAILINGS AND MOLTEN SLAG

Reaction equation	Temperature range /K	Enthalpy change /J
$(SiO_2)+(CaO)=(CaO\cdot SiO_2)$	298~1873	ΔH_1
$12(CaO)+(7Al_2O_3)+=(12CaO\cdot 7Al_2O_3)$	1373~1873	ΔH_2
$(MgO)+(CaO)+2(SiO_2)=(2CaO\cdot MgO\cdot SiO_2)$	298~2171	ΔH_3
$(3CaO\cdot SiO_2)+ (SiO_2)= 3CaO\cdot 2SiO_2$	298~1773	ΔH_4

TABLE 2 CHEMICAL COMPOSITION OF IRON TAILINGS AND MOLTEN SLAG

material	SiO_2	CaO	MgO
Blast furnace slag	32.6	36.43	8.72
Iron tailings	67.41	2.78	2.60
material	Al_2O_3	TiO_2	K_2O
Blast furnace slag	15.44	1.55	0.71
Iron tailings	12.13	0.31	1.25
material	Na_2O	Fe_2O_3	FeO
Blast furnace slag	0.55	0.62	0.88
Iron tailings	2.89	4.18	4.08

As can be seen from the phase diagram, mainly iron ore tailings and blast furnace slag in the SiO_2, CaO, MgO, Al_2O_3 between the four substances in the chemical reaction, therefore, the percentage of the four substances in iron tailings as the weight factor for the calculation of the mixed heat of chemical dissolution, so the calculation formula of the mixed heat of chemical solution is

$$\Delta H_m = 0.6741\cdot\Delta H_1 + 0.0278\cdot\Delta H_2 + 0.0260\cdot\Delta H_3 + 0.1213\Delta H_4 \quad (1)$$

3. THE MATHEMATICAL MODEL OF IRON TAILINGS DIFFUSION

According to the law of diffusion[5-7], in the period of *dt*, in the slag modifier diffusion along the normal direction through the N surface area is *ds*, the weight of fluid *dm* is:

$$dm = -D(x,y,z)\cdot\frac{\partial C}{\partial n}\cdot dS\cdot dt \quad (2)$$

Where $D(x,y,z)$ is the modifier diffusion into the diffusion coefficient in the slag, minus said matter is by the side of the high concentration of penetration to the side of the low concentration.

An arbitrary selection of a closed surface Γ, which is written in the area of Ω, from the moment t_1 to t_2 time to enter the material quality of this closed surface

$$m = \int_{t_1}^{t_2}\{-D(x,y,z)\cdot\frac{\partial C}{\partial n}\cdot dS\}dt \quad (3)$$

Because of Gauss formula[8]

$$\frac{\partial C}{\partial n}dS = \iiint_{\Omega}\{\frac{\partial}{\partial x}(D\frac{\partial C}{\partial x})+\frac{\partial}{\partial y}(D\frac{\partial C}{\partial y})+\frac{\partial}{\partial z}(D\frac{\partial C}{\partial z})\}dV \quad (4)$$

$$m = \int_{t_1}^{t_2}\{\iiint_{\Omega}\{\frac{\partial}{\partial x}(D\frac{\partial C}{\partial x})+\frac{\partial}{\partial y}(D\frac{\partial C}{\partial y})+\frac{\partial}{\partial z}(D\frac{\partial C}{\partial z})\}dV\}dt \quad (5)$$

At the same time, the conditioning agent penetrate into the area Ω, so that the internal concentration change, in the time interval $[t_1,t_2]$, the concentration change from $C(x,y,z,t_1)$ to $C(x,y,z,t_2)$, the increase of the material quality is:

$$\iiint_{\Omega}(C(x,y,z,t_2)-C(x,y,z,t_1))dV = \iiint_{\Omega}(\int_{t_1}^{t_2}\frac{\partial C}{\partial t})dV = \int_{t_1}^{t_2}(\iiint_{\Omega}\frac{\partial C}{\partial t}dV)dt \quad (6)$$

By mass conservation :

$$\int_{t_1}^{t_2}\{\iiint_{\Omega}\{\frac{\partial}{\partial x}(D\frac{\partial C}{\partial x})+\frac{\partial}{\partial y}(D\frac{\partial C}{\partial y})+\frac{\partial}{\partial z}(D\frac{\partial C}{\partial z})\}dV\}dt = \int_{t_1}^{t_2}(\iiint_{\Omega}\frac{\partial C}{\partial t}dV)dt \quad (7)$$

Without considering the chemical reaction and the mutual mixing between the solutes, the microscopic description of the diffusion of conditioner is:

$$\frac{\partial C}{\partial t} = \frac{\partial}{\partial x}(D\frac{\partial C}{\partial x})+\frac{\partial}{\partial y}(D\frac{\partial C}{\partial y})+\frac{\partial}{\partial z}(D\frac{\partial C}{\partial z}) \quad (8)$$

Further transformed into a standard type

$$\frac{\partial C}{\partial t}-\nabla(D\nabla C)+0=0 \quad (9)$$

Due to the existence of mixing between reaction and solute complex of iron tailings in the melting process, so in the region A, mixed solute density changes with time and space, the introduction of the source, can get the diffusion equation:

$$\frac{Dc}{Dt} = \nabla\cdot(D_b\nabla c)+S_c+R_A \quad (10)$$

$$S_c = \frac{\partial}{\partial x}\left[\rho D_b \frac{\partial}{\partial x}(C_l - C)\right] + \frac{\partial}{\partial y}\left[\rho D_b \frac{\partial}{\partial y}(C_l - C)\right] + \frac{\partial}{\partial z}\left[\rho D_b \frac{\partial}{\partial z}(C_l - C)\right] - \frac{\partial}{\partial x}\left[\rho v_x \frac{\partial}{\partial x}(C_l - C)\right] - \frac{\partial}{\partial y}\left[\rho v_y \frac{\partial}{\partial y}(C_l - C)\right] - \frac{\partial}{\partial x}\left[\rho v_z \frac{\partial}{\partial z}(C_l - C)\right] \quad (11)$$

In the formula, C_1 , C and D are the solute concentration in the liquid phase, the solute concentration in the solid-liquid phase and the mixed diffusion coefficient of the solid-liquid phase solute. S_C is produced due to the introduction of mixed solute concentration and mixed diffusion coefficients, which exist only in the paste zone. R_A is indicates the rate of solute mass produced by a chemical reaction. ρ is mixed density. v_x , v_y and v_z are the mixed velocity components in the direction of x, y, z respectively. Mixed solute concentration and mixed solute diffusion coefficients are expressed as:

$$C = \omega_s C_s + \omega_l C_l \quad (12)$$

$$D_b = \omega_l D \quad (13)$$

$$R_A = kC \quad (14)$$

In the formula, ω_l and ω_s are the mass fraction of the liquid phase and the solid phase. C_s is the concentration of the solute in the solid phase. k is constant.

4. ENERGY CONSERVATION EQUATION

In slag, solute diffusion caused latent heat, Coefficient of mixed heat conduction, latent heat, the density of solution in the chemical reaction heat source change. On the basis of solid-liquid phase transition in the continuous model the energy conservation equation of Bennon and Ineropera[9-10] are on the paper for the diffusion equation, the introduction of chemical reaction heat, can be obtained in the cylindrical coordinate system, the establishment of energy conservation equation

$$\frac{D\rho T}{Dt} = \nabla \cdot \left(\frac{\kappa}{c_p} \nabla T\right) + S_T \quad (15)$$

$$S_T = S_L + S_H \quad (16)$$

In the formula, κ and c_p were mixed and mixed thermal conductivity specific heat capacity, S_T is the total source term, S_L and S_H are phase change latent heat and chemical reaction heat source terms. Mixed heat conduction coefficient and specific heat are defined as:

$$\kappa = \varphi_s \kappa_s + \varphi_l \kappa_l \quad (17)$$

$$c_p = \omega_s c_{p_s} + \omega_l c_{p_l} \quad (18)$$

In the formula, κ_B , κ_l and c_{p_B} , c_{p_l} are respectively the thermal conductivity of the solid and liquid phase and the specific heat capacity of the solid and liquid phases. The expression of latent heat of phase change and chemical reaction heat source term is:

$$S_L = -\frac{1}{c_{p_l}} \frac{\partial(\rho L \omega_l)}{\partial t} + \frac{c_{p_l} - c_{p_s}}{c_{p_l}} \frac{\partial}{\partial t}(\rho \omega_s T) - \frac{1}{c_{p_l}}\left[\frac{\partial(\rho L v_x)}{\partial x} + \frac{\partial(\rho L v_y)}{\partial y} + \frac{\partial(\rho L v_z)}{\partial z}\right] \quad (19)$$

$$S_m = \frac{1}{c_{p_l}} \frac{\partial}{\partial t}\left[\rho\left(\omega_s \Delta H_{m_s} + \omega_l \Delta H_{m_l}\right)\right] + \frac{1}{c_{p_l}}\left[\frac{\partial(\rho \Delta H_{m_l} v_x)}{\partial x} + \frac{\partial(\rho \Delta H_{m_l} v_y)}{\partial y} + \frac{\partial(\rho \Delta H_{m_l} v_z)}{\partial z}\right] \quad (20)$$

In this formula, L is latent heat of phase change, ΔH_{m_B} is heat of chemical reaction of solid phase, ΔH_{m_l} is heat of chemical reaction of liquid phase.

5. NUMERICAL SOLUTION AND ANALOG SIMULATION

（1）In the numerical calculation process, first determine the parameter values of the initial time node. Suppose the initial volume of iron tailings is $3\times3\times3\text{mm}$, the volume of the weld pool is $10\times10\times10\text{mm}$, density of iron tailings (ρ_B) is $3\text{g}/\text{cm}^3$, the density of blast furnace slag (ρ_l) is 2.43kg/m^3 , thermal conductivity of iron tailings (K_s) is $3.65\text{W}\cdot\text{m}^{-1}\cdot^\circ\text{C}$, thermal conductivity of blast furnace slag (K_l) is $10.65\text{W}\cdot\text{m}^{-1}\cdot^\circ\text{C}$, specific heat capacity of iron tailings is $1.3\text{KJ/(Kg}\cdot^\circ\text{C)}$, specific heat capacity of blast furnace slag is $0.966\text{KJ/(Kg}\cdot^\circ\text{C)}$, latent heat of phase change (L) is $1.38\times10^5\text{J/K}$.

(2)ad then select the time step, at the time of solving the parameter values of the next time step, using the parameter values and temperature fields of the last time step to solve the diffusion equation and energy conservation equation of the next time step. Based on the calculation results of the parameter values and the temperature flied, then brought them into the equation to gain further solution. The diffusion equation and the energy equation are coupled to solve,

reach convergence turn to the next time step.

（3）Based on finite element method ,using PDE toolbox to emulate temperature field, the image at the last second of slag system temperature distribution is：

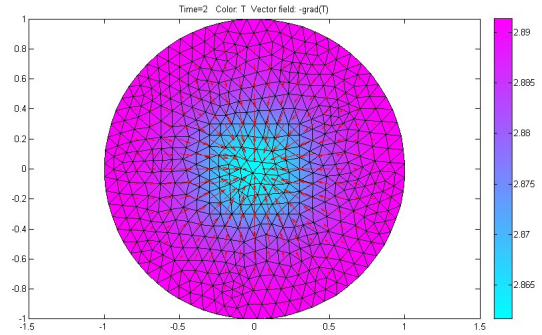

Figure 2. 2D temperature field distribution

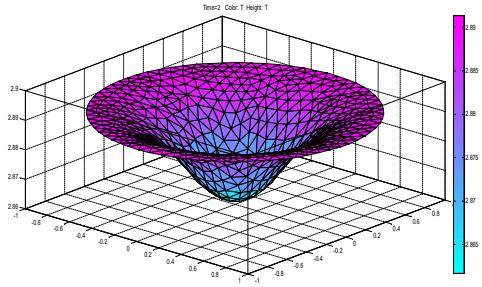

Figure 3. 3D temperature field distribution

Result Analysis ： When t=2min, the temperature difference between the highest point and the lowest point is less than 0.03, and it shows that it has achieved soaking. It can be known that molten pool achieve soaking after 2min under the condition of the specific value about the volume of the molten pool and the volume of the solute is 1000:27.

6. CONCLUSION

The material diffusion model and energy conservation equation is established based on partial differential equation, and it reveals the process of soaking: At the beginning of between the contact of iron tailings particles and blast furnace slag, iron tailings solids are heated, then the temperature of iron tailings rise and complete chemical reaction with blast furnace slag. Chemical reactions release heat, and it speed up the heating rate of iron tailings, accelerate melting, and improve the reaction rate and the heat transfer of the solute and blast furnace slag. After melting, complete two-dimensional and three-dimensional simulation of the temperature field about Solute diffusion, get put in the iron tailings particles in the slag and the system achieve soaking after 2 minutes.

7. ACKNOWLEDGMENT

The paper has got the support of the 2016 annual college students innovation and entrepreneurship training program in North China University of Science and Technology(project number: X2016141).

REFERENCE

[1] Jie Li, Yuzhu Zhang. Quenched and tempered blast furnace slag as slag fiber raw materials[J]. Chinese Journal of Environmental Engineering, 2013,7(12):4971-4977.

[2] Shuang Cai, Yuzhu Zhang, Junguo Li. Preliminary research on homogenization of adjusted molten BF slag[J]. Iron and Steel, 2016,51(6):34-38.

[3] Daxin Zeng, Junyi Su. Mathematical Modeling of Solid-liquid Phase Change Problems and Numerical Methods for Solving These Problems[J]. Journal of Hubei Autimotive Industries Institute, 2001,15(2):16-20.

[4] Hailong Wang, Xiuxi Wang, Haige Liang. MOLECULAR DYNAMICS SIMULATION AND ANALYSIS OF BULK AND SURFACE MELTING PROCESSES FOR METAL Cu[J]. ACTA METALLURGICA SINICA, 2005,41(6):568-572.

[5] Bitao Peng, Zhoushun Zheng, et al. Lattice Boltzmann method for solving two dimensional convection-diffusion equations[J]. Computer Engineering and Applications, 2015,51(23):68-73.

[6] Zhijie Cao, Yiping Lin, Jianwei Shen. Conservation laws for a variable coefficient nonlinear diffusion–convection–reaction equation Original Research Article[J]. Journal of Mathematical Analysis and Applications, 2014, (420):77-93.

[7] Douglas J. Nicolin, Diogo F. Rossoni, Luiz Mario M. Jorge. Study of uncertainty in the fitting of diffusivity of Fick's Second Law of Diffusion with the use of Bootstrap Method Original Research Article, Journal of Food Engineering, 2016(184):63-68.

[8] Jing Wu, Yafeng Yan. A Study on Gauss Formula by the Flow from a Fluid through a Curved Surface[J]. STUDIES IN COLLEGE MATHEMATICS, 2016,19(2):32-34.

[9] Gim Yau Soh, Guan Heng Yeoh, Victoria Timchenko. An algorithm to calculate interfacial area for multiphase mass transfer through the volume-of-fluid method[J]. International Journal of Heat & Mass Transfer, 2016,100:573-581.

[10] Daming Xu, Qingchun Li. NUMERICAL SIMULATION OF HEAT, MASS AND MOMENTUM TRANSFERS IN METALLIC INGOTS AND FREDICTION OF MACROSEGREGATION[J]. ACTA METALLURGICA SINICA, 1990,26(4):267-270.

Study On The Change Of Temperature In The Flowing Process Of Blast Furnace Slag

Yong Li[1], Minghui Zhang[2], Minghao Wang[3], Lianzheng Ma[1], Jie Li [4,], Weixing Liu[4]*
[1]Collage of Metallurgy and Energy, North China University of science and technology, Tangshan 063000, Hebei, China
[2]Collage of Information Engineering, North China University of science and technology, Tangshan 063000, Hebei, China
[3]Collage of Electrical Engineering, North China University of science and technology, Tangshan 063000, Hebei, China
[4]The ministry of education key laboratory of modern metallurgical technology, North China University of Science and Technology, Tangshan, 063000, Hebei, China

Abstract: Due to heat loss in the presence of liquid blast furnace slag while the slag pour, and the heat loss of the blowing process is very important. In order to effectively grasp the temperature variation of liquid blast furnace slag, the slag flow in the air flow in the process of heat loss points for liquid core to flow shares edge of heat conduction, heat conduction, convection and flow edge strands to outside air radiation heat exchange, and the convection heat were transferred into two parts to study. For the two parts of the problem of heat dissipation were established slag liquid core to the stream edge strands of infinite solid cylindrical heat source model and the heat from the stream edge to outside air heat transfer by radiation and convection heat transfer model, then by heat transfer analysis method to calculate the convective heat transfer of heat and radiation effect of heat diffusion and laminar flow state of liquid slag radius on the heat transfer, and carries on the analysis to the liquid slag in air cooling, to calculate the slag in the flow quantity of heat, then heat the total loss ratio.

Key words: Blast furnace slag; flow and heat transfer; solid cylinder heat transfer model; dissipate heat; radiation heat transfer

1. INTRODUCTION

Blast furnace slag is the main by-product of iron-making process. During the process of blast furnace slag disposal, not only the sensible heat of slag is recovered, but also the utilization of water slag is very low. As the blast furnace slag is between the ideal solid and liquid typical high temperature viscoelastic material, the classical heat transfer theory and related software is difficult to accurately describe and simulation. Therefore, to find a model which can effectively reflect the temperature variation law of liquid blast furnace slag, solving the problem of heat transfer and heat dissipation in slug flow in the air has become a research subject worthy of research. In this paper, the slag flow in the air and the slag in the slag flow is analyzed in the liquid-solid two-state coupled slag slag, and the heat transfer and heat dissipation of the stream in the air and slag are analyzed, And finally gives the total loss of heat ratio, blast furnace slag conditioning and direct laying a theoretical basis.

2. LIQUID CORE TO THE STREAM OF THE EDGE OF THE HEAT TRANSFER AND CONVECTIVE HEAT CONDUCTION

There are several factors that need idealization, such as the actual length of slag liquid column is not infinite solid cylinder, liquid column is affected by the ambient temperature and the distribution of heat in the liquid column is Inhomogeneous. Therefore, in order to solve the problem easily, we use the following three assumptions[1]:

1). Assuming that the air around the column is a semi-infinite uniform heat transfer medium, the initial temperature field is evenly distributed and its thermal property does not change with temperature.

2). It is assumed that the heat source in the cylinder model is considered as a uniform distribution in the cylinders inside the stream.

3). The blast furnace slag is assumed to be a homogeneous medium.

2.1 convective heat transfer model from liquid core to burden

In the process of liquid blast furnace slag, the slag is falling in the form of liquid column. When analyzing the heat conduction and convective heat conduction process from the liquid core to the strand edge, the heat transfer of the liquid core to convective heat transfer the amount[2]:

$$q_1 = h_1 \left(T_c - T_s \right) \tag{1}$$

Thereinto, T_c is liquid core temperature, the maximum temperature of the measurement is 1600℃, T_s is the boundary interface temperature, in this section, take the average of the measured temperature 1235℃, h_1 is the convective heat transfer coefficient of the liquid core to the stream edge, in general, the value is 2000W/(m^2 · k).

In order to solve the problem of heat dissipation

during pouring and falling of blast furnace slag, numerical model of infinite solid cylinder is introduced in this paper [3]. The slag liquid column of the liquid blast furnace slag is regarded as a solid cylinder with radius r_0 as infinite length, there into, The conditions for this one-dimensional cylindrical surface heat source model are as follows： The studied area is a homogeneous medium from the center of the cylinder of $r = 0$ to $r = r_0$, the slug flow column has an infinitely long constant heat flow q (in w / m) from the moment of $\tau = 0$ in the $r \in (0, r_0)$ zone.

The mathematical description of the one-dimensional cylindrical surface heat source model is given below：

When $0 < r < r_0, \tau > 0$ is present

$$\frac{\partial \theta_b}{\partial \tau} = a_b \left(\frac{\partial^2 \theta_b}{\partial r^2} + \frac{1}{r} \frac{\partial \theta_b}{\partial r} \right) \tag{2}$$

When $r > r_0, \tau = 0$ is present

$$\theta_b = 0 \tag{3}$$

When $r = 0, \tau > 0$ is present

$$\frac{\partial \theta_b}{\partial r} = 0 \tag{4}$$

Thereinto , Where $\theta_b = t_b - t_0$, $\theta_s = t_s - t_0$ is the excess temperature K ; t_b, t_s for the heat transfer area temperature K ; t_0 is the initial temperature of the heat transfer area K ; a_b is the hole medium diffusion rate m^2/s. Can be drawn flow within the temperature distribution, as shown in Figure 1.

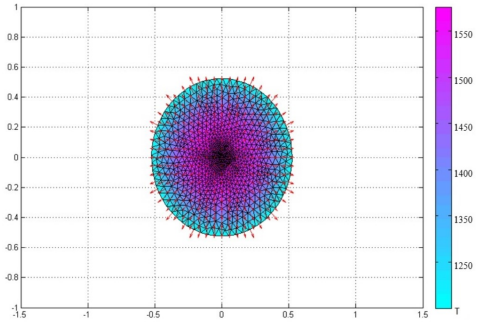

Figure 1 Distribution of two-dimensional temperature field

According to the above formula, the heat flux of convective heat transfer from the liquid core to the strand edge is: 184000 w/m^2.

2.2 thermal conductivity analysis from liquid core to burden

The heat flux from the liquid core to the edge of the stream is:

$$q_2 = -\lambda_s \frac{\partial T}{\partial x} \tag{5}$$

There into, λ_b is Slag thermal conductivity W/(m · k), Take 0.3 W/(m · k).

The heat conduction heat flux from the liquid core to the stream strand edge: $-0.3\dfrac{\partial T}{\partial x}$

3. STREAM EDGE TO THE OUTSIDE AIR CONVECTION HEAT AND RADIANT HEAT TRANSFER

3.1 stream edge to the outside air convection heat

Convection heat flux of air and slag flow is:

$$q_3 = h_3 \left(T_s - T_{m1} \right) \tag{6}$$

Thereinto, T_{m1} is Air temperature, take 30℃; h_3 take 7.1 w/(m^2 · k).

The heat flux of convective heat transfer between slag and air is:

$$Q_3 = A q_3 \tag{7}$$

Thereinto, Q_3 is the convection heat transfer heat; A is the contact surface area of the slag with the air. Through the above process and the actual measured data, the calculation can be obtained convective heat transfer heat:

q_3 =8555.5J/m^2, Q_3 =8555.5A

3.2 stream of air to the outside edge of radiative heat transfer

Heat transfer from the edge of the stream to the air is dissipated by radiation heat transfer. For this reason, we consider the slag flow column as a finite-length cylindrical surface heat source model, starting at any time τ , The molten slag flows as a cylindrical surface heat source q_s (heat flow per unit area) and starts to exothermal, At time τ , The actual temperature rise of a point around the slag liquid column $t - t_0$ is located at different locations, at different instantaneous point of the heat source at this point the corresponding temperature superposition, denoted by t_a , The virtual heat exchange method is adopted, that is, the ground is the symmetry plane, considering that there is a heat sink of intensity $-q_s$ above the ground (as shown in Figure 2), In this heat source, the role of heat sink, the ground temperature throughout the heat transfer process to maintain the same, The analysis of the element $d\theta dh$ at the cross section of h at time τ , As shown in Figure 2, the horizontal distance d of this cell to the calculated position $A(\mathrm{R}, \mathrm{z})$ is:

$$\begin{aligned} d &= \sqrt{\left(R - r_0 \cos\theta\right)^2 - \left(r_0 \sin\theta\right)^2} \\ &= \sqrt{R^2 + r_0 - 2Rr_0 \cos\theta} \end{aligned} \tag{8}$$

Thereinto: r_0 is slag liquid column radius, R is calculate the horizontal distance from the center of the slag column.

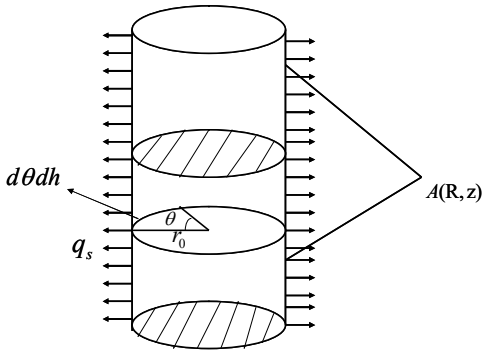

Figure 2 Heat source model of finite length cylindrical surface

By substituting (8) into the instantaneous heat source function, we can get the temperature response of the position $A(R,z)$ under the action of this micro element at time τ :

$$dt_a = \frac{1}{8\left[\sqrt{\pi a\left(\tau-\tau^{'}\right)}\right]^3} \mathrm{e}^{A} d\theta dh \tag{9}$$

Thereinto: $A = -\frac{R^2 + r_0^2 - 2Rr_0\cos\theta + (h-z)^2}{4a\left(\tau-\tau^{'}\right)}$, a is diffusivity（$m^2/s$）.

The temperature response dt_a integrates θ、h、τ and takes into account the effect of the virtual heat sink. The heat expression at any point around the slag liquid column can be obtained as follows:

$$t_a = \frac{q_s}{4\pi k}\int_0^H dh\int_0^{2\pi} \left\{\mathrm{erfc}\left(\frac{\mathrm{A}_1}{2\sqrt{a\tau}}\right)/\mathrm{A}_1 - \mathrm{erfc}\left(\frac{\mathrm{A}_2}{2\sqrt{a\tau}}\right)/\mathrm{A}_2\right\} d\theta \tag{10}$$

Thereinto:

$$\mathrm{A}_1 = \sqrt{R^2 + r_0^2 - 2Rr_0\cos\theta + (h-z)^2} \tag{11}$$

$$\mathrm{A}_2 = \sqrt{R^2 + r_0^2 - 2Rr_0\cos\theta + (h+z)^2} \tag{12}$$

k is Thermal Conductivity（W/m · ℃）, erfc(z)is waste heat error function. q_s has the following relationship with q_1 (the heat flow per unit length) in the finite heat source model:

$$q_s = q_1/(2\pi) \tag{13}$$

The heat flux of the radiant heat fluxes of air and slag flow is [4]:

$$q_4 = \varepsilon\sigma\left[(T_s+273)^4 - (T_{ml}+273)^4\right] \tag{14}$$

Thereinto: ε is the radiation coefficient, take 0.5; σ is the Stephen-Boltzmann constant, take 5.67×10^{-8} W/(m^2 · k^4)

The heat flux between the slag and the air radiates heat is:

$$Q_4 = Aq_4 \tag{15}$$

Thereinto: Q_4 is radiation heat flux of slag radiation.

Radiation heat flux

$$q_4 = 146369.2975 \text{ J/m}^2$$

$$Q_4 = 146369.2975\text{A}$$

The ratio of the convective heat transfer rate to the radiant heat dissipation flow rate is:

$$\eta = \frac{Q_3}{Q_4} \tag{16}$$

The above results are brought into the above equation η =0.0589<<1, It means that radiation is much larger than the convection heat dissipation.

According to the above analysis can be obtained slag flow into the air from the edge of the temperature distribution diagram shown in Figure 3.

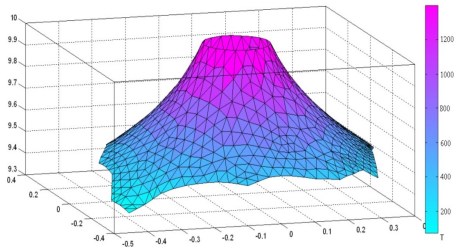

Figure 3 Distribution of the three-dimensional temperature field from the edge of molten slag to the air

Based on the above results, the percentage of convective heat transfer can be further found:

$$w_{Q_3} = \frac{Q_3}{Q_3+Q_4} = 5.5\% \tag{17}$$

Radiation heat transfer as a percentage of:

$$w_{Q_4} = \frac{Q_4}{Q_3+Q_4} = 94.5\% \tag{18}$$

It can be seen radiative heat transfer accounted for the largest percentage of the above data 94.5%.

4.ANALYSIS AND CALCULATION OF RESIDUAL HEAT OF PROCESS

The process of falling of the slag stream includes radiative heat transfer and convective heat transfer, However, the heat loss in the process of falling of the slag stream is mainly caused by radiation heat transfer, And in the process of research into the technology of blast furnace fiber[5], The final residual temperature of slag flow is an important research parameter, According to reference[6], the energy conservation equation of slag is as follows:

$$q_{in,i} = -q_{out,i} + \frac{m_{in,i}cT_{g,i} + q_{ex,i-1} - q_{ex,i}}{A_i} \tag{18}$$

According to the actual process of slag flow drop process can get the following changes in the residual heat of the slag formula:

$$Q_t - Q_s = Q_r \tag{19}$$

Thereinto: Q_t is total heat of blast furnace

slag; Q_s is heat loss of blast furnace slag: Q_r is residual heat of blast furnace slag.

Set the slag per unit volume of heat on the K, Therefore, the total heat of slag is Q_t:

$$Q_t = KV = Cm\Delta T = C\rho V\left(T_c - 298\right) \quad (20)$$

Thereinto: T_c means that the temperature of the molten slag is the temperature at the center of the stream.

In the research process will be slag stream as a cylinder, so the above equation can be expressed as:

$$Q_r = \pi Khr^2 - 2\pi hr\left(q_3 + q_4\right) \quad (21)$$

Thereinto: r is the slag flow radius.

The above equation can be simplified as:

$$Q_r = \pi h\left[Kr^2 - 2r\left(q_3 + q_4\right)\right] \quad (22)$$

From the above formula can be expressed that the remaining heat flow shares and the function of the radial flow function as a quadratic function, as shown in Figure 4.

$$Q_r = C\rho V\left(T_p - 298\right) \quad (23)$$

Thereinto, T_p is the temperature of the stream after the heat is dissipated from the slag flow

$$T_p = T_c - \frac{2\left(q_3 + q_4\right)}{Cr\rho} \quad (24)$$

According to heat loss flux and slag flow radius $\left(r = 1.2\text{cm}\right)$, Specific heat capacity $\left(C{=}1.1\right)$, density $\left(\rho{=}3.45\text{t}/\text{m}^3\right)$ Can be obtained stream heat loss after the heat flow center temperature of 1552 ℃.

In summary, can be obtained in the slag during the heat loss ratio η.

$$\eta = \frac{Q_s}{Q_t} \times 100\% = 3\%$$

5. CONCLUSIONS

In this paper, the heat dissipation of slag flow in air flow is divided into two parts: heat transfer and heat conduction from the liquid core to the edge of the stream, convective heat conduction and radiative heat transfer and convective heat transfer from the edge to the outside air. The main heat loss in the process of free falling and chute flow is obtained by establishing the infinite solid cylindrical heat source model and the radiation heat transfer and convective heat transfer model from the edge of the stream to the outside air. Is the key factor to decrease the heat loss of the slag flow, increase the temperature of the stream and reduce the surface area of the stream. It is the heat dissipation ratio of the slag slagging process, which can effectively

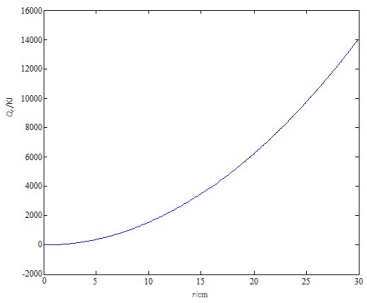

Figure 4 the flow of residual heat flow and the flow of the radius of the relationship diagram

From the practical point of view, when $r \to 0$ has $Q_r \to 0$, so one of the solutions to 0. when $r > 0$ has $Q_r > 0$, It can be deduced that the other solution of the equation is negative. This function can be seen from the relationship between the slag flow of residual heat and molten slag flow is proportional to the square of the radius, That is, the flow of stock radius, the relative increase in excess heat, heat loss less; the stream radius decreases, then the heat loss will increase rapidly.

Residual heat flow of molten slag

control the liquid state temperature variation of blast furnace slag.

6. ACKNOWLEDGMENT

The paper has got the support of the 2016 annual college students innovation and entrepreneurship training program in North China University of Science and Technology (project number: X2016140).

REFERENCES

[1] Zhan Guohui, Yu Yanan, Finite long cylindrical [D]. Journal of Zhejiang University, 2011, 6(6): 1104-1107.

[2] Yang Aimin, Research on heat transfer rule of blast furnace slag during fibe ring process [D]. Qin Huangdao: Yanshan University, 2015.

[3] Wu Dan, Fang Zhaohong, Zhang Wenke, Study of Infinite solid cylinder heat-source transfer model [D]. Refrigeration and Air Conditioning, 2009, 8(4): 101-104.

[4] Gong Shuwen, Chen Lingen, Xie Zhihui, Water wall and slag flow inside the stove reaction research [D]. Shang Hai:East China University of Science and Technology,2012.

[5] Husslage W M, Reuter M A, et al. Flow of Molten Slag and Iron at 1500℃ to 1600℃ through Packed Coke Beds[J].Metallurgical and Materials Transactions, 2005, 35B：765-776.

[6] Zhou Junhu, Kuang Jianping, Zhou Zhijun, Liu Jianzhong. Numerical Simulation for Pulverized Coal Gasifier'Heatong Nozzle and Slag Building Model [J]. Proceedings of the CSEE, 2007, 27(26): 1781-1786.

Study on the Heat Transfer Law of Juice Flow in Chute Based on Monte Carlo model

Minghui Zhang[1], Yong Li[2], Minghao Wang[3], Shuwu Lu[3], Jie Li[4,], Weixing Liu[4]*
[1]Collage of Information Engineering, North China University of science and technology, Tangshan 063000, Hebei, China
[2]Collage of Metallurgy and Energy, North China University of science and technology, Tangshan 063000, Hebei, China
[3]Collage of Electrical Engineering, North China University of science and technology, Tangshan 063000, Hebei, China
[4]The ministry of education key laboratory of modern metallurgical technology, North China University of Science and Technology, Tangshan, 063000, Hebei, China

Abstract: As the slag in the slag flow in the process of the main way of heat loss is in contact with the air radiation heat transfer. To solve this problem, according to the Monte Carlo model, the radiation heat transfer has the advantages of fast convergence and high precision, The Monte Carlo model was established to analyze the radiant heat transfer between slag and air in chute. Calculate the radiation heat loss of heat, Thereby accurately simulating the position, direction, and the energy beam absorption or reflection of the emitted energy beam. And then the temperature of a good exposition.
Keywords: Heat loss, Monte Carlo model, radiation heat transfer, heat loss.

1. INTRODUCTION

The slag is present in the blast furnace chute, and its temperature is very high, the main way of the slag in the slag flow in the process of cooling is radiation heat transfer, [1] but the heat transfer process is also accompanied by energy reflection, and the energy is directly absorbed by air and other processes. The traditional method is difficult to obtain the accurate numerical solution to calculate the radiation heat transfer. Therefore, it is an urgent problem to find a way to describe the position, direction and energy reflection of the beam. Monte Carlo method is based on statistical principles, using random numbers to carry out statistical experiments, and obtains the statistical eigenvalue as the numerical solution of the problem to be solved. [2] Monte Carlo method can avoid the solution of complex equations. At the same time, the method can also meet the accuracy requirements. In recent years, with the development of computer technology, Monte Carlo method has been widely used in air physics, space physics, remote sensing, nuclear physics and other fields. [3] However, the people of studying the application of Monte Carlo method in the calculation of slag in the blast furnace slag to the air heat radiation situation is still very few. Because the control equations between the radiation systems are complex and interrelated, many physical factors have an important impact on radiation heat transfer. Therefore, the Monte Carlo method has the advantages of fast convergence speed and high precision, so it is necessary to study the heat of slag to air radiation in chute, [4] so that the slag in the temperature of a good exposition.

2. ANALYSIS OF SLAG TEMPERATURE VARIATION BASED ON MONTE CARLO METHOD

In the calculation of radiation heat transfer of molten slag, the coupling factor (radiant energy transfer coefficient) is a key parameter. It is a surface-emitting radiation energy through one way to reach the other surface and the surface absorption where the ratio of absorbed energy to total radiant energy is the coupling factor. In order to apply the Monte Carlo method to calculate the coupling factor, we made the following assumptions:

1. Suppose that the energy radiated from the surface of the slag is composed of a strip of energy.
2. Suppose that the slag does not react chemically with air.
3. Suppose that the juice is well mixed, and the juice is a uniform temperature.
4. Suppose that where we study is the slag liquid surface and the air surface.
5. It is assumed that there is no transmitted radiation on each surface during the radiation process.

3. CORE ALGORITHM

According to Monte Carlo analysis, we can know that the orientation and position of an energy beam from the surface of the slag, the direction in which the incident energy of the energy beam is absorbed or reflected by the air surface, and the direction of the energy beam reflection are related to a corresponding probability distribution function, that is, is related with a certain random number. So, Monte Carlo's core algorithm is to calculate the

total energy of radiation and determine the direction of the energy beam and can be reflected.

3.1 calculation of total energy of slag liquid emission

The total radiation energy emitted by slag from the chute surface is：

$$E_i = \int_{A_i} XeT^4 dA \quad (1)$$

As the area integral is a double integral problem, for the slag radiation surface, as shown in Figure 1, the equation can be written as:

$$E_i = \int_{x=a}^{x=b} \int_{y_1(x)}^{y_2(x)} XeT^4 dydx = \int_{x=a}^{x=b} E_i'(x)dx \quad (2)$$

Here

$$E_i'(x) = \int_{y_1(x)}^{y_2(x)} XeT^4 dy \quad (3)$$

The total energy radiated from the slag surface can be calculated $Q_i = E_i$ =5490J.

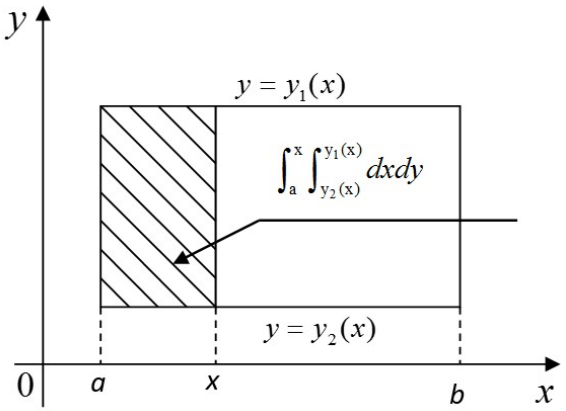

Figure 1 Plan of emission position of radiation beam

3.2 energy beam emission problem

The energy beam position and the emission direction of the slag surface are random, [5] when the energy beam reaches the air surface may be absorbed or may be reflected, and the direction of reflection is also random. If the energy beam tracking method is applied, assuming that the energy beam is reflected, it is necessary to continue tracking the energy beam to know the energy beam is absorbed by a surface or fly away from the system. But to determine the direction of the energy beam and energy beam is absorbed by the relationship.

First determine the emission direction of the energy beam

$$\cos\theta = \sqrt{R_\eta} \quad (4)$$

$$\varphi = 2\pi R_\varepsilon \quad (5)$$

Among them, the meaning of the θ , φ is the spatial angle and circumferential angle of the energy beam; R_η , R_ε is a uniformly distributed random number between 0 and 1, and it is randomly generated by the computer,(4) and (5) can determine the energy beam from the slag liquid surface of the emission direction, and at the same time the two equations are also suitable for determining the direction of reflection of the energy beam from the diffuse reflective surface. Because for diffuse reflection, the direction of reflection of the energy beam is independent of its incident direction.

Then, the reflectance of the reflector is used as the criterion for determining whether the energy beam reaches the surface of the air and is absorbed by the air surface. When the energy beam reaches a surface position, if the following conditions are met, it can be considered that the energy beam will be absorbed by the surface. Otherwise it is reflected, the body condition is

$$Rnd \le \varepsilon \quad (6)$$

Among them, *Rnd* is a randomly distributed random number between 0 and 1that produced by computer calculation; ε is the emissivity for the slag liquid surface. This article takes the emissivity of 0.9, we can use (4) to (6) to track the energy beam from the surface of the slag to the surface of the air being absorbed or exiting the system.

4. CALCULATION OF RADIATION HEAT BASED ON MONTE CARLO METHOD

4.1 the establishment of monte carlo

In this paper, the energy emitted from the surface of the slag is considered to be composed of the energy beam, and each energy beam has equal energy. Since the energy emitted by the surface of the slag liquid is related to the number of emitted energy beams. And so, in this paper, the possible pathways of each energy beam are selected until the energy beam is finally absorbed by the air surface or departs from the surface investigated in this paper. If the energy beam is absorbed by the air surface, then the entire trip is over, track the end of the travel of the energy beam. If the energy beam is reflected, it is necessary to continue to track the energy beam until it is absorbed by a surface. Because the number of beams selected is large enough, so the statistical results to the significance. Depending on the amount of energy absorbed by the air surface, you can determine the air surface to accept the radiation energy. Thereby determining the coupling factor between the surfaces.

Monte Carlo calculation of the specific process shown in Figure 2.

For the i (the slag liquid surface) and j (the air surface)two surfaces, let Q_i be the heat radiated from the i surface per unit time and N_i be the random beam radiation energy number of the i Surface and the energy of each energy beam is

$$W = Q_i / N_i \quad (7)$$

If the energy absorbed by the surface j is N_{i-j} .Then the energy transferred from i to surface j is:

$$Q_{i-j} = N_{i-j} - W \quad (8)$$

So it is easy to determine the coupling factor

between the two surfaces:

$$Ex_{i-j} = Q_{i-j} / Q_i = N_{i-j} / N_i \quad (9)$$

Among them, Ex_{i-j} represents the ratio of the radiant energy delivered from the surface i to the surface j of the total energy of the surface i emission, That is, the coupling factor.

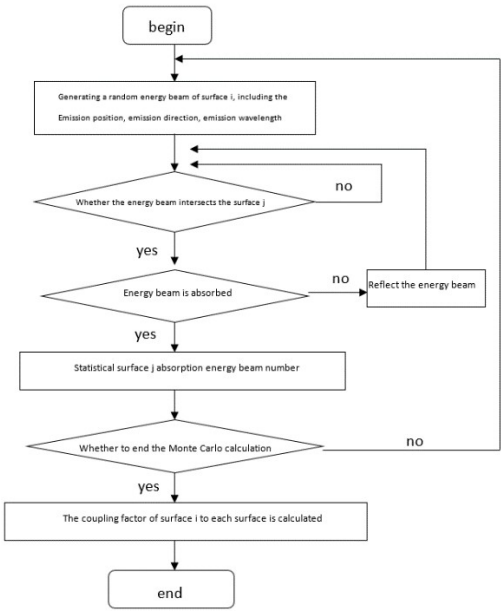

Figure 2 The flow chart of Monte Carlo method

4.2 calculate the heat of slag liquid based on monte carlo method

The chute size in this paper is 0.5m long, 0.05m wide and 0.1m high. The calculation model is shown in Figure 3.

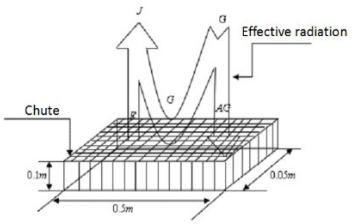

Figure 3 Computational model

According to the definition of effective radiation and projection radiation, the available radiation from the surface of slag liquid can be obtained

$$J_i = E_i + \rho_i G_i = \varepsilon_i E_{bi} + (1 - \alpha_i) G_i \quad (10)$$

Among them, J_i is the effective surface i radiation per unit area; ρ_i is the reflectance i per unit surface area; E_{bi} is the black body radiating force i per unit surface area; E_i is the radiation force i per unit surface area; α_i is the radiation absorption ratio i per unit surface area; G_i is the total radiant energy per unit time projected onto a unit surface area i . At the same time, because $\alpha = \varepsilon$,and so, the equation (10) can be changed to

$$J_i = E_i + \rho_i G_i = \varepsilon_i E_{bi} + (1 - \varepsilon_i) G_i \quad (11)$$

According to the definition of effective radiation and projection radiation can get the projection of radiation from the surface of the slag liquid

$$G_i = \sum F_{i-j} J_j \quad (12)$$

Among them, F_{i-j} is the angle of radiation between the surface i and the surface j .The net radiant heat flux leaving the surface is equal to the difference between the effective radiation and the projected radiation, which is

$$\Phi_i = (J_i - G_i) A_i \quad (13)$$

Among them, A_i is the surface area of the surface i

Net radiation heat flux is

$$q_i = \frac{\Phi_i}{A_i} = J_i - \sum_j^N J_i F_{i-j} \quad (14)$$

The effective radiant heat flux of the slag surface can be calculated from the effective radiation and the projection radiation of the slag liquid surface according to (11) and (12), the net radiant heat flux can be calculated, and the result is Q_{i-j} =3050J.

4.3 CALCULATION OF OPTIMUM BEAM NUMBER

According to equation (9), the coupling factor is 0.56, the coupling factor calculated by the Monte Carlo method. Comparing with the theoretical value of the coupling factor obtained by the traditional analytical method. As what is shown in Figure 4, A 1 is the isothermal radiating surface, A2 is the ideal blackbody, surface A1 and black body A2 in the radiation heat transfer system without other involved in the medium, the surrounding environment can be considered an infinite blackbody. Figure 5 and Figure 6 is the computer memory in the 128M, CPU PIII500, WinNT operating system under the conditions of the operating results.

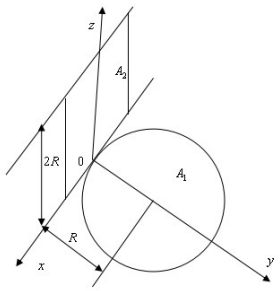

Figure 4 radiation heat transfer coefficient

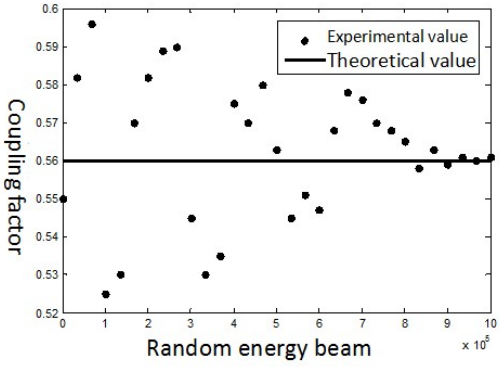

Figure 5 Results of Monte Carlo method for calculating coupling factor

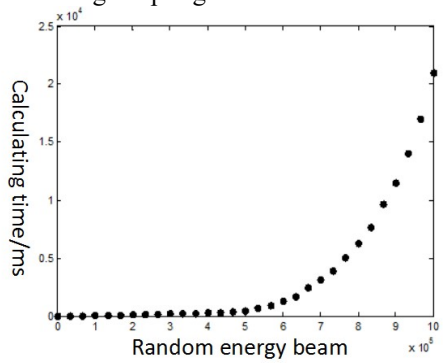

Figure 6 Monte Carlo method to calculate the coupling factor time diagram

It can be seen from Figure 5 that the calculated value of the coupling factor of the surface A1 to the surface A2 converges to the theoretical value in an irregular manner as the number of tracking energy beams increases. Therefore, the Monte Carlo method can improve the accuracy of the coupling factor by increasing the tracking energy beam number. As can be seen from Figure 6. When the tracking energy beam number is , the relative error of the calculated coupling factor is less than 0.3%. While the calculation time is less than 2.1 × 104 ms. Thus, the Monte Carlo method of radiation heat transfer calculation of convergence faster, higher accuracy, the description of the radiation situation is accurate.

5. THEORETICAL AND CALULATING PROCESS OF CONDUCTION HEAT FLUX OF SLAG AND SLAG FLOW

A flat wall of thickness is δ provided, thermal conductivity λ=$ConsT$,and no heat source which is $R=0$ .On both sides of the flat wall, the surface to maintain a uniform and stable temperature T_{w1} and $T_{w1} > T_{w2}$.

For a steady-state one-dimensional heat conduction problem with no internal heat source, due to temperature is changing, this is contradictory to the assumptions of the solution process. To this end, it is still assumed to be constant, λ to be constant, calculating the average thermal conductivity

$$\frac{\partial T}{\partial \tau}=\frac{\partial T}{\partial y}=\frac{\partial T}{\partial z}=\frac{\partial^2 T}{\partial y^2}=\frac{\partial^2 T}{\partial z^2}=\frac{qv}{\rho C_p}=0 \quad (15)$$

Differential equation of heat conduction

$$\frac{d^2T}{dx^2}=0 \quad (16)$$

The boundary condition is

$$\begin{aligned} x=0, T=T_{w1} \\ x=\delta, T=T_{w1} \end{aligned} \quad (17)$$

Equation (17) for the second-order linear ordinary differential equation, integral two times and then we can get

$$T=c_1 x+c_2 \quad (18)$$

Among them, c_1, c_2 is an integral constant which can be obtained from the boundary conditions.

Substituting the boundary condition (17) into (18) can be obtained

$$T_{w1}=c_1\cdot 0; T_{w2}=c_1\cdot\delta+c_2 \quad (19)$$

Joint solution available

$$c_2=T_{w1}; c_1=\frac{T_{w1}-T_{w2}}{\delta} \quad (20)$$

Substituting the general solution can be obtained:

$$T=\left(T_{w2}-T_{w1}\right)\frac{x}{\delta}+T_{w1} \quad (21)$$

Which is the expression of the temperature field of one-dimensional steady-state heat conduction problem of the flat wall, indicating the temperature inside the flat wall is a straight line. The temperature distribution of (21), the derivative can be obtained x can be obtained

$$\frac{dT}{dx}=\frac{T_{w2}-T_{w1}}{\delta} \quad (22)$$

Substituting into Fourier law can be obtained

$$q=\lambda\frac{T_{w1}-T_{w2}}{\delta} \quad (23)$$

Assuming that the side surface area of the flat wall is F , the heat flow is

$$Q=q\cdot F \quad (24)$$

Since the terms (22) and (23) are constants, indicating that heat flux and heat flux are constant, Q and heat flux q are constant. That is, in any section along the x direction, Q and q everywhere for a constant, and has nothing to do with x .This is an important conclusion of the one-dimensional thermal conductivity of the flat wall.

Because the thermal conductivity of the material is a function of temperature $\lambda=\lambda_0\left(1+aT\right)$, And along the direction of temperature is changing, x of

$$\lambda=\lambda_0\left(1+a\bar{T}\right)=\frac{1}{2}\left(\lambda_1+\lambda_2\right) \quad (25)$$

among them, λ_1, λ_2 respectively T_{w1} and T_{w2} lower

thermal conductivity, $W/(m\cdot℃)$, $\bar{T}$ is the average temperature,

$$\bar{T}=(T_{w1}+T_{w2})/2 \tag{26}$$

The following discussion of the concept of thermal resistance for further discussion, the common law of the various transfer processes can be described as

The amount of transfer in the process is the process of the driving force / process resistance in electricity is called Ohm's law, that is to say

$$I=\frac{\Delta U}{R} \tag{27}$$

The above procedure is combined in this section is slag and slag between the thermal conductivity Q_d , the expression corresponding to the conversion can be obtained：

$$Q_d=\frac{(T_w-T_v)}{\delta/\lambda F} \tag{28}$$

among them, T_v indicated the temperature of slag tank, we take it as 30℃ , the thickness of refractory bricks, and we take it as0.08m, λ refers to the thermal conductivity of refractory bricks, we take it as 0.61, the meaning of F is Said liquid slag and refractory brick contact area, we take it as 0.125m. So we can get $Q_d=1084J$

6. CALCULATION OF RESIDUAL HEAT OF SLAG IN SLAG

In the absence of an internal heat source, after a long period of slag flow, the heat transfer of molten slag in the chute reaches steady state. Then the amount of heat remaining is equal to the total heat minus the heat lost, the corresponding formula is

$$Q_r=Q_T-Q_s \tag{29}$$

The loss of heat mainly through radiation and conduction heat transfer in two forms

$$Q_s=Q_5+Q_d \tag{30}$$

7. CONCLUSIONS

In this paper, the dissipation of slag heat in slag trough movement is studied. The Monte Carlo model is established to deduce the radiation heat dissipation of air and slag flow, and then calculate its radiation heat flux and the amount of slag remaining in the slag. From the radiation and conduction heat transfer point of view, ignoring the chemical reaction heat. After deducting the theoretical formula, the heat flux of the radiation between the slag and the air is obtained. And the slag and slag between the thermal conductivity, and gives the slag in the slag tank heat balance of the calculation equation. It is concluded that the thermal residual is in direct proportion to the depth of the slag in the slag.

8. ACKNOWLEDGMENT

The paper has got the support of the 2016 annual college students innovation and entrepreneurship training program in North China University of Science and Technology(project number:X2016140).

REFERENCES

[1] Cheng Ke, Li Xinzhong, Shu Pengcheng. Monte Carlo method in the application of radiation heat transfer, Journal of Xi'an University of Technology, 2002, 18 (1): 44-47

[2] Xie Xiangqian. Master’s degree thesis, Monte-Carlo method for transient radiation propagation in multi-dimensional inhomogeneous media, Harbin Institute of Technology, 2012.7 (in Chinese with English abstract).

[3] Zhong Denghua, Bi Lei, Yu Jia, et al. Robustness analysis of underground powerhouse construction simulation based on Markov Chain Monte Carlo method, Science China(Technological Sciences, 2016.2

[4]Yang Yongguo, Chen Yuhua, Qin Yong, et al. Monte-Carlo Method for Coal bed Methane Resource Assessment in Key Coal Mining Areas of China, Journal of China University of Geosciences, 2008.4

[5] Huang Xiaochun, Hu Mingfu, Dong Fusheng. Energy saving method and development trend of radiant heat transfer in industrial furnace, investigation and analysis, 2013 (03)

[6] Zhang Tengfei, Luo Rui, Feng Wen, et al. Mathematical Model and Simulation of Radiation Heat Transfer in Furnace. Chinese Journal of Electrical Engineering, 2003, 23 (10): 23-27

[7] Yang Aimin. Study on Heat Transfer Law of Blast Furnace Slag Fibrous Process. Qinhuangdao: Yanshan University, 2015.

The Mathematical Model of Influence of Sintering Parameters on High Phosphorus Dephosphorization Rate

ZiJiao WU[1], Yang PENG[2], XiMeng ZHANG[3],WeiXing LIU[4],Wei ZHANG[5]*
[1]College of Metallurgy and Energy, North China University of Science and Technology, Tangshan 063000,Heibei,China,
[2]College of Electrical Engineering, North China University of Science and Technology, Tangshan 063000, Heibei, China;
[3]College of Economics, North China University of Science and Technology, Tangshan 063000,Heibei,China,
[4]Key Laboratory of Moderm Metallurgy Technology of Ministry of Education, North China University of Science and Technology, Tangshan 063000,Heibei,China,
[5]Moderm Technology Education Center, North China University of Science and Technology, Tangshan 063000,Heibei,China,

Abstract: Under the certain conditions of dephosphorizing agent and ratio,With Matlab software to establish the curve and surface fitting model to analyze the influence of technological parameters such as carbon content, alkalinity, ore grain size and sintering temperature on high phosphorus hematite Sintering gasification dephosphorization rate of the law. The results show that the dephosphorization rate of high phosphorus iron ore increases with the increase of carbon content, and the carbon content of 4.141% corresponds to the highest dephosphorization rate; with the increase of basicity, the dephosphorization rate of high phosphorus iron ore is the first The higher the dephosphorization rate, the higher the temperature, the higher the dephosphorization rate, taking into account the cost of the problem, the ore size in the selection of ore in the dephosphorization rate is higher, 0.1 ~ 0.15mm, sintering temperature of 1350℃ is appropriate. When the alkalinity is 1.2 and the temperature is 1400 ℃, the gasification dephosphorization rate is 42.92%, which is higher than that of alkalinity.

Keywords: High phosphorus hematite, Gasification dephosphorization, Curve Fitting, Interpolation Surface fitting

1. INTRODUCTION

China's rich mineral resources, there are eight deposits containing high-phosphorus iron ore, the amount of resources more than 10 billion tons. Phosphorus in the smelting process into the molten iron, will produce steel "cold and crisp", seriously affect the quality of steel. Therefore, although rich in resources, but basically can not be removed in the blast furnace smelting phosphorus, high phosphorus iron phosphate dephosphorization has become a worldwide problem. Therefore, it is of great significance to develop an effective dephosphorization method.

Throughout the study of dephosphorization of high-phosphorus iron ore at home and abroad [1-4], mainly in the following ways: the use of slag pre-treatment approach to control the required level of phosphorus, microwave carbothermal reduction technology, high phosphate ore smelting reduction dephosphorization method. These methods can dephosphorize to a certain extent, but the effect of dephosphorization is not very ideal. Therefore, it is necessary to study the influence of various technological conditions on the dephosphorization rate and find out the best combination of each process.

Through the multi reference data this research project,, the influence of single process conditions, such as carbon content, alkalinity, sintering temperature and ore grain size, on the sintering gasification dephosphorization rate of high phosphate rock was analyzed. The influence of single factor on gasification dephosphorization rate was analyzed. Relationship. Secondly, the influence of process conditions such as carbon content, alkalinity, sintering temperature and ore grain size on the dephosphorization rate of gasification was analyzed synthetically, and the mathematical model was established. Finally, the optimal cooperation was obtained, Which will provide theoretical and technical support for the effective utilization of high phosphate rock.

2.EFFECT OF SINGLE FACTOR ON DEPHOSPHORIZATION RATE OF GASIFICATION

2.1 gauss curve fitting of carbon content and alkalinity

Curve fitting is a kind of data processing method which approximate or depict the relation of discrete point group function by continuous

curve.At present, the more common method is the least square method to fit the curve,This paper is based on the least squares principle, with Matlab software fitting toolbox to achieve the curve fitting.

The influence of carbon content and alkalinity on the dephosphorization rate of gasification is approximately consistent with Gaussian distribution through prior knowledge,Take the Gaussian function template [5]

$$y = a_1 \exp(-((x - b_1) / c_1)^2) \quad (1)$$

Among them a_1, b_1 and c_1 are the parameters to be determined.

2.1.1 effect of carbon content on dephosphorization rate of gasification

In order to study the effect of carbon content on the dephosphorization of high phosphorus iron ore,at a temperature of 900℃,the carbon content was divided into five levels to carry out the experiment,then the allocation of carbon on the dephosphorization of the experimental program [6-9] in Tab. 1.

Table 1 The carbon content of gasification dephosphorization rate influence experiment

Fuel	Number	Carbon Content /%	Temperature /℃	Specific Surface Area/ m^2/g	Dephosphorization Rate %
Yangquang Anthracite	1#	3	900	13.728	2.25
	2#	3.5	900	13.728	2.84
	3#	4	900	13.728	9.82
	4#	4.5	900	13.728	5.78
	5#	5	900	13.728	3.13

Take the carbon content as the independent variable x,the dephosphorization rate of gasification is y.use MATLAB to exponential function curve fitting.The fitted formula is：

$$y = 8.454e^{-\left(\frac{x-4.141}{0.7602}\right)^2} \quad (2)$$

R^2=0.8128,more close to 1,indicating the use of Gaussian curve fitting degree is better.Derive the above formula,the maximum value of the corresponding function when the derivative is equal to 0.that is, $x = 4.414$, $y_{max} = 8.454$.

The results obtained by fitting the curve shown in Fig. 1.

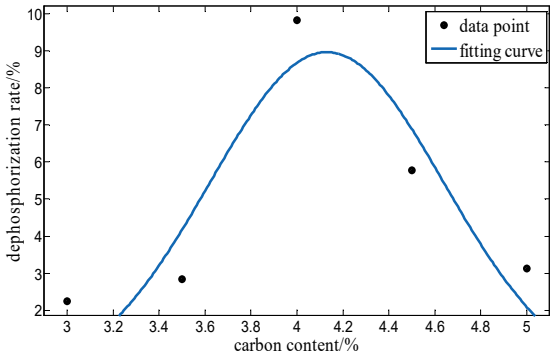

Figure 1. With the carbon content on the dephosphorization rate of fitting curve

As can be seen from the figure, the curve approximation accord with normal distribution.With the increase of carbon content, the dephosphorization rate of high phosphorus hematite increases and then decreases, and therefore there is a maximum value, The coordinates are (4.414, 8.454). When the carbon content is less than 3.5%, the dephosphorization reaction is difficult to occur due to the low carbon content and the contact chance between carbon and fluorine apatite.When the carbon content is more than 3.5%, the gasification dephosphorization rate rises sharply , and reached the maximum at about 4%. When the carbon content was too high, the iron oxides and phosphorus-containing minerals were reduced by carbon to produce FeP, FeP andO_2, CaOthe reaction of$Ca_3(PO_4)_2$, the product left in the sintering material, dephosphorization rate decreased.Therefore,the maximum dephosphorization rate is 8.454% when the carbon content is 4.141% and the temperature is 900 ℃.

2.1.2 effect of basicity on dephosphorization rate of gasification

In order to study the influence of alkalinity on the dephosphorization rate of gasification, at the temperature of 900 ℃, the carbon content of 4%, take 0.8, 1.0, 1.2, 1.4, 1.6, 1.8 and so on six different alkalinity levels of the experiment, the experimental program [6-9] See Tab. 2.

Table 2 The effect of alkalinity on gasification dephosphorization rate experiment

Temperature ℃	Carbon Content %	Basicity	Dephosphorization Rate%
900	4	0.8	11.55
900	4	1.0	13.21
900	4	1.2	18.40
900	4	1.4	15.82
900	4	1.6	14.85
900	4	1.8	14.20

Take the temperature change as the independent

variable x,the dephosphorization rate of gasification is y.use MATLAB to exponential function curve fitting.The fitted formula is：

$$y = 16.76e^{-\left(\frac{x-1.368}{0.9271}\right)^2} \quad (3)$$

Derive the above formula,the maximum value of the corresponding function when the derivative is equal to 0.that is, $x = 1.368$, $y_{max} = 16.76$

The results obtained by fitting the curve shown in Fig. 2.

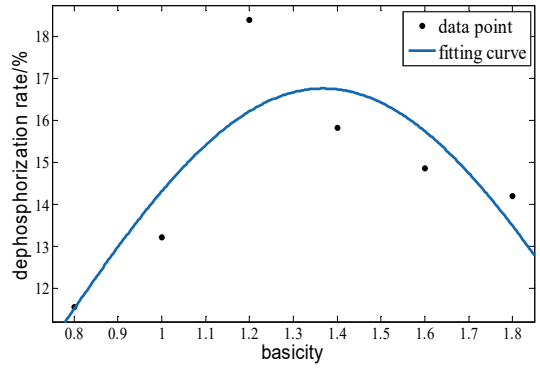

Figure 2 Influence of basicity on the dephosphorization rate curve

As can be seen from the graph, the alkalinity has a significant effect on the dephosphorization rate of gasification. The dephosphorization rate of gasification shows a tendency to increase first and then decrease with the increase of alkalinity.R=1.368 for the best alkalinity, when the alkalinity is too high, too much CaO will consume a large amount of SiO_2 generated$CaO·SiO_2$, $2CaO·SiO_2$, $3CaO·SiO_2$and other substances. SiO_2 plays a very important role in the gasification dephosphorization process, the reduction of SiO_2 generation is bound to affect the dephosphorus products.Therefore, when the alkalinity is high,indirectly restrict the dephosphorization reaction, the dephosphorization rate decreased .

In conclusion, the dephosphorization rate reached 16.76% when the temperature was 900℃ and the alkalinity was 4%.

2.2 power function curve fitting of ore particle size

In the study of the effect of ore particle size on the dephosphorization rate of high phosphorus hematite,the experimental conditions are as follows:carbon content 3%,alkalinity1,temperature 1300 ℃. Sinter test results and gas dephosphorization rate [6-9] in Table 6-3

Table 3 Experiment effect of ore size on gasification dephosphorization and results

Temperature /℃	Basicity	Carbon Content /%	Ore Particle Size /mm	Dephosphorization Agent	Dephosphorization Rate %
1300	1	3	0.18~0.55	2.31	17.3
1300	1	3	0.15~0.18	2.31	25.6
1300	1	3	0.0.96~0.15	2.31	31.2
1300	1	3	0.074~0.096	2.31	36.7

Taking the average of the grain size range as the independent variable x,the gasification dephosphorization rate is the dependent variable y.use MATLAB to exponential function curve fitting.The fitted formula is：

$$y = 10.2x^{-0.5222} \quad (4)$$

R^2=0.9957,It shows that the power exponent is used to fit the curve well, which is close to the actual situation.Fitting of the curve as shown in Fig. 3.

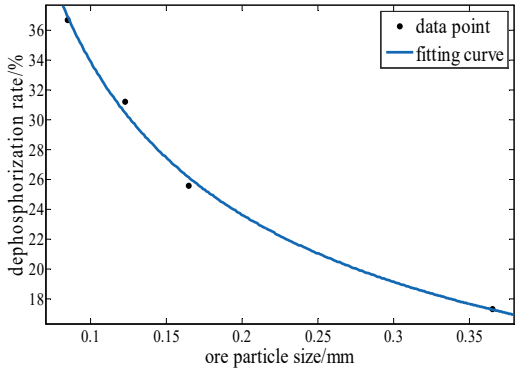

Figure 3 Ore particle size fitting curve

It can be seen from the figure: the smaller the particle size of ore, the higher the rate of gasification dephosphorization.The particle size is less than 0.2mm, as the particle size becomes smaller, dephosphorus rate change up to 12%. According to the high-phosphorus hematite microstructure we can see that the apatite and iron oxide particle size distribution is very fine, and there is a annular interphase structure between the two.As long as the high phosphorus iron ore particle size reaches a certain fineness,to make the iron mineral wrapped apatite exposed, Thereby increasing the contact area between the dephosphorizing agent and the apatite, thus creating favorable conditions for the gasification dephosphorization reaction.Taking the crushing cost into account , considering the ore particle 0.1~0.15.

2.3 curve fitting of exponential function for

temperature

the study of temperature on the high phosphorus iron ore under the influence of dephosphorization rate,the experimental conditions were as follows: carbon content 3%, alkalinity 1, particle size 0.15 ~ 0.18mm.The sinter test results and dephosphorus rate [6-9] see table 6-4.

Table 4 Effect of temperature on the gasification dephosphorization experiment scheme and results

Temperature /°C	Basicity	Carbon Content /%	Ore Particle Size /mm	Dephosphorization Agent /%	Dephosphorization Rate /%
1150	1.0	3.0	0.15 ~0.18	2.31	15.6
1250	1.0	3.0	0.15 ~0.18	2.31	23.9
1350	1.0	3.0	0.15 ~0.18	2.31	28.5
1400	1.0	3.0	0.15 ~0.18	2.31	42.8

Taking the temperature change as the independent variable x, the gasification dephosphorization rate is y,use MATLAB to exponential function curve fitting.The fitted formula is:

$$y = 0.1641e^{0.003929x} \quad (5)$$

$R^2 = 0.9226$,This value is very close to 1, indicating a higher degree of curve fitting, more realistic.Fitting of the curve as shown in Fig. 4.

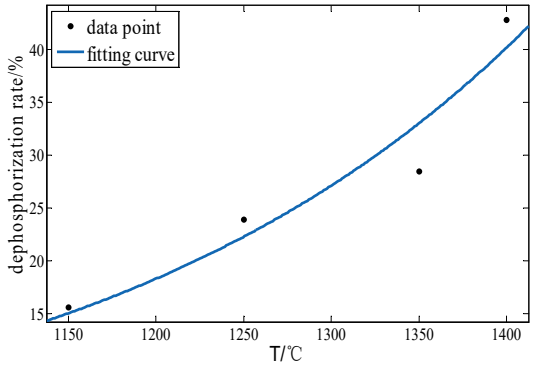

Figure 4. The temperature curve fitting

By the analysis of Figure 4, with the increase of system temperature, gasification dephosphorization rate is high.At 1250~1400℃ , the dephosphorization rate can be as high as 40%, a difference of 15%, indicating that the temperature impact on the dephosphorization rate greatly. According to the thermodynamic reaction of high phosphorus slag gasification dephosphorization analysis, dephosphorization agent of calcium phosphate reduction reaction is strong endothermic reaction, the higher the temperature is, the more favorable to the dephosphorus reaction, but the high temperature will affect the metallurgical properties of sinter, especially under high temperature conditions, easy decomposition of calcium ferrite. At the same time taking into account the cost of the problem, the final sintering temperature can be selected to 1350℃.

3.INFLUENCE OF GASIFICATION DEPHOSPHORIZATION RATE OF MULTI FACTORS

3.1 principle of surface interpolation fitting based on matlab

Due to the limited experimental data, it is impossible to do so many sets of experiments,So we can use the method of interpolation fitting,with the aid of Matlab software,fitting a smooth 3D surface,to study the influence of multi factors on the gasification rate of dephosphorization.

Through the experimental data in Table 5 [6-9] observation,Can be found as a temperature and alkalinity of the 4 by 3 matrix,So the interpolating function interp2 in Matlab can be used,And then use the surf statement to draw the surface can be[12].

Table 5 Effect of alkalinity on gasification dephosphorization experiment scheme and results

Temperature /°C	Basicity	Carbon Content /%	Ore Particle Size /mm	Dephosphorization Agent/%	Dephosphorization Rate /%
1150	1.0	3	0.15 ~0.18	2.31	15.6
1150	1.5	3	0.15 ~0.18	2.31	14.4
1150	2.0	3	0.15 ~0.18	2.31	12.8
1250	1.0	3	0.15 ~0.18	2.31	23.9
1250	1.5	3	0.15 ~0.18	2.31	21.2
1250	2.0	3	0.15 ~0.18	2.31	18.6
1350	1.0	3	0.15	2.31	28.5

			~0.18		
1350	1.5	3	0.15~0.18	2.31	30.3
1350	2.0	3	0.15~0.18	2.31	30.5
1400	1.0	3	0.15~0.18	2.31	42.8
1400	1.5	3	0.15~0.18	2.31	41.6
1400	2.0	3	0.15~0.18	2.31	35.4

3.2 Effect of alkalinity and temperature on the dephosphorization rate at high temperature

Under the experimental conditions of 3% carbon content and 0.15 ~ 0.18mm particle size,to study the effect of temperature and alkalinity on the dephosphorization rate,using MATLAB software for interpolation, draw a three-dimensional surface,See Figure 5,Through the observation of the curved surface can be obtained with the temperature rise of the surface, showing an upward trend, but in the direction of alkalinity fluctuations, but the overall alkalinity is mainly lower, the higher the rate of gasification dephosphorization,And the influence of temperature on dephosphorization rate of gasification is greater than that of alkalinity.

At the same time, when the alkalinity is 1.2 and the temperature is 1400℃, the dephosphorization rate of gasification reaches 42.92%, which is the maximum value under this experimental condition.

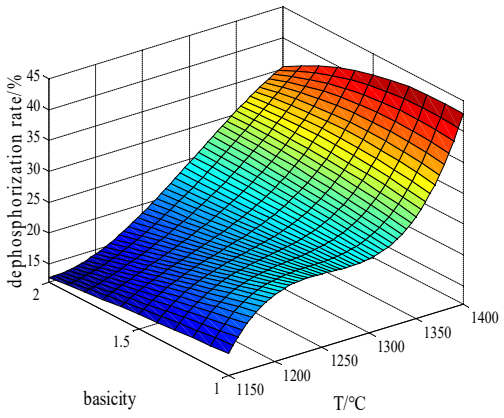

Figure 5 Temperature and alkalinity and dephosphorization rate of the three-dimensional surface

4. CONCLUSIONS

With the combination of thermodynamic calculation and gaussian curve, firstly you need to ascertain that each technological condition such as asamount carbon, alkalinity, sintering temperature, the ore granularity and so on makes influence rule towards the sintering gasification rate of dephosphorization of high phosphorus hematite. And then you can optimize and get the optimal cooperation of every factor to achieve the efficient dephosphorization during the sintering process of high phosphate rock.

1) With the increase of amount carbon, the variation tendency of the high phosphate rock's gasification rate of dephosphorization is first rising and then going down. In the temperature of 900℃ with 4.141% carbon, the dephosphorization rate reaches 8.454%.

2) With the increase of content of alkalinity, the gasification rate of the high phosphate rock presents the variation tendency which is first rising and then going down. In the temperature of 900℃, the alkalinity of 1.368, the dephosphorization rate up to 16.76%.

3) In the temperature of1300℃ with 3% carbon, and under the condition of alkalinity of 1, the smaller the granularity is, the higher the gasification rate of dephosphorization is.

4) Under the condition of 3 % carbon, the alkalinity of 1 and the granularity from 0.15mm to 0.18mm, the temperature increases and the dephosphorization will reach the highest level, which is 28.5%.

5) With the help of three-dimensional curved surface got from interpolation, we know that the gasification rate of dephosphorization at most up to 42.92%.

5. ACKNOWLEDGMENT

The paper has got the support of the 2016 annual college students innovation and entrepreneurship training program in North China University of Science and Technology(project number:X2016233).

REFERENCES

[1] Cheng Cheng, Qingguo Xue,Jingsong Wang, Guang Wang , Yuanyuan Zhang.The mechanism of high phosphorus iron containing minerals and gangue by carbothermal reduction [J].Journal of iron and steel research,2016,04:8-15.

[2] Jun Li, Guangqiang Li, Chengyi Zhu, Changan Wang.Progress in treatment of high phosphorus iron ore and dephosphorization of High Phosphorus Hot Metal Research [J].Journal of Materials and Metallurgy,2007,03:173-179.

[3] Wentang Xia, Xingyu Chen, Huiqiang Li. Dephosphorization of high phosphorus iron ore

wet process and phosphorus removal from wastewater recycling [J].Environmental Engineering, 2011, S1:4-6+40.
[4] Yuxiao Zhao,Qingguo Xue,Guang Wang,Cheng Cheng,Jingsong Wang.High phosphorus iron ore pellet containing carbon reduction smelting dephosphorization [J].Journal of iron and steel research,2015,07:26-31.
[5] Chong Tang, Huihui Hui. Solution of Gauss Curve Fitting Based on Matlab [J].Computer and Digital Engineering, 2013,08:1262-1263+1297.
[6] Wei Zhang, Weixing Liu, Jie Li,Yungang Li, Hongwei Xing.Experimental Study on Factors Affecting Dephosphorization of High Phosphorus Steel Slag by Gasification [J].Iron and steel,2015,01:11-14.
[7] Wei Zhang, Hui Wang, Hongwei Xing, Tielei Tian,Jie Li.Kinetics of dephosphorization of high phosphorus oolitic hematite by gasification [J]. Mining and Metallurgical Engineering, 2015, 01: 11-14.
[8] Hui Wang.Study on high phosphorus oolitic hematite sinter gasification dephosphorization[D]. North China University of science and technology, 2015.
[9]Tielei Tian. Study on sintering dephosphorization of high phosphate rock [D]. Hebei United University, 2012.
[10] Fukagai S, Hamano T and Tsukihashi F. Formation Reaction of Phosphate Compound on Multi Phase Flux at 1573K[J]. ISIJ International, 2007, 47(1): 187-189.
[11] Suito H, Inoue R. Behavior of phosphorous transfer from CaO-Fe_tO-P_2O_5(-SiO_2) slag to CaO particles[J]. ISIJ lntemational, 2006, 46(2): 180-187.
[12]Tingtang Ming. Data Visualization Programming of Matlab[J]. Computer Programming Skills and Maintenance, 2016, 02: 79-85.

Application of configuration software in cold water cooling system of traditional Chinese Medicine

*Yongfu Zhang, Bo Zhao, Yaoxin Wang, Desheng Liu**
College of Information and Electronic Technology, Jiamusi University, Heilongjiang, China,154007

Abstract: With the widely application of the traditional Chinese medicine liquid cold water cooling system, solved the problem of the cooling of the Chinese medicine liquid tank. However, because of traditional Chinese medicine liquid cold water cooling system structure is more complex, brought to the whole cooling system of the monitoring of trouble. In this paper, according to the scope of the functions of king view software and traditional Chinese medicine (TCM) solution to the specific requirements of the cold water cooling system, design the configuration system of traditional Chinese medicine liquid cooling cold water system. Experimental results show the system can monitor real-time solution of cold water cooling system of traditional Chinese medicines, makes the liquid cooling system more intelligent, automation.
Keywords: Configuration; Cold Water System; Real Time Protection

1. INTRUDUCTION

The design of traditional Chinese medicine liquid cooling monitoring and control system of traditional Chinese medicine (TCM) is applied with the king view software solution cold water cooling system for real-time monitoring. The monitoring main interface was designed based on actual hardware structure of the cold water cooling system , corresponding with the actual hardware structure of the cold water cooling system, and making relevant animation design to make the operator on the upper unit state clearly understand the cold water cooling system operation process[1,2]. The Chinese medicine liquid cold water cooling system used cold water cooling system to cool the liquid tanks storing liquid of traditional Chinese medicine, as shown in the Fig.2;Besides, the cold water cooling system was consisted of the water tank of backing cold water, cold water tank of water supply, water chiller, tanks, valves and piping.

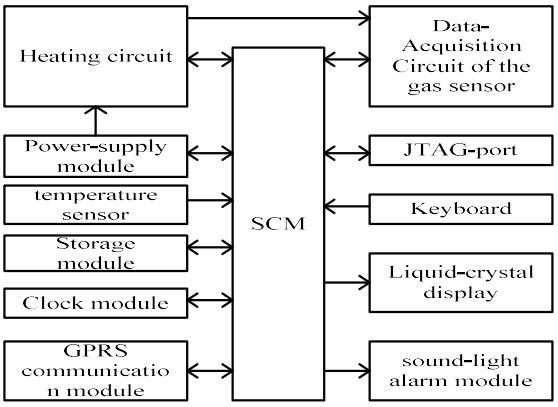

Figure 1 Cold water control system structure diagram

This configuration program is aimed to devise a sensor fault alarm module,which makes it convenient for operators to be aware of the working condition of all sensors in the system.Once sensors goes wrong,IPC configuration software will give an alarm[3].Operators can repair or replace sensors conveniently which went wrong according to the alarm information to ensure the normal operation of cold water cooling system.In this paper,the design of the IPC configuration software is aimed to devise real-time temperature curve interface establishing a real-time data curve in this interface.

When the whole system is operating,operators can check the temperature of each medicine liquid tank in real time in this interface.According to the functions of king view software and traditional Chinese medicine(TCM)solution to the specific requirements of the cold water cooling system,it is aimed to devise the history curve window function and the report data window.This system adopts the design of the integrated control system and upper and lower structure[4,5].As is shown in the picture,field device primarily includes temperature sensor, transducer valve pump package and so on;

The gathering data and the controller select the programmable controller (PLC) realization, completes the overall system the movement and the data analysis function, including each kind of function software design.The supervisory system stands the realization in the operator, the loading configuration king software realization monitors the software the design; Engineer stands is responsible for coordinating and the overall plan monitoring.

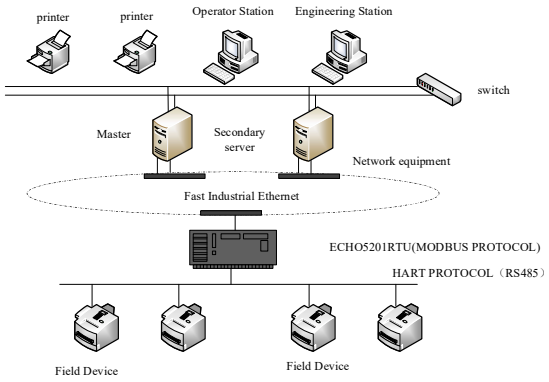

Figure 2 Schematic diagram of monitoring system

2. DESIGN AND IMPLEMENTATION

2.1 Configuration interface design

According to the technological requirements of Chinese traditional medicine, in order to meet the real-time monitoring of the temperature of the filling liquid medicine, should have the main technology interface monitoring function, temperature display function, real time temperature curve and history curve function, data report function, historical data display,storage function and parameter setting function, etc.

The main process interface includes the operation status of the process pipeline and all the equipment,generally providing the temperature of the display and alarm function,switch to other module functions. The main process template of Chinese medicine pharmaceutical industry includes three parts,the main process monitoring template of the cold water system of Chinese medicine pharmaceutical industry includes three parts.The three interfaces will be displayed at the same time of the configuration operation,so as to constitute the main interface of the configuration system.

The real time curve interface is drawn through the lower computer to the temperature value of the liquid medicine in the industrial computer software, and the temperature changes at any time, which reflects the result of the real-time collection of the temperature value of the liquid medicine.This is the current time graph interface of the system. There are four temperature curves which distinguished by different colors in each current time graph.

Figure 3 real-time curve

Data report module in this system configuration data report involving seven function, respectively the historical data query, print, print history real-time reports, statements, modify the report name and save real-time report page setup and historical data, historical data report report print preview. The seven functions will be integrated in data reporting interface, through to the command language to write, to achieve different functions.History data record system configuration module function unit is king view software to meet the requirements of special configuration program run time and open up the function of the unit, the unit including set up the development system, operation system, alarm configuration, historical data record, network configuration, the user configuration and print configuration. The Chinese medicine liquid cold water cooling system configuration program uses the set operation system, historical data record, and user configuration three functions, to realize the run time system configuration Settings, history, library and user safety configuration of three functions.

2.2 the interface implementation

History curve is a curve segment of historical data that storaged in the configuration program of the temperature of liquid medicine filling. The operator may set the historical curve related parameters according to the actual production to achieve reading of the historical data of temperature in liquid medicine filling. Interface defined in different colors representing different segments of liquid medicine filling temperature history data.

Real time curve showing interface is painted by the temperature of the medicine soup can real time delivered from lower computer to the soft ware of the industrial personal computer,The latest temperature varies with time ,showing the medicine soup can results collected real time..Every real time curve picture is able to draw no more than 4 temperature curve lines at the same time,and every curve line is distinguished by the color.

Choosing the options of the report window in the toolkit and drawing the report on the interface .Double-click the report window and seeing p to the table size .,through establishing the text ,seeing up to the text parameter ,realizing the table enroll and revealing put table the results ,its ways of setting up are the same with setting up of the above text object and expression choose the relevant the data variable .

3. CONCLUSIONS

The form of this system can conveniently indicate the temperature of medical pot,with an independent unit of alarm,which can realize actual time monitor to medical monitor.Use the user's authority function in the form of system.To edit the user's authority,for the users who use different authority to land.Classify the function which can be operate,so that it can realize the different function operations.This system form set variable quantity for tradition Chinese medicine cold water to lower the temperature,and design

specific parameter to set up interface,which benefits operators to design system data in different conditions.

4. ACKNOWLEDGMENT

This work was supported in part by a grant from Innovation and entrepreneurship training program for college students in Heilongjiang Province(201510222020).

REFERENCES

[1] AI Hon,point temperature monitoring system with configuration software of data communication [J].Instrument and Meter for Automation,2014,10:37-41.

[2] Weeing Z hang,Wezen Li,Yang Li,Jingly Li,Yong Go.Research of using PLC and configuration software building bio gas production automatic control[J].Research of Agricultural Mechanization,2014,03:216-219.

[3] Tao Z hang. Coal mine safety production monitoring and control system design for PLC and configuration software[J]. Journal of Reckoning Technical University (Natural Sciences) 2014, 02: 177-182.

[4] Ming Sun, BO Guam, Strongmen Sun.HART smart meters general configuration software development[J]. Journal of Jilin Institute of Chemical Industry, 2014, 03: 56-60.

[5] Ni Li.Production line sorting monitoring system design based on MCGS The comparison and application of industrial control configuration software, the computer automatic measurement and control.

The Development and Research of Two-wheeled Self-balancing Intelligence Vehicle System Based on 16-Bit MCU MK60DN512ZVLQ10

Nuonuo Xue, Zhaobo Liu ,Yi Han

Chang'an University, School of Automobile, Xi'an, Shannxi, 710064, China

Abstract: In this article, a two-wheeled self-balancing intelligence vehicle system based on the microcontroller MK60DN512ZVLQ10 is presented. This system uses sixteen microprocessors MK60DN512ZVLQ10 as the core control unit, and design speed monitoring module, inclination measurement module, cruise control module and so on through various sensors. Further, corresponding program to complete the balance control, speed control, steering control of the three major tasks are written. And the segmented Kalman filter and PI, PD control are used. After that, we carried out the installation and commissioning of the mechanical system. And we also carried out a static and dynamic adjustment of the three control parameters of modules. At last, this article carries on the real test of the entire system on the actual runway, whose results prove that the design of intelligent vehicle system can drive fast, steadily, flexibly and independently.

Keywords: self-balanced, intelligence vehicle, Kalman filter, PID control.

1. INTRODUCTION

Nowadays, vehicles are on a development way of intelligence and environmental protection. Smart cars have a wide application prospect in civil, military and scientific research. Among them, self-balanced intelligent vehicles, especially two-wheeled self-balancing intelligent vehicles, are becoming a new, environmentally friendly and convenient means of intelligent transportation. It is a high-order, unstable, non-linear system, which can be seen as a moveable inverted pendulum.

Under the control of the MCU (microprocessor control unit), the system presented in this paper controls the motor drive module of the intelligent vehicle according to the parameters of the functional modules, which can make the intelligent car run smoothly on the different road surface, and improve the safety and driving stability of the intelligent vehicle. At the same time, through the cruise control module, system can enter the cruise mode. The car can be independent at a fixed speed when driving in good condition, which reduces the operator's fatigue intelligently.

2. HARDWARE ASSEMBLY of SYSTEM

A self-balancing intelligent vehicle is introduced in this article, which includes a smart car body and an intelligent vehicle self-balancing control device. The small car includes body, wheels, frame, motor. The device comprises several modules as follows: a MCU, a speed detection module, an inclination measurement module, a electromagnetic wire detection module, a constant speed cruise module, a motor drive module, a battery management module, HMI module (human - computer interaction module) and debug module. They are shown in Fig.1.

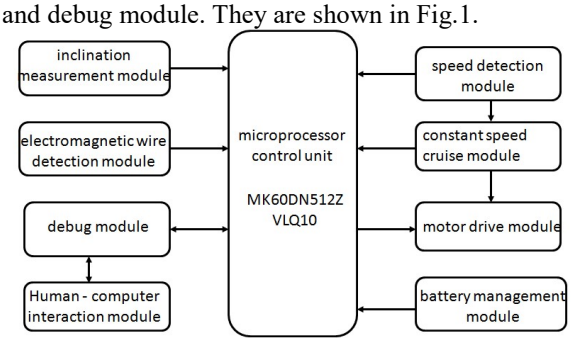

Figure 1 Logic diagram of intelligent vehicle self-balancing control device

The output of the speed detection module, the inclination measurement module and the electromagnetic wire detection module are all connected with MCU. The MCU comprises a sixteen-bit microprocessor, MK60DN512ZVLQ10. An output of the microprocessor control unit is connected to motor drive module. An output of the battery management module is connected to motor drive module and MCU, the output of the speed detection module is connected to the cruise control module. And the output of the cruise control module is connected to motor drive module and MCU. Further, the HMI module and the MCU are connected through the debug module.

3. THE FUNCTION MODULE OF SYSTEM

3.1 Cruise control

Cruise control can reduce the operator's fatigue intelligently. The cruise control module receives the wheel speed signal of the speed detection module. It

comprises a control unit, a distance sensor and a CMOS digital image sensor.

In the cruise control mode, the distance sensor collect the distance signals between the intelligent vehicle and the front and rear vehicles, CMOS digital image sensor collects the image signals around the intelligent vehicle, and the speed detection module get wheel speed signals. All of these signals are transmitted to the control unit which decide how fast the vehicle. At last, the decision signal on speed is transmitted to motor drive module. The process is shown in Fig.2.

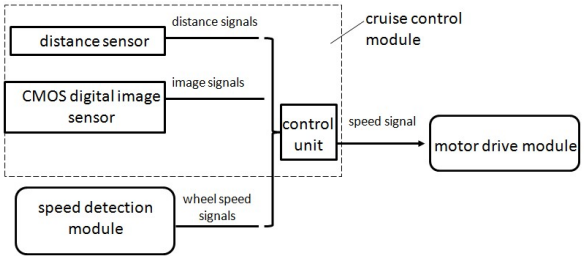

Figure 2 The working principle of cruise control module

3.2 Battery management

Different modules need different voltage supply. Therefore, the voltage 7.2V need to be converted to different voltage values. As shown in Fig.3, there is a 7.2V nickel-cadmium battery which offers power to the motor drive module in the battery management module. What's more, the microprocessor control unit, the speed detection module, the electromagnetic wire detection module and the man-machine interaction module are supplied by the nickel-cadmium battery through the 5.0V LM2940 chip. The inclination angle measuring module is powered by the nickel-cadmium battery through a 5.0V LM2940 chip and a 3.3V LM1117 chip.

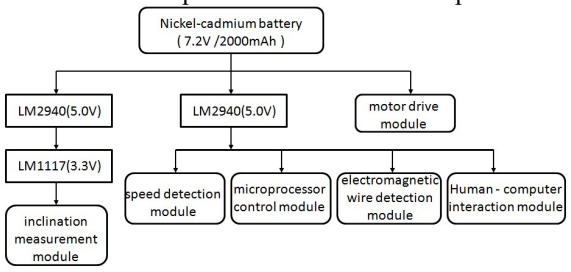

Figure 3 Battery management of intelligent vehicle system

HMI (human - computer interaction)

The HMI module comprises a liquid crystal display screen, an input device and a memory chip.

The memory chip is AT24C02 made by Atmel company.The AT24C02 is a memory chip with an operating voltage of 2.5-5.5V , a low-power CMOS type E2PROM and a memory space of 8 × 256 bits. Its connection circuit is shown in Fig.4.

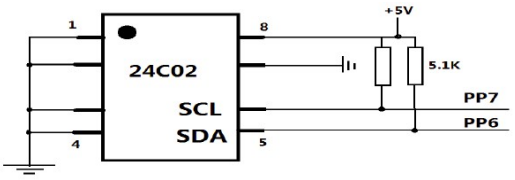

Figure 4 The connection circuit of the memory chip and MCU

Pins(1,2,3) of AT24C02 are three address lines used to determine the chip's hardware address. Pin(5), SDA, is a bidirectional I2C bus through which the data can be serially transferred.

Pin(6),SCL ,is for the serial clock, SDA and SCI are for the open-drain side. In practical application, there will be a 5.1k pull-up resistor respectively when connected the positive power supply. Pin(7) the write protection side.When it connects positive power supply

When it is connected to the positive power supply, only the read operation is allowed. when it is grounded, the chip is allowed to read and write operation. Fig.5 shows the flow diagram of reading data from the AT24C02.

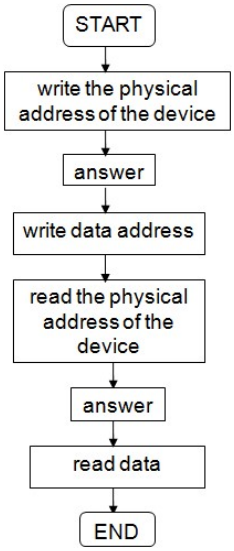

Figure 5 The flow diagram of reading data from the AT24C02

Liquid Crystal Display (LCD), NOKIA5110,communicates with MCU through serial interface. There are eight interface signal lines, 48 × 84 dot matrix LCD ,which support SPI serial peripheral interface, and can display 4 lines of Chinese characters.

We offer Input MCU digital input device which sets eight keys independently. And their funtion are +1, -1, +10, -10, +100, line, save, whose corresponding I/O port are A0, A1, A2, A3, A4, A5, A6, A7. The system can determine the status of input device by detecting the input device connected to the I/O port. The circuit schematic is shown in Fig.6.

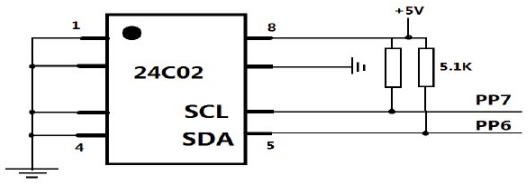

Figure 5 The circuit schematic of keyboard

When the switch is off, pull up PAx, it is in a high level. When the switch is closed, PAx is ground, it will generate a low pulse. when the pulse signal is detected, the corresponding program will be executed.

3.4 Inclination measurement and Kalman filtering

When smart car driving, its system needs to get the information of its inclination and acceleration. There are gyroscope and accelerometer in the inclination measurement module. The angular velocity of the smart car is obtained by the gyroscope and the angular velocity of it is obtained by the accelerometer. Then, system adopts the segmented Kalman filter for the inclination and angular velocity of the intelligent vehicle.

The accelerometer can output the gravity acceleration component in the Z-axis direction and calculate the inclination angle value according to the component value and the inverse trigonometric function. The gyroscope will output the angular velocity signal in the rotation direction of small car. Then the module gets the tilt angle of smart car by integrating the angular velocity.

The system integrates the data of accelerometer and gyroscope with segmented Kalman filter effectively, which can prevent the drift of gyro output from affecting the reliability of the signal and the angular velocity from accumulating error after integral operation. By this way the system can gather the correct information of inclination angle.

4. THE CONTROL ALGORITHM OF SYSTEM

The system program its control method with C language, based on a integrated development environment, CodeWarrior. The control method includes intelligent vehicle upright control algorithm, speed control algorithm, direction control algorithm, gyroscope and accelerometer Kalman filter algorithm. The steps of the control method are as follows.

The MCU initializes functional modules such as speed detection module, inclination measurement module, electromagnetic wire detection module, cruise control module.

The operator sets the parameters by the HMI module.

The MCU obtains the processed AD information from each function module.

Inclination measurement module obtains the inclination angle of the intelligent vehicle by segmented Kalman filtering of the signals from gyroscope and accelerometer.

Make PD calculation of the inclination so as to let the intelligent vehicle be upright.

MCU judges whether it is within the steering calculation period. If it is, then read difference and ratio of the electromagnetic sensor of electromagnetic wire detection module, and perform steering PD control calculation. If not, continue next step.

MCU judges whether it is within the speed calculation period. If it is, then read the feedback value of the photoelectric encoder of the speed detection module and clear it. Then system performs steering PD control calculation. If not, continue next step.

MCU converts the result of closed-loop control to a PWM (Pulse Width Modulation) duty cycle.

MCU judges whether the intelligent vehicle attitude is correct. If it is, PWM duty cycle output controls the motor and rotates to the third step. Otherwise, the motor stops rotating. Steps end.

5. RESULT

We compile and debug program combined with the above algorithm. And we adjust three control module control parameter statically and dynamically. What's more, we conduct the test and commissioning on the runway with a total length of 26.53m. After multiple adjustments on parameter and modifications on program we get the test results which are shown in Tab.1.

Table1 Test results

serial number	fastest time each lap	fastest speed	average speed	times-out of runway
1	14.90	1.9	1.78	0
2	15.24	1.8	1.74	0
3	15.16	1.8	1.75	0
4	17.22	1.7	1.54	0
5	16.69	1.7	1.59	0
6	14.66	1.9	1.84	0
7	16.69	1.7	1.59	0
8	14.74	1.9	1.80	0
9	15.80	1.8	1.65	0
10	15.61	1.9	1.70	0

6. CONCLUSION

In this article, the mechanical structure and principle of the system are introduced, and their connection relations are described in detail. In addition, the article introduces the debugging environment of the software system and the principle of the static and dynamic adjustment of the upright, speed and direction control parameters of vehicle model. After that, we debug it in the actual runway. The results show that the design of hardware and software of the system meet requirements, and have proved the feasibility of the design scheme. However, there are some shortcomings in the relevant hardware installation and procedures for further optimization, which are also the direction of future research.

REFERENCES

[1] Gong W, Research on Control Method of Vertical Two - Wheel Self – Balancing [D]. Changchun

Industrial University, 2016:6.
[2] Jeong S, Kouzai K, Noguchi S. Influence of a rider's rapid weight-shifting motion on the braking behavior of a self-balancing personal mobility vehicle[J].Advanced Robotics, 2016,307.
[3] Rafael N, Carlos C. Studying self-balancing strategies in island-based multimemetic algorithms [J]. Journal of Computational and Applied Mathematics, 2016:293.
[4] Zhu J, Liu H J, Li X J. Research on Multi-sensor Information Fusion of Self - balanced Two - wheeled Electric Vehicle Based on Kalman Filter[J]. Journal of Electrical Engineering, 2016,06:25-32.
[5] Fang J, Yau H T. The LQR Controller Design of Two-Wheeled Self-Balancing Robot Based on the Particle Swarm Optimization Algorithm[J].Mathematical Problems in Engineering, 2014.
[6] Gao X, Dai F Q, Li C Q. Two types of coaxial self-balancing robots[J]. Journal of Central South University, 2013:29-37.
[7] Chih C Y. Sliding-Mode Velocity Control of a Two-Wheeled Self-Balancing Vehicle[J]. Asian J Control, 2014: 166.

Precision Validation and Modification of CFD Simulation based on the Platform of Hydraulic Torque Converter

Li Wenjia[*]*, Wang anlin*
School of Mechanical Engineering, Tongji University, Shanghai, 201804, China

Abstract: In order to verify the simulation accuracy of torque converter CFD and modify the results of CFD simulation, a certain type of hydraulic torque converter was regarded as the research subject. The CFD simulation accuracy to the performance prediction of torque converter was validated based on bench test. The input shaft torque and output shaft torque of CFD simulation were corrected. The average prediction errors of torque converter efficiency, torque ratio and pump capacity are 0.75%, 1.06%, 0.96% respectively after corrected. A method of modifying the simulation results of CFD was provided.
Keywords: Hydraulic torque converter, CFD simulation, bench test, precision validation.

1. INTRODUCTION

Hydraulic torque converter (hereinafter referred to as "HTC") is widely used in ships, construction machinery, automobile, drilling equipment, air blower and other fields. With the rapid development of computer technology, computational fluid dynamics (hereinafter referred to as "CFD") simulation becomes an important means to study HTC gradually. According to CFD simulation, the internal flow field is observed and the HTC is optimized.

By means of flow field analysis, the stress and deformation of the torque converter were studied under the action of concentrated force and hydraulic pressure by Shivaramaiah. [1] Flack [2] discovered the law of the pump wheel pressure surface to the suction surface, and the law of the inner ring to the outer ring of the flow. Kubo [3] analyzed the influence of structural parameters on the flow field characteristics of the torque converter. Yang [4] discovered the law of second flow by using CFD to simulate the stator. Kunz [5] simulated the flow field of pump wheel. Won [6] calculated the flow field of torque converter by using commercial CFD software and analyzed the interaction between the 3 hydraulic components. Kesy [7] analyzed the design parameters of the main influence on the performance of HTC through a series of CFD simulation.

However, the accuracy and correction of CFD simulation were not researched a lot. The CFD simulation accuracy to the performance prediction of torque converter was validated based on bench test. The input shaft torque and output shaft torque of CFD simulation were corrected. The accuracy of correction was also validated in this paper.

2. VALIDATION OF CFD SIMULATION ACCURACY

For the accuracy of CFD simulation, this paper considers two angles from the forecast trend and the forecast precision. According to the manufacturing accuracy, sample A and sample B are classified as a group whose manufacturing accuracy are low, to verify the prediction with the model, and sample C is classified as a group whose manufacturing accuracy is low, to verify the prediction accuracy of the combined model.

The efficiency of bench test of sample A and sample B and CFD simulation of them are shown in figure 1.

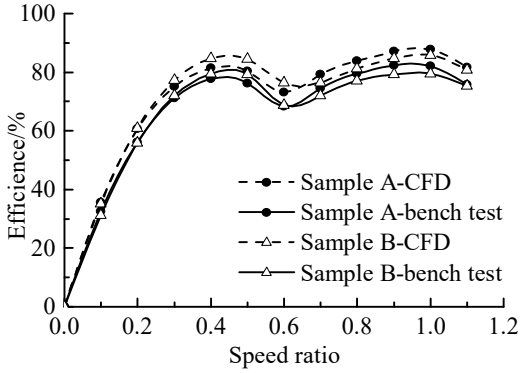

Fig 1 Efficiency comparison of bench test and CFD simulation of sample A and sample B

As can be seen from figure 1, the efficiency of CFD simulation of the two samples has some error to the bench test. The relative error can be calculated by formula 1.

$$\delta_\eta = \frac{|\eta_c - \eta_e|}{\eta_e} \times 100\% \tag{1}$$

Where:

δ_η - relative error of efficiency,

η_c - efficiency of CFD simulation,

η_e - efficiency of bench test.

The calculation result of the efficiency relative error is shown in figure 2.It can be seen from figure 1 and figure 2 that the efficiency trends and the error trends of the 2 samples are consistent. In the bench test, compared with sample B, sample A has a low

efficiency at low speed area and a high efficiency at high speed area. In the CFD simulation, compared with sample B, sample A has the same trend.

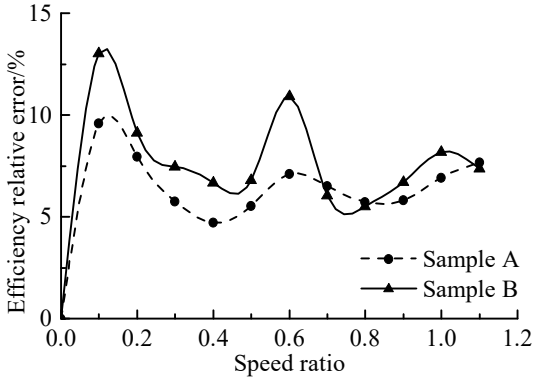

Fig 2 Efficiency prediction relative error of CFD simulation of sample A and sample B

The major reason that causes the efficiency prediction relative error of CFD simulation of sample A and sample B is that the two samples are manufactured by the method of rotary laser sintering. This causes high surface roughness and low efficiency of bench test. But the reliability of CFD simulation in different torque converter performance prediction trend is proved.

The efficiency, torque ratio and pump capacity of bench test and CFD simulation of sample C are shown in figure 3. It can be seen from figure 3 that the prediction accuracy of CFD simulation on efficiency, torque ratio and pump capacity at middle and high speed area is high, but the prediction accuracy on pump capacity at low speed area is low.

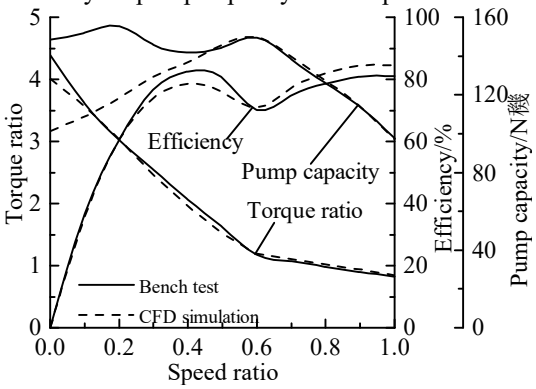

Fig 3 Efficiency, torque ratio and pump capacity comparison of bench test and CFD simulation

Relative errors in efficiency, torque ratio and pump capacity of sample C are solved and shown in figure 4, in order to verify reliability of the simulation results on the accuracy. It can be seen from figure 4 that the relative errors of CFD simulation in efficiency and torque ratio are in 5% mostly. The relative errors of CFD simulation in pump capacity are in 5% at low speed area, and are bigger at middle and high speed area.

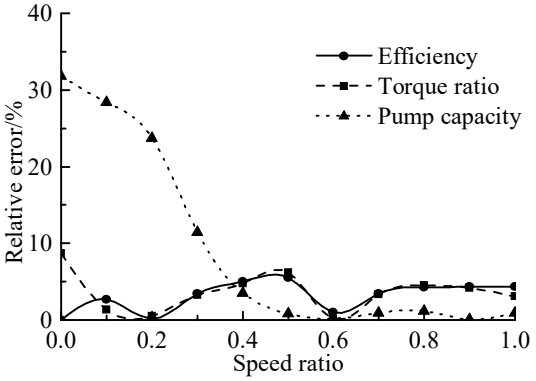

Fig 4 Performance prediction relative error of CFD simulation of sample C

The reasons of low accuracy of the CFD simulation in the low speed area to the pump round capacity prediction are mainly in two aspects. The first reason is that the efficiency of HTC is low in low speed area, and most of the mechanical energy is converted into heat energy. This leads to an increase in oil temperature in the torque converter and the change of hydraulic oil performance. But, CFD simulation does not take into account the effects of oil temperature rise. So a certain error is caused. The second reason is that the pump wheel is connected with the pump wheel shell when the torque converter is actually working. The pump wheel shell is outside the turbine, and there is a certain gap between them, which is connected with the gap between the impellers and full of hydraulic oil. When the HTC works, if there is a rotational speed difference between the pump wheel shell and turbine, there will be torque between them. When the HTC works in the low speed area, the pump wheel and the turbine speed vary greatly, so the torque between them is large. When the HTC works in the high speed area, the pump wheel and the turbine speed vary small, so the torque between them is small.

2. MODIFICATION OF CFD SIMULATION

In order to reduce the errors above, the input shaft and output shaft torque of the CFD simulation results are corrected by the bench test. According to the sample C, the rotation speed of pump wheel is set to 1200 r/min, 1400 r/min and 1600r/min. Input shaft and output shaft torque ratios between bench test and CFD simulation of different transmission ratio are shown in figure 5.

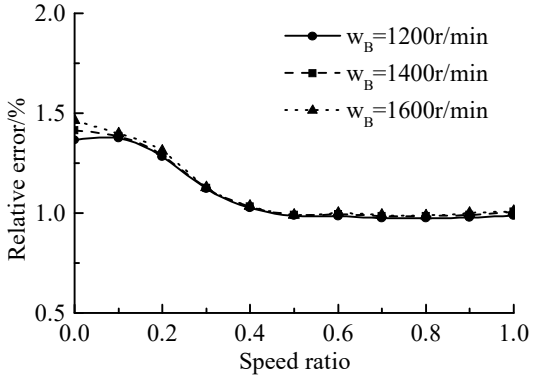

(a) input shaft torque ratios

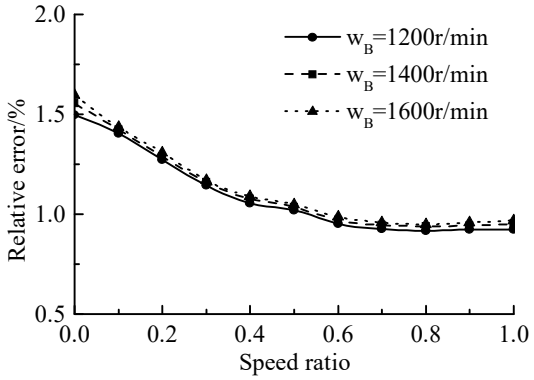

(b) output shaft torque ratios

Fig 5 Input shaft and output shaft torque ratios between bench test and CFD simulation

It can be seen from Figure 5 that the input shaft and output shaft torque ratios between bench test and CFD simulation have little business of pump speed. So it is considered that it has nothing to do with the pump wheel speed. Average values of bench test and CFD simulation of the input shaft and output shaft torque are got under different pump wheel speeds and transmission ratios. Correction coefficient formula of input shaft and output shaft torque is shown in formula 2.

$$k_B = \begin{cases} -3.5\times i^2 + 0.081\times i + 1.4 & i<0.35 \\ -0.035\times i + 1 & i \geq 0.35 \end{cases}$$

$$k_O = \begin{cases} -1.3\times i + 1.6 & i<0.34 \\ -0.52\times i + 1.3 & 0.34 \leq i < 0.67 \\ 0.019\times i + 0.93 & i \geq 0.67 \end{cases} \quad (2)$$

Where:

k_B - Correction coefficient of input shaft torque,

k_O - Correction coefficient of output shaft torque.

Input shaft and output shaft torque of CFD simulation can be corrected form formula 3.

$$\omega`_B = \omega_B k_B$$
$$\omega`_O = \omega_O k_O \quad (3)$$

Where:

$\omega`_B$ - input shaft torque after corrected,

ω_B - input shaft torque of CFD simulation,

$\omega`_O$ - output shaft torque after corrected,

ω_O - output shaft torque of CFD simulation.

3. ACCURACY VERIFICATION OF MODIFIED CFD SIMULATION

HTC performance contrast of bench test and corrected CFD simulation is shown in figure 6. The formula for calculating pump capacity is formula 4.

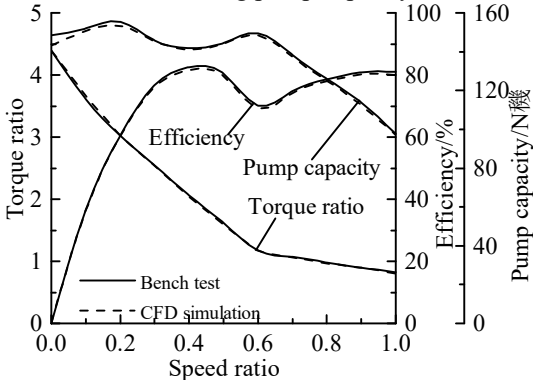

Fig 6 HTC performance contrast of bench test and corrected CFD simulation

$$M_{Bg} = M_B \left(\frac{1000\times 60}{2\pi\omega_B} \right)^2 \quad (4)$$

Where:

M_{Bg} - pump capacity,

ω_B -pump speed

HTC performance prediction errors of corrected CFD simulation are shown in figure 7.The average prediction errors of torque converter efficiency, torque ratio and pump capacity are 0.75%, 1.06%, 0.96% respectively after corrected.

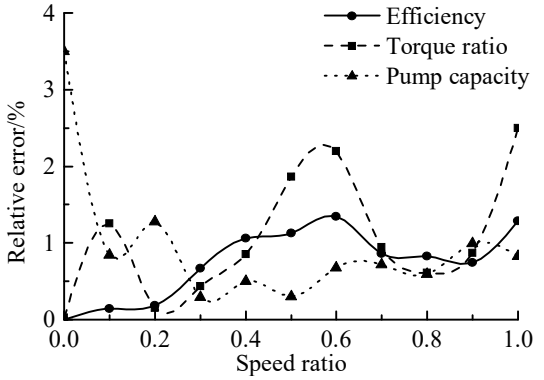

Fig 7 HTC performance prediction errors of corrected CFD simulation

4. CONCLUSION

In summary, the HTC performance prediction of CFD simulation has high reliability in the trend, which can reflect the different performance characteristics of HTC. The prediction accuracy of CFD simulation on efficiency, torque ratio and pump capacity at middle and high speed area is high, but the prediction accuracy on pump capacity at low speed area is low.

Through the input shaft and the output shaft torque correction of CFD simulation, the performance prediction is very high to satisfy the engineering requirements.

REFERENCES

[1] Shivaramaiah Subbaramu1, Banthia Vinod, Kumar, S. M. Structural assessment of torque converter at operating conditions-A numerical study [J]. ASME 2014 Gas Turbine India Conference. 2014, 12-15.

[2] Flack R, Brun K. Fundamental analysis of the secondary flow s and jet-wake in a torque converter pump---part IV: mode land flow in a rotating passage [J] . ASME Journal of Fluids Engineering, 2005, 127(1) : 66~ 74.

[3] Kubo. M.. A loss analysis design approach to improving torque converter performance. SAE paper 981100.

[4] Yang Seunghan, Shin Sehyun, Bae Incheol, et al. A computer-integrated design strategy for torque converters using virtualmodeling and computational flow analysis [C]. SAE Paper 1999-01-1046, 1999.

[5] R. R. By R. Kunz and B. Lakshminarayana. Navier-Stokes Analysis of the Pump Flow Field of an Automotive Torque Converter[J]. Journal of Fluids Engineering, 1995, 117(1): 116-122.

[6] Won Sik Lim, Chinwon Lee, Wookjin Jang etc. Three-Dimensional Flow Field Simulation to Estimate Performance of a Torque Converter [R]. SAE 2000-01-1146.

[7] A. KESY, A. KADZIELA. Construction optimization of hydrodynamic torque converter with application of genetic algorithm [J]. ARCHIVES OF CIVIL AND MECHNICAL ENGINEERING.2011, 6(4):905-920

Design of Intelligent Curtain Controller Based on Single Chip Microcomputer

GuoYanhua,Wang Mingxia*

School of mechanical and electrical engineering, Zhoukou Normal University, Zhoukou 466001, China

Abstract: Based on AT89C51 single-chip smart curtain controller can achieve automatic control and manual wireless control mode.In the automatic control mode, the system can be based on external signals (light, rain) changes in the curtains to make the appropriate adjustments.In the manual wireless control mode, the user can press the button to achieve the timing of the curtains and real-time opening and closing functions.The two models of the design can help people achieve the effective control of the curtains, reducing the traditional curtains in the use of cumbersome operation, so that people's lives more convenient.

Key words:single-chip microcontroller; ntelligent; wireless control

1. INTRODUCTION

Curtain is an indispensable item in people's daily life, but with the rapid development of people's living standards, traditional curtains using rope control or direct manual control has been unable to meet people's daily needs[1,2]. With the rapid development of intelligent, so smart curtains gradually into the people's attention.Smart curtains[3] can not only solve the complex problems of traditional curtains, and can make people's lives more intelligent, more comfortable and more convenient.

The application of single-chip microcomputer[4-9] in intelligent curtain system design can reduce the occupancy space and enhance the practicality and reliability of the system.The design of smart curtain system based on single-chip microcomputer can automatically control the external environment according to the change of the external environment, and realize the real-time manual control, so it has a strong practicability.

2. SYSTEM DESIGN

AT89C51 single chip microcomputer(SCM) was used as the control core of the system. Its main functional modules include wireless receiving / sending module,key / display module, detection module and execution module.Wireless send / receive module through the keyboard keys to send wireless signals. After signal processing, then passed to the microcontroller. The key / display module can be used to control the curtains accordingly. Detection module to detect changes in the external environment, then the analog signal into a digital signal to the controller. Implementation of the module is the signal from the controller to the stepper motor, the stepper motor driven by the wheel in series to achieve the opening and closing curtain control. The overall structure of the system block diagram shown in Fig.1:

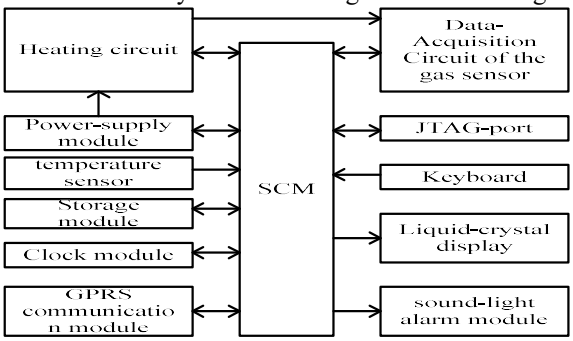

Figure 1 President of the system design

3. HARDWARE CIRCUIT DESIGN

The hardware circuit of the system includes a main control circuit, a detection circuit, a wireless transmission / reception circuit, a key / display circuit, an execution circuit ,etc.

3.1 main control circuit design

SCM control system is the main control circuit, the main control circuit directly determines the choice of the performance of the entire system. It can control and coordinate the normal operation of the entire system, while controlling the normal work of the CPU in the entire hardware plays a vital role in the operation of the system to provide the basis for implementation. The main control circuit design mainly includes three parts: power circuit design, clock circuit design and reset circuit design. Circuit was shown in Fig. 2.

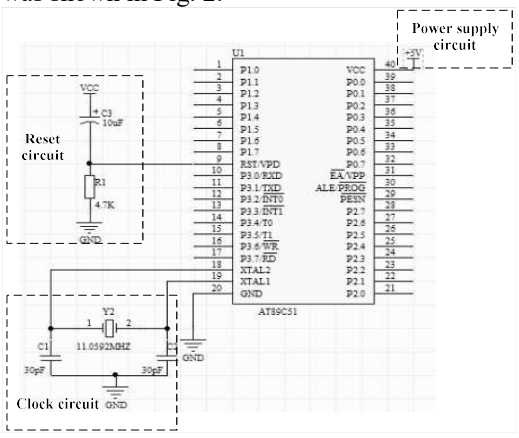

Figure 2 Main control circuit

3.2 detection circuit

The detection module of the system consists of external ambient light detection and raindrop detection. In the raindrop detection / light detection module, LM393 with the input side of the resistance divider is also used to form the raindrop / light reference voltage. When the external detection signal reaches the set value of the voltage comparator does not occur, continue to keep the curtains state. When the external detection signal reaches the set value, the output voltage will change, resulting in the input to the reverse input voltage changes, the voltage comparator action, the comparison of the digital signal is passed to the controller, and then close the curtain.

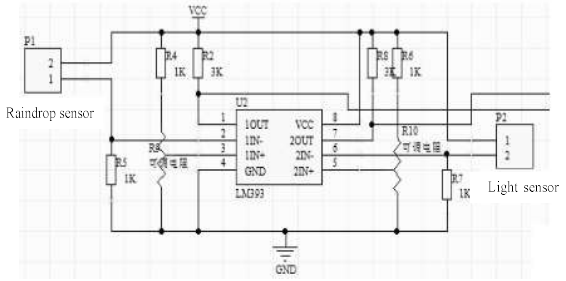

Figure 3 Detection circuit

3.3. wireless transmit / receive circuit

When people are not satisfied with the system automatically adjust the effect, want to manually adjust the opening and closing curtains, curtains through the remote control to adjust the opening and closing state, you need to send and receive wireless module to achieve the control signal transmission.

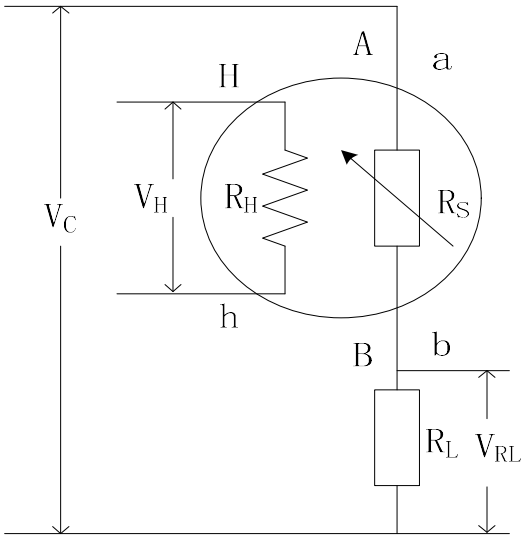

Figure 4 Wireless transmitter module

In the wireless transmission module, the encoder must be used to encode the information in order to send information through the wireless transmission device. This design used PT2262 and F05P as the encoder and wireless transmitter respectively. The circuit is shown in the Fig.4.

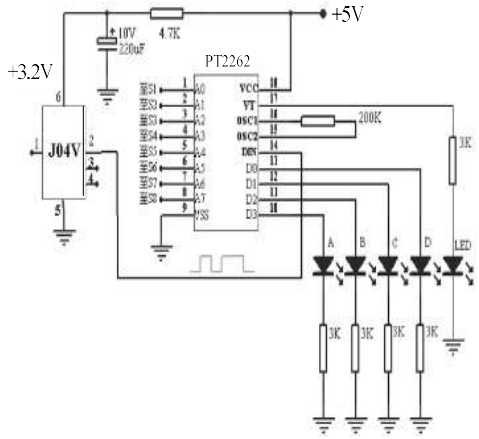

Figure 5 Wireless receiver module

Wireless receiver module is the main function of the wireless receiver to receive unlimited send module to send the signal, and then the signal sent to the decoder to decode the decoded signal sent to the controller, the controller generates the corresponding control signal. The design used PT2262 and J04V respectively as the encoder and RF wireless receiver was shown in Fig. 5.

3.4 button module

As shown in Fig.6, in this module using the microcontroller P1.0 ~ P1.3 port with a pull-up resistor between the key and the microcontroller. When the key is pressed, +5 V power supply voltage through the resistor R1 directly grounded, so P1.0 pin is low level; When the key release P1.0 port is high level. According to this principle can be detected by the number of I/O port on the level of the connection, so as to determine whether there is a key to press and determine the location of the press the button.

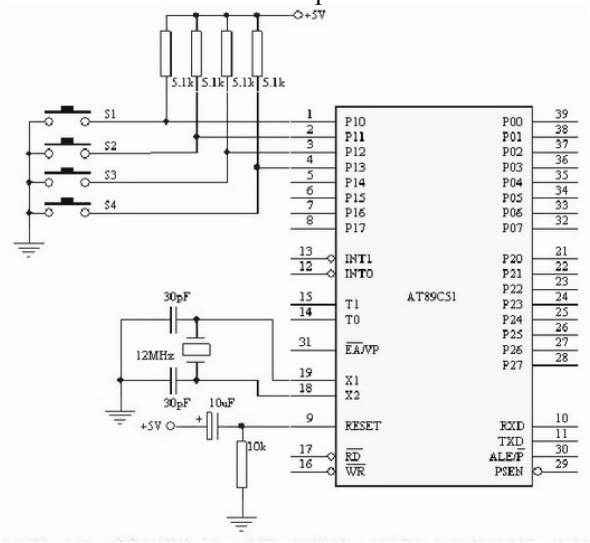

Figure 6 Key module

3.5 display the module

In order to compare the intuitive display related control, 1602 LCD module was used in the circuit system, which is mainly used in timing modules in the timing of the adjustment and motor action

display.

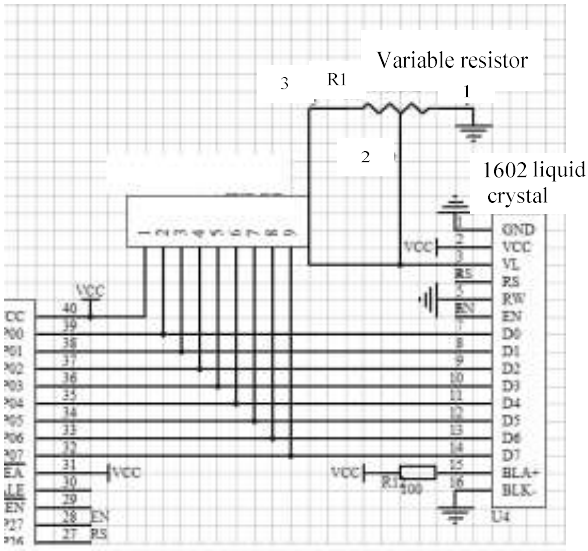

Figure 7 Display module

In this module, you need to use the 32 ~ 40 feet of SCM, and the display 1602 and the SCM were connected with 10K pull-up resistor, because VL is displayed in the bias signal, the need to connect 10K adjustable resistor, the data pin D0 ~ D7 connected to the single-chip P0.0 to P0.7, that was shown in Fig.7.

3.6 execute the module

When the microcontroller receives the external signal, will produce a certain control signal, and this signal through the I/O port to the driver chip ULN2003A(Fig.8), stepper motor driver chip receives a control signal, the drive stepper motor rotation, A pulse signal, the stepper motor rotation angle is pre-set, the entire rotation process is composed of a number of this rotation. In the motor work process, according to the principle can achieve precise control of the curtain.

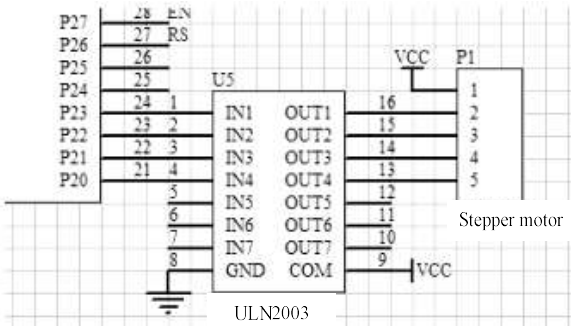

Figure 8 Execution module

4. CONCLUSION

The system has two operating modes: automatic mode and manual mode. In automatic mode, the system not only can automatically adjust the curtains according to the changes of external light and raindrops, but also can open or close the curtains according to the preset time. In the manual mode, one can control the degree of opening and closing curtains, curtains and can set the opening and closing time, to provide people with a great convenience. Intelligent curtain system has good reliability and anti-interference ability, more complete function, more convenient control, more human, so in the market has great application prospects, it is worth vigorously develop and promote.

5. ACKNOWLEDGMENT

Supported by Henan Provincial Department of Science and Technology Research Project (No. 162102210400). and Foundation from Education Department of Henan Province (No. 16B140006).

REFERENCES

[1] HUANG Quan-yuan, LI Yuan-yuan, Design of Smart Curtain Based on Single-chip Microcomputer , Information and Communication, 2015, 8: 71 -72.

[2] LI Qiang, TANG Mingzhuo, YANG Guiqin, Design and Realization of Wireless Transceiver Module , Jiangxi Communication Science & Technology, 2010, 1: 38-40.

[3] LIU Jin, TANG Lil, Design Intelligent Curtain System Based on Single Chip Microcomputer, Science and Technology Innovation Herald, 2015, 25: 14-15.

[4] Wang C W, Liu C L, Jiang W L, et al, Intelligent Curtain Controller based on Single-chip Microcomputer, Jilin Normal University Journal, 2010,1:93-95.

[5] Jia X J, Design of Intelligent Hanger Based on AT89C52 Single-Chip Microcomputer, Advanced Materials Research, 2013, 694-697:1475-1478.

[6] Zhao J, Shun-Wei W U, Chen X M, et al, Design of Photosensitive Curtain and Acoustic Control Lamp System based on Single-chip Microcomputer, Journal of Taishan University, 2013.35(3):101 -103.

[7] Sun Q, The electric curtain design based on single chip microcomputer, Microcomputer & Its Applications, 2012,16:32-37.

[8] Li J, Meng X L, Song W L, Intelligent Temperature Control System Design Based on Single-Chip Microcomputer, Journal of Harbin Institute of Technology(New Series, 2014, 21(3):91-94.

[9] Jiang J H, Xiao Z G, A Study on Liquid Level Measurement and Control System Based on Single Chip Microcomputer, Applied Mechanics & Materials, 2015, 713-715:369-372.

Study of Generalized Snell's law

Zhou Sihua[1], Wang Gaoliang[1], Guo Yanhua[2]*

[1]School of Physicsand Electromechnical Engineering, Zhoukou Normal University, Zhoukou 466001, China

[2]School of mechanical and electrical engineering, Zhoukou Normal University, Zhoukou 466001, China

Abstract: To further study on the laws of anomalous refraction and reflection, the Matlab software was used to simulate , the value of phase gradient was separately setted to $2\pi/1400$ or $2\pi/1200$, $\lambda_0 = 700nm$, $n_1 = 1$ and $n_2 = 1.5$. simulation results supported that incident wave come out abnormal refraction and reflection on the surface of superconducting materials. Choosing appropriate phase gradient could make abnormal reflection disappear. These laws will be applied widely in modulating phase, controlling light beams, et al.

Keywords: metasurface; phase gradient; reflection law; refraction law

1. INTRODUCTION

The Snell's law of Optical important foundation was overturned by was a kind of new metamaterial[1-5], Veselago, a scientist of The former Soviet union , has predicted the existence of it in theory.The metamaterial have different physical characteristics such as reverse Cerenkov radiation, inverse Doppler effect and inverse Snell's law.Electric field Intensity, magnetic field intensity and wave vector between present a left hand rule,When permittivity and permeability of materials is negative,so it was called left-handed materials, negative refraction materials[6] ,Han Lu[7] has derived generalized Snell's law from the Fermat's principle and boundary conditions.These materials with special properties[8-10] have been designed and manufactured in lab.The super interface is an important field of metamaterials,which was manufactured with orderly physical structure ,and can use in beam manipulation[11], wave plate[12] and polarization treatment[13,14] and other fields.

2. GENERAL OF THE SNELL'S LAW

If the interface is ideal,there will be no additional phase when a light ray passes from one medium(n_1) to another(), it is consistent with Snell's law.

$$\sin\theta_r - \sin\theta_i = 0 \quad (1)$$

$$n_\tau \sin\theta_\tau - n_i \sin\theta_i = 0 \quad (2)$$

There will be additional phase when the interface is not ideal. If rate of phase change ($d\phi/dx$) is a constant value, the generalized Snell's law [15]could be exported on base of Fermat's principle

$$\sin\theta_r - \sin\theta_i = \frac{\lambda_0}{2\pi n_i}\frac{d\Phi}{dx} \quad (3)$$

$$n_\tau \sin\theta_\tau - n_i \sin\theta_i = \frac{\lambda_0}{2\pi n_i}\frac{d\Phi}{dx} \quad (4)$$

Comparing equation (1,2) with equation (3,4),the gen eralized Snell's law(3,4) turn into the traditional Snell's law(1,2) as $d\phi/dx = 0$ .The relationship of Snell's law and the lgeneralized Snell's law Can be seen intuitively from the Matlab simulation diagram. The angle of reflection and refraction is not only connected with the incidence angle, the refractive index and wavelength but also phase gradient in the case of $d\phi(x)/dx \neq 0$ .Fig.1shows the relationship of reflection angle and incident angle.The solid line and dotted line show respectively traditional law of reflection and generalized law of reflection.The relationship of reflection angle and incident angle is not a straight line,it is different from the traditional law of reflection.Reflected light will disappear when the incident angle is greater than the critical value,the result indicates that critical value are decreasing with the phase gradient increasing.If the critical value is negative, then the corresponding angle of reflection is positive, it means that reflection angle and incident angle are both on the same side of the normal in physics,this phenomenon is negative reflection.People can take advantage of this phenomenon to design stealth material.

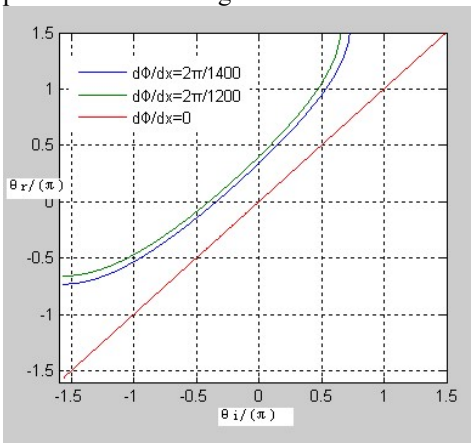

Figure 1 The relationship of reflection angle and incident angle

Fig 2 shows the relationship of refraction angle and incident angle when light from optically thinner

medium into the optically denser medium.The solid line and dotted line show respectively traditional law of refraction and generalized law of refraction.Refracted light will disappear when the incident angle is greater than the critical value,but total reflection will occur.The result indicates that critical value are decreasing with the phase gradient increasing.If the critical value is negative, then the corresponding angle of refraction is positive, it means that refraction angle and incident angle are both on the same side of the normal in physics,this phenomenon is negative refractions.People can take advantage of this phenomenon to design stealth material.

Negative refraction and negative reflection will appear at the same time if the choice of wavelength, refractive index and phase gradient is appropriate.

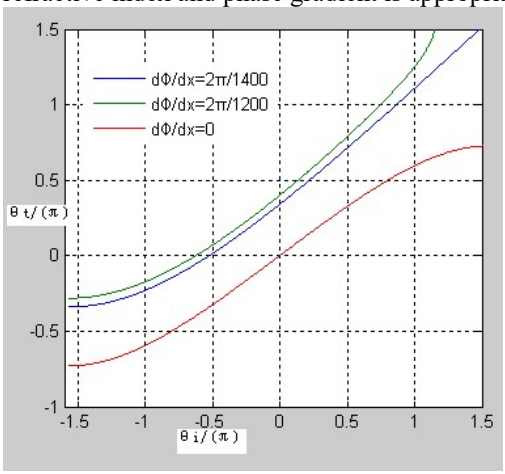

Figure 2 The relationship of refraction angle and incident angle.

3. ABNORMAL REFLECTION AND ABNORMAL REFRACTION

In Fig.3, traditional Snell's law shows that incident light and reflected light(refracted light)separated on both sides of the normal.Abnormal reflection and abnormal refraction are shown in fig.4,it is obviously different between traditional Snell's law and generalized Snell's law.

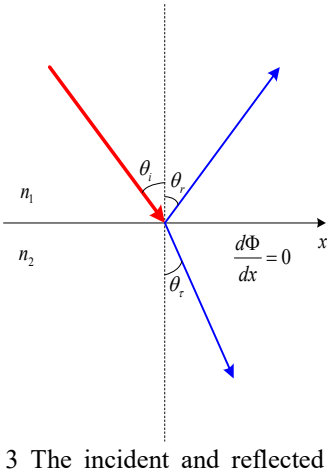

Figure 3 The incident and reflected light of Snell's law

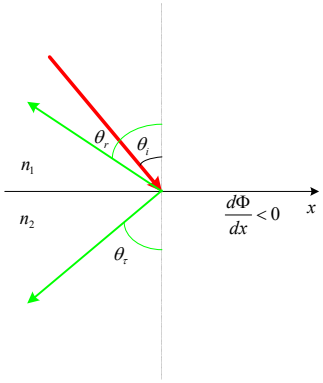

Figure 4 The incident and reflected light of generalized Snell's law

If the incident light is perpendicular to the interface,that is $\theta_i = 0$,the equation of (3) and (4) become into

$$\sin\theta_r = \frac{\lambda_0}{2\pi n_i}\frac{d\Phi}{dx} \quad (5)$$

$$n_\tau \sin\theta_\tau = \frac{\lambda_0}{2\pi}\frac{d\Phi}{dx} \quad (6)$$

for θ_r and θ_τ are real numbers,there are $|\sin\theta_r| \le 1$ and $|\sin\theta_\tau| \le 1$,so

$$-\frac{2\pi n_i}{\lambda_0} \le \frac{d\Phi}{dx} \le \frac{2\pi n_i}{\lambda_0} \quad (7)$$

$$-\frac{2\pi n_\tau}{\lambda_0} \le \frac{d\Phi}{dx} \le \frac{2\pi n_\tau}{\lambda_0} \quad (8)$$

The constraint equation of（7） and（8）are abnormal reflection and refraction respectively.

4. CONCLUSION

If the interface is designed into a structure composed of many small antenna array group, refracted light will disappear when the incident angle is greater than the critical value,but total reflection will occur. The critical value is negative, then the corresponding angle of refraction is positive, it means that refraction angle and incident angle are both on the same side of the normal in physics. Negative refraction and negative reflection will appear at the same time if the choice of wavelength, refractive index and phase gradient is appropriate.

5. ACKNOWLEDGMENT

Supported by National Nature Science Foundation of China(No. 11405280) and Foundation from Education Department of Henan Province (No. 16B140006).

REFERENCES

[1] A. V. Kildishev, A. Boltasseva, and V. M. Shalaev,Planar photonics with metasurfaces,Science, 2013,

339, 1232009.
[2]Alexandra Boltasseva , Harry A. Atwater, Low-Loss Plasmonic Metamaterials,Science ,2011,331 (6015): 290–291.
[3]Gong Boyi,Zhou Xin,Zhao Xiaopeng, Numerical study of three-dimensional isotropic left-handed metamaterials at visible frequencies , Acta Phys. Sin,2011,60(4),044101.
[4] SuYanyan,Gong Boyi Zhao Xiaopeng, Zero-index Metamaterial Based on Double-negative Structure, Acta Phys. Sin,2012,61(8),084102.
[5] J. Cheng and H. Mosallaei, Optical metasurfaces for beam scanning in space , Opt.Lett,2014,39, 2719.
[6]Huang Zhenyong, Dispersion and equal-inclination interference characteristics of left-handed materials, Laser & Optoelectronics Progress, 2012, 49(9),091602.
[7] Han Lu, Wang Zhaona, Two methods for general laws of reflection and refraction for Metasurface with phase discontinuity, College Physics, 2013,32(03):49-52.
[8] Hou Shanglin, Zhang Shujun, Li Suoping, et al, Investigation on transmission characteristics of doubly cladding fiber with an inner cladding made of negative refractive-index material, Acta Optica Sinica,2011,31(5),0506004
[9] Zhou Cheng,Gao Yanxia,Liang Zhixia, Research of second-harmonic conversion efficiency with high intensity of fundamental frequency light in negative-index materials, Acta Optica Sinica,2010,30(7):2074-2079.
[10] Liang Lanju,Yan Xin,Yao Jianquan et al, Two-dimensional left-handed material based on parallel metallic double rods in terahertz wave, Acta Optica Sinica,2012,32(3),0316001.
[11] A. Pors, M. G. Nielsen, and S. I. Bozhevolnyi, Broadband plasmonic half-wave plates in reflection, Opt. Lett,2013,38, 513.
[12] M. Farmahini-Farahani and H. Mosallaei, Birefringent reflectarray metasurface for beam engineering in infrared, Opt. Lett,2013,38, 462.
[13] N. K. Grady, J. E. Heyes, D. Roy Chowdhury, et al, Terahertz metamaterials for linear polarization conversion and anomalous refraction, Science, 2013,340, 1304.
[14]Parazzoli C G, Greegor R B, Lik, et al, Experimental verification and simulation of negative index of refraction using snell's law, Physics Review Letter,2003,90,107401.

Designing of Mooring System

Chengran Ren[1], Huiqi Zhang[1], Shihao Zhao[2], Jianhui Wu[3,]*
[1]College of metallurgy and energy of North China University of Science and Technology, Tangshan, Hebei 063000, China.
[2]College of Information Engineering of North China University of Science and Technology, Tangshan Hebei,063000, China.
[3]College of Science of North China University of Science and Technology, Tangshan Hebei,063000, China

Abstract: According to the problem, we establish the catenary equation model for the anchor chain part. The result shows that the tangent angle between the anchor chain and the anchor chain is 2.3750 when the wind speed is 12m / s, the horizontal distance of the point is 8.5014m, and the curve of the anchor chain and the area of the swimming area are 227.05m2 according to the catenary equation. When the wind speed is 24m / s, the tangent direction of the connection of anchor chain and anchor and the horizontal angle is 8.510, the horizontal distance from the mooring point to the hanging point is 14.3641m, and the area of the swimming area is 648.20m2. The force balance equations between steel and buoy are established. The force balance equations between force and inclination angle are established, and the inclination of steel drum and steel pipe is obtained when wind speed is 12m / s and 24m / s respectively. Angle and draft, and the drafts were 0.732 m and 0.75 m, respectively.

Keywords: Theoretical Mechanics, Catenary equation, Newton iteration method

1. INTRODUCTION

The catenary coordinate system of the chain is established, and the related unknown quantity is obtained by solving the catenary equation. We need to establish the relationship between the inclination angle of the steel pipe required, the inclination angle of the steel drum, the shape of the anchor chain, the buoy draft and the swimming area, the anchor chain and the anchor are respectively subjected to the force analysis, and the relationship between the inclination angle and the force is established so as to obtain the result.

2. EXPERIMENTAL

2.1The establishment of model 1: The Catenary Model of Chain [1,2]

The coordinate system with anchor as the coordinate origin, parallel to the seabed direction as the x axis and perpendicular to the seabed direction as the y axis is set up and the catenary equations are listed

$$y = a\left[\sec^T\left(ch\frac{x}{a}-1\right)+tgTsh\frac{x}{a}\right] = \frac{R}{w}\left[\frac{1}{\cos T}\left(\frac{e^{\frac{xw}{R}}+e^{\frac{-xw}{R}}}{2}-1\right)+\frac{1}{\cos T}\cdot\frac{e^{\frac{xw}{R}}-e^{\frac{-xw}{R}}}{2}\right] \quad (1)$$

From the above formula can be seen that y is a function of $y=f(R,x,T,w)$. Known R,x,T,w can be obtained water depth y .Under normal circumstances the depth of the water instead is known, so often from the y to seek x. Obviously, it is difficult to derive its inverse function $x=f_2(y)$ from the formula. $y=f_1(x)$, and it is difficult to obtain y by substituting a different value of x into the formula (1), which is the value we want when the calculated water depth is exactly equal to the water depth. Process more cumbersome, in the use of Excel software processing[3,4], let the computer to complete. After obtaining, then followed by the following formula to find the chain length:

$$l = a\left[tgT\left(ch\frac{x}{a}-1\right)+\sec T\cdot sh\frac{x}{a}\right] = \frac{R}{w}\left[\frac{1}{tgT}\left(\frac{e^{\frac{xw}{R}}+e^{\frac{-xw}{R}}}{2}-1\right)+\frac{1}{\cos T}\cdot\frac{e^{\frac{xw}{R}}-e^{\frac{-xw}{R}}}{2}\right] \quad (2)$$

Through access to relevant information,

$$S = \frac{T_H}{w}(\tan\beta-\tan\alpha) \quad (3)$$

$$x = \frac{T_H}{w}\left[\sinh^{-1}(\tan\beta)-\sinh^{-1}(\tan\alpha)\right] \quad (4)$$

$$z = \frac{T_H}{w}(\cosh\left[\sinh^{-1}(\tan\beta)\right]-\cosh\left[\sinh^{-1}(\tan\alpha)\right]) \quad (5)$$

2.2The establishment of model 2: The model of the inclination and force of each object is established [5-7]

First of all, observe the link between the various objects in the figure, the force of each part of the analysis: Set buoy draft depth h, given by the wind in the formula can be obtained, this time the size of the wind:

$$F = 0.625\times(2-h)\times 2\times v^2 \quad (6)$$

From the buoyancy formula:

$$F_1=\rho g\pi h \quad (7)$$

1.Analysis of the buoy can be obtained by force

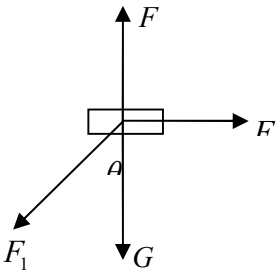

Figure 1 Stress analysis

$$F_1\cos\theta_1+G=F \quad (8)$$

(θ_1 is the first section of the steel tube tilt angle, F_1 is the first section of the steel tube pull.)

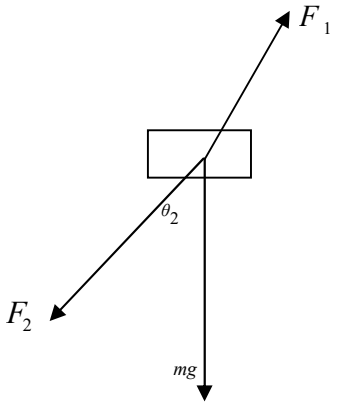

Figure 2 Stress analysi

2.The first section of the steel pipe force analysis available

$$F_1\cos\theta_1=mg+F_2\cos\theta_2 \quad (9)$$

$$F_1\sin\theta_1=F_2\sin\theta_2$$

The second section of the steel pipe force analysis available.

$$F_2\cos\theta_2=mg+F_3\cos\theta_3 \quad (10)$$

$$F_2\sin\theta_2=F_3\sin\theta_3$$

Analysis of the third section of the steel pipe available.

$$F_3\cos\theta_3=mg+F_4\cos\theta_4 \quad (11)$$

2.3 The Establishment of Model 3:The model between the inclination angle and the water depth is established.

From the depth of the sea and steel pipe, steel drum, the length of the anchor chain, so you can establish the relationship between the tilt angle and water depth:

$$22.05\times\cos\theta_6+1\times\cos\theta_5+1\times\cos\theta_4+1\times\cos\theta_3+1\times\cos\theta_2+1\times\cos\theta_1+h=18 \quad (12)$$

Set up

$$g(h)=22.05\times\cos\theta_6+1\times\cos\theta_5+1\times\cos\theta_4+1\times\cos\theta_3+1\times\cos\theta_2+1\times\cos\theta_1+h-18 \quad (13)$$

3. RESULTS AND DISCUSSION

The solution to the above equation, and then tested $g(h)$ = 0, the draft is the depth. The above 15 equations can be obtained immediately tilt angle and force, through the MATLAB programming (code see appendix) finally obtained:

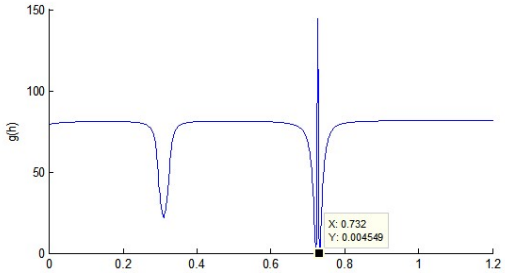

Figure 3 Curve of water depth and a curve when wind speed is 12m / s

It can be seen from Fig.1, $g(h)$ = 0 point appears in = 0.732, so when the wind speed of 12m / s, h = 0.732; h into (1) (2), inferred $\theta_1=0.9635^0$;

In the same way, $\theta_2=0.97065^0$, $\theta_3=0.9779^0$, $\theta_4=0.98527^0$, $\theta_5=0.99275^0$.

Buoy draft depth h = 0.732m. The model can also be used to determine the angle between the top tension of the chain and the horizontal plane, ie, θ_6=31.38^0 and the wind force $F=228.24$N, and substituting the two into (3),We can calculate the anchor angle α=2.375^0

Put the size of the anchor angle into (1) and (4) ,we can get $x=8.5014$, and then get the floating area of the buoy as the center of the anchor, 8.5014 radius of the circular area, the area S = 227.05.

Anchor chain equation

$$y=3.3271\times\left[\sec 2.375^0\times\left(ch\frac{x}{3.3271}-1\right)+tg2.375^0\times sh\frac{x}{3.3271}\right] \quad (16)$$

Thereby obtaining an anchor chain shape map,

as

shown in Fig.d

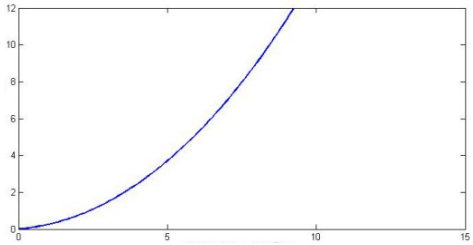

Figure 3 Chain shape when wind speed is 12m /s

REFERENCES

[1] LingbinHu,Tang Jun . Solution of catenary equation and its application [J]. Ship, 2004,01: 17-20.

[2] Mengda Wu, LiZhi Cheng, etc. Mathematical modeling tutorial [M]. Higher Education Press, 2011.

[3] Yi-hua Su, Jian-min Yang, Long-fei Xiao, Xin Li.Multi-objective optimization design of mooring system based on static similarity for water depth truncation [J] .Ocean Platform of China, 2008,01: 14-19.

[4] Xiao-ping Li, Shu-xinWang,Man-li He, Hai-gen Zhang.Theoretical Model of Underwater Cable Dynamics [J].

[5] Meng-xi Nie, Xu-sheng Wang, Xiao-ming Wang, Lin Wang. Time domain method for mooring forces of wind, wave and current flow [J].

[6] Xin Yang. Mooring system of fast calculation and its application [D]. Dalian University of Technology, 2015.

[7] Long Yu, Jiahua Tan. Optimization of Multi-component Mooring Line Based on Quasi-static Method [J].

Study On The Application Of Internet Of Things Technology In Agriculture

Yu Mingxi, Wang Rui
University of Science anf Technology Liaoning,Anshan Liaoning

Abstract: Directing at the current development condition of the internet of things and based on the available technology analysis of the internet of things, the paper makes analysis and research on the internet of things in terms of technological levels and systems. Started from three aspects, respectively, data collection, network service, date fusion and computation, the paper analyzed the technologies like RFID, ZigBee, sensors, Cloud Computing and so on, based on which the paper further brought forth the technological system framework of the internet of things. By combining the technology system framework, the paper carried out the application research in aspect of intelligent agriculture and raised the system construction of production monitoring system of agriculture standardization which is based on the internet of things. Moreover, the paper carried analysis and research works on the sensor nodes of the system, made analysis and discussion on the various technologies involved.
Keywords: the internet of things, intelligent agriculture, information collection, ZigBee, Sensor.

1. INTRODUCTION

Internet of Things refers to a network allows a series of intelligent activities like identification, positioning, tracking, monitoring and management by linking devices like RFID, Smart Sense, GPS (Global Positioning System) and 2-D Code, etc. in objects to wireless network via interfaces to endow objects with intelligence, therefore realize the communication and dialogue between human and objects as well as objects and objects.

IOT and relevant technologies have already been highly values by enterprises and in academic circles both inside and outside the country. Moreover, series of research and exploring works have been launched. However, both inside and outside the country, IOT's research and development works still remain in a preliminary condition and their architecture and system model haven't been developed. There are certain blindness in the research and development of the IOT technology. In terms of the proper definition, the fundamental principles, the architecture and the system

model of IOT, there are plenty of questions to be considered and discussed. Based on the current IOT technology analysis, by analyzing and discussing the technological levels and systems of IOT, the paper is going to start the research on the architecture and the framework of IOT.

Started from the intelligent transportation, logistic scheduling and tracing and base station monitoring, IOT extends its application domain to public oriented personal medical treatment, intelligent home furnishing and so on, and its applications can be found in all walks of life. However, being in the preliminary stage and asking for innovations, IOT hasn't been popularized in large scales. The IOT industry covers sensors, transmission tunnels, computation and process, industrial application and so on, which involves technologies like RFID, sensors, wireless network transmission, computation with high-performance, intelligent control and so on. The paper is going to unfold the introduction by combing the application of IOT in the monitoring system for the agricultural standardized production.

2. KEY TECHNOLOGIES OF IOT

Internet of Things is an open architecture with a variety of technical supports, including radio frequency identification technology, middleware technology, logistics management, e-commerce technology and so on. It involves three key technologies:

(1) sensing technology—obtain the object information simultaneously and accurately through the use of RFID, sensor, two-dimensional product code and other equipments and technologies; (2) information transfer technology— deliver real-time and accurate object information by using the deep integration between a variety of telecommunications networks and the Internet; (3) intelligent processing technology— analyze and sort out large amounts of information and data as well as implement intelligent control of the goods through cloud computing and fuzzy intelligent recognition technology. Considering the content of IOT, in the following part, we are mainly focused on analyzing and researching the information collection technology (ID identification, location information), network service technology (wireless sensor networks, core network element and so on), data merger and computation technology (Cloud computing, mass data merger) and so on.

2.1 Technology of Information Collection

The gathering technology of IOT is sensing technology which is the foundation of IOT. Currently, information collection mainly depends on electronic tags and sensors, etc. In sensing technology, the electronic tag is used to standardize the identification of the collected information; and the data acquisition

and device control are realized through radio frequency identification and two-dimensional code readers, etc. In data collection and processing stages, it mainly uses various types of sensor technologies, RFID, two-dimensional code and other information gathering techniques to collect data and then receive the control signals from upper receiver, respond, and complete the corresponding actions to process information.

RFID is a non-contact automatic identification technology and it identifies targets automatically and collects relevant data by radio-frequency signal. By affixing

electronic labels to the objects, RFID realizes high efficient and flexible management and it becomes the most critical technology for IOT. Typical RFID system is comprised by electronic labels, readers and information process system. Without the manual involvement, the identification process is capable of all kinds of severe environment. RFID is able to identify high-speed traveling object and multiple labels at the same time, with great convenience and efficiency in operation. By absorbing technologies like internet, communication and so on, RFID realizes the object tracing and the information sharing all around the world.

Currently, in the field of RFID, most of researches are based on label cost, uniform technology standard, key technology and so on. Besides RFID, the sensor technology is another frequently applied technology in the ITO. Sensor refers to devices and equipment which are able to perceive the determined test object and the transform it into useful signals in accordance with certain rules. In most cases, the sensor is comprised by sensitive element and conversion element, which are able to detect, perceive external signals, physical and chemical and physical conditions. Meanwhile, the sensor technology is the premise of the sensor node technology.

2.2 Technology of Network Communication

In communication technologies of IOT, there are a variety of technologies to choose. They are mainly divided into two types, wired technology (e.g. DSL, PON, etc.) and wireless technology (e.g. CDMA, GPRS, IEEE 802.1 la/b/g and WLAN, etc.), which are relatively mature. Referring to the implementation of IOT, the wireless sensor network technology is particularly important.

WSN is a network system which integrates distributed data collection, transmission and process technology and it is widely concerned for its network method and installation method with low cost microminiaturization, feasibility, reliability and flexibility and its capacity for moving object. By sensor node and networks spread in different place, IOT is able to perceive the world. The network construction of WSN can be classified into physical layer, data link layer, internet layer, transmission layer and application layer. The basic composition of sensor's network node includes sense unit, process unit, communication unit and energy unit.

In the technologies of IOT's network and communication, ZigBee is not only a technology between wireless labeling technology and Bluetooth, but also a bidirectional wireless communication technology with close range, low complexity, low power consumption, low cost. ZigBee is applicable in the domain of automatic control and long-range control. ZigBee, as a transmission standard, can be applied in multiple frequencies and working segments and is widely applied for its low power consumption and low cost. In domains of safety system, sensor network, industrial monitoring and other IOT areas, ZigBee has great development space. Moreover, by integrating IPv6 technology into the IOT, we can realize the end to end communication with the current network equipment and improve the retransmission efficiency, which further enhance the safety of information transmission.

2.3 Technology of Data Fusion and Computing

IOT is comprised by numerous nodes in the sensor network. In the process of information perception, it is not feasible to adopt the method of single nodes

transmitting the date to the sink independently. Because there is enormous redundant information, they would waste much communication width and precious energy resource. Besides, they would lower the efficiency of information collection and affect the timeliness of information collection. For this reason, we need to adopt data merger and intelligent technology to deal with the problem, during which distributed data merger and cloud computing are involved.

Cloud computing is one of distributed computing. By automatically dissembling the huge computing and processing processors into countless subprograms, it handled these subprograms to the huge system composed by multiple servers for searching, computing and analysis, after which it transfers the procession result to the user. Via this technology, web service providers is able to process millions and millions, even billions and millions of information, and thus be capable of net service as powerful as "super computer". By taking advantage of the low cost, super powerful procession ability and storage ability of Cloud Computing Center, and the everywhere information collection of IOT, we combined them together, and enable all kinds of objects to exchange and communicate, thus realizing the intelligent identification. By means of visualization technologies, single server can support multiple virtual machines in running multiple operating systems, and therefore improving the use ratio of servers. Cloud Computing is a service which provides those dynamic, scalable and visualized computing resources by internet.

Visualization, elastic range extension, distributed storage, distributed computing and multiple lessees

are critical technologies of Cloud Computing. Distributed storage aims at the target of satisfying the storage requirement which can't be satisfied by single server by utilizing the storage resources of multiple servers inside the cloud environment, and its characteristic is that storage resource is able to be expressed abstractly and be managed in uniform. Moreover, it is capable of ensuring the security and reliability and other requirements generated in the data read-write and operation.

3. PROCESSOR ARCHITECTURE OF IOT SYSTEM

Based on the research and analysis on IOT's critical technologies, in the general technological system architecture of IOT, we shall ensure the size of IOT (only with certain size can we enable the object intelligence to play their role), mobility (we need to ensure the object can realize instant communication under moving condition even with high speed) and security (as for those which involve national security, trade secret and personal privacy, core technology with proprietary intellectual property rights are necessary) The application of IOT is still relatively fragmented in China, and there is no large-scale, systematic development trend, so a scalable and open architecture of IOT should be established in the industrial chain technology as well as application and formation system in ideal aspects in order to break through the barriers of application in large-scale and promote the IOT industry's transition from the start-up period to the growth period. The overall technical architecture of IOT includes data acquisition layer, information exchange layer and application layer. The overall technical architecture of IOT is shown in Figure 1.

Data collection layer consists of two-dimensional code tags and readers, RFID tags and readers, cameras, sensors, GPS, sensor gateways, sensor networks and other equipment and technologies. In this layer, it mainly solves the issues like data collection and object identification, etc. It is composed by the various types of acquisition and control modules, and the main function is to complete IOT's information perception, data collection and the control of facilities. It is an important foundation of IOT.

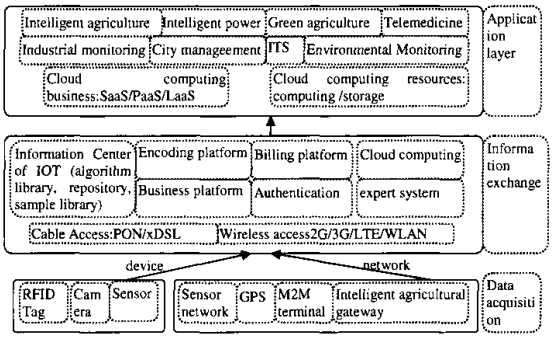

Fig 1 The technical architecture of IOT

The layer of information exchange is based on the network of IOT and communication technologies, such as mobile communication network and the Internet, which is a converged network formed by a variety of communication networks and the Internet. It includes information center, management center of IOT, expert systems and cloud computing platform, which are responsible for the massive part of Intelligent Information Processing. Therefore, the network layer not only requires the ability to operate the network, but also the ability to enhance operational efficiency of information. It is the infrastructure to make the IOT become a universal service.

Application layer refers to solutions of integrating IOT technologies with industrial technical expertise to achieve a wide range of application with intelligent technologies. Through the application layer, IOT ultimately realizes deep integration with information technology and industrial professional technologies. The application layer lies on the top which is the ultimate goal of IOT applications. It consists of a variety of servers and its main functions include the collection, transformation and analysis of the gathered data as well as the adaptation and triggers of things for users. The key issue in this layer is socialization of information's sharing and information security.

4.MONITORING SYSTEM FOR AGRICULTURAL STANDARDIZED PRODUCTION BASED ON IOT

In the process of agricultural production, the most critical part is the true time data collection in terms of temperature, moisture, carbon dioxide content, and soil temperature and soil moisture content. By making use of the IOT platform and GPRS/TD, by means of SMS, WEB, WAP and other methods, we can make the users dealing with agricultural production acquire these real-time information. Monitoring System for Agricultural Standardized Production based on IOT aims at the target of making information collection towards several indexes in crop growing and carrying out systemic monitoring towards the plantation area, crop pattern, crop growing, the breaking out and development of agricultural damages, crop output and so on.

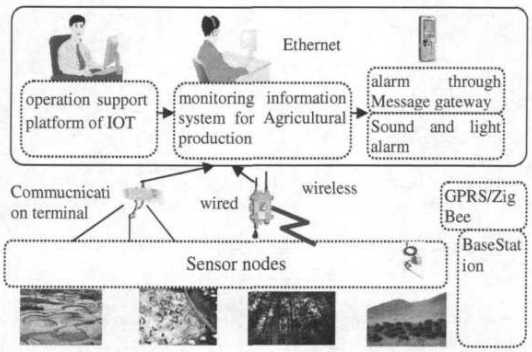

Fig 2 The system architecture of Monitoring system

The monitoring system is composed by the wireless sensor monitoring network and distant monitoring information system. ZigBee sensor nodes set in the plastics tents or greenhouse collect the critical index in crop growing like air temperature, moisture, soil temperature, moisture, illumination intensity, C02 concentration and so on. Moreover, by means of ZigBee short range wireless communication technologies, we can realize the date transmission and transmit all the node date to the base state where we can carry out TCP/IP packaging on the data we've received, after which we can send them to the remote control center by means of GORS. The control center receives data, analyze and express them. Moreover, they can make parameter setting. Once environmental parameters go beyond the set values, it is possible to make acousto-optic alarming or message alarming. By making use of cell phone or remote computer, researchers can make real-time control on the environmental conditions and information in the crop growing spot. The architecture of monitoring system is shown by the Picture 2.

Monitoring system is composed by three parts: (1) sensor node, sending the information like atmosphere collected by the senor in periodicity to the monitoring and management center of agricultural environment by means of multiple hop transmission.

(2)gate way. Located in the edge of sensor network. Realizing the interconnection and communication between the sensor network and internet. In the gateway, we can realize the conversion from the sensor network protocol to the internet protocol. (3) Monitoring and management center of agriculture environment (user), being responsible for the information storage, procession, evaluation and so on. One management center usually is capable of managing multiple monitoring areas. Remote control and PDA users are able to visit the data of the environmental monitoring center by means of internet and they can make real-time inquiry via the center.

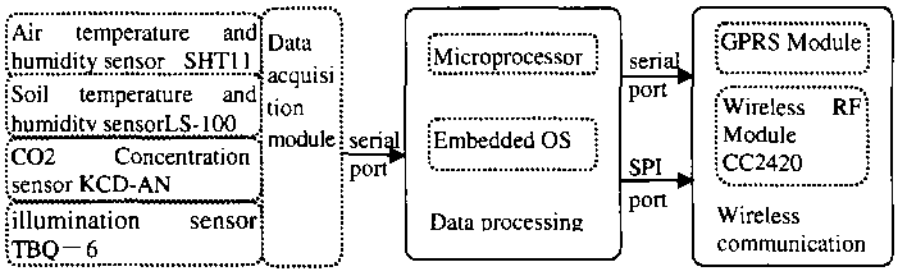

Fig 3 Structural framework figure of the sensor nodes

Sensor network is basically comprised by sensor board which is set with sensors of air temperature and moisture, soil moisture and temperature, soil PH value, light intensity and C02 concentration. These sensors can be selected and set in the sensor board. The sensor board makes adjustment on the input signals of sensors which is collected by the terminal node of wireless sensor network. The general architecture of sensor node is shown by picture 3. Temperature and moisture sensors are more and more widely applied in the areas of industrial and agricultural production, whether, environment protection and so on. We've selected the SHT11, a digital moisture and temperature sensor with high-accuracy, which is produced by Sensirion in Switzerland. The sensor is a new typed and digital relative moisture and temperature sensor with two passes of serial interface. The sensor has monolithic calibration and can be used to measure relative moisture, temperature, dew point and other parameter, with characteristics of digital output, adjustment free, standardization free, peripheral circuit free, good exchanges. As for the air moisture and temperature sensor, we've adopted SHT11, digital moisture and temperature sensor with high accuracy, which is produced by SENSIRION in Switzerland. As for the soil temperature moisture sensor, we've adopted the LS-100, soil moisture sensor, which is produced by domestic companies. As for the C02 concentration sensor, we've adopted KCD-AN, produced by Korean companies.

Data procession module is comprised by micro processor, data storage circuit and embedded operation system and it is the core component of sensor node. Moreover, it is responsible for data's storage and procession, scheduling system tasks, carrying out the communication protocols and so on. Wireless communication module is responsible for the communication among the sensor nodes and between the nodes and the station, information exchange and control among sensor nodes and the data collected by the receiving and sending station. When design the system, we adopted CC2420 ship which supports ZigBee protocols, with a frequency band of 2.4 GH z. we've adopted DSSS (Direct Sequence Spread Spectrum) under the specification of IEEE 802.25.4.

5. CONCLUSION

The paper has analyzed the current situation of IOT and made analytical research on the major technologies of IOT. Directing at the practical requirement of national agricultural environment, we've design a agricultural standardized production monitoring system based on the IOT. The system can

realize the automatic configuration and self organized transmission of information collected node, realized the real-time collection, transmission, expression and storage of agricultural environmental information. By applying it to the construction agriculture, we can better solve the defect in the traditional monitoring system of green house and plastic tents and make people acquire agricultural environment information at any time. Moreover, we can realize the remote, real-time and accurate monitoring on the agricultural environment. In many aspects, IOT has displayed its promising research and application values. What is more, its application in agriculture has become one of hotspots because it constructed a precious technological platform for the precision agriculture in turning from demonstration to the practices. IOT enables traditional agricultural pattern to evolve into a information network centered production mode and brings automation, networking and intelligentializing to the agricultural production.

REFERENCES

1. Cai, B., Bi, Q.-S., Li, F.-C., Wang, D., Yang, Y., Yuan, C.: Research and Design of Agricultural Environment Monitoring System Based on ZigBee Wireless Sensor Network. Acta Agriculturae Jiangxi (11) (2015)
2. Xu, X.-R., Gao, Q.-W., Li, Z.-Y.: Design of wireless sensor networks applied to survey of agriculture environment communication. Transducer and Microsystem Technologies (07) (20014)
3. Zhang, W., Yu, J., Yu, F., Luan, R.: Study on Agricultural Distance Monitoring and Diagnosing Integration Platform Based on XMPP. Chinese Agricultural Science Bulletin
(11)(2015)
4. Liu, Z.-S., Wei, F., Chai, Y.-T., Shen, X.-S.: Study on the Construction of the Internet of Things in China. Logistics Technology (07) (2015)
5. Li, G.-G., Li, X.-W., Wen, X.-C.: Influence of Internet of Things Technology on the Development of Automatic Environmental Monitoring System. Environmental Monitoring in China (01) (2014)
6. Liu, H.-J.: Research on Key Technology for Internet of Things. Computer Era (07) (2015)
7. Shen, S.-B., Fan, Q.-L., Zong, P., Mao, Y.-Q., Huang, W.: Study on the Architecture and Associated Technologies for Internet of Things. Journal of Nanjing University of Posts and Telecommunications (Natural Science) (6) (2014)
8. He, K.: The Key Technologies of IOT with Development & Applications. Radio Frequency Ubiquitous Journal (1) (2015)

A New Machine Vision System for Print Defect Detection

*Caijian Hua, Yan Zhang**
School of Computer Science, Sichuan University of Science and Engineering, Zigong, 643000, China

Abstract: Traditional machine vision systems for printing-defect detection sample images at a fixed resolution and a presetting speed in one inspection. When detecting small defects in a large print data background, there is usually a large amount of redundancy in the image data. To solve this problem, a machine vision system with master-slave imaging function is presented in the paper. The system can passively sample images with a high resolution in the defect area and actively a relative low resolution in the background area, which reduces the total data in image processing and increases the speed and accuracy of real-time inspection significantly.
Keywords: machine vision system, printing-defect detection, master-slave imaging, multi-resolution

1. INTRODUCTION

The traditional machine vision systems sample printing images at a presetting speed with a fixed resolution, and process all the images in the same data size [1-2]. However, the size, shape and distribution of print-defects in backgrounds are not regular in practice – they vary randomly in time and space [3]. When the visual information of the defect areais less than 5% of the total inspection area, high resolutioncameras are usually used in order to enable ahigh-speed-and-accuracy real-time inspection [4]. As a result, the host computer must be able to store, transmit and process a huge amount of image data, most of which are redundant. This slows down the inspection speed. In some cases, only very fast algorithms can be employed, which may reduce the quality of the inspection. The redundant data problem has been a bottle neck for a long time in machine vision, cumbering improvement of the speed and accuracy of machine vision systems.

One of the key points using a machine vision system for inspection of small defects in a large background is how to irregularly sample images. In this paper, we present the principle and structure of a machine vision system with amaster-slave imaging function, and study the real-time defect object the master-slave images in detail.

2. MATERIAL AND METHODS

2.1 Machine vision detection system

The principle and structure of our machine imaging detection system for print-defect are shown in Fig.1.

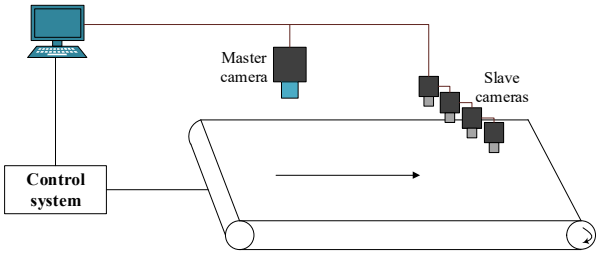

Figure 1 Machine vision system with an master-slave imaging function

The master camera was located far away from the conveyor surface for acquisition of global images. A group of the slave cameras were installed in a line closely to the platform surface. They captured local images of a small area at high spatial resolution. The host computer drove some of the slave cameras to “work” while others were “sleeping” according to the global image. Thus the local images were irregularly sampled in time and space. The areas related to the target would have a high spatial resolution, and the others would have a low resolution or even not any data. Comparing our system with the traditional ones, the total image data would be significantly reduced, but the spatial resolution of the target area would be noticeably increased.

After the initially global image processing, the host computer made a note of the suspecting defect area. Information about the suspected area with the corresponding local images is then retrieved and used for further image processing such as filtering, segmentation, extracting features and defect classification.

Our experimental system consisted of 4 slave cameras with a maximum resolution of 1392× 1040 pixels and a master camera with resolution of 2048 × 1536 pixels. An example of the global image and local image of package printing is shown as Fig.2.

a) Global image

b) Local image

Figure 2. Comparing the two types of images in the system

2.2 Image processing algorithm

2.2.1Fast and adaptive template matching

Template Matching is a high-level machine vision technique that identifies the parts on an image that match a predefined template [5-6]. Advanced template matching algorithms allow to find occurrences of the template regardless of their orientation and local brightness. The conventional methods have been commonly used as metrics to evaluate the degree of similarity (or dissimilarity) between two compared images. The methods are simple algorithms for measuring the similarity between the template image (*T*) and the portions of the target image (I).Then, the process will classify the corresponding object. The matching procedure calculates a resulting pixel using various matching methods, such as sum of squared differences (SSD), normalized cross correlation (NCC)[7] and zero-mean normalized cross correlation (ZNCC).

SSD works by taking the squared difference between each pixel in *T* and the corresponding pixel in the portions of image being used for comparison in *I*. Squared differences are summed to create a simple metric of similarity.

NCC works by taking the product of each pixel in *T* and corresponding pixel in the portions of image being used for comparison in *I*. The normalization process allows for handing linear brightness variation. The main advantage of NCC over the cross correlation is that it is less sensitive to linear changes in the amplitude of illumination in the two compared images.

ZNCC is even a more robust solution than NCC since it can also handle uniform brightness variation.

In this paper, we adopt a fast template matching algorithm named NCC-based image matching. In the first stage, a target image is accordingly remodeled following the interested object position, then standard robust matching NCC is applied to this image. This stage reduces the computational cost to a large extent. In the second stage, the object location is identified and the correct positions are updated properly in the whole target image, while the template image is adapted properly. This stage shows the efficiency of tracking method.

2.2 Defect detection

Print-defect detection works on the principle of comparing two images during the identification of faults. One image is called thereference image, while the other image is the actualprint image. To have both images compared, they must bein the same position during comparison. The object of interest is storedin the reference image area in the initial stagesof printing, and an image for comparison is acquired on aregular basis for defect checking. During acquiring ofimages, there is always shifting in the images. This can bedue to many reasons like accuracy in synchronizing camerasystems to trigger pulses, sudden jerks, vibration causingthe camera to shake, etc. This is assumed to happen should take into consideration of all the changes.The basic defect detection can be separated into the followingmajor steps. Step1.The system detects and tracks the interested object in the object detection process.

Step2. The template image is updated suitably on the object location and updating template process.

Image subtraction can be done by using equation as under[8]:

where Z is the output image, X is the reference input image, Y is the inspected input image, represents exclusive OR operation.

In Fig3, it has been shown that if the pixels value of reference image are not equal to pixels of test image, then there is a defect.

Figure 3. An example of bar code defect detection. a): reference image, b): image with a structural fault, c): defect detection result.

3. DISCUSSION

In this paper, we have described a vision system in terms of its principle and structure, as well as the image processing algorithms that it utilizes to locate areas of defect from the printing. The algorithm for this defect detection process was developed in

Future research will mainly focus on global image processing by simulation of human visual attention. The computational models in the top-down and top-down combining bottom-up approaches, together with their theory and methods on the image saliency map, top-down knowledge, context-based experience and probabilistic framework should also be used for reference. Besides, algorithms for the image processing in locating defect area and defect object detecting techniques with a high speed and high accuracy should be developed for real-time inspection.

4. ACKNOWLEDGMENTS

We are particularly grateful to Mr. Zhenwei Su for his

valuable suggestions in the academic studies. This work wassupported by the Sichuan Provincial Department of Education Fund (Grant No.13ZB0139 and No. 14ZB0217) and Key Laboratory of Higher Education of Sichuan Province for Enterprise Informationlization and IOT Open Fund (Grant No.2013WYY04 and 2015WYY02).

REFERENCES

[1] Shankar, N. G., N. Ravi, and Z. W. Zhong, A real-time print-defect detection system for web offset printing, Measurement, 2009, 42(5): 645-652.

[2] Vans, Marie, et al. Automatic visual inspection and defect detection on variable data prints, Journal of Electronic Imaging, 2011, 20(1): 1-13.

[3] Lundström, Jens, and Antanas Verikas. Assessing print quality by machine in offset colour printing. Knowledge-Based Systems, 2013, 37: 70-79.

[4] Xiaomei, Zhao, and Xie Bing. Research on Online Detection Algorithm for Printed Matter Based on Image Processing. Proceedings of the 17th IAPRI World Conference on Packaging, 2010.

[5] Yoon, Young-Geun, et al. An effective defect inspection system for polarized film images using image segmentation and template matching techniques. Computers & Industrial Engineering, 2008, 55(3): 567-583.

[6] Chantara, Wisarut, and Yo-Sung Ho. Object detection based on fast template matching through adaptive partition search. Computer Science and Software Engineering (JCSSE), 2015 12th International Joint Conference on. IEEE, 2015.

[7] Wei SD, Lai SH. Fast template matching based on normalized cross correlation with adaptive multilevel winner update. IEEE Transactions on Image Processing. 2008,17(11):2227-2235.

[8] Kaur, Beant, Gurmeet Kaur, and Amandeep Kaur. Detection and Classification of Printed Circuit Boards Defects. Open Transactions On Information Processing, 2014, 1(1): 8-16.

Design of Indoor Air Quality Monitoring System Based on Embedded

Guangjian Chen, Huaping He, Xiaoling Wang*
School of Computer Science, Sichuan University of Science & Engineering, Zigong,643000, China

Abstract: With the development of embedded system technology and GPRS wireless communication technology, remote data acquisition technology has been widely used. This thesis designs the air quality monitoring system based on AT89C2051 SCM and GPRS. The control module of the data acquisition terminal is made up of AT89C2051 SCM, which is responsible for controlling liquid-crystal display, GPRS module, indoor air quality parameter acquisition module and so on. GTM900-B transfers the information collected by terminal to the DC of upper monitor through GPRS network for analysis and processing. The system realizes the collection, display and long-distance transmission of air quality parameter.
Keywords: Air quality; data acquisition; GTM900-B; SCM;

1. INTRODUCTION

With economic development and social progress, more and more people are in favor of the superior living environment. Various types of building materials and household appliances enter indoor and make the indoor pollutants complicated and various. Indoor air pollution causes huge losses to society, family and individual and the global annual total death toll due to indoor air pollution reaches 2.8 million. Therefore, indoor air pollution has been listed as one of the four most critical environmental problems in the world[1].

At present, there are two main problems of indoor air quality problems in people's daily life. The first problem is the noxious gas brought by housing decoration, toys and pesticide, such as formaldehyde, volatile organic compounds (VOCs: containing benzene) and other carcinogenic substances. The second problem is noxious gas leakage caused by carelessness or equipment failure, such as water gas, natural gas and liquefied petroleum gas, which are harmful to human body. Therefore, it is necessary to design a set of indoor air quality monitoring device with integration of these two noxious gas monitoring, which can detect, give an alarm and remind people to take certain measures of the noxious gas in the living environment promptly, accurately and effectively. It can not only effectively protect people's health but also make a lot of family avoid disasters.

2. Hardware system design

2.1 The basic structure of hardware system

The system hardware is mainly composed of three parts. The first part is sensor array circuit for air quality monitoring system, including sensor heating circuit, sensor signal acquisition circuit. The second part is acquisition circuit for DS18B20 single wire digital temperature sensor. The third part is typical AT89C2051 peripheral circuit, including voltage conversion circuit to realize the system, GPRS module in communication, memorizer for procedure and data storage, liquid crystal display circuit to display a variety of current gas concentration, audible and visual alarm circuit, keyboard circuit and JTAG interface circuit for debugging. The hardware structure of indoor air quality monitoring system is shown in Figure 1.

Gas transducer and temperature sensor transfer the real time air quality information into effective signal and then transmit SCM for related processing. SCM on one hand will have status display for air quality monitoring data after treatment and on the other hand will send it to GPRS module and control the operation of GRPS itself, including starting and closing services, establishment, close junction and mode conversion. It then sends the data after encryption and fault-tolerant treatment to the remote detection centre.

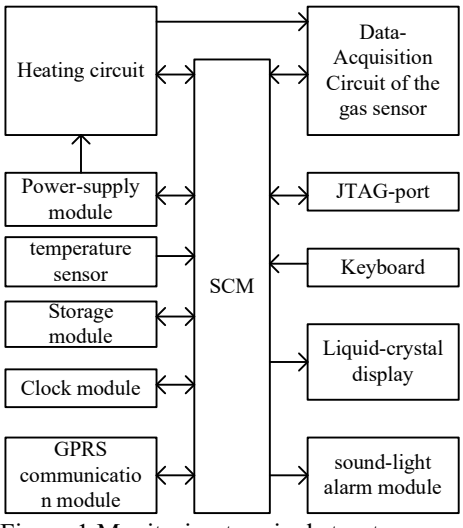

Figure 1 Monitoring terminal structure

2.2 Key chip selection and local design

2.2.1 scm

AT89C2051 is low voltage, high performance CMOS 8 bit SCM produced by the United States and it is fully compatible with the MCS-51 instruction system, which includes 2K bytes rewritable 1000 Flash flash memory and 128 bytes of internal RAM, 15 I/O lines, two 16 bit timer counter, a communication full

duplex serial port and a built-in precision comparator. At the same time, it can be reduced to 0Hz static logic operation, and support the power saving mode. Therefore, AT89C2051 is especially suitable for the portable, power saving and information collection system.

2.2.2 GPRS communication module

GPRS communication adopts GTM900-B module by HUAWEI. This module has simple interface, and supports the PPP protocol. It is mainly compatible with SIEMENS C35 module, supports standard AT commands and enhances AT commands through the UART interface and external CPU communication. It mainly realizes the wireless sending and receiving, baseband processing, audio processing and other functions. GPRS module and data acquisition module communicate through the serial port and the maximum rate of communication can reach 115200 bit/ s. Data acquisition module can send the data to the PC upper monitor through GPRS network.

2.2.3 One-wire digital thermometer

DS18B20 is a one-wire digital thermometer produced by America DALLAS. It integrates all digital conversion circuits, eliminates switching and amplifying part in the circuit and saves a large number of lead wires and logic circuit to control channel switching. Compared with the traditional thermal resistance, it can directly read the measured temperature and realize the temperature resolution of 9-12 through simple programming. The temperature range is -55℃~+125℃ and its precision is±0.5℃ with the temperature range -10℃~+85℃. The temperature within 750 ms can be changed to 12 digital quantities. It is connected with the microprocessor and can realize two-way communication with only one signal line. The unique structure is not only simple and economical, its digital transmission but also greatly improve the anti-interference of the system. Therefore, it is very suitable for the construction of temperature measurement system.

The connection between temperature transmitter DS18B20 and SCM AT89C2051 is shown in Figure 2. DQ pin is the connection between data wire and SCM P3.4. At the same time, a 4.7KΩ pull-up resistor also needs to be connected so that the data line in the idle state can automatically pull up to a high level.

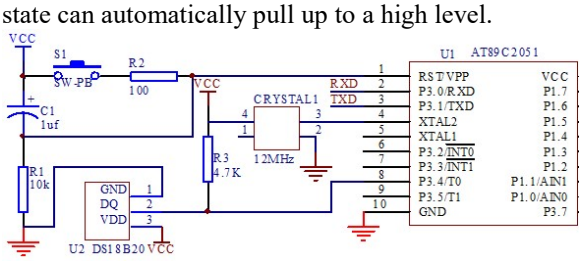

Figure 2 DS18B20 and AT89C2051 hardware connection diagram

Although the accuracy of DS18B20 is + 0.5 C, it is found that higher accuracy can be obtained by other methods. First, the temperature value between 0 and 1 bite is read from DS18B20 scratch pad memory. The lowest significance bit is removed and the 0.5℃is thrown from the value red. The value is denoted by T, and then read the 6 byte cache, denoted as R, finally read scratchpad memory byte 7, denoted as C. The calculation formula of the temperature value of the extended precision is as follows.

$$Temperature = t - 0.25 + \frac{c - r}{c} \tag{1}$$

According to the communication protocol of DS18B20, the host control DS18B20 must go through three steps for the temperature conversion. DS18B20 needs to be reset before each read-write. After the success of the reset, a ROM instruction is sent. Finally send the RAM directive, so that the DS18B20 can be scheduled for the operation.

2.2.4 Gas transducer

MQ-135 gas sensor selection in the design is suitable for the measurement of formaldehyde, toluene, smoke, carbon dioxide and other harmful gases. MQ-9 sensor is used to measure carbon monoxide, methane, liquefied petroleum gas and other combustible gas. DHT21 temperature and humidity sensing module is selected for temperature and humidity measurement.

The measurement circuit of MQ-135 and MQ-9 is shown in Figure 3. The measuring circuit is composed of two parts, the test loop and the heating circuit. In the test circuit, the sensor surface resistance RS changes with the measured gas concentration. The output of the effective voltage signal VRL in series with the load RL reflects the concentration of the gas to be measured in the air, and the relation between the VRL and the RS is shown in the Formula (2):

$$V_{RL} = \frac{V_C}{(1 + \frac{R_S}{R_L})} \tag{2}$$

In Figure 3, A, a, B, B, H, h are the 6 connectors of gas transducer, VC is loop voltage. VH is the heating voltage. RH is the heating resistance. RS is the sensor surface resistance. RL is the sampling resistance. VRL is the output voltage[2].

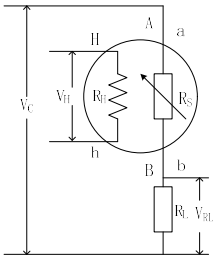

Figure 3 Signal pick-up circuit schematic diagram of gas transducer

For the heater voltage VH in Figure 3, MQ-135 uses 5V DC voltage as the heating voltage. MQ-9 uses 5V

high voltage, 1.4V low voltage cycle heating mode. For MQ-9, when VH=5 V, cleaning sensor price is 1.4 V, the sensor works, you can collect the gas concentration, among which, the high level duration is 60 s and the low level duration is 90 s.

3. SOFTWARE SYSTEM DESIGN

The system software design is divided into the upper and lower monitor. The lower monitor completes the data collection, display, alarm, data processing and then sends out by the GTM900-B module via GPRS network. The upper monitor receives the information transmitted over the GPRS network through the GTM900-B module and has real-time display after handling of monitoring software. The upper monitor can also transfer control information to the lower monitor through GPRS network.

3.1 Core control program design of lower monitor

First of all, the monitoring terminal has SCM, clock chip and GPRS module and other hardware initialization and then SCM controls collection and processing of air quality parameter. Then, the monitoring terminal is connected to GPRS network. After the successful connection of GPRS network, air quality parameter is transmitted to GPRS module through SCM serial port. At this time, SCM can communicate with GPRS module. When the data sent by GPRS module has the response signal, it will be sent to remote air quality monitoring centre. The system sends the air quality monitoring data to the GPRS network through the GPRS module. GPRS network then sends the data to Internet through gateway. The monitoring terminal can be automatically attached to the GPRS network, establish a connection with the data centre and send air quality parameters at any time through the software program. Users do not need to carry out complex settings, as long as the data centre determines the IP address and port number[3]. The software design flow of the monitoring terminal is shown in Figure 4.

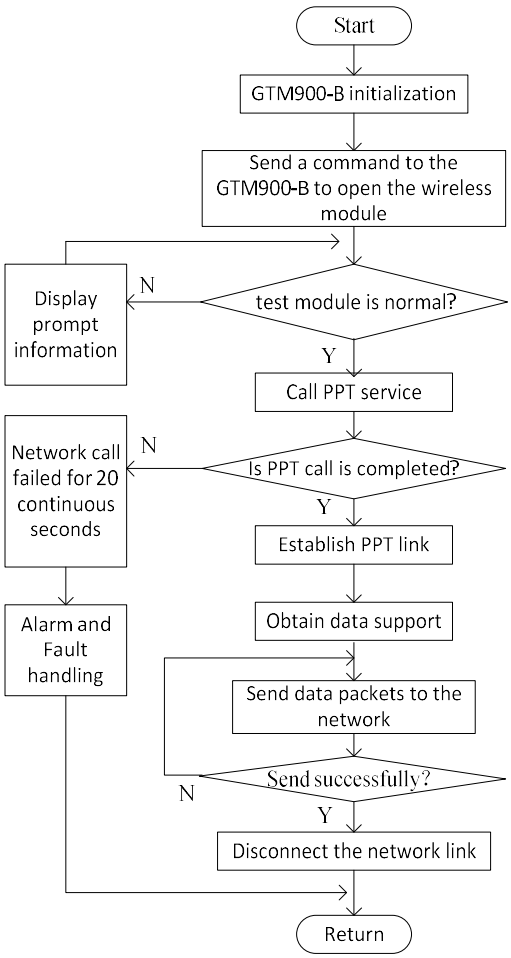

Figure 4 The flow chart of main program

3.2 GPRS data transmission protocol

GTM900-B integrates TCP / IP protocol and uses the internal extension of AT instructions to achieve data communication. The specific steps of the AT command of data transmission in the design are as follows[3].

1. AT is used to confirm the status of the current network and module

AT+ CSQ is used to check the local network signal strength. When this command is idle, you can send cycle and understand the status of network signals;

AT+ CPIN is used to check whether SIM work is normal;

AT+ CGREG is used to check the network registration. When the command is idle, you can send cycle and understand the status of the module registered network.

2.AT is used for data transmission

AT+ CGDCONT = 1, " IP", "CMNET" is used to set APN wireless access point;

AT% ETCPIP= 0, 0 is used for PPP dialling;

ETCPIP AT% used to check the local IP address and DNS server address. It can send data after several connections.

After the completion of data transmission, using the command "AT% IPCLOSE = 1" to close the TCP SOCKET connection, and then use the command

"AT% IPCLOSE= 5", otherwise there may be an abnormal termination of TCP connection, causing the client IP address residue. The process of GPRS Network Driver is shown in Figure 5[3-4].

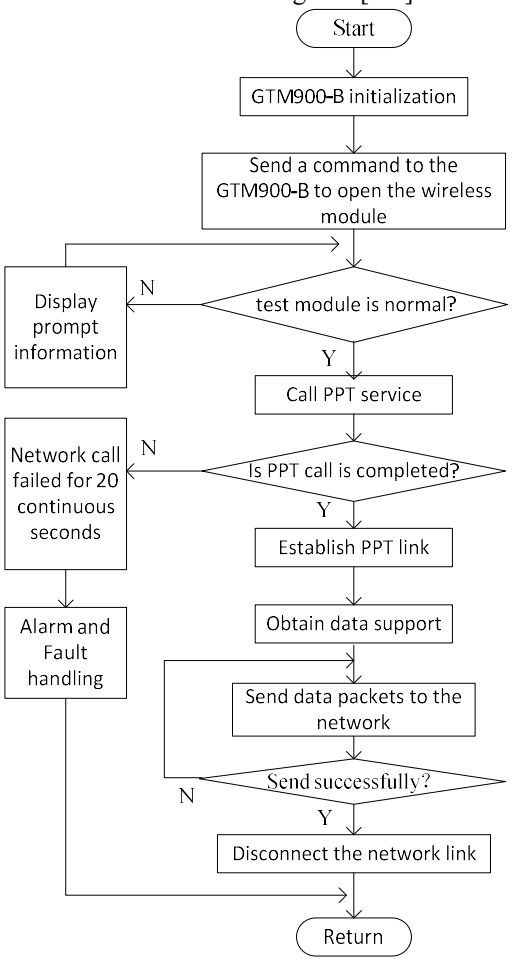

Figure 5 The process of GPRS Network Driver

3.3 The design of management software

The management software of monitoring center is seamless connected with each monitoring terminal by GPRS and Internet to collects data. Its function includes: data processing, real-time display, storage and statistical reports. In order to provide a visual manipulation platform, the operation interface is developed by Visual C++, the backstage database uses Microsoft Access to manage, and connected with the front stage operation by ADO. Its main function includes:

(1)Establish connection with each monitoring terminal.

(2)Real time receiving, processing, displaying and storing air quality parameters from monitoring terminal.

(3)Realize the remote control of the monitoring terminal, as the time interval of GPRS sending data, the time interval of collection, upper and lower limit values of alarm parameters, etc.

4 Conclusion

With formaldehyde, natural gas and temperature as the object, we designed the IAQ monitor system, and its function includes data acquisition, alarm display, feedback control. The system takes the GPRS mobile public network, which has the advantage of high transmission rate and low system delay, as the wireless data communication platform to realize the remote control of the monitoring terminal. After a series of tests, it proves the monitoring system has the advantages of real time, accuracy, convenience, reliability and so on.

5. ACKNOWLEDGMENT

This work was supported by the Artificial Intelligence Key Laboratory project of Sichuan Province (No.2014RYY03), the research project of Sichuan Provincial Key Lab of Enterprise Information and Control Technology for Internet of Things (No.2015WYY03),the research project of Sichuan University of Science & Engineering (No.2013PY06),The fund Project of Sichuan Provincial Academician (Expert) Workstation (No: 2015YSGZZ01).

REFERENCES

[1] GUO Wei-tong, SONG Hai-sheng, YANG Hong-wu, PEI Dong.Design of a portable rapid detection instrument for indoor air quality. Transducer and Microsystem Technologies,2015.4(in Chinese)

[2] LI Ping, SU Yan-chen, GUO Tai-chun. Design of indoor air quality monitoring system based on ARM. CHINA MEASUREMENT&TEST, Vol.36(5), 2010.9 (in Chinese)

[3] LUO Dongsong, LI Qiong.The research and design of environm ent protecting data acquisition and transm ission system based on GPRS. Industrial Instrumentation & Automation | Ind Instrumm Autom,2011.2 (in Chinese)

[4] Sun Xiaochun, He Dongjian. Study on Soil Information Acquisition System Based on GPRS. Journal of Agricultural Mechanization Research,2010,2(2):123-125(in Chinese)

Optimizing Study on Low Pressure Casting Process for Aluminum Alloy Impeller and Designing Scheme for the Gating System

Xu Wenbo, ZONG Xuewen

College of Mechanical Engineering, Xi'an University of Science and Technology, Xi'an710054, China

Abstract: The characteristics of low pressure casting process and the designing scheme for its gating system were discussed.UG software was used to model.Numerical simulation for the low pressure mold filling and solidification process of the aluminum alloy impeller by using ProCAST,and analyze two different scheme of gating system.Pouring temperature,mold preheating temperature and pressure-time parameters for aluminum liquid filling state and solidification sequence are analyzed.The research results that,the low pressure casting process and design of gating system of aluminum alloy impeller can be optimized and selected the best scheme by ProCAST software.

Key words: impeller; low pressure casting; gating system; ProCAST software; numerical simulation

1. INTRODUCTION

Casting process include Sand casting,gravity casting,centrifugal casting,investment casting, pressure casting, plaster casting and etc.Among them, low pressure casting is use pressure of air or electromagnetic force to the liquid metal into the mold to achieve filling,the pressure of air or the electromagnetic force on the alloy surface causes it to move,and alloy liquid is raised along the tube,finally filling and solidification of the casting under the effect of pressure.Therefore,uniform microstructure of castings can be obtained.The casting process for aluminum alloy impeller was introduced in this paper is low pressure casting,it can produce high performance,high life,high quality of the impeller[1].

At present, the research on Optimization Design of low pressure casting process parameters for aluminum alloy impeller is relatively few[2-4],Using ProCAST software to simulate the process and using VE-Mesh on the casting and the mold finite element mesh division[5-8].In this paper, the low pressure casting process of different gating system is based on the Visual-CAST module of the Visual Environment software.Besides,quantitative design and optimization Based on die preheating temperature, casting speed, pouring temperature, heat transfer coefficient, cooling mode and pressure-time parameter.

2. PROCESS ANALYSIS AND MOLD DESIGN OF CASTING STRUCTURE

2.1 Product Structure Analysis

Point cloud data measured by three coordinate measuring instrument,and three dimensional design of the impeller in 3D software as shown in Figure 1.Can be seen from the figure,the overall size of casting is relatively small and central symmetry.The maximum height of the impeller is 19.7mm,the maximum diameter is 150mm,and the minimum axis hole diameter is 35.6mm.There are 29 blades of the same size and distributed along the circumference.And the blade is variable cross section and uneven thickness,the most important is that minimum wall thickness is 0.5mm.The material used in the impeller is YL112 aluminum alloy,properties of the material:mechanical properties is tensile strength 320MPa, elongation rate of 3.5%, hardness 85HBW.

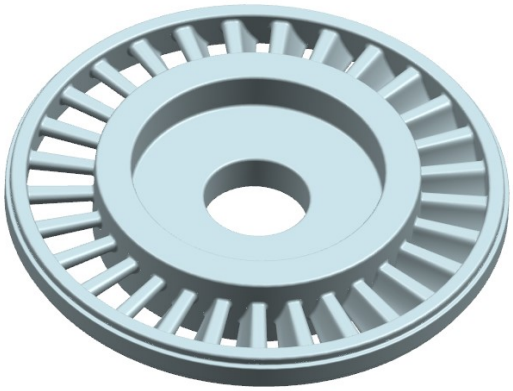

Fig 1 Three-dimensional model of impeller

2.2 Mold Design And Material Selection

The three-dimensional modeling of the mold can be done by the characteristics of the impeller and the low pressure casting process requirements as shown in Figure 2.Mold parting surface is located in the largest section of the shape of casting part,in order to facilitate the completion of the casting can be successfully mold release.In the process of low pressure casting,the aluminum liquid is solidified and shrunk up and down by the effect of low pressure for feeding casting.And cast away from the gate position of first solidification as far as possible,then gate finally solidified,ultimately in the solidification process of casting sprue finally achieve feeding and sequential solidification.Therefore,12 exhaust holes

of 2mm diameter are arranged on the upper surface of the mold.

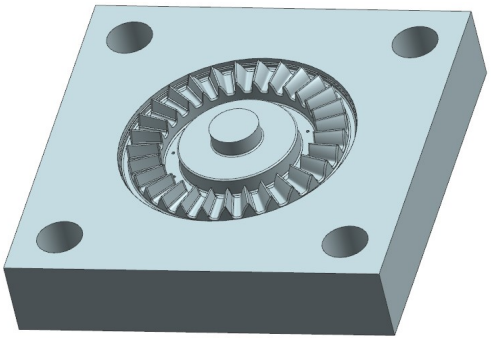

(a) Upper mold

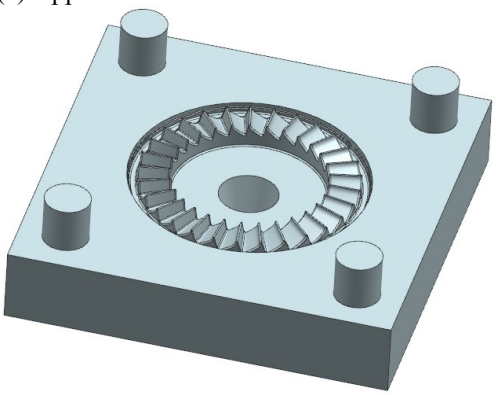

(b) Lower mold

Fig 2 Upper mold and lower mold of impeller

Contrast on the upper mold,the lower mold does not need to be provided with exhaust holes,but it need to put it in a good design of the gating system.The rise of liquid alloy gating system in liquid distribution pipe and into the casting.A typical low pressure casting gating system consists of a straight runner,and it connected to the liquid rising pipe,and then the alloy liquid is introduced into the mould through the runner and the inner gate.According to the diameter of the variable section, the straight runner is roughly divided into two forms,one is gating system with isosceles trapezoid,the other one is gating system with inverted trapezoid[9],As shown in Figure 3.The advantages and disadvantages of the two different gating systems are compared in the following chapters.

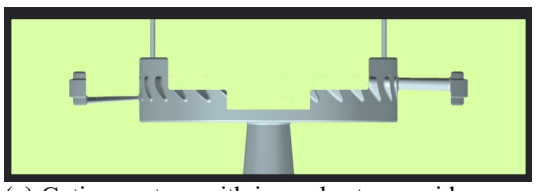

(a) Gating system with isosceles trapezoid

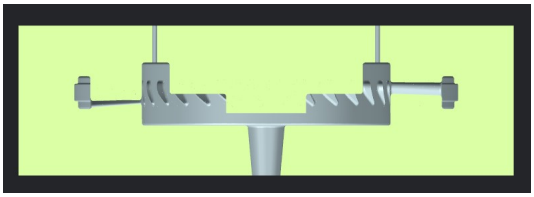

(b) Gating system with inverted trapezoid

Fig 3 Two kinds of gating systems

The material used in the mold selection of H13 steel,The performance in the medium temperature (600 ℃) is better than 4Cr5MoSiV steel.In addition, adding Mo, V, W and other metal elements will produce two times the hardening effect of tempering process on the dissolve into austenite in H13 steel.Therefore, H13 steel is extremely suitable for die casting mold.

3. PRE-PROCESSING OF NUMERICAL SIMULATION

3.1 Finite Element Mesh Generation

In the use of ProCAST software for numerical simulation of the casting and mold to be carried out on the tetrahedral finite element mesh, it is difficult to affect the efficiency of ProCAST simulation[10].We can use Visual-Mseh to quickly divide the tetrahedral mesh of the impeller and the mold,through the test of MeshCAST,and the mesh quality is higher than MeshCAST.According to the above methods, two different types of gating system are obtained as shown in Figure 4.

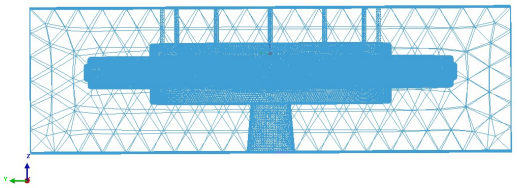

Fig 4 Volume mesh of impeller mold

3.2 Set Pouring Process Parameters

In the Visual-Cast module, the first set of gravity direction,Because the low pressure casting is the counter gravity casting, the setting of the gravity direction is opposite to the direction of the sprue.There is a principle of low pressure casting in the setting of pouring temperature,in order to ensure that the casting under normal conditions as far as possible to reduce the temperature,and to reduce the metal liquid suction feeding effect.The filling ability of aluminum alloy liquid is higher than the gravity casting in low pressure casting.Therefore,The pouring temperature of low pressure casting is 20℃ lower than that of gravity casting, set pouring temperature 700℃.

The preheating temperature of the mold has a certain effect on the mold filling of molten metal,mold preheating temperature higher will be beneficial to the metal liquid filling,but on the other hand, it will affect the solidification of the molten metal[11].For the irregular thin-walled complex part of impeller, the

blade is prone to the phenomenon of insufficient filling when filling,so H13 steel mold preheating temperature should be slightly higher.In summary,the preheating temperature of H13 steel mold is set to 400℃,meanwhile aluminum alloy ZL112 molten liquid preheating temperature is set to 700℃.The heat transfer coefficient between the surface of the casting and the upper and the lower mold is set to h=1280W/（m2·K）.In order to make the simulation more realistic,using Visual-CAST in the low pressure casting default boundary conditions.Besides,H13 steel mold cooling mode is set to air cooling.

Filling and solidification process of pressure - time parameters are shown in table 1.

Tab.1 Pressure time parameters

	lift	filling	pressurize	Holding pressure	decompression
pressure/MPa	0.005	0.01	0.05	0.05	0.005
time/s	—	0.8	3	80	5

4. NUMERICAL SIMULATION AND RESULTS ANALYSIS OF OPTIMIZATION SCHEME

The solidification time distribution of two different gating systems can be concluded by Figure 5.The structure of the isosceles trapezoid can ensure casting to achieve top-down sequential solidification,but the trapezoidal structure does not guarantee the order from top to bottom of the casting solidification.It is very important to ensure the solidification of castings,because it is necessary to ensure that the sprue in the final solidification and play a role in the repair.In summary,the impeller casting gating system should select isosceles trapezoid form.

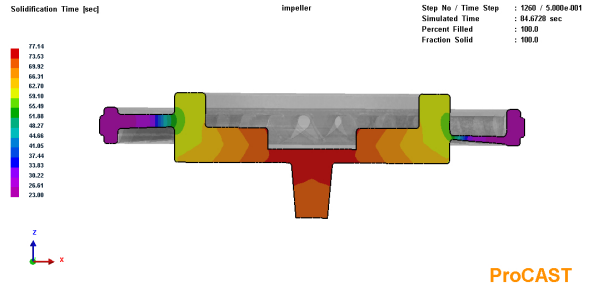

(a) Solidification time of gating system with inverted trapezoid

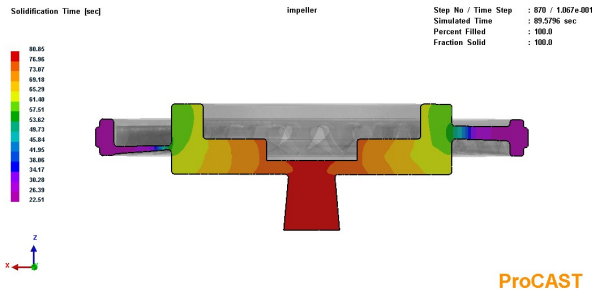

(b) Solidification time of gating system with isosceles trapezoid

Fig 5 Comparison of solidification time from two kinds of gating systems

Set the pouring temperature to 700℃,Preheat temperature of H13 steel mold is 400℃,The preheating temperature of aluminum alloy liquid is 700℃,the pressure-time parameters are shown in table 1.The filling stage after the pressure time parameter optimization is shown in Figure 6,it can be seen in the impeller filling stage, the pressure of the molten flow of aluminum alloy is more stable,and there are no defects such as isolated weld pool and rolling gas.The solidification stage is shown in figure 7,The solidification sequence of the impeller is solidified in the horizontal direction from the edge of the impeller to the center of the sprue,and from top to bottom in the vertical direction.It can be proved that the 12 exhaust holes can play the role of cooling and solidifying the top layer,and the spure in the final solidification played a role in the repair.

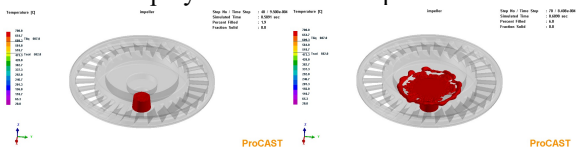

(a) t=0.5891s (b) t=0.6098s

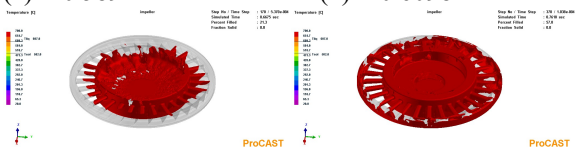

(c) t=0.6675s (d) t=0.7618s

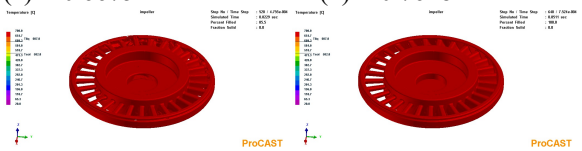

(e) t=0.8229s (f) t=0.8511s

Fig 6 Filling state of impeller

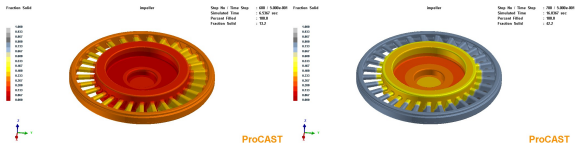

(a) t=6.5367s (b) t=16.0367s

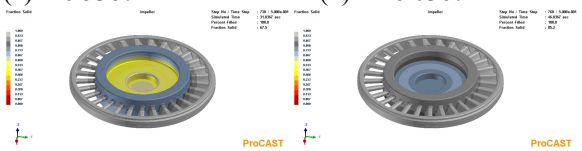

(c) t=31.0367s (d) t=46.0367s

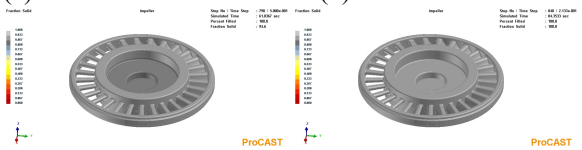

(e) t=61.0367s (f) t=84.3533s

Fig 7 Solidification state of impeller

Figure 8 shows the state distribution of the pressure mutation in the filling process,the pressure is basically stable in general.But at the time of filling 0.7646s,the inner ring edge of the impeller appears a small range of mutation pressure.This shows that the local stress increases at this time,and metal liquid on the mold caused a big shock and has certain influence to the mold life.However, due to the smaller impact area and the stress mutation occurs only in 0.0026s, it will disappear immediately.Therefore, the effect of stress mutation can be neglected.

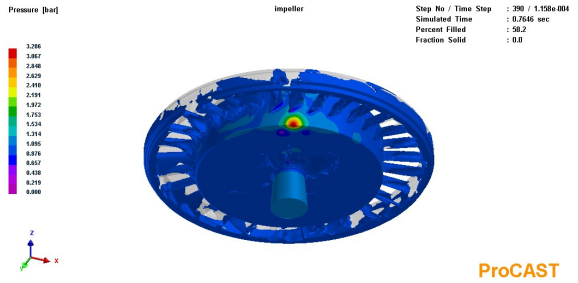

(a) t=0.7646s

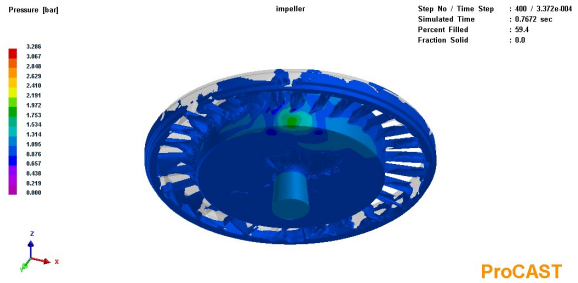

(b) t=0.7672s

Fig 8 Drawing abrupt pressure change

The parameters of the impeller can be observed through the Niyama criterion as shown in Figure 9,finally the volume fraction of shrinkage is less than 0.80%.There are no casting defects and satisfy technical requirement.At present, in the aluminum casting process of the casting shrinkage prediction method,Niyama criterion is not only accurate for the prediction of shrinkage and shrinkage of castings,but also this module is widely used in the domestic and foreign casting software[12-13].

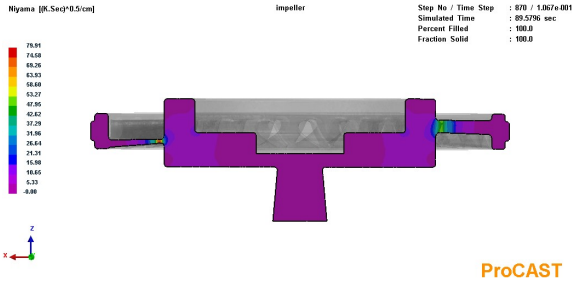

Fig 9 Niyama criterion graph

5. CONCLUSION

The numerical simulation of different gating system was carried out by ProCAST software,In order to determine a suitable gating system and casting process scheme by using different parameters to numerical simulation.It make the casting can be solidified in sequence and avoid shrinkage porosity and the emergence of abrupt pressure.At the same time, it also can solve the problem of the mold design, the low pressure casting process and the control parameters of the impeller type casting.Not only greatly shorten the actual production cycle, but also to ensure the quality of the impeller castings.This provides a reliable basis for the optimization of the parameters of the impeller and all kinds of complex parts in low pressure casting process.

REFERENCES

[1] Li Jiqiang,Dong Xuanpu.Foundry technology [J]. 2009.

[2] Kang Daoan,Yang Yi,Wu Min,et al.Research status and development of numerical simulation of filling and solidification of aluminum alloy casting [J]. hot working technology, 2008, 37 (23): 109-113.

[3] Wang Yingying.Design and numerical simulation of low pressure die casting for aluminum alloy impeller [D]. Shandong University, 2012.

[4] Wang Y C, Li D Y,Peng Y H, et al. Numerical simulation of low pressure die casting of magnesium wheel[J]. The International Journal of Advanced Manufacturing Technology, 2007, 32(3):257-264.

[5] Liu Liqun.Reverse engineering and finite element analysis of turbocharger compressor impeller [D]. Northeastern University, 2009.

[6] Ji Xiaogang.Research on key technology of reverse engineering of turbocharger impeller [D]. Nanjing University of Science and Technology, 2006.

[7] Xiong S M, Lau F, Lee W B, et al.Numerical methods to improve the computational efficiency of thermal analysis for the die casting process[J]. Journal of Materials Processing Technology, 2003, 139(1-3):457-461.

[8] Wang Y C, Wang W M, Da-Yong L I, et al. The Simulation Analysis of Cooling Capacity in Mold during LPDC of Magnesium Wheel[J]. Journal of Shanghai Jiaotong University, 2005.

[9] Jie Wanqi.Casting technology [M]. higher education press, 2013.

[10] Wang Yuanqing, Liu Jing, Chen Qiang, et al. Application of Procast software in large and complex aluminum alloy castings [J]. special casting and nonferrous alloys, 2011, 31 (11): 1024-1027.

[11] Liao Haihong, Liang Minjie, Cheng Jun. CAD design of aluminum alloy low pressure casting gating system[J]. rare metals, 2006, 30 (z2): 43-48.

[12] Lee P D, Chirazi A, See D.Modeling microporosity in aluminum–silicon alloys: a review[J]. Journal of Light Metals, 2001, 1(1):15-30.

[13] Pan Liwen, Zheng Lijing, Zhang Hu, et al. Applicability of Niyama criterion to prediction of shrinkage porosity in castings [J]. Journal of Beihang University, 2011, 37 (12): 1534-1540.

Application of Improved Genetic Algorithm in Coal and Gas Outburst Hazard Prediction

*MingLong Xu, ZhiXue Wang, ZhiWei Li, Nan Ji**
North China University of Science and Technology, Tangshan, 063000, China

Abstract: In this paper, the Genetic Algorithm and Neural Network are combined to improve the performance of each other, so that the search ability to further improve the combination of the two methods for solving coal and gas outburst prediction model, and through some measured data for simulation. The experimental results show that the combination of the two algorithms has obvious effect on the prediction of coal and gas outburst risk, and it is faster and more accurate.
Key words: Coal and gas outburst, Neural Network, Genetic Algorithm, characteristic index, prediction.

1. INTRODUCTION:

China is one of the most serious countries of coal and gas outburst in the world. Therefore, the prediction of coal and gas outburst danger has important practical significance for coal mine safety production. However, because coal and gas outburst are very complex dynamic phenomena and influential factors, some traditional methods such as Single Index Method, Gas Geostatistics Method, Comprehensive Index Method, Shimen Cuttings Index Method, Borehole Gas Emission Initial Velocity Method, R Value Index Method, and Indexing Method of Drilling Cuttings, etc. These methods and indexes are mainly obtained by regression analysis method, which considers the individual or important factors affecting coal and gas outburst, and does not comprehensively consider the influence of coal and gas outburst Of the factors, predictions are often not very accurate.[1-3] Based on the Genetic Algorithm and BP Network, this paper uses the improved algorithm to model the coal and gas outburst danger. And verifies the feasibility and validity of the forecasting method.

2. DATA SEIECTION AND PROCSSING

The input data is Normalized before inputting the Neural Network. Normalization is a kind of non-dimensional processing method, which makes the absolute value of the physical system value become a relative value relation and the effective method of reducing the value. [0, 1]. After the normalization of data more concise, convenient, but also in the same order of magnitude. For the input samples, the Normalized processing formula is

$$y = \frac{x - x_{min}}{x_{max} - x_{min}} \tag{1}$$

In the formula (1), y is the Normalized data, x_{min} x_{max} is the minimum value and the maximum value of the sample.

In this paper, we selected 40 coal and gas outburst data of 14 mines in Tangshan area as learning samples, among which 1 ~ 10 groups are non-prominent and 11 ~ 20 groups are outstanding data. The training model is trained by the Neural Network prediction model. And then the remaining 20 groups of prominent points of data to verify the network prediction effect is good or bad

Table 1. the data of multiple mine coal and gas outburst in Tangshan area

Test number	crustal stress (PO) /MPa	Gas pressure(Pg) /MPa	Coal thickness(hm) /mm	Coal sample screening modulus(sc)
1	0.6999	0.1290	0.5902	0.3137
2	0.6999	0.1774	0.0564	0.1275
3	0.8619	0.1935	0.0489	0.6078
4	0.6074	0.0484	1.0000	0.2843
5	0.9074	0.1774	0.4135	0.9608
6	0	0.2097	0	1.0000
7	0.6276	0.0645	0.3421	0.2745
8	1.0000	0.2742	0.0188	0.8137
9	0.4924	0.1613	0.4925	0.2647
10	0.8619	0	0.8421	0.2157
11	0.6768	0.1613	0.5602	0
12	0.6999	1.0000	0.4135	0.1275
13	0.7462	0.5484	0.3647	0.6176
14	0.7462	0.4194	0.2368	0.6176

15	0.6074	0.4032	0.2218	0.2353
16	0.8619	0.4032	0.7256	0.6078
17	0.5842	0.5323	0.7105	0.3824
18	0.7231	0.6129	0.2820	1.0000
19	0.4924	0.6774	0.0226	0.7059
20	0.4924	0.7258	0.2744	0.7056
21	0.6761	0	0.0248	0.1863
22	0.6761	0.2021	0.0248	0.1863
23	0	0.1489	0.2795	0.2745
24	0.7121	0.2766	0.2795	0.3725
25	0.9459	0.0319	0.5466	0.8137
26	0.5504	0.2340	0.4161	0.2647
27	0.6580	0.2872	0.2640	0.7451
28	0.6580	0.1809	0.1615	0.7451
29	0.8383	0.2766	0.6957	0.2157
30	0.6941	0.5532	0.4627	0
21	0.6220	0.1489	1.0000	0.6765
32	0.6220	0.5638	0.2733	0.6765
33	0.7121	0.4574	0.4938	0.3137
34	0.6406	0.6702	0.8789	0.2353
35	0.8738	0.6383	0.5435	0.0980
36	0.6552	0.6383	0.8199	0.2843
37	0.6220	0.8298	0.0404	0.3824
38	0.7301	1.0000	0	1.0000
39	0.5685	0.7340	0.8106	0.2647
40	1.0000	0.4149	0.4783	0.1667

3. MODEL STRUCTURE

Neural Network model uses three layers of BP Network, namely input layer, hidden layer and output layer, the structure shown in Figure.1In this paper, the number of input units n = 4, the number of output units m = 1; among them p_i (i=1, 2, 3, 4) is the input of the sample in the network, W_j (j=1) is the actual output of n samples in the network; t_j (t_j =($t_{1,j}$), j=1) is the expected output of n samples in the network; V_1 is the connection weight between the input layer and the hidden layer, V_2 is the connection weight between the hidden layer and the output layer; B_2 is the threshold of the hidden layer unit, B_2 is the output layer unit threshold.

The selection of the number of neurons in the hidden layer generally does not have a fixed choice, mostly through experiments to adjust the number, until the network has a faster convergence. [5]

(2n + 1) = 2 × 20 + 1 = 41 for the hidden layer neurons selected in this pap

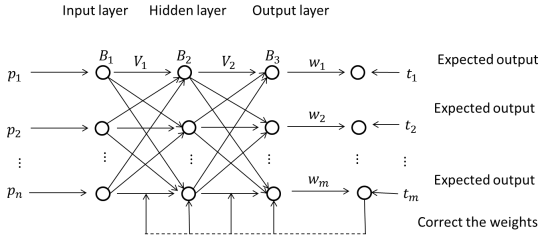

Figure 1 Schematic diagram of BP Neural Network

4. MODEL OF THE INITIAL WEIGHT AND THE THRESHOLD OF THE GENETIC ALGORITHM OPTIMIZATION

4.1 The basic idea

Genetic Algorithm is a search for the full range of algorithms. In order to speed up the convergence speed of BP Algorithm, we need to encode the initial weights and thresholds, form the initial population, then form the next generation population according to the genetic operators, then eliminate the individuals in the population, The optimal weight is obtained by decoding the optimal individual. If the conclusion satisfies the actual demand, the optimal weight is retained. Otherwise, the operation is continued until the optimal individual of a generation satisfies the demand. At this time, the corresponding weight, The threshold is the result of the global optimal weight of the network, and then get the results to the BP Network for further optimization.[4, 6]

4.2 Design methods

Coding methods Genetic Algorithms are the main coding methods of binary coding, real coding, Gray code encoding. Binary coding has some errors and

shortcomings. In this paper, a real-coded method is adopted to realize genetic searching in a large space, and the precision is higher than that of binary coding. The GA-optimized real-coded strings are successively decoded as $V_1 \rightarrow V_2 \rightarrow B_1 \rightarrow B_2$ Judge the Genetic Algorithm in the individual after decoding the corresponding solution in the problem is accurate, the standard is the fitness function. The greater the fitness of the general fitness function, the more accurate the solution, the more realistic. Define the fitness function as

$$y = \frac{1}{x}, \qquad x = \frac{1}{m}\sum_{j=1}^{m}\left\|W_j - t_j\right\| \tag{2}$$

The weights and thresholds of the individuals are taken into the BP Network to obtain the actual output (W_{i1}, W_{i2}, …, W_{im})of each sample, and the fitness value of a single sample p_i can be obtained from the above formula.

4.3 Genetic parameters

Each generation in the Genetic Algorithm has to go through the elimination of bad individuals, retain excellent individuals, in order to produce a new generation of population. After a generation of these operations, so that each generation of individual evolution, the quality of the population continues to increase.[7, 8]

4.3.1 The selection operator is a Normalized preference operator. In order to achieve the purpose of preserving the best individual, do not participate in the next crossover, mutation operation, in order to avoid damage by genetic operations to ensure that the optimal solution can be.

4.3.2 The crossover operator adopts the adaptive crossover operator, and the crossover probability changes with the value of the fitness function, which not only can improve the searching efficiency of Genetic Algorithm, but also avoids searching only local. The expression of the crossover probability is

$$\mathrm{k}_c = \begin{cases} n_1 (f_{\max} - f_c) \big/ (f_{\max} - f), f_c \geq f \\ n_2, f_c \leq f \end{cases} \tag{3}$$

In the expression, f_c is the greater fitness of the two individuals to be crossed; $f_{\max}$ is the maximum fitness value of each generation; f is the average fitness value of each ; n_1, n_2 Is a constant less than or equal to one.

4.3.3 The mutation operator adopts the adaptive mutation operator, and the mutation probability changes with the change of the fitness function value. The expression of the mutation k_m probability is

$$k_m = \begin{cases} n_3 (f_{\max} - f_m) \big/ (f_{\max} - f), f_c \geq f \\ n_4, f_c \leq f \end{cases} \tag{4}$$

In the expression, k_m is the greater fitness of the two individuals to be mutated, n_3 n_4 is a constant less than 1 or equal to 1.

4.4 The feasibility of Genetic Algorithm combined with BP Network

BP Network can learn and store a large number of input and output mode mapping, without the need to reveal the mathematical relationship between the description of the mathematical equation. Its learning rule is to use the steepest descent method, and adjust the network and threshold value by back propagation so as to minimize the square of the error of the network. However, the search space of the steepest descent method for multi-peak distribution will fall into the local optimal solution. The improved Genetic Algorithm is robust to global optimization and has strong parallel and global search ability. It is suitable for solving nonlinear complex system optimization problems, which solves the shortcomings of BP Network.

5 OPTIMIZATION PROCESS OF BP NEURAL NETWORK BASED ON GENETIC ALGORITHM

5.1 Normalize the data.

5.2 Generate the initial network. The number of network layers, the input layer, the hidden layer and the number of neurons in the output layer are determined by some of the first known conditions and some determined practical requirements. According to the initial weights, the thresholds are combined with the generated network to determine the fitness of the initial population size.[9]

5.3 According to the fitness of individuals to normalize the survival of the fittest selection, the formation of a new generation of sub-populations.

5.4 Each individual represented by the coded string is decoded into the weights and thresholds of the network by the coding method. The network is obtained by running all the training samples, and the mean square error of the whole sample set is calculated. Equation (2) determines the fitness value of each individual.

5.5 Repeat steps 3 and 4 above until the population reaches the maximum evolutionary number n.

5.6 The optimal weights of the Genetic Algorithm are substituted into the initial weights and thresholds of the BP Algorithm to train the Neural Network. According to the training function of the BP Algorithm, the fine adjustment of the weight threshold is adjusted until the mean square error $\sigma < z$, Where z is a pre-assumed expected index.

6. THE EXPERIMENTAL SIMULATION

Genetic Algorithm to optimize the network, select the initial population, is the number of network training samples P0 = 20, evolutionary algebra is 200, the

crossover probability of 0.4, the probability of variation 0.01, the choice of probability determined by the roulette wheel method. Using MATLAB simulation to get the best fitness value, evolutionary algebra is 149 generations. The original Neural Network is modified by using the weights and thresholds of the optimized network. Figure.2 and Figure.3 are Neural Network trained by experimental data and Neural Network after optimization using Neural Network and Genetic Algorithm.

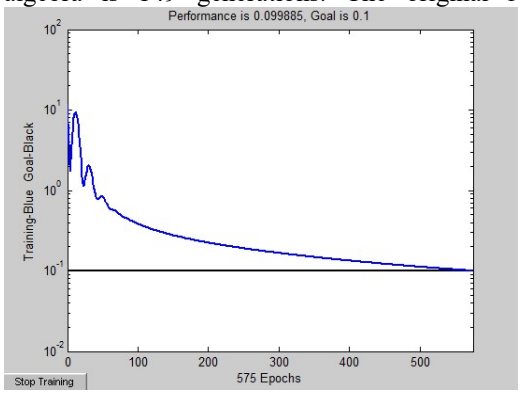

Figure 2 not optimize neuralnetwork rendering

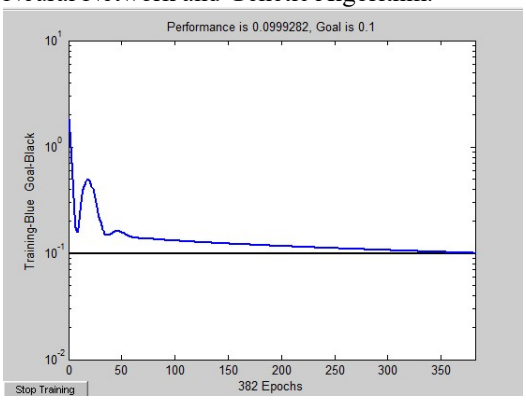

Figure 3 optimize neuralnetwork Network rendering

7. THE ERROR ANALYSIS

The actual value	Neural Network predictive value	The optimized network predictive value	The Neural Network predictive value and the actual value error	With the actual and estimated values of the optimized network error
0.5309	0.0829	0.0968	1.15615	0.338482
0.3434	0.054	0.3267	0.842749	0.794118
-0.1152	-1.8266	0.6889	14.8559	21.8359
0.3843	0.4875	0.314	0.26854	0.45147
0.022	-0.4663	0.4161	22.19545	40.10909
-0.0517	0.1673	0.3439	4.23598	3.41586
-0.2296	0.3544	0.6195	2.54355	1.15462
0.2122	-0.1644	0.4297	1.774741	2.799717
0.2282	0.0157	0.1466	0.931201	0.57362
0.2724	0.7852	0.688	1.882526	0.356828
0.193	-0.3263	1.174	2.690674	7.773575
1.1663	1.3278	0.9777	0.138472	0.30018
1.1561	1.0989	0.3203	0.049477	0.673471
0.7263	0.9844	1.0479	0.355363	0.087429
0.9016	0.9266	0.5625	0.027728	0.403838
0.5367	1.1235	0.9657	1.093348	0.294019
0.6781	1.2735	0.9693	0.878042	0.448606
0.9866	1.2911	0.5696	0.308636	0.731299
0.8379	1.6552	1.2498	0.975415	0.483829
1.2802	1.2424	0.3185	0.029527	0.721684

No optimization is obtained by diagram can forecast the network of the two groups with the actual value deviation is too big, can appear error due to data collection and 11 groups of predicted value and actual value is very close, after optimization of Neural Network forecast with 15 group to close to the actual value, the precision of prediction is greatly convergence rate is faster, and error analysis shows that this method is more accurate.

9. ACKNOWLEDGMENT

increased.

8. CONCLUSION

The results show that the combination of the two algorithms is effective for the prediction of coal and gas outburst hazard, and it can be used to predict the coal and gas outburst. And its

This work is supported in part by a grant from College students' innovative projects in hebei province(201610081075), North China university of

science and technology college students' innovative projects(X2016075), Innovation ability enhancement project in hebei province(15456252) .

REFERENCES

[1] Prediction of coal and gas outburst based on PCA-BP Neural Network [J]. Chinese Journal of Safety Science, 2013, 04: 45-50.

[2] NIE Baisheng, HE Xueqiu, WANG Enyuan, LIU Zhentang, SA Zhanyou.Study on the status and development of coal and gas outburst prediction technology [J]. Chinese Journal of Safety Science, 2003, 06: 43-46 + 83.

[3] GUO De-yong, LI Nian-you, PEI Da-wen, ZHENG Deng-feng.Neural Network method for prediction of coal and gas outburst [J]. Journal of University of Science and Technology Beijing, 2007, 04: 354-357.

[4] GUO De-yong, FAN Jin-zhi, MA Shi-zhi, WANG Yi-bin.Hierarchical analysis of coal and gas outburst prediction-fuzzy comprehensive evaluation method on, 2016, 15: 455.

[J]. Journal of University of Science and Technology Beijing, 2007, 07: 660-664.

[5] Tian Yunli, Zhou Lihua.Study on prediction method of coal and gas outburst based on BP Neural Network [J] .Systems Engineering -Theory & Practice, 2005, 12: 102-106.

[6] Cao Daoyou. Based on the application of improved Genetic Algorithm [D]. Anhui University, 2010. [7] Cui Shanshan.Genetic Algorithm of some improvements and its application [D]. University of Science and Technology of China, 2010.

[8] LIU Jian-wen, DING Jie-yu, PAN Kun, ZHANG Xiao-qiang.Advance of adaptive Genetic Algorithm based on individual similarity [J]. Journal of Qingdao University (Engineering & Technology Edition), 2016, 01: 16-19.

[9] Liang Wang, Li Liang, Wang Fushun. Basic Research on Genetic Algorithms [J]. Modern Economic Informati.

Design and Realization of GPS Navigation Toy Car Based on Arduino

Fangwei Lü
Senior high school of Fugou County, Zhoukou, Henan Province, 461300, China.

Abstract: An GPS navigating car that can automatically travel to the target location has been designed. Its control system is realized based on Arduino microcontroller, which consists of 4 modules including GPS signal processing module, electronic compass signal processing module, target distance and heading angle calculating module, motor and servo closed-loop controlling module. We further describe the hardware and software design of the GPS navigation car in detail. And, the experimental results illustrate that the GPS navigation car has the characteristics of high stability and fast response.
Key words: ATmega2560 microprocessor, GPS, Control system

1. INTRODUCTION

GPS is a global positioning system for short. Using the positioning satellites in the global, GPS realizes a global real-time positioning [1]. With the development of science and technology, the application field of GPS navigation is more and more diversified. The application of GPS technology in the field of automatic navigation has become one of the popular research directions. Using GPS to achieve automatic navigation, the vehicle can be achieved in harsh environments unmanned. In this paper, a toy car which could be navigated by GPS has been designed and realized.

2. HARDWARE DESIGN

Figure 1 represents the hardware structure of the control system for our designed toy car. In order to realize the GPS navigation control of the car, the control system uses the GPS sensor to get the position information, utilizes electronic compass to obtain the traveling direction of the car and then employs the microprocessor to analyze and calculate the collected information. Based on that, the motor and Servo are controlled correspondingly and the car reaches the target location ultimately.

The GPS module refreshes the GPS coordinates every 1 seconds while the electronic compass achieve a current heading angle every 15 milliseconds.

In order to give full play to the characteristics of the rapid response of electronic compass, we design the control system with two controllers working together in the program, that is, the use of the main controller and co-controller. As shown in Figure 1, the co-controller is responsible for receiving and parsing GPS information, and obtaining the target coordinates through the XBEE module which is transferred over from host computer.By calculating the difference between the target coordinate and the current coordinate, the co-controller calculates the distance between the car and the target. In the meantime, the co-controller calculate the target heading angle and transmit all the data to the main controller through serial communication.

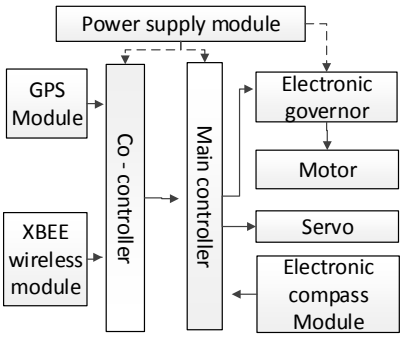

Fig.1 Control system hardware structure

The main controller receives the distance and target heading information from the co -controller once per second. In the interval of receiving information from co-controller, the main controller receives the heading angle from the electronic compass module every 15 milliseconds. The rudder angle is corrected by the control of the servo so that the car continues to move towards the target.

2.1 Microcontroller

Fig.2 Arduino Mega

Arduino is a low-cost, open-source, user-friendly development tool [2], which includes hardware (various Arduino boards) and software (Arduino IDE).

The microcontrollers used in the toy car are Arduino Mega, which consists of an ATmega2560 microprocessor and a circuit board. It provides 54 digital pins, 4 hardware serial ports and 16 analog output pins, which can be powered by USB or 9VDC power supply . Arduino can provide a variety of powerful expansion board (Shield) and library files. So, we can call a variety of functions to achieve the required functions of the project, such as the analysis of GPS coordinate information, control of the servo and motor. The use of Arduino to develop the control logic provides us great convenience.

2.2 GPS module

The type of GPS Module is EM-408, whose chip is SIRF III. The positioning accuracy is 1m and the data refresh rate is 1Hz. This GPS module is powered by the Arduino motherboard and uses serial communication. The data protocol of SIRF III chip is NMEA-0183 [3]. The format of the output packets is presented in table 1.

Table 1 Packet data format

Name	Examples	Description
Packet ID	$GPRMC	RMC packet header
UTC coordinates	161229.487	hhmmss.sss
Status	A	A = Data Valid V = Data Invalid
Latitude	3723.2475	ddmm.mmmm
North or south hemispheres	N	N = northern S = Southern
Longitude	12158.3416	dddmm.mmmm
East and West hemispheres	W	E = Eastern W = Western
Speed	0.13	
Date	120598	Ddmmyy
Magnetic change		E=east or W=west
Checksum	*10	
<CR><LF>		Terminator

By analyzing the data packets, the controller can get the current latitude and longitude information of the car.

2.3 Electronic compass module

Electronic compass module is a critical module for car navigation. We can monitor the real-time heading angle of the car continuously through this module. A magnetized magnetic needle is used to sense the earth's magnetic field in the traditional compass . The magnetic force between the magnetic field of the earth and the magnetic needle causes the magnetic needle to rotate until both ends of the magnetic needle point to the magnetic South Pole and magnetic North Pole of the earth respectively. Similarly, in the electronic compass, the magnetic needle is replaced by a magnetoresistive sensor. Magnetoresistive sensor will feel the geomagnetic information and converts it to digital signal. Through the programming, the electronic compass could output the triaxial magnetic force information, then obtains the current heading angle of the car. In our designed toy car, the used electronic compass chip is LSM303DLH, and its performance parameters are presented in table 2 .

Table 2: Electronic compass performance parameters

Power supply	2.5-3.3V
Communication	IIC communication protocol
Measuring range	± 1.3-8.1 Gauss
Resolution	2 m gauss

2.4 Servo and motor modules

Servo is a kind of position servo drive, mainly composed by the shell, circuit board, non-core motor, gears and position detector components.Here, the type of servo model is S3001, of which the operating voltage is 4.8V to 6V. The performance parameters corresponding to different voltages are shown in table 3, which can meet the need of car controlling.

Table 3. S3001 Servo Performance parameters

Operating Voltage	4.8v	6v
Torque	2.4kgf*cm	3kgf*cm
Rotational speed	0.28s/60°	0.22s/60°

The rotation of the servos is achieved by adjusting the duty cycle of the PWM (pulse width modulation) signal. S3001-type servo control PWM control signal cycle is 20ms. Pulse width 0.5ms and 2.5ms of the high-level PWM signal can realize steering servo 90 degrees turning right and 90 degrees turning right control respectively [4] [5].

Motor is controlled with the electronic governor which amplifies and adjusts the PWM control signal outputted by the controller and then controls the rotation speed and direction of the motor. In this way, the control of the car speed is realized [6]. The control signals to the motor and the servo are shown in table4.

Table 4: Control signal to motor and servos

Control Object	Target Action	PWM High Level Time
Servo	Turn left 90 degrees	0.5ms
	Turn right 90 degrees	2.5ms
Motor	Full-speed reverse	1ms
	Full speed forward	2ms
	Stopped	1.5ms

3. SOFTWARE DESIGN

Control logic of the main controller is shown in Figure 3. By comparing the target location and the car's operating parameters (position coordinates and running angle), the controller performs closed-loop

control of the servo and the motor until the car travels around the target.

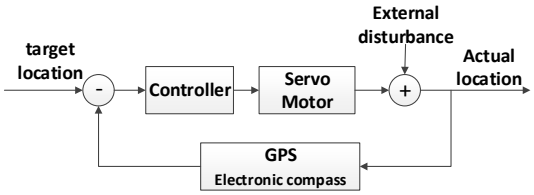

Fig.3 Closed-loop control of motor and servos

The the control software was carried out in the Arduino IDE development environment. The main functions of the car control software include GPS signal processing, the calculation of distance and azimuth angle between the target and the car, the acquisition of the car heading angle, closed-loop control of the servo and the motor. The main program flow chart is shown in Figure 4.

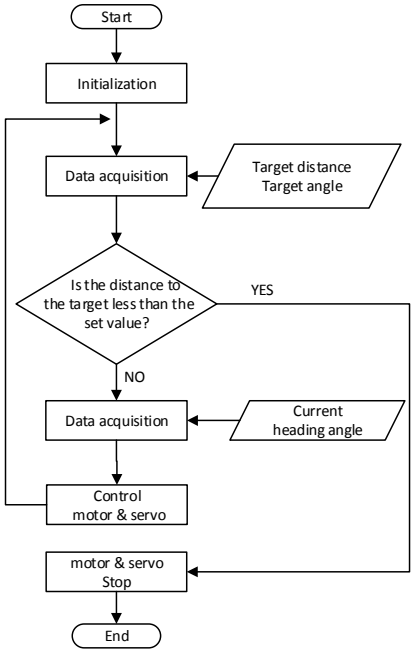

Fig.4 Main program flow chart

4. SUMMARY

In conclusion,, based on Arduino microcontroller, we realized a GPS navigation car by using GPS chips and electronics compass. The control system of the motor and servo is developed and the closed-loop control of the car is implemented. The car can automatically travel to a destination in the GPS-navigation. This GPS navigation car shows the characteristics of high stability and fast response in experimental tests.

REFERENCES

[1] BAI Xue, LIU Guo-hai, HUANG Zhen-yue. A system design for gathering GPS position information based on micro computer system [J]. CONTROL & AUTOMATION. 2008，24（8）：228-229.

[2] CAI Rui-yan. Principle and application of Arduino[J]. ELECTRONIC DESIGN ENGINEERING, 2012,20(16) : 155-157. DOI:10.3969 /j.is sn.1674-6236.2012.16.048.

[3] FANG Min, LIU Xing-rong. Applications of GPS Inertial Navigation and Combination Navigation Techniques in Motor Vehicle Navigation [J]. AUTOMOBILE TECHNOLOGY, 2000, (5):1-3.DOI:10.3969 /j.issn.1 000-3703. 2000.05.001.

[4] LIANG Li-Qin, WANG Yan, ZHANG Bao-Jian. The Design of Intelligent Vehicle Model Based on Freescale MCU [J]. DEVELOPMENT & INNOVATION OF MACHINERY & ELECTRICAL PRODUCTS，2010(6)：114—116.

[5] WEI Nan, ZHOU Bin. Smart Car's Software Design Based on S12 Microcomputer [J] . MICROCOMPUTER APPLICATIONS ， 2010(11)：28—33.

[6] ZHOU Quanz, WANG Gui-youg, JIA Xian-guang, ZHAO Ying-bing. Design of Smart Car Based on MC9S12DG128B [J]. JOURNAL OF KUNMING UNIVERSITY OF SCIENCE AND TECHNOLOGY （SCIENCE AND TECHNOLOGY），2010(5)：37-40.